An Investigation into the Characteristics and Potential Therapeutic Application of Human Neural Progenitor Cell-Derived Astrocytes in Experimental Spinal Cord Injury

Von der Fakultät für Mathematik, Informatik und Naturwissenschaften der RWTH Aachen University zur Erlangung des akademischen Grades eines Doktors der Naturwissenschaften genehmigte Dissertation

vorgelegt von

Diplom-Biologe Tobias Führmann

aus Essen

Berichter:

Privatdozent Dr. Gary Anthony Brook

Universitätsprofessor Dr. Hermann Wagner

Tag der mündlichen Prüfung: 3. November 2011

Diese Dissertation ist auf den Internetseiten der Hochschulbibliothek online verfügbar.

Summary

English version

Damage to the spinal cord leads to severe, and often permanent, motor, sensory and autonomic disturbances. A multitude of mechanism may contribute to spinal cord injury (SCI), including apoptotic and necrotic death of neurons, astrocytes and oligodendrocytes, axonal injury, demyelination, excitotoxicity, ischemia, oxidative damage, and inflammation. The lack of axonal regeneration is not primarily due to an inherent lack of capacity for axonal growth potential, but rather to the overall balance of axon-growth promoting (e.g. migration of Schwann cells into the lesion site and the local presentation of growth promoting factors and extracellular matrix proteins) and axonal growth inhibitory/repulsive molecules (e.g. myelin-associated proteins, the presence of a physical barrier presented by the glial scar and the development of fluid-filled cystic cavities) at- and around the lesion site. Over recent years, increasingly more detailed knowledge has been gained that demonstrates the potential for axonal regeneration within the nervous system of both experimental animals and humans. While the strongest regenerative capacity has been identified in the lesioned peripheral nervous system (PNS), it could also be demonstrated that axonal regeneration and compensatory sprouting takes place in the injured central nervous system (CNS). Such findings have led to the development of a number of interventional approaches to support or enhance the regenerative capacity of the CNS. Within the CNS, the main thrust of these approaches has focused either on new surgical methods, novel medications (including the use of blocking/neutralising antibodies and peptides), cell-based intervention strategies (including stem/progenitor cells) or, most recently, the application of tissue engineering strategies using biomaterials.

The aim of the present study was based on the two latter approaches, combining the growth promoting properties of human neural progenitor-derived astrocytes and a highly

orientated three dimensional collagen matrix in a tissue engineering strategy to bridge acute spinal cord lesions in adult rats.

The present investigation is separated into two parts:

The first part of the thesis addresses the issue of cell characterization, cell-cell and cell-substrate interactions *in vitro*. Human neural progenitor cells (hNPC) are characterized by their expression of certain stem/progenitor markers as well as for their ability to show multi-potency. Furthermore their ability to generate highly enriched populations of human neural progenitor-derived astrocytes (hNP-AC) is demonstrated. The axon growth promoting effects of the hNP-AC are shown in a simple 2D- as well as in a more complex 3D-culture system. After seeding onto orientated electrospun nanofibres hNP-AC show the ability to adhere, extend processes and migrate. Following seeding onto 3D collagen scaffolds, hNP-AC survive, proliferate and form columns of cells along the orientated pores of the scaffold. The highly orientated, porous microstructure of the scaffold also supports substantial intermixing of hNP-AC and migrating Schwann cells / fibroblasts from the DRG explant, cell populations that are normally mutually repulsive. This suggests that the topography of 3D scaffolds may not only influence cell-substrate interactions but also cell-cell interactions within the scaffold.

The second part of the thesis addresses the integration and functional benefits of transplanting hNP-AC into spinal cord injured rats *in vivo*. Two different types of experimental spinal cord injuries are investigated. In the **first *in vivo* SCI model**, hNP-AC are transplanted one week after a balloon compression injury and animals are subjected to standard behavioural tests (i.e. BBB, open field and gridwalk scores, as well as the Hargreaves' heat sensitivity test) with correlative morphological investigations (i.e. amount of spared tissue, survival of transplanted cells, glial scarring, microglia activation, Schwann cell migration and axonal regeneration).

Transplantation of hNP-AC promotes a better functional recovery compared to the control, but not the control + immunosuppression and the hFbl + immunosuppression (cell control group). hNP-AC integrate well into the host spinal cord in 90% of host animals, where they reduce glial scarring and promote a greater extent of axonal regeneration into the lesion site. Furthermore, Schwann cell migration into the lesion site is enhanced in the presents of hFbl and microglia activation is enhanced by immunosuppression.

In the **second *in vivo* SCI model**, hNP-AC seeded collagen scaffolds are implanted into a partly transected spinal cord directly after lesion. Since the lesioned animals show a faster recovery with this lesion model (compared to the compression model), more sophisticated behavioural analyses are possible (CatWalk, gridwalk (footfalls) and von Frey filaments). Morphological analysis includes survival of the transplanted cells, integration of the scaffold, neurite regeneration into the scaffold, glial scarring and microglia activation.

Survival of the cells within the implanted collagen scaffold is surprisingly low, with only half of the animals demonstrating morphological signs of viable donor hNP-AC, and only 10% for the donor hFbl. Although the hNP-AC fail to promote a greater functional recovery than the other investigated control groups (i.e. scaffold + immunosuppression (IS) and hFbl-seeded scaffold + IS), they lead to a greater graft-host integration and reduced host glial scarring. Furthermore microglia activity is reduced by hNP-AC compared to the control + IS, indicating a modulated immune response.

German version / deutsche Version

Verletzungen des Rückenmarks führen zu schwerwiegenden und meist permanenten Schädigungen motorischer und sensorischer Nerven sowie des autonomen Nervensystems. Eine Vielzahl von Mechanismen können zu Rückenmarksverletzungen beitragen, dazu zählen apoptotischer und nekrotischer Tod von Neuronen, Astrozyten und Oligodendrozyten, Schädigungen des Axons, Demyelinisierung, Excitotoxizität, Ischämie, oxidativer Stress und Entzündungen.

Die ausbleibende axonale Regeneration liegt nicht an einem fehlenden inhärenten Potential für axonales Wachstum, sondern eher an einem generellen (Un-)Gleichgewicht von wachstumsfördernden (z.B. der Migration von Schwann-Zellen in die Läsionsstelle und die lokale Bereitstellung von Wachstumsfaktoren und extrazellulärer Matrix) und wachstumsinhibierenden, -repulsiven Molekülen (z.B. Myelin-assoziierte Proteine, der Ausbildung einer physikalischen Barriere in Form der glialen Narbe und die Entwicklung von mit Flüssigkeit gefüllter Hohlräume) an der Läsionsstelle und um sie herum.

Im Laufe der letzten Jahre wurde ein immer detaillierteres Wissen über das regenerative Potential von Axonen im Nervensystem von Tieren und Menschen gewonnen. Das periphere Nervensystem weist dabei ein großes regeneratives Potential auf, jedoch konnte darüber hinaus gezeigt werden, dass axonale Regeneration und kompensatorisches Nervenwachstum auch im verletzten zentralen Nervensystem (ZNS) selbst stattfindet. Diese Erkenntnisse führten zur Entwicklung einer großen Anzahl von verschiedenen Strategien, um die Regeneration im ZNS zu unterstützen und zu fördern. Im Bereich des ZNS fokussieren sich diese Strategien vor allem auf neue operative Methoden, neue Medikamente (zu denen auch blockende/neutralisierende Antikörper und Peptide gehören), zellbasierte Strategien (u.a. Stamm- und Vorläuferzellen) und neuerdings die Anwendung von Biomaterialien als eine Zell- und Gewebeersatz-Strategie.

Die vorliegende Studie basiert dabei auf den beiden letztgenannten Ansätzen und beschreibt die Nutzung der wachstumsfördernden Eigenschaften von aus humanen neuralen Vorläuferzellen gewonnenen Astrozyten (hNV-AZ) alleine oder in Kombination mit einer orientierten dreidimensionalen Kollagenmatrix in einer Zell- und Gewebeersatz-Strategie, um funktionelle Regeneration nach akuten Rückenmarksverletzungen in erwachsenen Ratten zu fördern.

Die Dissertation gliedert sich in zwei Teile:

Der erste Teil der Dissertation befasst sich mit Zellcharakterisierung, Zell-Zell- und Zell-Substrat-Interaktionen *in vitro*. Humane neurale Vorläuferzellen werden sowohl anhand der Expression verschiedener Stamm- und Vorläuferzellenmarker charakterisiert als auch anhand ihrer Fähigkeit, Multipotenz zu zeigen. Zudem wird ihre Fähigkeit, sich in nahezu reine Populationen von hNV-AZ zu differenzieren, dargestellt. Die wachstumsfördernde Eigenschaft der hNV-AZ auf Axone wird sowohl in einem relativ einfachen 2D- als auch in einem komplexeren 3D-Zellkultur-System gezeigt. Die hNV-AZ sind in der Lage, auf elektro-gesponnenen Nanofasern zu adhärieren, Fortsätze zu bilden und entlang der Fasern zu migrieren. Nach Besiedlung auf eine 3D-Kollagenmatrix überleben die hNV-AZ, proliferieren und bilden Zellkolumnen entlang der orientierten Poren der Matrix. Die stark orientierte, poröse Mikrostruktur der Matrix fördert zudem die Vermischung von hNV-AZ mit aus DRG Explantaten, migrierenden Schwann-Zellen und Fibroblasten. Diese Zellpopulationen bilden normalerweise klare Grenzen zwischen einander. Dies deutet an, dass die Topographie der 3D-Kollagenmatrix nicht nur die Zell-Substrat, sondern auch die Zell-Zell-Interaktionen innerhalb der Matrix beeinflusst.

Der zweite Teil der Dissertation befasst sich mit der Integration und den funktionellen Vorteilen nach Transplantation von hNV-AZ in das verletzte Rückenmark von Ratten *in vivo*. Zwei verschiedene Arten von experimentellen Rückenmarksverletzungen werden untersucht.

Bei dem **ersten *in vivo* Rückenmarksverletzungs-Modell** werden die hNV-AZ eine Woche nach einer Ballon-Kompressions-Verletzung transplantiert und die Tiere den üblichen Verhaltenstests (BBB, Gridwalk und dem Hargreaves Hitze Sensitivitäts Test) und morphologischen Untersuchungen unterzogen (Anteil des verschonten Gewebes, Überleben der transplantierten Zellen, Ausmaß der glialen Narbe, Aktivierung von Mikroglia, Migration von Schwann-Zellen und axonale Regeneration).

Die Transplantation der hNV-AZ führt zwar zu einer besseren funktionellen Regeneration im Vergleich zu der Kontrolle, aber nicht im Vergleich zu der Kontrolle + Immunsuppression (IS) oder den humanen Fibroblasten + IS (hFbl, Zell-Kontrolle). Bei 90% der untersuchten Versuchstiere sind die hNV-AZ in der Lage, sich gut in das Gewebe zu integrieren. Dort reduzieren sie die gliale Narbe und fördern das Wachstum von Axonen in die Läsionsstelle. Zudem fördern die hFbl die Migration von Schwann-Zellen in die Läsionsstelle und die Immunsuppression bewirkt die Aktivierung von Mikroglia.

In dem **zweiten *in vivo* Rückenmarksverletzungs-Modell** wurde die Kollagenmatrix mit hNV-AZ besiedelt und direkt in das teilweise durchtrennte Rückenmark implantiert. Da diese Tiere schneller regenerieren als die Tiere in dem Kompression-Modell sind technisch versiertere Verhaltenstests möglich (CatWalk, Griwalk (Anzahl der Fehltritte) und der von Frey Filamenten-Test). Mit Hilfe morphologischer Methoden wurden das Überleben der transplantierten Zellen, die Integration der Matrix, das axonale Wachstum in die Matrix, das Ausmaß der glialen Narbe und die Aktivierung von Mikroglia untersucht.

Die Zellen überleben überraschenderweise nur sehr schlecht in der implantierten Matrix: Am Ende wurden nur bei der Hälfte der Versuchstiere noch lebende hNV-AZ nachgewiesen und lebende hFbl nur bei 10% der Versuchstiere. Obwohl die hNV-AZ nicht in der Lage sind, eine bessere funktionelle Regeneration als bei den anderen untersuchten Gruppen (naive Matrix + IS und hFbl besiedelte Matrizes + IS) zu fördern, kann eine bessere Integration der Matrix in das Rückenmark und eine Reduzierung der glialen Narbe hervorgerufen werden. Zudem reduzieren die hNV-AZ die Aktivierung von Mikroglia im Vergleich zu der Kontrolle + IS, was auf eine Modulation der Immunantwort hinweist.

Contents

1. Introduction **18**

1.1. Pathophysiology of Spinal Cord Injury 19

1.2. Myelin-Associated Axon Growth Inhibitors 21

1.3. Astroglial Scarring & Axon Growth-Repulsive Molecules 22

1.4. Spontaneous Axon Sprouting and Regeneration 24

1.5. Strategies to Promote Recovery after SCI 25

1.6. Neural Progenitor Cells 27

1.7. Astrocytes as Promoters of Axon Regeneration 29

1.8. Hypotheses Investigated in this Thesis 30

2. Material & Methods **31**

2.1. Tissue Culture 31

2.1.1. Human Neural Progenitor Cells (hNPC) 31

2.1.2. Human Neural Progenitor-Derived Astrocytes (hNP-AC) 31

2.1.3. Preparation of hNP-AC Extracellular Matrix (hNP-AC-ECM) 32

2.1.4. Preparation of hNP-AC Conditioned Media (hNP-AC-CM) 32

2.1.5. Human Foreskin Fibroblasts (hFbl) 32

2.1.6. Cell Counting 33

2.1.7. Fixation 33

2.2. Immunohistochemistry 33

2.3. Scanning Electron Microscopy (scanning EM) 35

2.4. Production of the Orientated Nanofibers 35

2.4.1. Glass-Coverslip Preparation 35

2.4.2. Electrospinning of Oriented Nanofibers 36
2.4.3. Seeding of the Orientated Nanofibers 36
2.4.4. Cell-Adhesion Assay & Cell-Number Counting 36
2.4.5. Process Length 36
2.4.6. Cell-Migration Assay 37
2.5. Gene Expression Analysis 37
2.6. Preparation of Adult Rat Dorsal Root Ganglia Neurons 38
2.7. Evaluation of Axonal Growth on 2D Substrates 39
2.8. Orientated 3D Collagen Scaffold 40
2.8.1. Preparation 40
2.8.2. Cell Seeding 40
2.8.3. Processing 40
2.8.4. Evaluation of Proliferation 41
2.8.5. Evaluation of Axonal Growth on 3D Substrates 41
2.8.6. Evaluation of Schwann Cell Migration 41
2.8.7. Preparation for *in Vivo* Studies 41
2.9. Animals 42
2.10. Balloon Compression Injury 42
2.10.1. Cell Transplantation 42
2.11. Lateral Funiculotomy 43
2.12. Immunosuppression 45
2.13. Behavioural Analyses 45
2.13.1. Behavioural Studies for Animal Groups Subjected to Balloon Compression 45
2.13.2. Behavioural Studies for Animal Groups Subjected to Lateral Funiculotomy 46
2.14. Tissue Fixation and Processing: 48
2.15. Morphological Investigations 49
2.15.1. Axon Regenerating/Axonal Sparings 49
2.15.2. Schwann Cell Migration 49
2.15.3. Inflammatory Response 49

2.15.4. Reactive Gliosis/CSPG Immunoreactivity 50
2.15.5. Survival of Transplanted Cells 50
2.15.6. Spared Tissue 50
2.16. Statistical Analysis 53

3. Cell Characterisation, Cell-Cell and Cell-Substrate Interactions 54

3.1. Introduction 54
3.2. Results 57
3.2.1. Cell Characterisation 57
3.2.2. Axon Regeneration by Dissociated Adult Rat DRG 60
3.2.3. Orientated Nanofibres 62
3.2.4. Micro-porous Collagen Scaffolds 66
3.3. Discussion 71
3.3.1. Cell Characterisation 72
3.3.2. Axon Growth Promoting Properties of hNP-AC in 2D Cultures . . . 72
3.3.3. Cell-Substrate Interactions of hNP-AC on Orientated Nanofibres . . . 73
3.3.4. Cell-substrate Interactions between hNP-AC and Orientated 3D Collagen Scaffolds 75
3.3.5. Axon Growth Promoting Properties of hNP-AC Seeded 3D Scaffolds 76
3.4. Conclusion 78

4. Experimental Spinal Cord Injury 80

4.1. Introduction 80
4.2. Results 82
4.2.1. Characterization of hFbl 82
4.2.2. Balloon Compression Model with Cell Implantation 83
4.2.3. Tissue Engineering Approach to Promote Repair after Lateral Funiculotomy of the Thoracic Spinal Cord 100
4.3. Discussion 111
4.3.1. Characterization of hFbl 113
4.3.2. Comments on the behavioural analyses of both SCI models 113

4.3.3. Survival of transplanted cells 117
4.3.4. Axonal regeneration 120
4.3.5. Schwann cell migration 121
4.3.6. GFAP and CSPG expression 122
4.3.7. Inflammatory response 125
4.3.8. Spared tissue 127
4.4. Conclusion 128

5. General Discussion **130**
5.1. To generate highly enriched populations of immature astrocytes from human neural progenitor cells (hNP-AC) 131
5.2. To determine cell-substrate interactions between hNP-AC and orientated bioengineered substrates 131
5.3. To identify the axon growth-promoting properties of the hNP-AC in 2D and 3D systems using adult neuronal populations 133
5.4. To determine the axon growth promoting properties/ graft-host interactions of hNP-AC when implanted into experimental models of SCI, either alone- or in combination with a 3D collagen scaffold 134
5.5. Conclusion 138

A. Publications **186**

B. Acknowledgments **188**

List of Tables

2.1. Antibodies 34
2.2. Forward and reverse primer sequences used for the detection of RT-PCR for GFAP, CD44 and GAPDH. 38
2.3. Gridwalk test score 45
2.4. List of animal numbers used in each experimental group. 49

3.1. Quantification of the extent of neuritic outgrowth from dissociated DRG neurons over the different substrates. 61

List of Figures

1.1. Edwin Smith Surgical Papyrus 19
1.2. Schematic diagram, spinal cord lesion 21

2.1. Schematic diagram, dissociated DRG 39
2.2. Schematic diagram, balloon compression injury 43
2.3. Schematic diagram, lateral funiculotomy 44
2.4. Schematic diagram, evaluation balloon compression 51
2.5. Schematic diagram, evaluation lateral funiculotomy 52

3.1. Scanning EM of hNPC 57
3.2. Characterisation, hNPC 58
3.3. Characterisation, hNP-AC 59
3.4. Evaluation, dissociated DRG 61
3.5. Scanning EM, nanofibers 62
3.6. Characterization, hNP-AC on nanofibres 64
3.7. hNP-AC migration on nanofibers 65
3.8. Scanning EM, collagen scaffold 66
3.9. Scaffold, proliferation of hNP-AC 67
3.10. Scaffold, hemisected DRG outgrowth 69
3.11. Scaffold, cell-cell interactions 70
3.12. Scaffold, evaluation of DRG outgrowth 71

4.1. Characterisation, hFbl 83
4.2. Behavioural Analysis, Balloon Compression 85
4.3. Survival hFbl, Balloon Compression 87

4.4. Survival hNP-AC, Balloon Compression 88
4.5. Evaluation Survival, Balloon Compression 89
4.6. Axon Regeneration along hNP-AC, Balloon Compression 90
4.7. Axon Regeneration/Sparing, Balloon Compression 91
4.8. Schwann Cell Migration, Balloon Compression 93
4.9. GFAP and CSPG Immunoreactivity, Balloon Compression 95
4.10. Immune Response, Balloon Compression 97
4.11. Spared Tissue, Balloon Compression 99
4.12. Catwalk Gait Analysis, Lateral Funiculotomy 103
4.13. Gridwalk, Lateral Funiculotomy 104
4.14. Von Frey Filaments, Lateral Funiculotomy 104
4.15. Survival of Transplanted Cells, Lateral Funiculotomy 106
4.16. Axon Regeneration, Lateral Funiculotomy 107
4.17. GFAP and CSPG Immunoreactivity, Lateral Funiculotomy 109
4.18. Immune Response, Lateral Funiculotomy 111

Abbreviations

5-HT	5-hydroxytryptamine
ANOVA	analysis of variance
BBB	Basso, Beattie, and Bresnahan locomotor rating scale
BDNF	brain-derived neurotrophic factor
BMP4	bone morphogenetic protein 4
bFGF	basic fibroblast growth factor
BOS	base of support
BSA	bovine serum albumine
CD	cluster of differentiation
cDNA	copy deoxyribonucleic acid
CGRP	calcitonin gene-related peptide
ChABC	chondroitinase ABC
CNTF	ciliary neurotrophic factor
CNS	central nervous system
C/PCL	collagen/polycaprolactone
CSPG	chondroitin sulphate proteoglycans
DAPI	4',6-Diamidino-2-phenyindole
DIV	days *in vitro*
DMEM	Dulbecco's modified Eagle medium
DNA	deoxyribonucleic acid
dpo	days post operation
DRG	dorsal root ganglia
DRGM	dorsal root ganglia media
ECM	extracellular matrix
EGF	epidermal growth factor
FBS	fetal bovine serum
g	gram
GAM	goat anti mouse
GAPDH	glyceraldehyde 3-phosphate dehydrogenase

GARb	goat anti rabbit
GDA	glial restricted progenitor-derived astrocytes
GFAP	glial fibrillary acidic protein
GTP	guanosine triphosphate
HBSS	Hank's buffered salt solution
hFbl	human foreskin fibroblasts
hNestin	human nestin
hNP-AC	human neural progenitor-derived astrocytes
hNP-AC-CM	human neural progenitor-derived astrocytes conditioned media
hNP-AC-ECM	human neural progenitor-derived astrocytes extracellular matrix
hNPC	human neural progenitor cells
hNuc	human nuclei
Iba1	ionized calcium binding adaptor molecule 1
IgG	immunoglobulin G
IL	interleukin
INF-γ	interferon-γ
iPS	induced pluripotent stem cell
IS	immunosuppression
kg	kilogram
LIF	leukemia inhibitory factor
MAP2a+b	microtubule-associated protein (a+b)
MAG	myelin associated glycoprotein
mg	milligram
MIP-1	macrophage colony stimulating factor-1
MSC	mesenchymal stromal cells
mTOR	mammalian target of rapamycin
NF	neurofilament
NG2	neuronglial antigen 2
NGF	nerve growth factor
NgR	NOGO receptor
NGtS	normal goat serum
NPBM	neural progenitor basal media
NPC	neural progenitor cells
NPDM	neural progenitor differentiation media
NPPM	neural progenitor proliferation media
NSF-1	nerve survival factor-1
OMgp	oligodendrocyte-myelin glycoprotein

PBS	phosphate buffered saline
PCL	polycaprolactone
PCR	polymerase chain reaction
PDGF	platelet-derived growth factor
PFA	paraformaldehyde
PirB	paired immunoglobin like receptor B
PLL	poly-L-lysine
PNS	peripheral nervous system
PSA-NCAM	poly-sialylated neural cell adhesion molecule
PSN	propriospinal neurons
PTEN	phosphatase and tensin homolog
RNA	ribonucleic acid
RohA	ras homolog gene family, member A
RT	room temperature
RT-PCR	reverse transcription polymerase chain reaction
scanning EM	scanning electron microscopy
SCI	spinal cord injury
SEM	standard error of the mean
sPEG	star-shaped poly-ethylene glycol
TGF-β	transforming growth factor-β
TNF-α	tumor necrosis factor-α
TuJ1	β-III tubulin
μg	microgram
μm	micrometer

1. Introduction

The devastating consequences of traumatic spinal cord injury (SCI) depend on the level and severity of the injury but include permanent locomotor and sensory deficits, neuropathic pain, spasticity, urinary and respirator dysfunction, metabolic problems as well as obvious psychological problems associated with a poor prognosis. The first medical documentation of SCI was recorded on Egyptian papyrus, dating from the sixteenth century B.C. (Figure 1.1). The first indications of the cellular basis for the poor outcome after SCI were described by Santiago Ramón y Cajal and his students in the late early 20th century using silver impregnated tissue sections of experimental spinal cord lesions. Ramon y Cajal reported that *"In adult centres the nerve paths are something fixed, ended, immutable. Everything may die, nothing may be regenerated. It is for the science of the future to change, if possible, this harsh degree"* [70]. For a long time, the apparent inability of the mature mammalian central nervous system (CNS) to generate new neurons (neurogenesis) and the failure of axons to regenerate were generally regarded as "laws of nature" [70, 82, 149]. This was in stark contrast to the behaviour of lesioned peripheral nervous system (PNS) axons, which could undergo successful regeneration leading to the re-innervation of their targets [69, 176, 180, 401]. The opinion that brain and spinal cord lesions were irreversible has now been revised, partly due to Cajal's original descriptions, showing damaged CNS axons forming regenerative sprouts that were unable to extend for more than 1-2 mm alone, but much further with the use of peripheral nerve grafts [70]. A few examples of endogenous axonal regrowth were demonstrated in recent years [33, 58, 94, 458] and the existence of multi-potent progenitor populations was demonstrated in the adult hippocampus (dentate gyrus), sub-ventricular zone and spinal cord [6, 7, 21, 122, 155, 199, 223, 229, 273, 344]. Thus it has become clear that the adult CNS is able to respond to CNS injury by: (i) the anatomical reorganization of spared axonal connections (plasticity) and (ii) the generation of new precursor cells. This

has motivated numerous scientific studies to better understand the pathophysiology of SCI and to further challenge the dogma of the irreversibility of CNS injury.

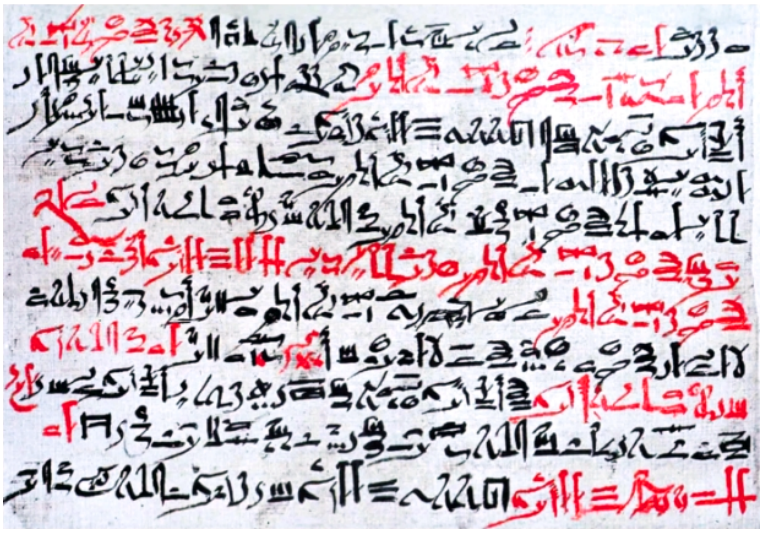

Figure 1.1.: Instructions concerning a dislocation of a vertebra in the neck. *"If you examine a man with a neck injury... and find he is without sensation in both arms and both legs, and unable to move them, and he is incontinent of urine... it is due to the breaking of the spinal cord caused by dislocation of a cervical vertebra. This is a condition which cannot be treated."* Edwin Smith Surgical Papyrus, Case 31. Thebes, c. 1550 BC. Taken from Breasted. J.H. (ed.) The Edwin Smith Surgical Papyrus© The University of Chicago Press, 1930.

1.1. Pathophysiology of Spinal Cord Injury

Traumatic human SCI is widely acknowledged to be a highly heterogeneous disorder and the characteristics of the lesion site are known to depend on a number of parameters including type of injury, severity and time after injury. Nonetheless, 4 main types of injury have been identified [65, 66]: (i) compression injury, (ii) contusion injury, (iii) laceration injury, and (iv) solid core lesions. This has resulted in the development of a number of experimental models of SCI, which mimic (to a greater or lesser degree) the pathophysiology seen in the range of different human spinal cord injuries. These models have also been used to investigate the cascade of cellular and molecular events that are initiated by the primary insult, as well as for the development and evaluation of a range of therapeutic strategies intended to promote tissue repair e.g [416].

Immediately after SCI, numerous descending and ascending nerve fibre pathways are mechanically damaged and the highly organised cytoarchitecture of the spinal cord white matter

is disrupted. Since primary, mechanical injury to the CNS gray and white matter results directly from the trauma, such destruction cannot be avoided and may result in immediate partial or total paralysis. Such primary degenerative events are followed by a cascade of secondary degenerative events including bleeding, ischaemia, free-radical production, oedema, excitotoxicity, inflammation, programmed cell death, scarring and cystic cavitation, all of which contribute to the augmentation of tissue loss [65, 369] (see schematic illustration in Figure 1.2). The dynamics of the secondary degenerative events take place over a time scale of hours, days, weeks and even months after the injury [201, 248, 368]. Inflammatory processes are a major contributor to secondary degeneration. The current view is that the inflammatory response after CNS injury is a "double-edged sword", having both early neurodegenerative and later neuroprotective aspect [74, 248]. Disruption of the blood-spinal cord barrier leads to the recruitment of intrinsic (microglia) and extrinsic inflammatory cells (neutrophils, macrophages, lymphocytes, natural killer cells), which express proteolytic enzymes that in turn, degrade extracellular matrix proteins and contribute to blood-brain barrier degradation and oedema. The processes initiated by the pro-inflammatory cytokines and chemokines (i.e. IL-1, IL-α, IL-β, IL-6, interferon (INF)-γ, macrophage colony stimulating factor (MIP-1), tumor necrosis factor (TNF)-α) as well as reactive oxygen species, oxidative enzymes, and metalloproteinases exacerbate secondary tissue damage and the formation of an inhibitory glial scar [141, 142, 220, 253, 325, 326, 482]. Cell death resulting from all these mechanisms occurs through necrotic or apoptotic phenomena [117] as well as through autophagia [368]. Inflammatory processes also participate in the demyelination of still intact axons [31]. The body's immune response may facilitate the recovery from injury by reducing the size of lesion, facilitating wound repair by clearance of hemorrhagic and necrotic tissue as well as by releasing trophic factors and cytokines which can be neuroprotective and stimulate axonal regeneration (e.g. interleukin (IL)-10, transforming growth factor (TGF)-β) [25, 48, 74, 111, 116, 138, 139, 237, 253, 404].

Wallerian degeneration, with death of oligodendrocytes, cyst formation within grey and white matter and the development of scar tissue (mainly composed of astrocytes and fibroblasts [8]) represent the final histopathologic evolution of SCI in the chronic stage [31, 369]. The evolution of the cellular and molecular responses to SCI may result in the re-organisation of spinal cord circuitry that could be functionally useful (e.g. spasticity) or detrimental (e.g.

neuropathic pain [31]). It is now widely acknowledged that the lack of any functionally significant axon regeneration in the lesioned CNS is due to an imbalance of local axon growth-promoting and growth-inhibitory mechanisms, including the relatively poor expression of neurotrophic factors and guidance cues at the lesion site, as well as the presence of potent molecular (myelin inhibitors) and physical barriers (glial scar) to axon growth [130, 199, 201, 381].

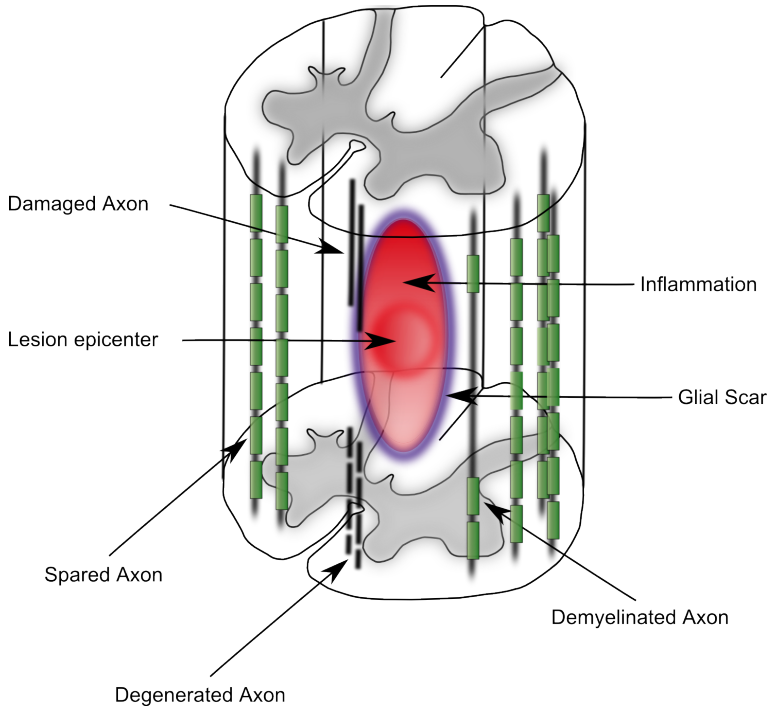

Figure 1.2.: *Schematic diagram of the pathological events initiated by compression- or contusion-type traumatic injury to the spinal cord.* The injury causes rapid degeneration of the neural cell bodies and processes within the spinal cord grey matter at the lesion epicentre, accompanied by local bleeding. The ensuing ischaemia, free-radical production, excitotoxicity, inflammation, oedema and programmed cell death all contribute to secondary degeneration which increases the size of the lesion over time. Reactive astrocytes express elevated levels of CSPGs and contribute to scar formation. Oligodendrocytic necrosis and apoptosis result in myelin debris being released at and around the lesion site and some degree of demyelination of spared axons. Mild- and moderate compression and contusion injuries often demonstrate some sparing of axons at the outermost aspect of the white matter.

1.2. Myelin-Associated Axon Growth Inhibitors

The primary and secondary degenerative events caused by traumatic injury release, as debris, a number of potent myelin-associated axon growth-inhibitory molecules into the lesion site and surrounding tissues. The first of these molecules to be identified was NI-35/250

(recently cloned and renamed NOGO-A) [79, 170, 330]. This membrane-bound glycoprotein constitutes only a few percent of the total protein content of mature central myelin but is an extremely potent inhibitor of axon growth. It induces the rapid, Nogo receptor (NgR)-mediated collapse of axonal growth cones by activation of the small GTP-ase RhoA [145, 146, 299]. The development of a monoclonal antibody (IN-1) which blocks the inhibitory activity of NOGO-A has proved to be extremely useful in promoting regeneration of axotomised corticospinal axons, as well as substantial sprouting and re-organisation of non-lesioned axonal projections [22, 54, 427, 479]. Other potent myelin-associated inhibitors are myelin associated glycoprotein (MAG) and oligodendrocyte-myelin glycoprotein (OMgp), both of which also act via NgR and share the same intracellular signalling pathway [109, 282, 293, 455, 456]. NOGO-A, MAG and OMgp have also recently been found to act via a supplementary receptor system, via paired immunoglobin like receptor B (PirB) [15]. However, it seems that MAG plays no significant role in the inhibition of CNS axons *in vivo* [29, 259] and is lost or degraded very early after SCI [68]. Recent investigations have clearly demonstrated that the myelin-associated axon growth inhibitory molecules stabilise existing connections within the mature CNS and suppress plasticity. In this context, the use of anti-NOGO-A antibodies or blocking peptides has been shown to promote functional recovery by supporting some degree of regeneration by lesioned corticospinal axons as well as compensatory (or collateral) sprouting [166, 260]

1.3. Astroglial Scarring & Axon Growth-Repulsive Molecules

It has been known for over 100 years that lesion-induced scars of the CNS were inhibitory to axon regeneration. The long-standing emphasis on inhibitory glia has led to a generalized notion that reactive astrogliosis *per se* is a detrimental phenomenon contributing to neurotoxicity, inflammation and chronic pain [397].

A prominent hallmark of reactive gliosis is hypertrophy of the astrocytic cell body and processes with increased production of intermediate filaments, such as glial fibrillary acidic protein (GFAP, [27, 119]), as well as renewed expression of vimentin [95, 96, 267, 465] and

nestin [59, 81, 152]. The hypertrophic processes extend and interweave with each other at the edge of the injury site; eventually forming a thick mesh-work of cells and processes, supported by tight- and gap junctions. The resulting astroglial scar represents a major mechanical and molecular barrier to axonal regeneration [151, 185, 473]. In lesions that spare the dura mater, the scar is composed primarily of astrocytes, but in more severe lesions (which open or rupture the meninges) invading connective tissue elements (e.g. fibroblasts, endothelial cells, ependymal cells) and Schwann cells come into close contact with the reactive astrocytes [33, 58, 60, 381]. Other inflammatory cell types such as microglia, macrophages and also oligodendrocytes participate to scar formation [31]. Eventually, a scar-encapsulated cavity forms, which may be many times the size of the initial wound [17].

Further proof that the SCI-induced glial scar presented an inhibitory environment to axons was the identification of the re-expression of axon-repulsive extracellular matrix (ECM) molecules such as tenascin and four classes of proteoglycans [219, 227, 281, 393, 418]. Members of the proteoglycans that were detected included the large family of chondroitin sulphate proteoglycans (CSPG), of which aggrecan, brevican, neurocan, neuronglial antigen 2 (NG2), phosphacan and versican are prominent members [173, 292]. In addition, a number of other extrinsic and intrinsic factors have been shown to be axon growth-inhibitory, including the up-regulation of ECM-related molecules such as ephrins and semaphorins, [129, 173, 315], as well as the intrinsic neuronal molecules phosphatase and tensin homolog (PTEN), a negative regulator of the mammalian target of rapamycin (mTOR) pathway [313].

Nevertheless, axon growth-supportive molecules are also expressed by reactive astrocytes, for example laminin, fibronectin, and poly-sialylated neural cell adhesion molecule (PSA-NCAM) have also been reported [174, 345, 381, 394, 422]. Although the expression of both growth-inhibitory and growth-promoting ECM molecules increases in reactive astroglia, the inhibitory ECM components are almost always more markedly up-regulated [280]. The interactions of these and other axon growth-repulsive and growth-promoting molecules results in an environment which is overall supportive or inhibitory to axon regeneration [202, 394].

However, other studies have shown a beneficial role of the glial scar during the acute phase (1-2 weeks) after spinal cord injury. Elimination of reactive astrocytes or preventing their proliferation and contribution to scar formation after CNS injury resulted in a failure of blood-brain barrier repair, accompanied by massive inflammatory cell infiltration

and increased loss of neurons and oligodendrocytes and the eventual worsening of the functional outcome [127, 305]. Moreover, transgenic mice showing enhanced astrocytic migration and premature glial scar formation facilitated recovery [305]. Thus, an acute astrocytic response appears important to limit and restrain the inflammatory response, but this may be at the expense of reduced axonal regrowth. Since the late 90's, many studies using transgenic and experimental animal models have provided compelling evidence that reactive astrocytes are important for the protection of the CNS by: (1) uptake of potentially excitotoxic glutamate [67, 349, 410], (2) protection from oxidative stress via glutathione production [80, 378, 410, 444], (3) neuroprotection via adenosine release [268], (4) protection from NH_4^+ toxicity [340], (5) neuroprotection by degradation of amyloid-beta peptides [240], (6) facilitating blood-brain barrier repair [67], (7) reducing vasogenic oedema after trauma, stroke or obstructive hydrocephalus [67, 475], (8) stabilizing extracellular fluid and ion balance and reducing seizure threshold [475], and (9) limiting the spread of inflammatory cells or infectious agents from areas of damage or disease into healthy CNS parenchyma [67, 110, 127, 194, 258, 295, 305, 397, 448]. Together, these findings indicate that there is a normal process of reactive astrogliosis and glial scar formation that exerts various beneficial functions, including protecting neural cells and their function, restricting the spread of inflammation and infection, as well as promoting tissue repair. It is important to distinguish this normal response to injury with the potential of dysfunctional reactive astrocytes to contribute to CNS disorders.

1.4. Spontaneous Axon Sprouting and Regeneration

Although there is no spontaneous functional axon regeneration by long distance projecting neurons after SCI, it has become clear that axonal sprouting and cellular re-organisation following SCI are more extensive and organised than had previously been appreciated. Experimental models of SCI (i.e. compression- and lacerating-type injuries) have revealed that the ECM framework deposited during early bleeding in the lesion site supports the migration of different populations of cells, i.e. polymorphonuclear neutrophils, followed by endothelial cells, meningeal fibroblasts, macrophages, activated microglia and Schwann cells [369]. The presence of migrating Schwann cells appears to tip the balance of growth-promotion versus

growth-inhibition towards the support of axon regeneration, predominantly by populations of local intrinsic spinal cord GABAergic and glycinergic interneurons [33, 57, 60, 177]. All of the axonal re-growth taking place after compression- and laceration-type injuries appears to be associated with a framework of overlapping Schwann cell bodies and processes which present important growth promoting cell adhesion molecules, such as L1 [60]. The glial framework is remarkable in that, in many places, it demonstrates a high degree of orientation, in parallel with the longitudinal axis of the spinal cord. Similar observations of orientated Schwann cells and axons have been reported within human spinal cord lesions [458].

An even more striking, plasticity-mediated return of function has been demonstrated following partial thoracic (hemisection-type) injuries [23]. Lesioned lumbar-projecting corticospinal axons were found to sprout and innervate short- and long distance projecting propriospinal neurons (PSN). With time, contacts with the short distance projecting PSN were lost, while those with the long distance projecting PSN were maintained. The long distance projecting PSN extended synaptic contacts to include deafferented lumbar motoneurons. The spontaneously sprouting corticospinal axons, thus established contacts which effectively by-passed the lesion site [23]. A better understanding of the regulation and restrictions of these spontaneous events may lead to the identification and manipulation of novel targets which enhance and maintain endogenous tissue repair processes.

1.5. Strategies to Promote Recovery after SCI

The complex nature of SCI has resulted in the development of many different repair strategies. Of the myriad of intervention strategies, **cell-implantation therapies** may offer a number of advantages: in addition to presenting an avenue for continuous growth factor delivery, transplanted cells may act as a bridge across the lesion across which axonal regrowth may occur. Donor cells may replace lost glia and neurons, and contribute to the re-establishment of new functional local circuits.

In the early 1980s, pioneering research demonstrated that adult CNS neurons could regenerate axons into implanted PNS or foetal CNS tissues [98, 303]. In later experiments, successful axonal regeneration could also be supported after implantation of foetal spinal cord [10]. Grafting of peripheral glia (either alone or in combination with a growth promoting

scaffold) into the lesion site to promote axon regeneration was the next step. Both Schwann cells [64, 239, 261, 471] and olfactory ensheathing cells [337, 338] have been extensively investigated and have generated promising results. However, more recently the potential of progenitor cell-based strategies has become apparent. The potential sources of such donor progenitor cells include embryonic- [277], foetal- or adult-derived neural progenitors cells (NPC, [231, 321, 322, 359, 367]), and more recently, induced pluripotent stem cells (iPS) [436]. Such neural progenitor-based strategies have been reported to promote functional improvement in experimental models of CNS injury, but their beneficial mechanism(s) of action remain poorly defined [52, 114, 121, 156, 306]. Furthermore, mesenchymal stromal cells (MSC) have also been suggested as potential candidates for neural repair. This suggestion is particularly interesting bearing in mind the relative ease of harvesting such autologous cells: being readily isolated from bone marrow, adipose and other tissues [16, 243, 331]. Motor and sensory improvements in rodent models [11, 196, 411] as well as in phase I clinical trials [311, 412] have been reported following implantation of MSC.

A variety of studies have also suggested that the **inhibition or stimulation of inflammatory responses** can be beneficial to functional recovery following SCI. Experimental studies investigating inhibitors of cellular inflammatory responses include the administration of corticoids [9, 368], the depletion or suppression of mononuclear phagocytes [44, 325], inhibition of leukocyte, macrophage/monocyte, and neutrophil infiltration [160, 419, 420], inhibition of inflammatory angiogenesis [453], administration of classical immunosuppressives [32], administration of anti-inflammatory cytokines [36, 37, 55], or pharmacological agents capable of reducing macrophage activation [400, 482]. All the above studies suggested that inhibition of inflammation was important for the promotion of tissue sparing and/or improvement of functional recovery in animal models of SCI [9].

In contrast to these findings, other work has demonstrated that stimulation of cellular inflammatory responses via administration of activated T-cells , implantation of stimulated homologous macrophages, vaccination with myelin self-antigens or NOGO-A-derived peptides can promote functional recovery after SCI [186–188, 233, 341, 370, 474]. A Phase I clinical trial applying anti-Nogo-A antibody to subjects with acute SCI has been successfully conducted and a multicentric, multinational Phase II trial is in preparation [485].

In most of these studies, recovery was improved, but the orientation of axonal regeneration

within the lesion site was poorly controlled. Since the orientation of axonal regeneration is likely to play an important role in the eventual efficiency of bridging strategy, a number of orientated scaffolds have been developed. The first of such guidance channels were simple hollow tubes, into which the proximal and distal stumps of transected spinal cord could be inserted and the tube filled with a gel-like matrix or with donor glia [291, 469, 470]. Such guidance channels supported significant axonal in-growth, which mainly occurred on the inner surface on the tubes.

Recent advances in **bioengineering** have resulted in the development of a number of artificial 3D, highly orientated, biodegradable matrices [200, 316, 426] which have been transplanted into the injured spinal cord. It is assumed that the biodegradability of these scaffolds plays an important role in promoting tissue repair, since non-degradable matrices could induce a harmful foreign body response, potentially leading to the constriction of the scaffold [484]. Significantly, it has been recognized that such bioengineering strategies are sufficiently versatile to be able to import functional molecules, drugs or cells into areas of pathology.

Although a large number of intervention strategies have been investigated, it is unlikely that any one strategy, alone, would be able to promote dramatic functional improvement. It is more likely that combined approaches will yield greater benefits: for example the combination of grafting PNS nerves [432], Schwann cell-seeded guidance channels [76] or neural stem/progenitor cell [206, 225] with the administration of the enzyme chondroitinase ABC (ChABC) has resulted in improved axonal regeneration in all cases. The ChABC is important for breaking down sugar side-chains of inhibitory CSPGs. Similarly, the combination of growth factor treatment via genetic modification of donor cells (such as fibroblasts, NPC and Schwann cells) has resulted in enhanced axonal regeneration and, in many cases, functional recovery [171, 172, 217, 232, 269, 285, 294].

1.6. Neural Progenitor Cells

Stem cells are non-specialized cells that have the capacity to give rise to more stem cells (termed self-renewal) for an extensive period of time, as well as producing progeny that undergo terminal differentiation into the major cell types of their tissue of origin (termed

multi-potency) [154, 372]. It is widely appreciated that adult neural stem cells *in vivo* are slowly dividing, long-term BrdU-retaining cells that exhibit several common features of subventricular radial glia-like astrocytes and ventricular ependymal cells, including morphological characteristics and expression of the glial fibrillary acidic protein (GFAP) and the glycoprotein CD133 [274]. However since only a small proportion of cells in an *in vitro* neurosphere population seems to fulfil the criteria of a stem cell, here the term neural progenitor cells (NPC) is used to describe a more restricted oligopotent cell population, which has only a limited capacity of self-renewal [343].

NPC may be obtained from the inner cell mass of the blastocyst, from embryonic- [235, 429] and foetal-tissue [409, 440], and from neurogenic regions in the adult CNS [165, 398]. Even *post mortem* CNS tissue has been suggested to be a source for NPC [133, 252, 371], where harvested cells maintain the capacity for self-renewal, and the generation of neurons, astrocytes and oligodendrocytes [154, 278, 398, 425].

In spite of many studies indicating a beneficial role of stem cell transplantation following SCI, there is still limited mechanistic insight. The simplest interpretation of how transplanted stem cells promote functional recovery is that donor cells replace lost neurons and glia. Other possible, but more indirect mechanisms include (i) the expression and release of growth factors, cytokines and neurotrophic factors (trophic support); (ii) effects on the vasculature or the modulation the inflammatory response; (iii) acting as a substrate for axonal regeneration; (iv) the promotion of endogenous progenitor proliferation [24, 314].

The use of NPC isolated from foetal tissues attenuates the risk of oncogenic transformation (as observed with embryonic stem cells), especially after they have undergone differentiation prior to transplantation [230]. Undifferentiated foetal human NPC have been transplanted into mice [92, 93, 359], rat [224, 264, 304, 421, 460, 468] and primate [212] models of spinal cord injury, with encouraging results. Following transplantation of human, rat or mouse NPCs into the intact or injured murine spinal cord, donor cells were only found to primarily differentiate into astrocytes and, to a lesser extent, into oligodendrocytes [71, 100, 264, 367, 379, 395, 421, 450, 460]. However transplantation of NPC-derived oligodendroglia has been shown to promote remyelination and improvement in locomotor function after spinal cord injury [126, 230, 301]. Promoting the generation of oligodendrocytes (at the expense of astrocytes) by transplanted neural stem cells further facilitates sensory and

locomotor recovery [197]. Following a similar logic, the transplantation of foetal hNPC-derived astrocytes might represent an attractive cell type to support spinal cord repair by an alternative mechanism, namely by promoting axon regeneration.

1.7. Astrocytes as Promoters of Axon Regeneration

Astrocytes are phenotypically heterogeneous, and it is not clear to what extent different phenotypes play different roles in the pathophysiological response to traumatic injury. The glial scar is composed of both local hypertrophic astrocytes and newly formed astrocytes, derived from stem/progenitor cells that invade the lesion area [397]. However, it is clear that the developmental status of the astrocytes exerts a marked influence on the axon growth-inhibitory/promoting properties of the reactive cells [28, 381]. The first indications of the beneficial (i.e. axon growth promoting) effects of reactive immature astroglia to injury were reported in the late 1980s: astrocytes from the developing brain were suggested to be an ideal substrate for neuron regeneration *in vitro* [124, 125, 131, 302, 433, 434] and *in vivo* [380, 382, 390, 391]. Since then, numerous studies have suggested that immature astrocytes may provide a favourable substrate for axon regeneration following SCI [38, 99, 100, 128, 431]. Most importantly, in contrast to type I astrocytes, which induced robust axonal regeneration, differentiation and grafting of type II astrocytes has been reported to induce allodynia-like symptoms (pain in response to a normally nonpainful stimuli) [99, 197]. The axon growth promoting properties of different subpopulations of animal-derived astroglia (e.g. immature and reactive astrocytes) were reported to be due to the production of particular ECM components (including laminin and fibronectin) as well as to the expression and release of certain growth factors (including bFGF, BDNF, NGF) [113, 329, 463].

1.8. Hypotheses Investigated in this Thesis

Following the simple idea that immature rat astrocytes promote axonal regeneration and scaffold integration [236, 380, 389–391], the main hypothesis investigated in this thesis can be formulated as: *"Human immature neural progenitor-derived astrocytes are capable of promoting axon regeneration and scaffold integration, similar to properties demonstrated for immature rat astrocytes."*

To answer this hypothesis the following goals were formulated:

1. To generate highly enriched populations of immature astrocytes derived from human neural progenitor cells (hNP-AC).

2. To determine cell-substrate interactions between hNP-AC and orientated bioengineered substrates.

3. To identify the axon growth-promoting properties of the hNP-AC in 2D and 3D systems using adult neuronal populations.

4. To determine the axon growth promoting properties/graft-host interactions of hNP-AC when implanted into experimental models of SCI, either alone- or in combination with a 3D collagen scaffold.

2. Material & Methods

2.1. Tissue Culture

2.1.1. Human Neural Progenitor Cells (hNPC)

Cells were purchased from Lonza Sprl. (Verviers, Belgium). The donated cells had been obtained from anonymous human foetus' (week 18) according to state and federal guidelines. Cells were cultured as neurospheres in neural progenitor proliferation medium (NPPM) consisting of Dulbecco's modified Eagle medium (DMEM)/F12 (high glucose, 1:1) containing Glutamax (1:100, Invitrogen), human recombinant epidermal growth factor (EGF 20 ng/ml, Cell Concepts), human recombinant basic fibroblast growth factor (bFGF 20 ng/ml, Invitrogen), neuronal stem cell supplement (1:50, PAA) and penicillin/streptomycin (1:100, PAA) at 37°C with 5% CO2. Medium was changed every 2-3 days. Spheres were passaged following incubation in Accutase (undiluted solution, PAA) and triturated as described by others [451]. Multi-potency of hNPC was monitored by *in vitro* differentiation to astrocytes, neurons and oligodendrocytes. To induce differentiation, hNPC were plated onto poly-L-lysine (0.01%, Sigma-Aldrich, Steinheim, Germany) and laminin (10 μg/ml, Roche, Mannheim, Germany, PLL/laminin) coated 8-well chamber slides (Nunc, Langenselbold, Germany) and cultured in neural basal progenitor media (NPBM, Lonza) supplemented with nerve survival factor (NSF-1), gentamicin (both ready for use solutions, Lonza), B27 (1:50 Invitrogen) and platelet-derived growth factor AA (PDGF-AA, 20 ng/ml, Peprotech).

2.1.2. Human Neural Progenitor-Derived Astrocytes (hNP-AC)

hNPC were grown as spheres as described previously [461] in neural progenitor differentiation medium (NPDM) composed of Neurobasal A (Invitrogen) containing EGF (20 ng/ml), bFGF

(20 ng/ml), human recombinant leukemia inhibitory factor (LIF, 10 ng/mL; Chemicon), human recombinant bone morphogenetic protein (BMP4, 20 ng/mL; R&D Systems), neuronal stem cell supplement (1:50, PAA), Glutamax (1:100, Invitrogen) and penicillin/streptomycin (1:100, PAA), leading to the generation of a highly enriched population of progenitor-derived type I astrocytes after 8 passages [461].

2.1.3. Preparation of hNP-AC Extracellular Matrix (hNP-AC-ECM)

hNP-AC cultures were seeded onto PLL/laminin coated 24-well plates and maintained in NPDM. At 1 week after reaching confluency, cells were lysed by incubation in distilled water for 30 min at 37°C. The excess cell debris was removed by washing the substrate several times in 0.1M phosphate buffered saline (PBS); the remaining ECM substrate was stored in PBS at 4°C and used within 2 days of preparation [287].

2.1.4. Preparation of hNP-AC Conditioned Media (hNP-AC-CM)

hNP-AC cultures were grown to confluence in 12-well plates and fed with fresh dorsal root ganglia medium (DRGM) composed of Neurobasal A supplemented with B27 (1:50 Invitrogen), Glutamax (1:100 Invitrogen), 10% fetal bovine serum (FBS, PAA), and penicillin/streptomycin (1:100 PAA). After 3 days conditioning, the medium was removed from the cultures and mixed 1:1 with fresh DRGM prior to being given to the cultured DRG neurons.

2.1.5. Human Foreskin Fibroblasts (hFbl)

Purified hFbl were used a control cell type for the *in vivo* investigations. They were donated following informed consent following approval of the local ethics committee of the University of Montpellier. Fibroblasts were cultured on normal tissue culture plastic in DMEM/F12 containing 10% FBS and penicillin/streptomycin (1:100 PAA).

2.1.6. Cell Counting

To estimate the proportion of undifferentiated or differentiated hNPC that were immunoreactive for a particular antigen, cell numbers were quantified by counting at least 9 non-overlapping, randomly chosen, microscopic fields (200x magnification, area of interest: 280 μm x 212 μm) from three independent experiments.

2.1.7. Fixation

For Fluorescence microscopy, samples were exposed to cold 4% paraformaldehyde (PFA, AppliChem) and allowed to fix at room temperature (RT) for 30 min. For scanning electron microscopy, samples were exposed to 2.5% glutaraldehyde for 2 h. .

2.2. Immunohistochemistry

After fixation, samples were processed for immunocytochemical staining as described previously [137, 159]. Primary antibodies were diluted in 0.1 M PBS with 1% BSA and 3% normal goat serum (NGtS, Sigma-Aldrich) and incubated with the preparations overnight at room temperature. The following polyclonal antibodies were used: anti-fibronectin (1:500, DAKO), anti-glial fibrilary acidic protein (GFAP, 1:2000, DAKO, Hamburg, Germany), anti-Iba1 (1:1000, Wako), anti-laminin (1:200, Sigma-Aldrich), anti-Musashi (1:2000, Millipore), anti-nestin (1:500, Millipore), anti-neurofilament (1:2000, Sigma-Aldrich), anti-p75 (1:1000, Sigma-Aldrich), anti-S100ß (1:2000, DAKO) and anti-sox2 (1:2000, Millipore) as well as the following monoclonal antibodies: anti-A2B5 (1:200, Millipore), anti-CD44 (1:200, Sigma-Aldrich), anti-CSPG (1:200, Sigma-Aldrich), anti-ED1 (1:500, Santa Cruz), anti-human nestin (1:200, Millipore), anti-human nuclei (1:200, Millipore), anti-Map2a+b (1:500, Sigma-Aldrich), anti-neurofilament 200kDa (1:2000, Sigma-Aldrich), anti-04 (1:200, Millipore), anti-p75 (1:1000, Millipore), anti-TuJ1 (1:500, Sigma-Aldrich) and anti-vimentin (1:10.000, Sigma-Aldrich). Primary antibodies were detected by a combination of secondary antibodies for 2.5h at RT: Alexa Fluor© 488 goat anti-rabbit IgG (1:500, Invitrogen), Alexa Fluor© 488 goat anti-mouse IgG (1:500, Invitrogen), Alexa Fluor© 594 goat anti-rabbit IgG (1:500, Invitrogen) and Alexa Fluor© 594 goat anti-mouse IgG (1:500, Invitrogen)

diluted in 0.1 M PBS with 1% BSA. Cell nuclei were counterstained with 4,6-diamidino-2-phenylindole dihydrochloride (DAPI; 1 μg/ml, Invitrogen). For a complete overview of all antibodies/counterstains used, see Table 2.1. Coverslips were then mounted onto the samples using Fluoroprep (BioMerieux, Nürtingen, Germany) and, unless otherwise mentioned, samples were visualized using an inverted Zeiss Axioplan/Apotome fluorescence microscope coupled to an on-line digital camera (Axiovision software) for evaluation of the dissociated DRG and spinal cord sections, or an inverted Leica fluorescence microscope coupled to an on-line digital camera (Discus, Leica software) for evaluation of hNPC, hNP-AC and the scaffold preparations.

Table 2.1.: Antibodies

Monoclonal antibodies		
Antibody	*Dilution*	*Supplier*
A2B5, clone A2B5-105	1/200	Millipore (MAB342R)
CD44, clone A3D8	1/200	Sigma-Aldrich (C7923)
CSPG, clone CS-56	1/200	Sigma-Aldrich (C8035)
ED1, CD68	1/500	Santa Cruz (SC-59103)
Human nestin, clone 10C2	1/200	Millipore (MAB5326)
Human nuclei, clone 3E1.3	1/200	Millipore (MAB4383)
Map2a+b, clone AP-20	1/500	Sigma-Aldrich (M1406)
Neurofilament 200kD, clone NE14	1/2000	Sigma-Aldrich (N5389)
O4, clone 81	1/200	Millipore (MAB345)
p75, clone 192	1/1000	Millipore (MAB365)
TuJ1, Clone SDL 3D10	1/500	Sigma-Aldrich (T8660)
Vimentin, clone V9	1/10000	Sigma-Aldrich (V6630)
Polyclonal antibodies		
Antibody	*Dilution*	*Supplier*
Fibronectin	1/2000	DAKO (A0245)
GFAP	1/2000	DAKO (Z0334)
Iba1	1/1000	Wako (019-19741)
Laminin	1/200	Sigma-Aldrich (L9393)
Musashi	1/2000	Millipore (AB5977)
Nestin	1/500	Millipore (AB5922)
Neurofilament	1/2000	Sigma-Aldrich (N4142)
p75	1/1000	Sigma-Aldrich (N3908)
S100ß	1/2000	DAKO (Z0311)
Sox2	1/2000	Millipore (AB5603)
Secondary antibodies / nuclear counter stain		
Antibody	*Dilution*	*Supplier*
Alexa Fluor 488, goat anti-mouse	1/500	Invitrogen (A11029)
Alexa Fluor 488, goat anti-rabbit	1/500	Invitrogen (A11034)
Alexa Fluor 594, goat anti-mouse	1/500	Invitrogen (A11032)
Alexa Fluor 594, goat anti-rabbit	1/500	Invitrogen (A11037)
DAPI (1 μg/ml)	1/1000	Invitrogen (D1306)

2.3. Scanning Electron Microscopy (scanning EM)

Scanning EM was used to visualise the fine details of hNPC and hNP-AC, as well as their interactions with nanofibers and the 3D collagen scaffold. The 2.5% glutaraldehyde-fixed samples were dehydrated in acetone using a Polaron E3000 critical point dryer. The specimens were then mounted on stubs and sputter coated with gold, loaded into an ESEM XL30 FEG scanning electron microscope (Philips EO, Eindhoven, Netherlands) and viewed under an accelerating voltage of 5 kV. In this context, I would like to thank Manfred Bovi (Department of Pathology, UK Aachen) for the excellent technical support with the scanning EM.

2.4. Production of the Orientated Nanofibers

The glass coverslips and orientated nanofibers were kindly provided by José Gerardo-Nava and were prepared as described previously [159]. Experiments were performed on low density fibers.

2.4.1. Glass-Coverslip Preparation

Glass coverslips (12 mm diameter; Marienfeld Lauda-Königshofen, Germany) were surface-functionalized, dried with toluene and placed in a N_2-containing glove box prior to nanofiber collection, as described previously [175]. Within the glove box, 20 mg of star-shaped polyethylene glycol (sPEG, MW 12000 Da) was dissolved in 0.2 ml tetrahydrofuran. Before use, 1.8 ml deionized water was added and the mixture was allowed to partially crosslink for 5 min. The sPEG solution was sterile-filtered (0.2 μm filters) and applied to coverslips by spin-coating, undergoing 5 s of acceleration to 4000 rpm and then maintaining this speed for 40 s. Approximately 30 min was allowed for crosslinking between the sPEG and the activated cover-slips prior to binding with the nanofibers. Poly-L-lysine (100 ng/ml, 1 h) coated coverslips were used as a positive-control substrate.

2.4.2. Electrospinning of Oriented Nanofibers

Pure PCL (Sigma-Aldrich, MW 65000 Da), dissolved in chloroform/methanol (75:25 vol%) or a blend of PCL and calf skin type I collagen (Sigma-Aldrich, 75:25 wt%), then dissolved in 1,1,1,3,3,3-hexafluoro-2-propanol (Sigma-Aldrich) was prepared as a 9 wt% solution and electrospun as described previously [364]. Electrospun nanofibers were deposited between parallel metal bars (4 cm apart), which were positioned 20 cm from the spinneret and acted as grounded nanofiber collectors. The nanofibers were then collected by passing the sPEG-coated glass coverslips through the array [364].

2.4.3. Seeding of the Orientated Nanofibers

Nanofiber-coated coverslips were placed in four-well plates, sterilized with 70% ethanol (30 min) and washed twice with sterile PBS before cell seeding. hNP-AC cell suspension was prepared in DMEM/F12 (1:1, Invitrogen) with 10% FBS (PAA), penicillin/streptomycin and Glutamax (both 1:100, Invitrogen; 10,000 cells/well). Culture medium was replaced every third to fourth day.

2.4.4. Cell-Adhesion Assay & Cell-Number Counting

The cell-adhesion assay, based on crystal-violet staining 90 min after cell seeding, was performed as described previously [364]. Cell proliferation/survival was determined by counting the number of DAPI-stained cell nuclei that were associated with the PCL or C/PCL nanofiber preparations after 1, 4 and 7 days *in vitro* (DIV). The cell counts were performed in five rectangular fields of 345 x 435 μm (0.15 mm^2) that were selected randomly for each sample.

2.4.5. Process Length

Process lengths of hNP-AC were measured from the edge of the DAPI-labeled cell nucleus to the tip of the cell's longest process. The lengths of the longest 10% of at least 50 randomly chosen processes were measured for each sample.

2.4.6. Cell-Migration Assay

Astrospheres of hNP-AC were used for the migration assay. Migration away from the spheres was assayed on three different substrates: (I) orientated C/PCL nanofibers, (II) PCL nanofibers, and (III) PLL-coated tissue culture plastic which served as a non-oriented adhesion/migration-promoting substrate. Each assay was performed in triplicate, with a total of 12-15 spheres of uniform diameter (242 $\pm$ 18.5 μm) being plated in wells containing the different substrates. After 2 days, the spheres were fixed and processed for immunocytochemistry. Samples were observed and photographed with an inverse microscope (Leica, 10x objective) coupled to an online digital camera (Leica, Diskus software). For quantification, nine spheres from each condition were evaluated. The distance of the 10% farthest migrating DAPI nuclei along the axis of the oriented nanofibers was measured using ImageJ software. For estimation of cell migration on the non-oriented PLL substrate, a line was drawn at random through the centre of the sphere. The farthest 10% migrating cells along this axis was then measured.

2.5. Gene Expression Analysis

RNA was isolated using the RNeasy Mini Kit (Qiagen, Hilden, Germany) according to the manufacturer's protocol. RNA concentrations were measured using a Nanodrop photometer (Nanodrop Technologies, Montchanin, USA). For PCR analysis, 2 μg RNA was reverse transcribed to cDNA with Omniscript Reverse Transcriptase (Qiagen, Hilden, Germany) according to the manufacturer's protocol using oligo-d(T) primers and random hexamers. For amplification of target genes, 0.2 units Taq polymerase (Amersham Biosciences, New York, USA) were used with a standard PCR program (denaturation: 10 sec at 96°C; primer hybridisation: 2 min at various target specific temperatures, see Table 2.2; elongation: 2 min at 72°C). PCR products were analyzed by electrophoresis on a 1.7% agarose gel and visualized with 0.5 μg/ml ethidium bromide. The cDNA from the human astrocytoma cell line (U373) and human leukemia cell line (ThP-1) were used as positive controls. *Evaluation of mRNA expression:* The optical density of the PCR bands were analysed with ImageJ (http://rsbweb.nih.gov/ij/index.html) and calculated as a ratio in relation to the house

keeping gene, GAPDH (internal control).

Table 2.2.: Forward and reverse primer sequences used for the detection of RT-PCR for GFAP, CD44 and GAPDH.

Primer	forward (5´- 3´)	reverse (5´- 3´)	hybridization temperature	cycles	amplicon size (bp)
GFAP	gtg gta ccg ctc caa gtt tgc ag	aat ggt gat ccg gtt ctc ctc	59 °C	40	373
CD44	tgc ttc aat gct tca gct cca cct g	tga ttc aga tcc atg agt ggt atg	64 °C	33	375
GAPDH	tga agg tcg gag tca acg gat ttg gt	cat gtg ggc cat gag gtc cac cac	62 °C	30	983

2.6. Preparation of Adult Rat Dorsal Root Ganglia Neurons

DRG neurons were harvested from adult female Lewis rats (Charles River, Sulzfeld, Germany) as described elsewhere [102, 137]. Briefly, rats were killed by terminal inhalation anaesthesia (Isofluran, Abbott GmbH, Wiesbaden, Germany), DRG rapidly dissected and either used for the generation of neuronal suspensions for 2D tissue cultures or were hemisected and placed on top of cell seeded- or non-seeded (control) collagen scaffolds for 3D tissue cultures. DRG were maintained in DMEM/F12 (1:1) containing Glutamax (1:100), 10% FBS and penicillin/streptomycin (1:100) for 3D experiments. For 2D tissue culture, DRG were dissociated in collagenase (0.8% w/v collagenase CLS I, Biochrom AG, Berlin, Germany) for 2 hours followed by 0.5 ml of 0.25% trypsin (Invitrogen) for 30 min at 37°C. Trypsinisation was stopped by removal of the digestion solution and washing with DRGM. To remove myelin debris and the majority of Schwann cells, the solution was centrifuged (1200 g for 12 min at room temperature) through a freshly prepared Percoll density gradient (GE Healthcare Europe GmbH, Munich). The resulting pellet was resuspended in l ml of DRGM and the viable cells counted in a haemocytometer. Approximately 400-500 neurons were seeded with DRGM on to (A) PLL/laminin (positive control) substrate, (B) PLL/laminin in combination with hNP-AC-CM, (C) confluent layers of hNP-AC or (D) hNP-AC-ECM in 12 mm microwells (Figure 2.1). After 24h the preparations were fixed.

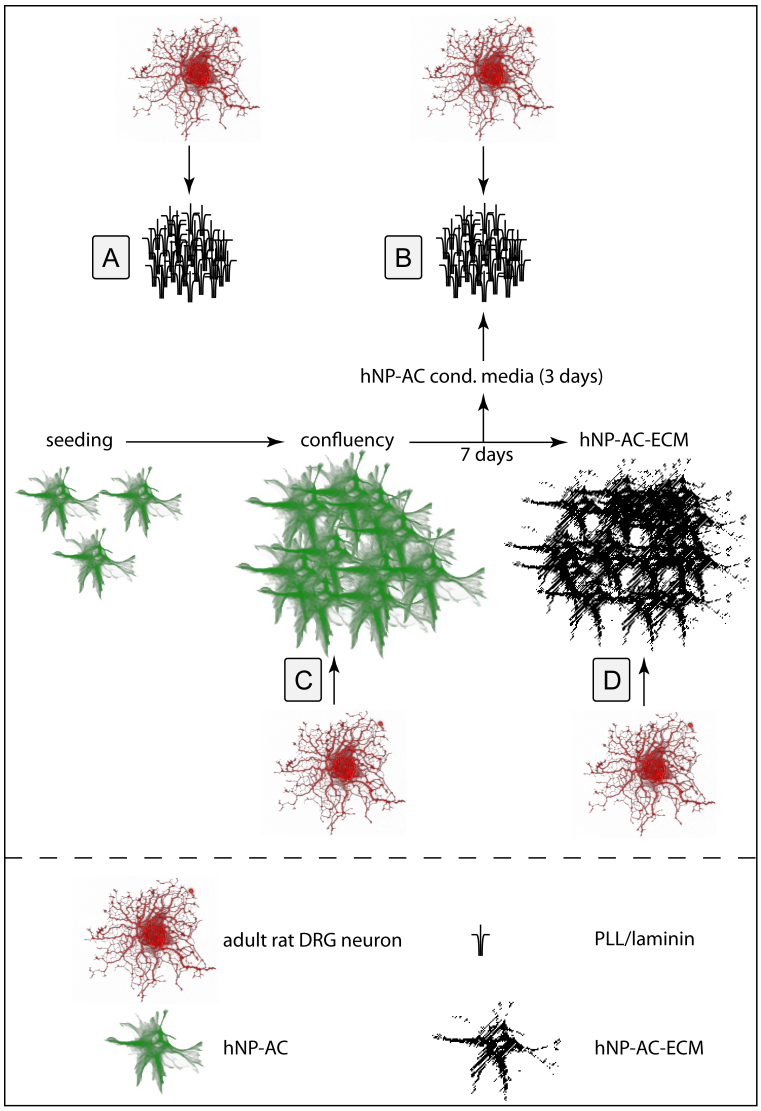

Figure 2.1.: *Schematic diagram of the experimental design for studying the axon growth promoting properties of hNP-AC.* Dissociated DRG neurons were seeded onto PLL/laminin positive-control substrate (A), PLL/laminin with hNP-AC conditioned media (B), hNP-AC confluent monolayers (C) or hNP-AC-ECM (D).

2.7. Evaluation of Axonal Growth on 2D Substrates

All experiments were performed in duplicate and a total of 100 DRG neurons per condition were evaluated. Digital images of MAP2a+b/NF200-positive DRG cell bodies and neurites were acquired for all experimental conditions. *Total neurite length* was measured by manually tracing all processes using Adobe Photoshop, followed by single pixel skeletonisation of the images using ImageJ. The total length of the neurites was estimated by counting the total

number of pixels per neuron. All analyzed data was standardised in relation to the values obtained using the PLL/laminin positive control.

2.8. Orientated 3D Collagen Scaffold

2.8.1. Preparation

The sterile scaffolds (diameter: 5 mm; thickness: 3 mm) used in this study were supplied by Matricel GmbH (OptiMaix-3D, Herzogenrath, Germany). The 3D-collagen scaffolds contain densely packed, longitudinally orientated micropores and were prepared according to the patented directional freezing process, as described previously [50, 245].

2.8.2. Cell Seeding

Scaffolds were seeded by dropping the dry scaffold into a 200 μl cell suspension (*in vitro* studies: hNP-AC: 20,000 cells/μl; *in vivo* studies: hNP-AC: 30,000 cells/μl, hFbl: 20,000 cells/μl). The seeded scaffolds were further processed for cell proliferation and distribution data after 1, 7 and 14 days *in vitro*. Other hNP-AC seeded scaffolds were kept in an incubator overnight prior to having the hemisected DRG placed on their open, porous ends (as described earlier [50]) or prior to transplantation into the injured spinal cord (lateral funicolotomy, see below).

2.8.3. Processing

Scaffolds were fixed and after multiple washes in PBS either frozen and cut on a cryostat (100 μm thick sections for the proliferation assay) or embedded in gelatine for the preparation of thinner (25μm) cryostat sections to assess DRG neurite in-growth. For embedding, samples were incubated in a 5% (w/v) gelatine (Merck), 5% (w/v) sucrose (Merck) solution in 0.1M PBS and kept in a humidified chamber at 45°C overnight. Gelatine was allowed to polymerize the next day, at 4°C, for half an hour and was then frozen at -80°C in isopentane.

2.8.4. Evaluation of Proliferation

DAPI nuclei from fifteen non-overlapping, randomly chosen, microscopic fields (100x magnification) from three sections obtained from three scaffolds were counted to estimate proliferation activity. The doubling time was calculated using the number of DAPI positive nuclei from days 7 and 14.

2.8.5. Evaluation of Axonal Growth on 3D Substrates

For measuring DRG neuritic length through the scaffold, 8-9 hemisected DRG were placed on top of the scaffolds and cultured for 21 days (DRG isolated from 2 animals). Three scaffolds were processed per group for evaluation (i.e. hNP-AC-seeded and control, non-seeded samples). Adjacent serial sections (following the longitudinal axis of the micropores) were collected onto adjacent slides. At least six slides, evenly spaced throughout the scaffolds, were then processed for immunohistochemical demonstration of regenerating axons and the different cell types. All neurite lengths were measured and the figure for the longest 10% calculated.

2.8.6. Evaluation of Schwann Cell Migration

The proportion of migrating p75-positive Schwann cells (expressed as a percentage of the total population of cells within the initial part of the scaffold) was calculated using a series of images taken with 100x magnification (area of interest: 4100 x 850 μm)

2.8.7. Preparation for *in Vivo* Studies

The seeded scaffolds were incubated in growth medium for 1 day to assure cell adhesion to the matrix. Before implantation, the scaffolds were washed in Hank's buffered salt solution (HBSS). Scaffolds were then kept in cooled HBSS and cut into approximately 1-2mm thick slices prior to implantation.

2.9. Animals

Animals were socially housed on sawdust, 4-5 animals/cage, in standard type 4 macrolon cages, with free access to water under a 12:12 h light regime. All procedures involving animals in this study were approved by the responsible ethical committee (Aachen: AZ 50.203.2-Ac 23,11/06, Liège: 814).

2.10. Balloon Compression Injury

These investigations were performed at the Institute for Anatomy, University of Liège. Compression injury was performed as described earlier [443]. Briefly, under isoflurane inhalation anaesthesia, the Th10 vertebra of adult female Wistar rats (body weight approximately 270 g) was exposed and a Fogarty 2F inflatable balloon passed into the epidural space via a small burr hole and gently moved rostrally for approximately 1 cm. The compression injury at level Th8 was caused by inflation of the balloon (15 μl of water for 5 minutes), after which it was deflated and removed. The dura was then closed using 10/0 suture, and the muscle layers closed using resorbable 6/0 suture. The skin was closed using 4/0 sutures and the animals were allowed to recover.

2.10.1. Cell Transplantation

One week post operation, animals were reanaesthetised and the original surgical wound reopened. Small bur-holes were drilled into the vertebral laminae to allow the transplantation of either (I) hNP-AC, or (II) hFbl (as a control cell population). Donor cells were grafted into the lesion epicentre (5 μl) as well as 1 cm rostral and caudal to the injury (2.5 μl each, therefore a total volume of 10 μl at 100,000 cells/μl, Figure 2.2). All transplantation procedures were performed using a glass micropipette under stereotaxic control as described earlier [118]. After the grafting of cells was completed, the muscle layers and skin were again closed using sutures (see above) and the animals received 10 ml of saline, immunosuppression (cyclosporine, methylpredisolone and azathioprine, see below), antibiotics (0.01%

baytril) and were allowed to recover. Non-implanted controls groups included lesioned animals without- or with immunosuppression (i.e. control group (III) and control + IS group (IV), respectively). Those animals only received the initial lesion with no further surgical intervention. Animals were sacrificed 9 weeks after injury. Animals that were not correctly lesioned (based on BBB score 1 day postoperative) were excluded from the study.

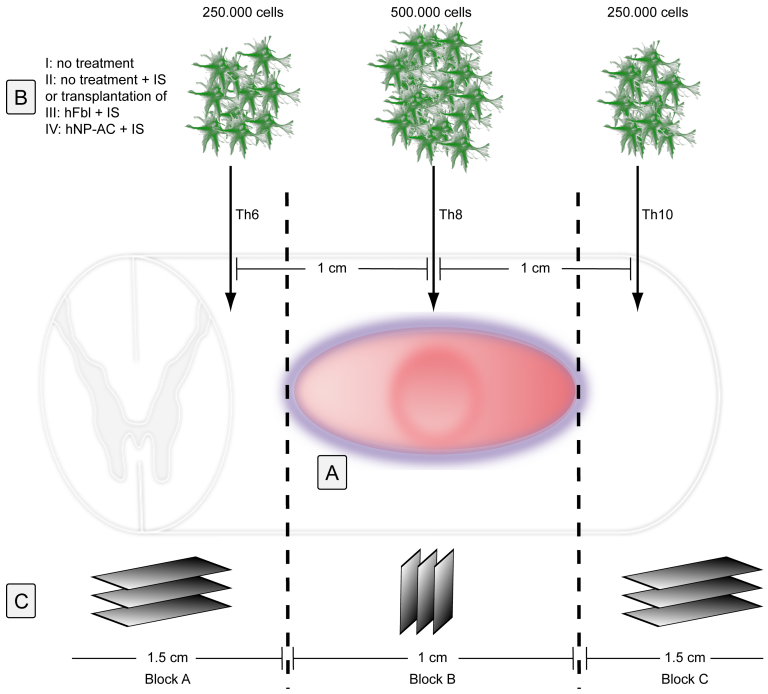

Figure 2.2.: *Schematic diagram of the experimental design for the balloon compression injury model.* The spinal cord was compressed (A) and left either untreated without (B-I) or with (B-II) immunosuppression (IS), or animals received transplants of hFbl (B-III) or hNP-AC (B-IV) one week after injury. Nine weeks after injury, animals were transcardially perfused with 4% PFA, the spinal cords removed, divided into three blocks and processed for serial longitudinal (block A and block C) or transverse (block B) cryosectioning.

2.11. Lateral Funiculotomy

Adult female Lewis rats (age $>$ 3 month) were used for this *in vivo* study (mean body weight 200 g; range 178-227 g). The low thoracical lateral funiculotomy (Th10) was performed as described earlier for the cervical area [269]. Under isoflurane inhalation anaesthesia, the back was shaved and the skin sterilized with 70% alcohol prior to incision along the midline, exposing the back musculature. Using blunt dissection, the superficial muscle layers were cleared from the deeper layers, a midline incision was made and the superficial and deep

muscle layers retracted to expose the dorsal surface of the Th9 - Th12 vertebrae. Fine bone rongeurs were used to perform a laminectomy of the Th10 and the Th11 vertebra, exposing the dorsal surface of the spinal cord. The dura was cut and reflected, after which a simple lateral funiculotomy involving the resection of 1-2 mm lateral spinal cord tissue was performed. The animals then received scaffold implants as follows: (A) non-seeded with IS, (B) hFbl-seeded with IS, or (C) hNP-AC-seeded with IS (Figure 2.3). The dura was then closed using 10/0 suture, and the muscle layers closed using resorbable 6/0 suture. The skin was closed using 4/0 sutures. After the operation, animals received 10 ml of saline, immunosuppression (cyclosporine, methylpredisolone and azathioprine, see below) and antibiotics (0.01% baytril) and were allowed to recover. The following day, the vast majority of the animals moved freely in their cage, fed and drank without any indication of pain or discomfort. While bladder dysfunction lasted - usually for not more than 7 days - the bladders were manually voided. Animals were sacrificed 8 weeks after injury.

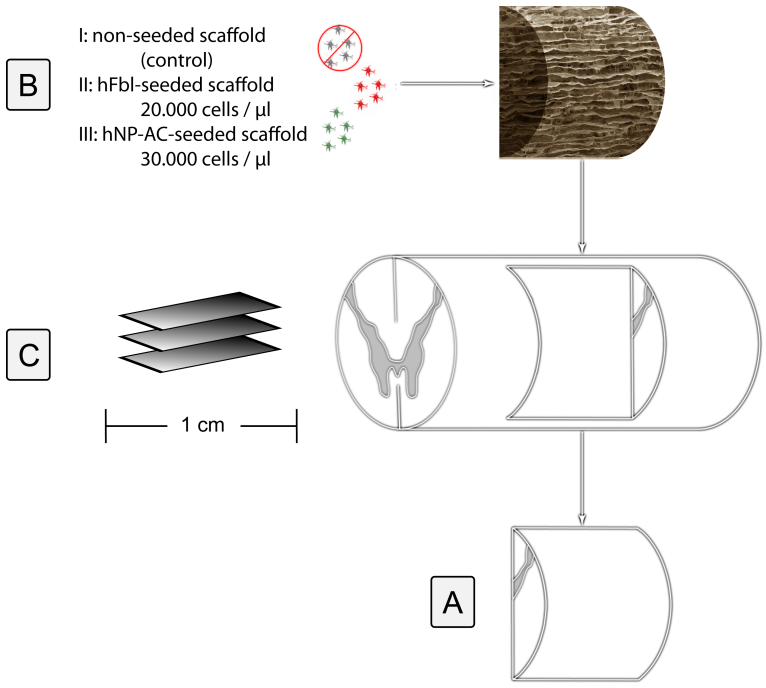

Figure 2.3.: *Schematic diagram of the experimental design for the lateral funiculotomy.* Part of the lateral white matter tract was resected (A) and substituted by a non-seeded scaffold (control, B-I), a hFbl-seeded scaffold (B-II) or a hNP-AC-seeded scaffold (B-III). Eight weeks after injury, animals were transcardially perfused with 4% PFA, the spinal cords removed and a 1 cm block containing the scaffold was processed for serial longitudinal cryosectioning (C).

2.12. Immunosuppression

The lesioned animals receiving cell transplants as well as those controls receiving immunosuppression were administered intraperitoneal (i.p.) injections of a combination of cyclosporine A (Novartis), azathioprine (GlaxoSmithKline) and methylpredisolone (Sanofi Aventis) in the following concentrations: 10 mg/kg cyclosporine starting from one day before transplantation (lateral funiculotomy injury model) / injury (compression injury model) and every day until animals were sacrificed, 4 mg/kg azathioprine starting on the day before transplantation as well as on the day of transplantation (subsequent daily injections included azathioprine at 2 mg/kg), 2 mg/kg methylpredisolone for one week starting at the day of transplantation, for the second week the dose was reduced to 1 mg/kg after which all remaining daily injections contained methylpredisolone at 0.5 mg/kg [5, 34, 204, 255, 318, 335].

2.13. Behavioural Analyses

2.13.1. Behavioural Studies for Animal Groups Subjected to Balloon Compression

These investigations were performed at the Institute for Anatomy, University of Liège, and were subject to the local ethics committee permission. The "Basso, Beattie, Bresnahan or BBB open field" locomotor rating scale was used to assess general locomotor performance [30]. In addition, fine motor coordination was assessed using a horizontal wire grid (Gridwalk, 50-cm long runway grid with 50 X 50 mm spacings, Table 2.3) [247], and a commercially available "plantar test" apparatus was used to assess sensitivity of the plantar hind-paws to a brief noxious heat stimulus in unrestrained rats (Hargreaves heat test [183]). The different test scores were assessed before injury and at 5 and 9 weeks post injury by 2 observers.

Table 2.3.: Gridwalk test score

0	No foot placement
1	Attempted foot placement, but grid is missed
2	Foot is occasionally placed on the grid, but slips
3	Foot is placed, but slips
4	Foot is placed, but does not grip the grid, many footfalls
5	Foot is placed and the grids are gripped, few footfalls

2.13.2. Behavioural Studies for Animal Groups Subjected to Lateral Funiculotomy

Function was assessed before injury and at 4 and 8 weeks after injury using the CatWalk gait analysis system, a gridwalk test and a sensory function test (von Frey filament test). CatWalk data could be acquired only after the animals regained body weight supporting stepping (BBB 11 or higher). Most animals achieved this level of recovery by one one week after injury, but some required a longer recovery time of up to three weeks.

CatWalk

The analysis of gait using the CatWalk system and the required training protocol has been described in detail elsewhere [181, 241, 449]. Briefly, during a 2-3 week-period in which a 12 g/day food restriction protocol was used (to provide for motivation), the animals were trained to make consecutive runs (without any stops or hesitation) over a glass runway. Each run made by the animals was rewarded by receiving foot pellets (Noyes Precision pellets PJPPP-0045; Sandown Chemical Ltd., Hempaton, UK) which were placed at the end of the runway. For correct locomotor analysis, the following criteria concerning walkway crossing were used: (1) the rat needed to cross the walkway, without any interruption or hesitation, and (2) a minimum of three correct crossings per animal were required (eight were usually recorded). For reliable comparison between the gait parameters of animals in the different groups it is of utmost importance that there is no difference in speed of gait [241]. This could be controlled by monitoring the time taken to cross the walkway. For this purpose, the 3 crossings closest to 1.4 seconds were chosen. In the present study, all individual crossings were analyzed for the duration of walkway crossing, the regularity index, base of support (for the fore- and hind-limbs), intensity of signal on paw placement, paw print area and maximum area, stance duration, swing duration, stride length and duty cycle (hind limbs).

Values for the duty cycle (stance duration divided by the sum of stance and swing duration), stride length, stance duration, swing duration, max area, print area and intensity were always calculated as the ratio of the ipsilateral (i.e. affected) side to the contralateral (i.e. unaffected, control) side and standardised in relation to the preoperative values.

Gridwalk

Fine motor coordination was assessed using a horizontal wire grid (50-cm long runway grid with 50 X 50 mm spacings) [247]. Animals were trained for 1-2 weeks until they were able to cross the grid without any interruption or hesitation to reach their food pellet rewards. A minimum of four correct crossings were performed and recorded using a digital video camera (Sony). Those videos were then used for slow motion replays to allow the quantification of the number of footfalls made.

Von Frey Filaments

Paw withdrawal in response to a mechanical stimulation to the plantar surface was determined using a series of von Frey filaments (Stoelting, Wood Dale, IL), which were graded from 1.08 to 21.09 g. For this test, animals were placed in a perspex box containing a metal mesh floor, where they were allowed to get accustomed to their surroundings for approximately 15 min prior to testing (by which time cage exploration and major grooming activities had ceased). Von Frey filaments were then applied to the mid-plantar surface of all four paws through the wire mesh floor. Probing was only performed when the animal's paw was in contact with the floor. Each probe was applied to the foot until the filament bent, and was kept in this position for 6-8 s [75]. The time interval between consecutive filament tests was at least 5 s. The 50% withdrawal threshold was determined using the up-down method of Dixon [75, 108]. In this paradigm, testing was initiated with the 2.0 g filament (i.e. the filament in the middle of the series). Stimuli were always presented in a consecutive fashion, whether ascending or descending. In the absence of a paw withdrawal response to the initially selected filament, the next strongest filament was presented; in the event of paw withdrawal, the next weakest filament in the series was chosen. The first paw withdrawal response was selected as the second response in one series. Four additional responses, either up or down, based on the rat's respone completed the series (in total six responses, all close to the 50% threshold).

2.14. Tissue Fixation and Processing:

Animals in experimental groups were terminally anaesthetized and transcardially perfused either 8 or 9 weeks after injury (for the lateral funiculotomy- and balloon compression models respectively) with 4% PFA (pH 7.4). For a list of animal numbers per experimental group, see Table 2.4. The spinal cords were removed, post-fixed, cryoprotected with 30% sucrose and, for tissues obtained from the lateral funiculotomy lesion model (e.g. Figure 2.3), were processed for serial longitudinal cryosectioning (section thickness, 20 μm). Sections were collected onto 15 adjacent slides such that the effective interval between neighbouring sections on the same slide was 300 μm. For tissue obtained from the balloon compression injury model, the spinal cord was divided into three blocks. Blocks A and C contained the transplant areas caudal and rostral to the lesion epicentre (block lengths: 1.5 cm, Figure 2.2) and block B contained the lesion site itself (block length 1 cm, Figure 2.2). Block B was processed for serial transverse crysoectioning (section thickness, 20 μm), every fifth section was collected onto 20 adjacent slides such that the effective interval between neighbouring sections on the same slide was 2000 μm. A sample series, composed of each 4th slide was stained with thionin (a form of Nissl stain) and were then used for morphometric analysis. In total, twenty-five thionin stained sections per animal (with a spatial sampling interval of 400 μm) were used to assess the amount of tissue sparing. The section with the least amount of tissue sparing was considered to be the epicenter of the lesion. Block A and C were processed for serial longitudinal cryosectioning (section thickness, 20 μm). Serial sections were collected on 20 adjacent slides such that the effective interval between neighbouring sections on the same slide was 400 μm. Two different slides (representating a total of 8 sections equally distributed throughout the spinal cord) were processed for double immunofluorescence using a range of different primary antibody combinations.

Table 2.4.: List of animal numbers used in each experimental group.

Lateral funiculotomy lesion model plus implantation strategy	**N**	**Balloon compression injury model**	**N**
		Lesion only (control group)	8
Lesion + empty scaffold implantation + IS (control group)	9	Lesion + IS (control group)	8
Lesion + hFbl seeded scaffold + IS (control group)	10	Lesion + hFbl implantation + IS (control group)	7
Lesion + hNP-AC seeded scaffold + IS (test group)	11	Lesion + hNP-AC implantation + IS (test group)	8

2.15. Morphological Investigations

2.15.1. Axon Regenerating/Axonal Sparings

In the compression injury model, the amount of regenerated and/or spared nerve fibers was estimated by counting the number of NF200-positive pixel in three randomly chosen images/section (400x magnification, area of interest: 222 μm x 166 μm, Figure 2.4A). To assess the amount of axonal regeneration into the implanted scaffold, the number of NF200-positive axons crossing 3 virtual lines within the scaffold were counted. These lines were drawn 100 μm from the rostral and caudal graft-host interface and also at the mid-point of the scaffold (Figure 2.5A).

2.15.2. Schwann Cell Migration

In the compression injury model, the extent of Schwann cell migration was estimated by counting the number of p75-positive pixels within three randomly chosen images/section (400x magnification, 222 μm x 166 μm, Figure 2.4B). Only limited migration of p75-positive Schwann cells was observed following lateral funiculotomy and implantation of the collagen scaffold, therefore quantitative evaluation was omitted.

2.15.3. Inflammatory Response

To assess the inflammatory response in the compression injury model, three randomly chosen images/section were processed for Iba1-immunohistochemistry (e.g. Figure 2.4D). To assess the extent of the inflammatory response to the implanted scaffold and/or cells, four images

per antibody were chosen to represent the events at the rostral, caudal and lateral interfaces, as well as within the centre of the scaffold (400x magnification, area of interest: 222 μm x 166 μm; e.g. Figure 2.5B). The inflammatory response to scaffold implantation was assessed using ED1- and Iba1-immunohistochemistry. The intensity (i.e. mean grey value) of the immunoreactivity was assessed in images that were captured using the same exposure time using ImageJ. Data was standardised to the maximal possible mean grey value (i.e. value of a completely white image).

2.15.4. Reactive Gliosis/CSPG Immunoreactivity

To assess the extent of reactive gliosis and CSPG deposition, immunostained sections were photographed as described above for the inflammatory response (400x magnification, area of interest: 222 μm x 166 μm for the compression injury model and area of interest: 116 μm x 105 μm for the scaffold implantation strategy; Figure 2.4C and Figure 2.5C respectively). The intensity of GFAP- and CSPG-(CS-56)-immunoreactivity was measured as described above. For the comparison of the immunohistochemistry for particular antigens, the staining procedure for all relevant samples were processed at the same time.

2.15.5. Survival of Transplanted Cells

Survival of transplanted cells was estimated by counting the number of animals with cells that could be identified by immunohistochemistry for species specific antigens, e.g. antibodies against human nuclei (i.e. for hFbl and hNP-AC) and human nestin (i.e. for hNP-AC).

2.15.6. Spared Tissue

Thionin staining was performed to enable (1) the identification of white matter and grey matter in the spinal cord at low magnification, and (2) a clear discrimination between the spared tissue and newly formed connective and vascular scar tissue following compression injury. For morphometry, sections were captured by digital camera, and high-resolution images were used to trace the areas of spared grey matter and white matter, respectively. The identified areas in individual sections were measured using image analysis software (GIMP). The graphical presentation of this data resulted in a U-shaped curve, and the

center of the lesion was defined as a level at which the 2 halves of the U-shaped curve could be most evenly divided.

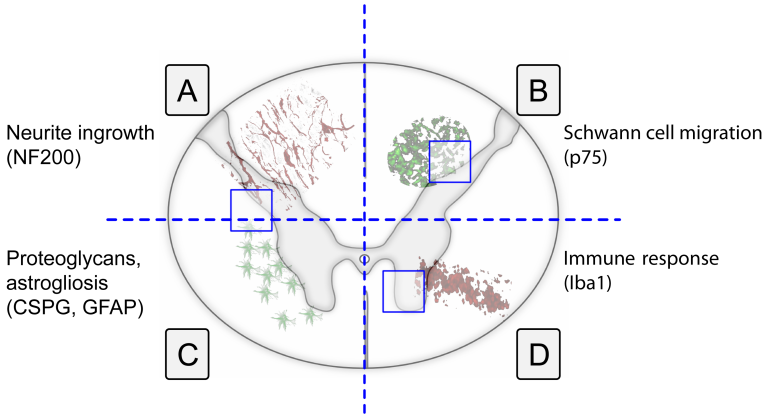

Figure 2.4.: *Schematic diagram of the evaluation of block B in the balloon compression injury model.* To estimate the amount of neurite ingrowth, Schwann cell migration, inflammatory response, gliosis and CPSG deposition three images for each antibody were taken randomly (blue boxes). For an estimation of the neurite ingrowth into the lesion site, the number of pixels relating to NF200-positive axons were counted (A). P75-positive Schwann cell migration was evaluated in the same manner (B). CSPG, GFAP (C) and Iba1 (D) immunoreactivity were estimated by measuring the intensity of the immunofluorescence.

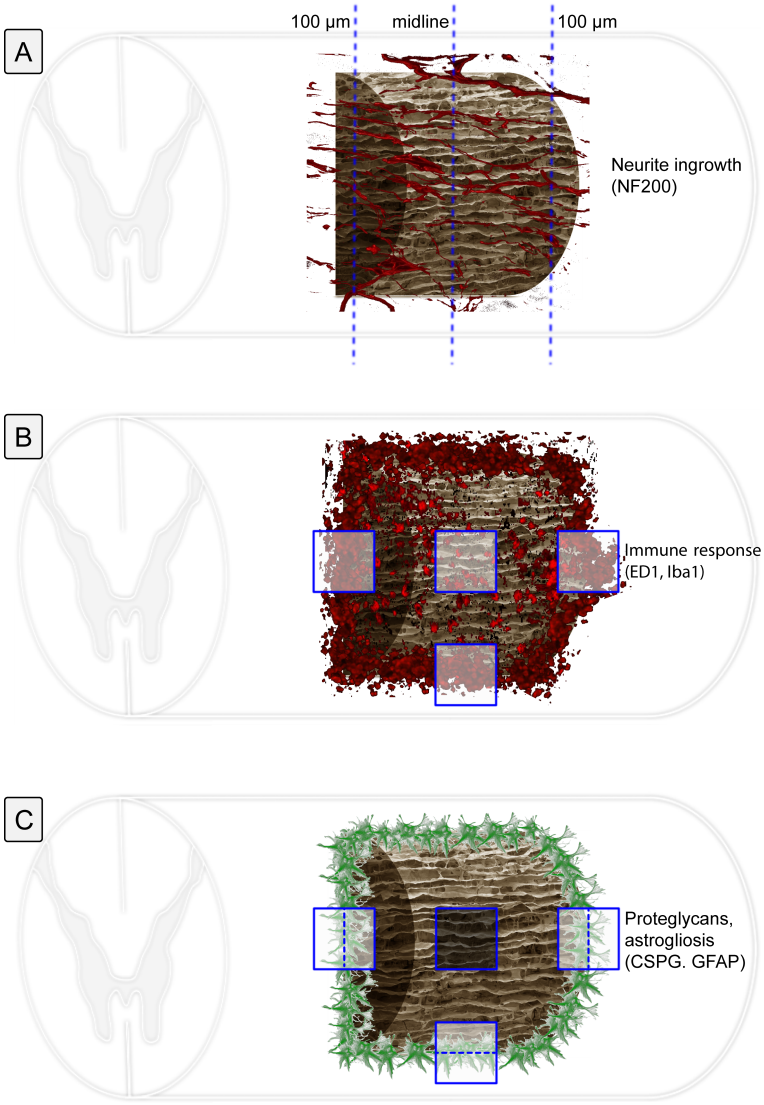

Figure 2.5.: *Schematic diagram of the morphometric evaluation of graft-host interactions after the lateral funiculotomy and scaffold implantation.* For an estimation of the neurite ingrowth into the scaffold after injury, all NF200-positive fibers crossing the three individual lines (dotted, blue lines) were counted (A). The inflammatory response was assessed by taking four different images at the indicated locations (blue boxes) for ED1 and Iba1 stained sections (B). CSPG and GFAP expression was also measured using a similar protocol to that used for the inflammatory response. For this purpose the line of GFAP-positive cells followed the midline of the images (dotted line, except for the dark shadowed middle box, C).

2.16. Statistical Analysis

Data are plotted as mean ± standard error of the mean (SEM). Data was subjected to an analysis of variance (ANOVA) followed by a Bonferroni's test for multiple comparisons between pairs of means (for the *in vitro* investigations) or followed by a Dunnett's test for comparisons between means (for the *in vivo* investigations). p values of < 0.05 were regarded as significant (i.e * $p < 0.05$, ** $p < 0.01$, *** $p < 0.001$). All tests were performed using statistical software GraphPad Prism version 4.0.

3. Cell Characterisation, Cell-Cell and Cell-Substrate Interactions

3.1. Introduction

Attempts to bridge the axon growth-inhibitory environment of the lesioned adult mammalian spinal cord have included the implantation of oriented growth-promoting tissues (e.g. peripheral nerve) and, more recently, various biomaterials including oriented structures that are capable of supporting directional axon regeneration and tissue repair (reviewed in [14, 97, 308, 363, 480]). Attempts to design the ideal scaffold for such bridging strategies have prompted numerous investigations of cell-substrate interactions. The influence of substrate topography and chemical composition on cell form and function has thus become a subject of increasing interest in the field of tissue engineering research [77, 78, 107, 384, 385, 480]. The size and shape of 2D substrates coated with purified extracellular matrix (ECM) molecules clearly influence the fate and function of adherent cells; for example, relatively large islands of ECM have been reported to promote proliferation while, in stark contrast, small islands induce apoptosis [77, 78, 384]. Furthermore, vascular endothelium cell-cell interactions have been demonstrated to be critically dependent on the width of ECM substrate stripes: 50-100 μm wide stripes only resulted in cell proliferation, while 30 μm wide stripes supported cell-cell interactions that resulted in the formation of tubular (capillary-like) structures [107]. Other studies have shown that aligned ECM, as well as the micron-scale topography of fibres or grooves, exert substantial effects on the guidance and orientation of neural cells and their processes [50, 51, 159, 266, 289, 364, 462]. This is of particular interest in the development of biomaterial-based scaffolds intended to promote the repair of nervous tissues which are endowed with their own highly orchestrated and longitudinally oriented topographies, such

as nerves of the peripheral nervous system (PNS) or white-matter tracts of the central nervous system (CNS) [35, 276, 360, 407, 408]. *In vitro* studies have demonstrated the influence of fibre diameter on the orientation of process outgrowth. The greater surface curvature of small-diameter fibres prompted an increasing tendency for neurite outgrowth to follow the longitudinal axis of the fibres: small-calibre fibres (5-30 μm diameters) promoted much greater oriented process growth than large-calibre fibres (up to 500 μm diameter). It is believed that this phenomenon is not due to chemotropism but rather to the topographical effect of the fibre on neurite growth [386, 387]. Recent advances in nanotechnology and a renewed focus on electrospinning has led to an interest in cell interactions with substrates in the sub-micron range [364]. The ability of fibres with diameters in the sub-micron range to affect the behaviour of non-neural cells [290, 406, 483] as well as neural cells of the PNS has been demonstrated in *in vitro* assays [47, 86, 364]. Oriented fibres promoted longer axonal extension than non-oriented fibres but fibre composition also has a role; functionalization of polycaprolactone (PCL) fibre surfaces with type I collagen (C/PCL) or with the peptide sequence GRGDS supported improved glial attachment, proliferation, migration, process extension and an enhanced rate of axonal growth [47, 86, 87, 364]. Collagens are among the most popular materials in bioengineering, being used for soft- and hard-tissue (e.g. bone) reconstruction [346]. Biomaterials made from collagen have, until recently, offered a number of advantages over many synthetic polymers, including biocompatibility, non-toxic degradation products, and the induction of minimal foreign body responses [354, 355]. Collagen is also amenable to controlled manipulation of its shape, microstructure, and stability including the possibility to prepare 3D constructs [13, 84, 211]. The recent advances in surface modification of electrospun substrates have resulted in many of the above mentioned advantages also being applicable to synthetic polymer nanofibres [169]

Investigations of biomaterials in the context of regenerative medicine and nerve repair have recently expanded to include the seeding of 3D scaffolds with neural progenitor cells (or their derivatives) as a means of promoting optimal cell survival, integration and regeneration, e.g. [327]. Such studies have made it increasingly clear that a better understanding of cell-substrate interactions, as well as cell-cell interactions within 3D scaffolds, is required for the optimal design of biomaterial-based scaffolds and tissue engineering strategies intended to promote functional repair. Although the potential benefits of implanting neural

progenitor-derived type I rat astrocytes into experimental models of spinal cord injury have been demonstrated [99], the axon growth promoting effects of the equivalent human cells, alone or in combination with bio-engineered 3D scaffolds remain poorly defined, and in some aspects are completely unknown. It is possible that the influence of scaffolds on the interactions of (donor) neural progenitor-derived astrocytes with other populations of (host) cells may have important consequences on the extent of graft-host integration as well as the development of scarring or barrier-forming tissues around the implant.

Schwann cells and astrocytes occupy mutually exclusive territories within the nervous system, being located in the PNS and CNS respectively. The only point where they come into close contact with each other, in normal development, is in dorsal and ventral roots, at the transitional zone where the spinal nerve roots enter the brain stem and spinal cord [147, 148]. A boundary forms at such transitional zones between the PNS Schwann cells and CNS astrocytes and these boundaries have been identified as natural barriers to cell migration and axon regeneration, e.g. [73, 162, 270]. The formation of similar boundaries has also been described following the implantation of peripheral nerve segments into the CNS [98, 383, 470]. The cell-cell interactions that are pivotal to the establishment of such boundaries include Schwann cell - astrocyte and fibroblast - astrocyte interactions, both of which have been modelled in relatively simple 2D *in vitro* confrontation experiments [2–4, 459, 464]. Although bioengineered 3D scaffolds intended for PNS or CNS repair will ultimately host the infiltration and migration of a number of different cell types following implantation into the recipient, the possible influence of scaffold topography on the ensuing cell-cell interactions remains obscure.

The present *in vitro* investigation includes a study of the growth promoting properties of hNP-AC in a simple 2D culture system. Astroglial interactions with electrospun PCL and C/PCL fibres (i.e. adhesion, morphology, proliferation and migration) were also studied. Although morphology and alignment of human astrocytes were clearly influenced by their interactions with both fibre-types, the functionalisation of the surface of the nanofibres by incorporation of type I collagen significantly improved the extent of cell migration by hNP-AC. Furthermore the axon growth promoting effects of hNP-AC were investigated in more complex 3D culture systems. The influence of a micro-structured, 3D collagen scaffold on cell-cell interactions between the seeded hNP-AC and migrating Schwann cells/fibroblasts

was also studied, revealing an interesting and possibly novel aspect in cell-substrate biology.

3.2. Results

3.2.1. Cell Characterisation

Characterisation of hNPC

The hNPC were grown as neurospheres which, by scanning EM, appeared as large, tightly bound clusters of cells with heterogeneous morphologies: small diameter, rounded cells being found on the surface of the neurospheres which were otherwise composed of a smoother, more flattened population of cells (Figure 3.1A). Plating of the neurospheres onto PLL/laminin-coated substrates caused rapid adherence, with the flattening of the sphere as cells migrated away in a radial pattern. Scanning EM showed a close relationship between the flattened, (presumably) astrocytic precursors and the migrating, bipolar, spindle-shaped (presumably) neuronal precursors (Figure 3.1B). Immunocytochemistry of these non-differentiated migrating hNPC demonstrated a filamentous cytoskeletal distribution for nestin (91 ± 3% of cells; Figure 3.2A), a diffuse cytoplasmic stain for Musashi (92 ± 2%; Figure 3.2B) and a nuclear distribution for SOX2 immunoreactivity (89 ± 3%; Figure 3.2C). Differentiated hNPC demonstrated a few rounded, multiple process-bearing, O4-positive oligodendrocytes (6 ± 4% of cells; Figure 3.2F), as well as many flattened and process bearing astroglia and glial-restricted progenitors which expressed GFAP- (30 ± 3%; Figure 3.2D), S100β- (66 ± 8%; Figure 3.2E) and A2B5- (12 ± 9%; Figure 3.2D) immunoreactivity respectively, and also bipolar, spindle-shaped, TuJ1-positive neuronal cells (32 ± 4% of cells; Figure 3.2E).

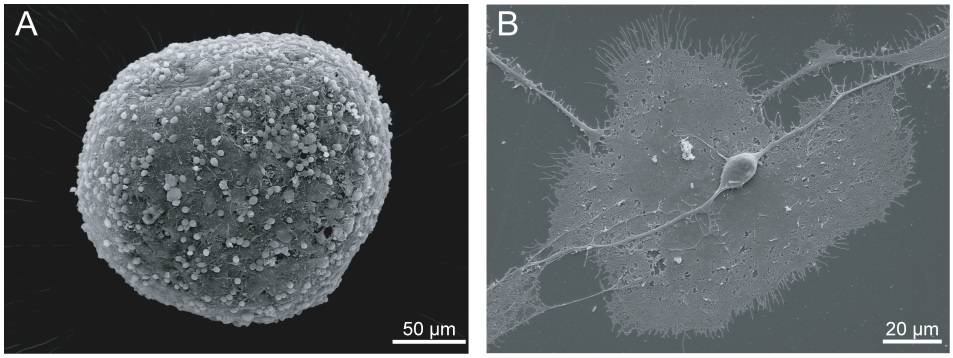

Figure 3.1.: *Scanning electron microscopy of hNPC* **A:** Low magnification image of a neurosphere. **B:** A bipolar cell (likely neuroblast) growing on top a flattened cell (likely astrocytic).

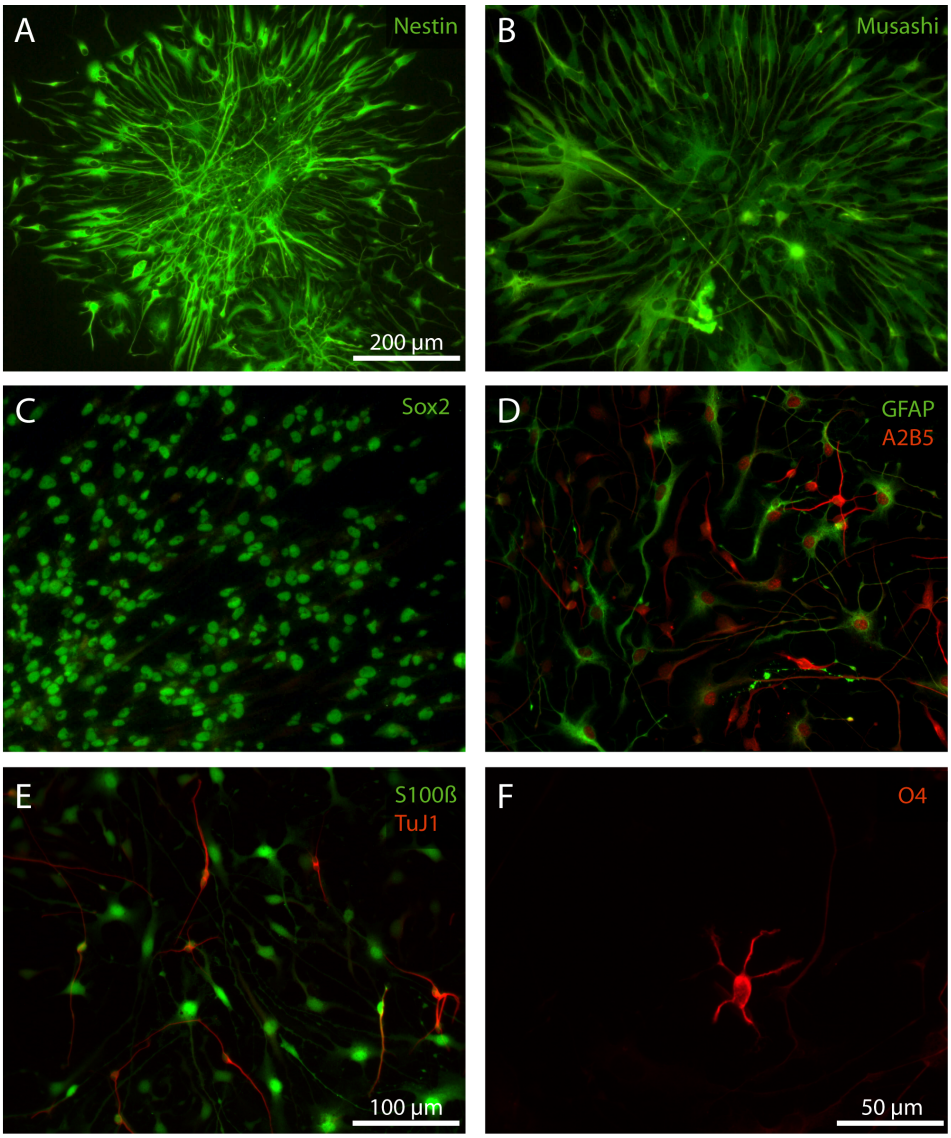

Figure 3.2.: *Stem cell marker expression and differentiation capacity of hNPC.* **A-C:** Characterization of undifferentiated cells plated onto PLL/laminin for 1 day, with antibodies recognising nestin (*A*), Musashi (*B*) and SOX2 (*C*). The expression of these markers shows the progenitor characteristics of these neural cells. **D-E**: Cells grown in differentiation media for 1 week showing immunoreactivity for GFAP (green, *D*) and A2B5 (red, *D*), S100b (green, *E*) and Tuj1 (red, *E*), and O4 (red, *F*). These markers show the potential of the hNPC to differentiate into astrocytes, neurons and oligodendrocytes. Scale bar in E for B-E.

Characterisation of hNP-AC

Plating of the differentiated hNP-AC astrospheres onto a PLL/laminin-coated substrate also caused rapid adhesion and flattening of the sphere with a radial pattern of cell migration. Immunocytochemistry of these differentiated, migrating hNP-AC revealed that they were GFAP- and vimentin-positive (>95% purity; Figure 3.3A-C), as well as CD44-positive

(Figure 3.3A). Only occasional TuJ1- or Map2a+b-positive neurons could be found after incubation in the LIF- and BMP4-containing differentiation medium (arrow; Figure 3.3D). Gene expression analysis: RT-PCR was used to confirm that the LIF/BMP4-mediated differentiation was associated with a significant up-regulation of GFAP- and CD44-mRNA ($p < 0.01$ and $p < 0.001$ respectively; Figure 3.3E, F).

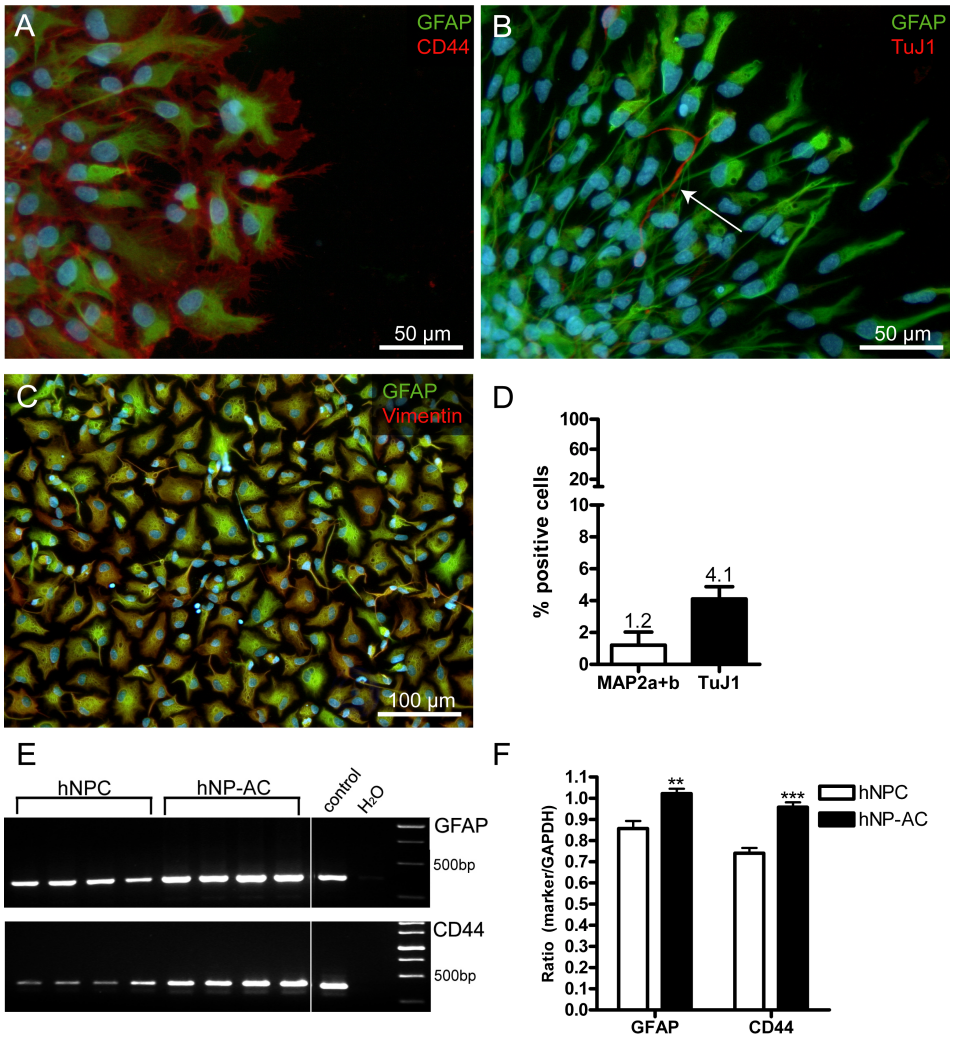

Figure 3.3.: *hNP-AC express GFAP, vimentin and CD44* **A-C:** Immunofluorescence of hNP-AC at passage 3. **A:** Cells are positive for the astroglial marker GFAP (green) and the surface marker CD44 (red). **B:** The vast majority of cells are GFAP (green)-positive astroglia while only occasional cells were positive for the early neuronal marker TuJ1 (red, arrow). **C:** Almost all cells GFAP (green)-positive hNP-AC are also vimentin (red)-positive. The expression of the markers GFAP, vimentin and CD44 together identifies the cells as immature astrocytes. **D:** Histogram showing the estimated purity of the hNP-AC cultures. Only 4.1% and 1.2% of cells stained with the neuronal markers MAP2a+b and TuJ1 respectively (n=9 images). **E:** RT-PCR of hNPC and hNP-AC: Differentiation to hNP-AC is associated with an increased expression of GFAP and CD44 mRNA. **F:** Quantification of CD44 and GFAP up-regulation following hNP-AC differentiation. Values normalised to GAPDH expression (n=4). Data represent means ± SEM, ** $p < 0.01$, *** $p < 0.001$.

3.2.2. Axon Regeneration by Dissociated Adult Rat DRG

Quantification of DRG axon regeneration over 2D hNP-AC substrates: Dissociated DRG were seeded onto PLL/laminin-coated tissue culture plastic and incubated in DRGM as an example of axonal growth on a positive control (i.e. axon growth-promoting) substrate (e.g. Figure 3.4A). DRG outgrowth was also assessed on the PLL/laminin-coated substrate following incubation in hNP-AC conditioned medium (hNP-AC-CM, e.g. Figure 3.4B), as well as on confluent hNP-AC cultures (e.g. Figure 3.4C) and on hNP-AC-derived ECM (e.g. Figure 3.4D). Seeding onto the PLL/laminin, positive control substrate, confirmed the presence of enriched populations of DRG neurons with rounded cell bodies (55±6 μm in diameter) from which multiple regenerating primary neurites grew (e.g. Figure 3.4A-D). There was very little glial contamination of such cultures, as reported by others [102, 366]. The regenerating DRG neurites achieved substantial growth and arborisation patterns within 24 hours, generating a relatively symmetrical halo of NF200/MAP2a+b-positive neurites around a centrally-positioned cell body (Figure 3.4A-D). Quantification of total neurite length revealed that axonal growth over hNP-AC was significantly greater than that seen over the PLL/laminin, positive control substrate ($p < 0.001$; Figure 3.4E, Table 3.1). Similarly strong neurite outgrowth was supported by the hNP-AC-ECM but the greatest overall neuritic extension was seen over the PLL/laminin substrate supported by hNP-AC-CM ($p < 0.001$; Figure 3.4E, Table 3.2). This however, did not reach statistical significance when compared with neuritic growth over the hNP-AC or hNP-AC-ECM ($p > 0.05$; Figure 3.4E, Table 3.1).

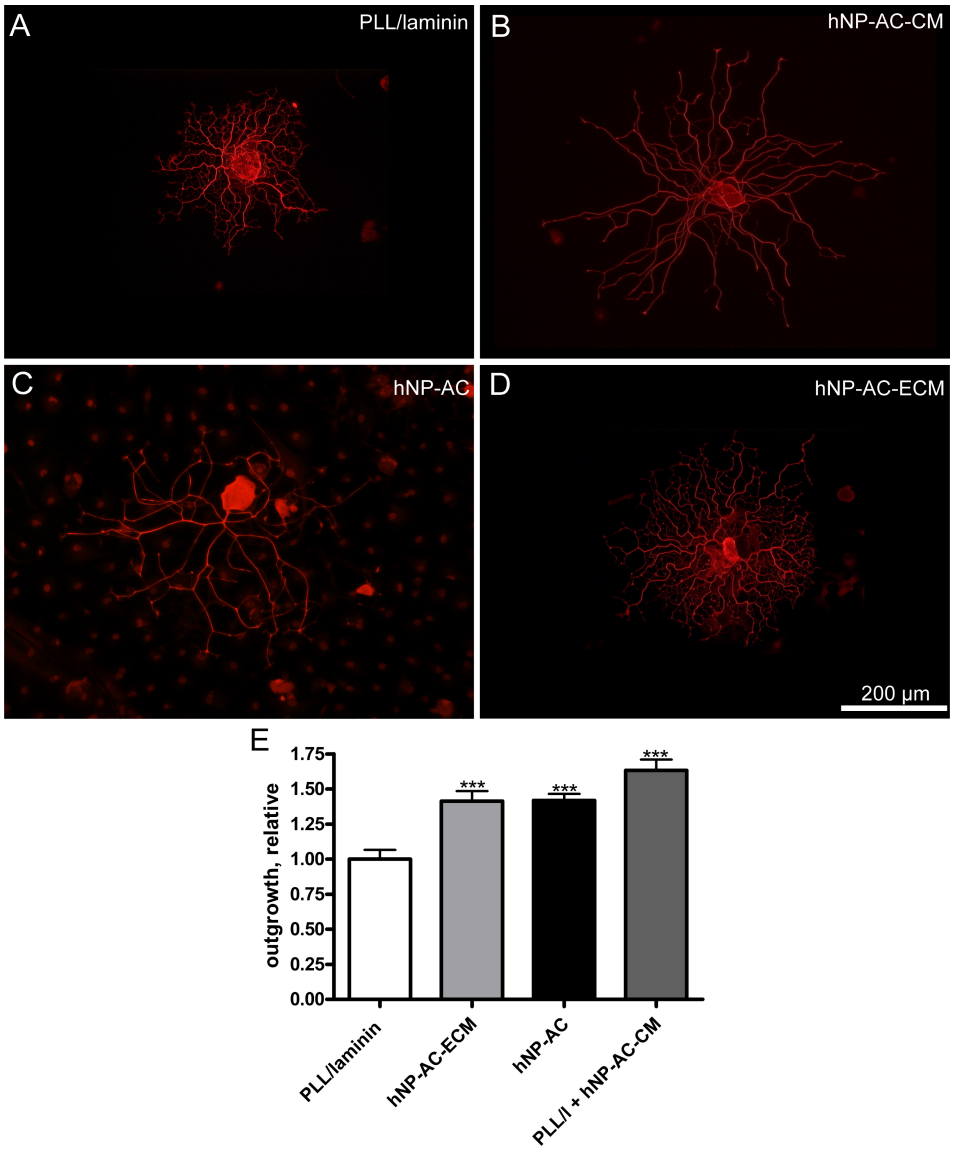

Figure 3.4.: *hNP-AC-ECM as well as the conditioned medium enhance neurite outgrowth.* **A-D:** NF200/MAP2a+b immunoreactive DRG neurite regeneration over PLL/laminin control substrate (*A*), over PLL/laminin plus hNP-AC-CM (*B*), over confluent, viable hNP-AC (*C*), and over hNP-AC-ECM (*D*). **E:** Histogram of the overall neurite outgrowth, standardized to that over the PLL/laminin control substrate. Significantly greater neuritic outgrowth is observed over hNP-AC, hNP-AC-ECM and PLL/laminin plus hNP-AC-CM. Scale bar in D for A-D. Data represent means ± SEM, n=100, *** $p < 0.001$ compared to PLL/laminin positive-control substrate

Table 3.1.: Quantification of the extent of neuritic outgrowth from dissociated DRG neurons over the different substrates.

	PLL/laminin	**hNP-AC**	**hNP-AC-ECM**	**hNP-AC-CM**
Overall neurite outgrowth [μm]	3581±236	5083±174	9206±471	10633±503
standardised	*1±0.07*	*1,419±0.05****	*1,413±0.07****	*1,633±0.08****

3.2.3. Orientated Nanofibres

Scanning EM of oriented PCL & C/PCL nanofibres: Highly oriented PCL or the blended C/PCL nanofibres were prepared by electrospinning and collected onto sPEG-coated glass coverslips. Similar to previous reports [364], the diameter of both types of nanofibre was in the sub-micron range (PCL nanofibres mean diameter ± standard deviation: 564.4 ± 208.8 nm; C/PCL nanofibres: 601.4 ± 151.2 nm) [159]. These fibres were uniform in diameter, highly oriented and could be collected at both high and low density (Figure 3.5). An estimation of the density of nanofibres collected under low density conditions (i.e., short electrospinning times) was obtained by counting the number of fibres crossing a sample line (345 μm in length) drawn perpendicular to the axis of the fibres. Under these conditions, the density of oriented PCL nanofibres was 60 ± 14 fibres/mm (average interfibre distance 16.6 μm) and, for C/PCL fibres, was 57 ± 7 fibres/mm (average interfibre distance of 17.4 μm) [159]. High-density fibres were spun to generate a dense mat of oriented fibres that covered the glass coverslips completely.

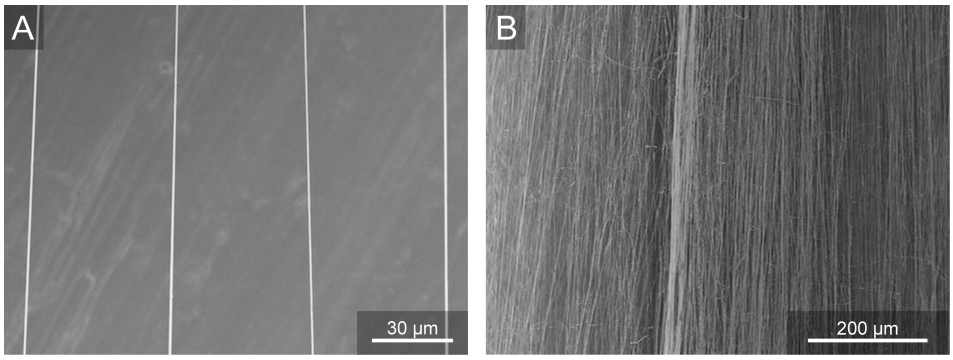

Figure 3.5.: *Scanning electron microscopy of oriented PCL nanofibers.* Electrospun C/PCL fibers are similar and therefore are not shown. **A:** Low density, oriented nanofibers. **B:** High density, oriented nanofibers. Electrospun nanofibers of either polycaprolactone or C/PCL are largely uniform in diameter and unbranched.

Cell Adhesion & Proliferation/Survival

Adhesion and proliferation/survival assays were used to establish the cytocompatibility of the PCL and C/PCL nanofibres. Very few cells bound to the poorly adhesive sPEG substrate (which served as a negative-control substrate). The functionalised C/PCL nanofibres, however, demonstrated a significant improvement in adhesion when compared with the PCL

nanofibres or PLL substrates ($p < 0.05$; Figure 3.6H). As a second measure of the suitability of the nanofibres for CNS-related cell interactions, the survival and proliferation of the cells that were bound to the nanofibres were assessed by comparing the number of bound cells detected at 1, 4 and 7 DIV to the number of cells that were initially seeded. No proliferation of hNP-AC could be detected over 1, 4 and 7 DIV on either PCL or functionalised C/PCL nanofibres. This effect was not brought about by nanofibre-induced cytotoxicity to hNP-AC because both immunocytochemistry and DAPI staining failed to reveal necrotic cells, cellular debris or fragmented nuclei. The only statistically significant increase of hNP-AC numbers was observed on the PLL-substrate between 4 and 7 days post-seeding ($p < 0.05$; Figure 3.6G).

Cell Morphology & Process Length

The morphology of hNP-AC on all substrates was investigated by double immunofluorescence for the cytoskeletal proteins GFAP (green) and vimentin (red; Figure 3.6A-F) as well as by scanning EM (Figure 3.7). hNP-AC grown on the PLL surface adopted a pleiomorphic, "fried-egg"-type morphology with only a small proportion of cells showing clear process formation (Figure 3.3C). All hNP-AC were vimentin- and GFAP-immunoreactive. By 1 and 4 DIV, most nanofibre-bound hNP-AC had adopted either a unipolar or bipolar morphology (e.g. Figure 3.6A-F). The length of the processes of hNP-AC had already reached well over 100 μm by 1 DIV on both fibre types (hNP-AC on PCL: 124 ± 25.9; hNP-AC on C/PCL: 125.3 ± 27.2; $p > 0.05$ for all comparisons; Figure 3.6I). Scanning EM clearly revealed the close interaction between hNP-AC and the nanofibres. Single cells that adhered to individual fibres demonstrated a strong tendency to align their processes in parallel with the orientation of the nanofibres, the slender processes growing directly over the surface of the nanofibres (Figure 3.7A-B). Following the seeding of hNP-AC suspensions onto nanofibres, cells occasionally managed to span the gap between adjacent fibres, spreading their cell bodies in a flattened, sheet-like manner (Figure 3.7A-B). This behaviour was even more pronounced in the area of cell migration immediately adjacent to the zones of astrosphere placement (Figure 3.7A). In areas where hNP-AC suspensions settled, by chance, in higher numbers they demonstrated the capacity to form bundles of multiple processes that followed the orientation of single nanofibres. Where the cell density was high enough, even the areas between

nanofibres became populated with oriented cell bodies and processes (Figure 3.7A-B).

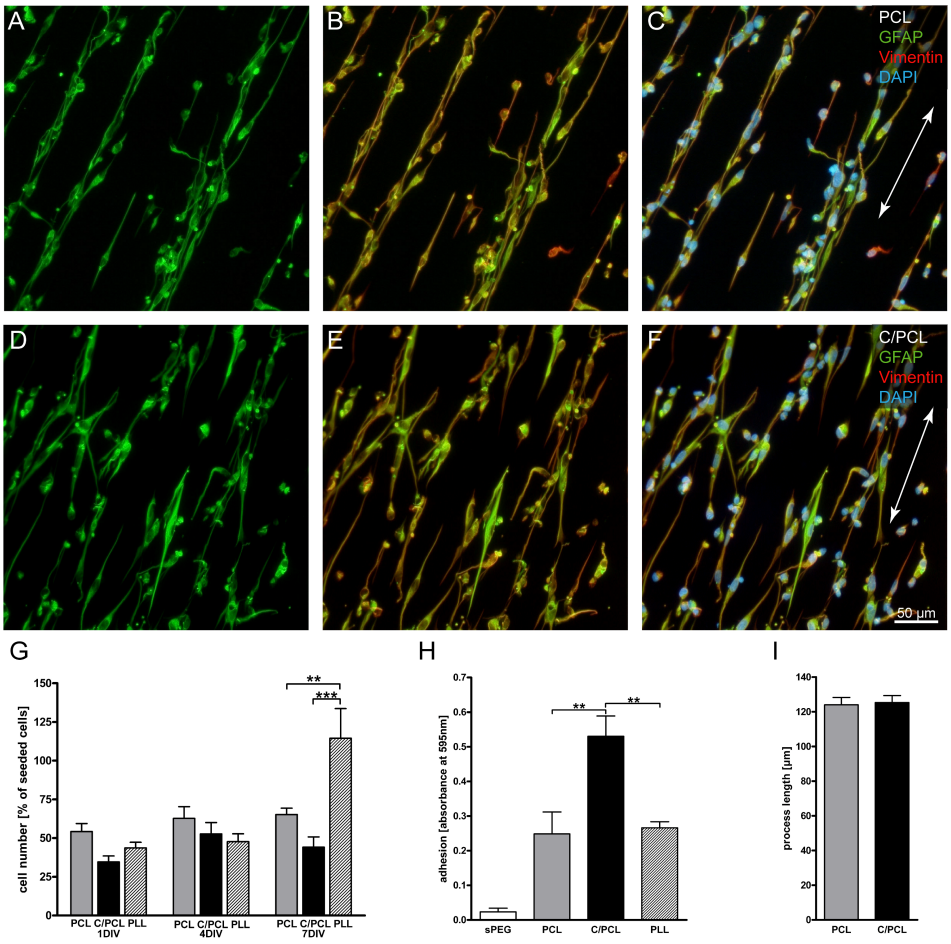

Figure 3.6.: *hNP-AC align their processes along PCL and C/PCL nanofibres.* **A-F:** Immunofluorescence for GFAP (green) and vimentin (red). Morphology and aligned process extension of hNP-AC along PCL (*A-C*) and C/PCL nanofibres (*D-F*). A non-oriented pleiomorphic appearance is adopted by most hNP-AC when allowed to spread freely on a non-oriented substrate (see Figure 3.3C for an example). Orientation of nanofibres is indicated by the double-headed arrow. **G:** Survival and proliferation of cells on PCL and C/PCL nanofibres after 1, 4 and 7 days. hNP-AC demonstrate no proliferation over 7 days on either PCL or C/PCL nanofibres ($p > 0.05$). Cell proliferation is, however, apparent on the PLL (positive control) substrate, being significantly greater than that on PCL or C/PCL at 7 days (** $p < 0.01$, *** $p < 0.001$; n=15 images). **H:** Quantification of cell adhesion of hNP-AC to sPEG (negative control), PCL nanofibres, C/PCL nanofibres and PLL (positive control) positive control substrate. Few hNP-AC adhere to the sPEG substrate. hNP-AC adhere equally well to PCL nanofibres and the PLL substrate ($p > 0.05$). hNP-AC adhesion to C/PCL nanofibres is significantly greater than that on PCL nanofibers or PLL (** $p < 0.01$; n=15 images). **I:** Quantification of process length, measured at 1 DIV after seeding onto PCL and C/PCL nanofibres. hNP-AC extend processes of similar length on both types of nanofibre ($p > 0.05$; n=50 processes). Scale bar in F for A-F.

Extent of Cell Migration along Nanofibres

The migration of hNP-AC along PCL and C/PCL nanofibres was investigated at 2 DIV after astrosphere adherence to the fibres. Cell migration away from the astrospheres resulted in an

elliptical distribution of cells around the astrosphere, with the greatest migration following the orientation of the nanofibres (Figure 3.7A-B). In contrast cell migration away from astrospheres plated onto the PLL-coated substrate was uniform in all directions. The PLL-coated substrate acted as a non-oriented, positive control for cell migration. Migration by hNP-AC on both nanofibre substrates was significantly better than that demonstrated on PLL and was clearly enhanced on the functionalised C/PCL nanofibres ($p < 0.01$; Figure 3.7C).

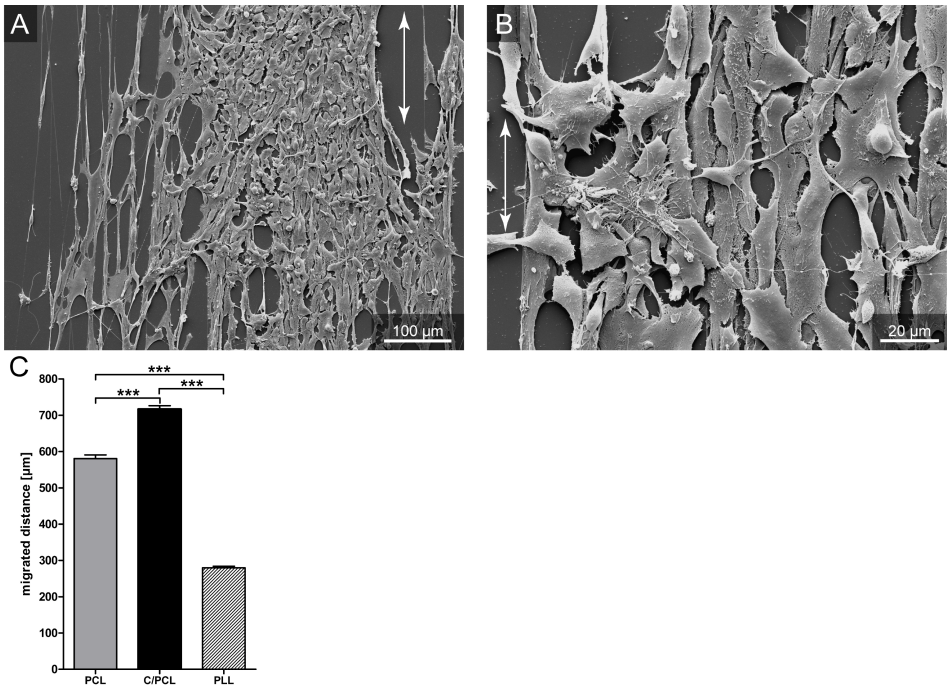

Figure 3.7.: *hNP-AC migrate further on C/PCL nanofibres compared to PCL nanofibres or PLL substrate.* **A-B:** Scanning electron microscopy of migrating hNP-AC from astrosphere preparations. **A:** Low magnification of the sheet of densely packed cells, having just migrated away from the astrosphere. To the left of the image, individual cells associated with single fibres have adopted an elongated, spindle-shaped morphology. Migration of cells away from the astrosphere is strongly influenced by the nanofibre substrate; cells following the orientation of the fibres migrate for significantly greater distances than those that attempt to migrate perpendicular to the main axis of nanofibre orientation. This results in an ovoid distribution of cells around the astrosphere. **B:** Higher magnification of hNP-AC that have migrated a short distance away from the astrosphere. Sheets of overlapping, flattened cells can be seen that still adopt a longitudinal orientation. Other more rounded and process bearing cells can be seen growing over the surface of the flattened cells. Orientation of nanofibres is indicated by the double-headed arrow. **C:** Quantification of migration of hNP-AC along PCL and C/PCL nanofibres after 2 days. hNP-AC migration is significantly improved by functionalization of the nanofibre surface, being significantly greater on the C/PCL than on the PCL nanofibres (*** $p < 0.001$; n=9 spheres).

3.2.4. Micro-porous Collagen Scaffolds

Scanning electron microscopy of the 3D type-I collagen scaffolds: scanning EM revealed that the scaffolds were composed of tightly packed and longitudinally oriented pores (Figure 3.8A-C). Higher magnification demonstrated that the longitudinally oriented pores were interconnected via numerous fenestrations in the scaffold walls (Figure 3.8B). Scanning EM of cross sections of the collagen scaffold demonstrated that the micro-channels had a profile that was disc-shaped (e.g. highlighted in red Figure 3.8C). Quantitative morphometry revealed that the shortest distance between the flattened edges of the disc-like micro-channels was approximately 84 $\pm$ 4.5 μm.

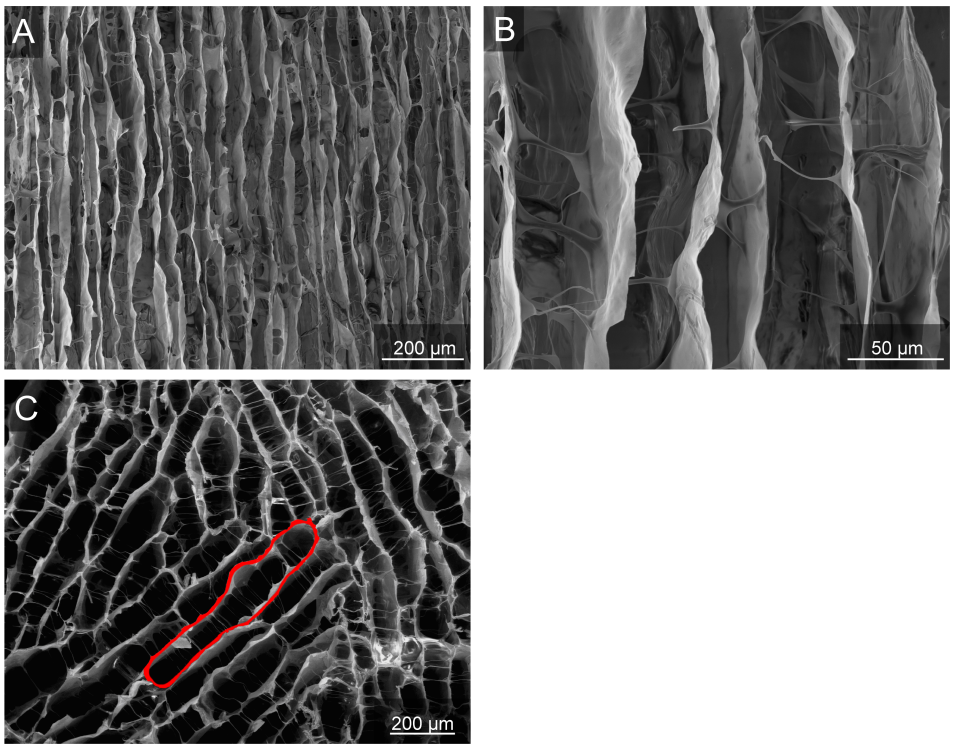

Figure 3.8.: *Scanning EM of the highly orientated collagen scaffold.* **A-B:** Low and high magnification images demonstrate the uniform orientation of the microchannels. The average distance between the (roughly) parallel walls of the scaffold is 84$\pm$4.5 μm. **C:** Scanning EM of a cross section of the collagen scaffold demonstrates that the microchannels have a transverse, disc-shaped, profile (e.g. highlighted in red).

Cell-Substrate Interactions Following the Seeding of hNP-AC on to 3D Collagen Scaffolds

The 3D collagen scaffolds were hydrophilic and became rapidly hydrated when incubated with an excess volume of cell suspension. By as early as 1 day *in vitro* (DIV), hNP-AC demonstrated an even distribution throughout the whole scaffold (e.g. Figure 3.9A). However, by 14 DIV, proliferation and redistribution had resulted in the formation of cell columns which followed the internal orientation of the scaffold micro-channels (Figure 3.9B, D). Quantification of the DAPI-labelled nuclei within the sections demonstrated an increase in the number of hNP-AC over the 14 day period (Figure 3.9E). This rate of proliferation is the equivalent to a doubling time of 5.0 ± 0.1 days which compares with that of 3.2 ± 0.06 days by hNP-AC on PLL/laminin-coated tissue culture plastic.

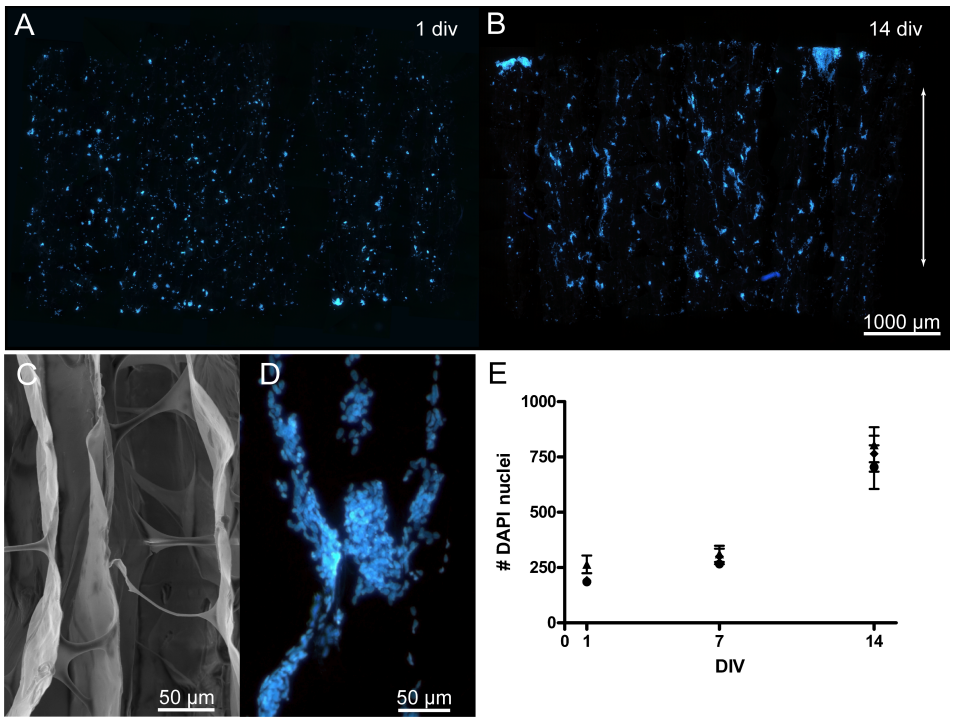

Figure 3.9.: *hNP-AC proliferate and grow as orientated columns of cells which follow the orientation of the micro-channels.* **A-B:** Cryosections reveal DAPI-labelled hNP-AC within the collagen scaffolds at 1 day (*A*) and 14 days (*B*) post-seeding. The double headed arrow in (*B*) indicates the orientation of the pores. **C-D:** High magnification scanning EM of the orientated scaffold (*C*) and the DAPI-labelled hNP-AC (*D*). **E:** Quantification of the DAPI-labelled hNP-AC nuclei demonstrates cell proliferation on the scaffold. The different symbols represent the data from three independent experiments. Scale bar in B for A and B.

Cell-Cell Interactions and Axon Growth Promoting Properties of hNP-AC Seeded Collagen Scaffolds

Hemisected DRG adhered well to the surface of both seeded- and the non-seeded scaffolds and extended NF200-positive axons into the orientated micro-channels (e.g. Figure 3.10A, red signal). Regenerating neurites were mostly associated with migrating, S100β-positive, GFAP-negative spindle-shaped, Schwann cells (Figure 3.10A, F for an example of neurofilament (red) and S100β (green) staining). However, some of the regenerating axons were also associated with either cell-free regions, or with S100-negative fibroblasts or GFAP-positive hNP-AC. Seeded hNP-AC were immunohistochemically identifiable by their intense staining for human nestin and human nuclei (Figure 3.10D-E). Double immunofluorescence demonstrated that hNP-AC were also intensely immunoreactive for S100β and GFAP (Figure 3.10D-E). The majority of the seeded hNP-AC adopted a flattened morphology with no clear indication of cell orientation (e.g. Figure 3.10E and Figure 3.11D), however, in those instances where processes were detectable, they tended to demonstrate an orientation that followed the longitudinal axis of the micro-channels (e.g. Figure 3.10D and Figure 3.11A). Where seeded hNP-AC happened to be located near the surface of the scaffold (i.e. close to the cut surface of the hemisected DRG), they were often found to be intermingled with columns of NF200-positive axons and Schwann cells (Figure 3.10G). Rather surprisingly, migrating vimentin-positive fibroblasts and p75-positive Schwann cells exhibited close spatial relationships with the seeded hNP-AC (Figure 3.11A-C, Figure 3.11D-F respectively). The migrating fibroblasts possessed large, DAPI-labelled nuclei with a polymorphic, flattened vimentin-positive/GFAP-negative cell cytoplasm and appeared to intermingle freely with the vimentin-positive/GFAP-positive hNP-AC (Figure 3.11A-C). The cell bodies and processes of migrating Schwann cells were p75-positive/GFAP-negative and followed the longitudinal orientation of the scaffold, often following a trajectory that brought them in close association with the seeded hNP-AC (Figure 3.11D-F). A fibronectin-rich ECM was found to be evenly distributed throughout the whole scaffold (Figure 3.11G-I).

Quantification of cell migration and axonal growth into the scaffold demonstrated that the presence of hNP-AC had no effect on the migration of p75-positive Schwann cells from the hemisected DRG explants (Figure 3.12B). However, hNP-AC did influence the extent of axon

growth, with a statistically significant increase of the 10% longest NF200-positive neurites found within the scaffold. The 10% longest axons within non-seeded scaffolds extended for 737±15 μm while the value for axon regeneration in to hNP-AC seeded scaffolds was 817±24 μm ($p < 0.01$; Figure 3.12A).

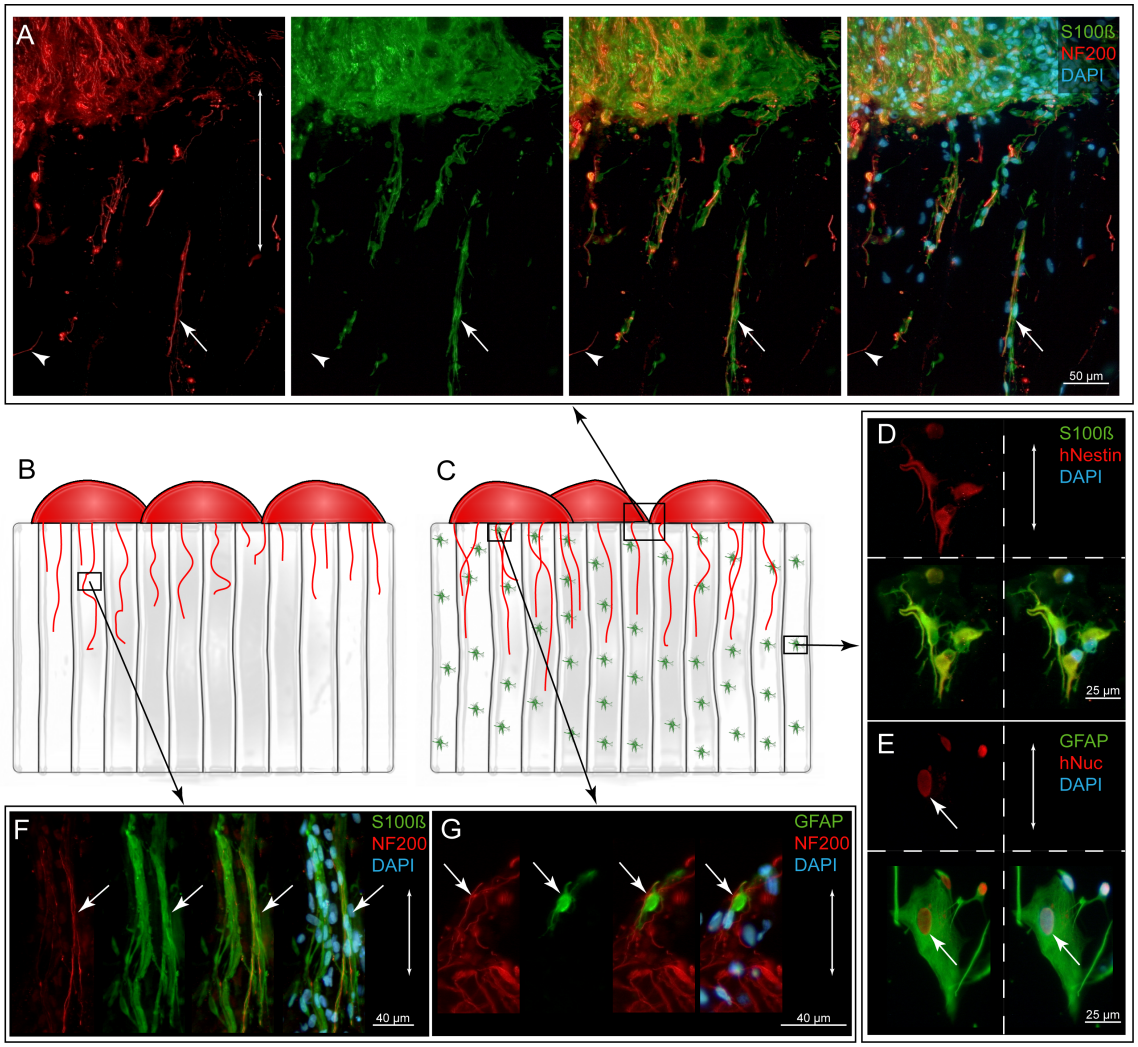

Figure 3.10.: *Cell-substrate and cell-cell interactions in the 3D collagen scaffold.* **A:** S100β-positive Schwann cell (green) migration and NF200-positive (red) axon regrowth from hemisected adult rat DRG closely follow the orientation of the microchannels. **B,C:** Schematic diagram of the experimental design for investigating cell migration and axon growth from hemisected DRG (red) placed onto the surface of non-seeded (B) and hNP-AC seeded (green stars, C) scaffolds. **D:** Small clusters of S100β-positive (green)/human nestin-positive (red) hNP-AC within the microchannels. Unlike the migrating Schwann cells, the seeded hNP-AC generally fail to extend long processes that follow the orientation of microchannels. **E:** Flattened morphology of the seeded GFAP-positive (green)/human nuclei-positive (red) hNP-AC within the microchannels. **F:** Not all bundles of migrating Schwann cells deep within the scaffold are associated with regenerating axons. Only 1 of these 2 parallel S100β-positive (green, arrow) Schwann cell bundles contains NF200-positive (red) axons. **G:** GFAP-positive (green) hNP-AC can be found in association with the regenerating NF200-positive (red) axon bundles, close to heir exit point form the hemisected DRG. Double headed arrows indicate the pore orientation for each series of images.

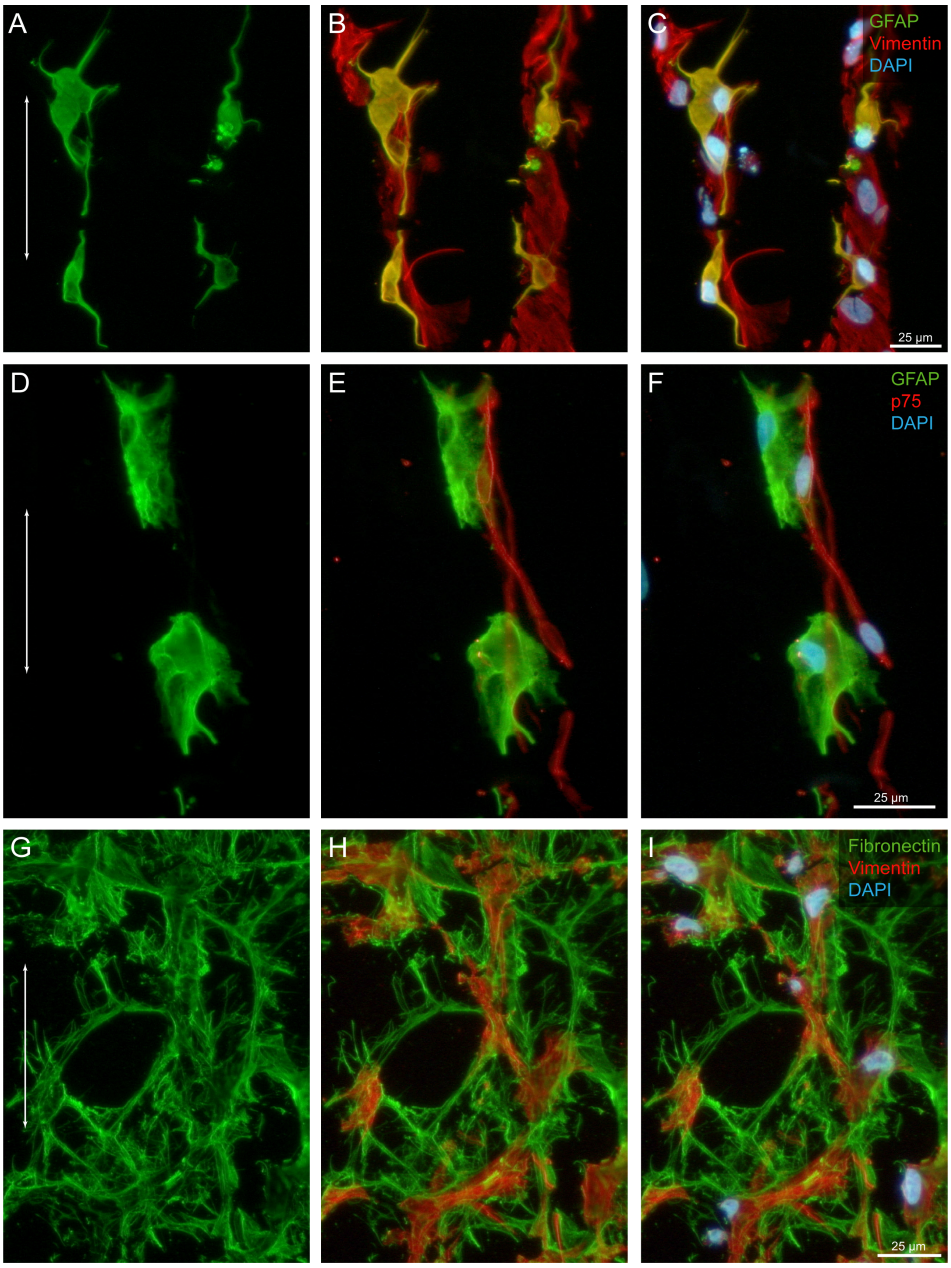

Figure 3.11.: *Cell-cell interactions within the 3D collagen scaffold.* **A-C:** Some GFAP-positive (green) seeded hNP-AC extend processes which appear to follow, to some extent, the orientation of the scaffold, where they can be seen intermingling with vimentin-positive (red) fibroblasts. **D-F:** The majority of the GFAP-positive (green) hNP-AC adopt a flattened morphology which does not follow the orientation of the scaffold, but which comes into close contact with the cell bodies and orientated process of migrating p75-positive (red) Schwann cells. **G-I:** The loose fibrillar distribution of the ECM molecule, fibronectin (green), is extensively distributed throughout the whole scaffold and is most likely produced by the migrating vimentin-positive (red) fibroblasts. Double headed arrows indicate the pore orientation for each series of images.

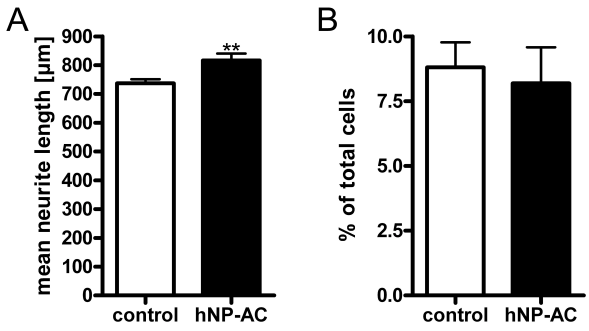

Figure 3.12.: *hNP-AC promote greater neurite extension into the scaffold.* **A**: The seeded hNP-AC significantly increase the extent of axon regeneration through the scaffolds. **B:** Non-seeded (control) collagen scaffolds supported migration by Schwann cells, the extent of which was not affected by the presence of hNP-AC (** $p < 0.01$; n=6 slides).

3.3. Discussion

Advances in biomaterial engineering and their potential contribution to regenerative medicine for neural tissue repair is a rapidly expanding area of interest. The development of scaffold concept and design requires a fundamental understanding of the influence that such engineered substrates may exert on adherent cell morphology and function, e.g. [77, 384]. This not only includes the ability of substrate bound cells to promote axon regeneration but also the influence of the substrate on cell-cell interactions. Substrate geometry has demonstrated a profound influence on adherent cell behaviour [77, 78, 107, 384, 385]. Aligned ECM, as well as micron- and submicron-scale topography of the substrate have been demonstrated to exert substantial effects on neural cell form and function [50, 51, 86, 159, 266, 289, 364, 462]. This is of particular interest for the development of biomaterial-based scaffolds intended to promote regeneration of peripheral nerves or CNS white matter tracts which are endowed with their own, highly orchestrated geometries, e.g. [35, 276, 360, 407, 408]. The intrinsic geometry of such PNS and CNS fibre pathways has been reported to play an important role in the success or failure of axonal regeneration [319, 320]. Earlier cell implantation studies of grafting immature astrocytes into experimental animals with CNS or spinal nerve root lesions (either alone or in combination with crude scaffolds composed of Millipore filters) have demonstrated some beneficial effects in terms of reduced host scarring and increased host axon regeneration [236, 390, 454]. More recent studies have identified that type I rat astroglia

are capable of promoting CNS tissue repair in the absence of unwanted side-effects [99, 100]. The mechanisms by which the equivalent, human-derived cells exert their axon growth promoting effects in simple 2D culture systems as well as in more complex, scaffold-associated, 3D systems remain largely unknown. Furthermore, the interactions between immature astrocytes and the crude scaffolds of earlier studies or with more modern, sophisticated scaffolds or nanofibers have been obscure.

3.3.1. Cell Characterisation

In the present investigation, it was important to demonstrate that the human cells under investigation actually conformed to the current descriptions of neural progenitors and progenitor-derived type-I astrocytes. The hNPC were characterised by the expression of progenitor-related markers nestin, SOX2 and Musashi [256, 358, 476] and were able to differentiate into neurons, astrocytes and oligodendrocytes. Differentiation with BMP4 and LIF induced elevation of mRNA levels and immunoreactivity for GFAP and CD44, confirming the generation of human neural progenitor-derived immature astrocytes, as described by others [461]. Mature, adult rat-derived DRG neurons were chosen for the axon growth promoting assays because their properties were likely to be more representative of the cell types that would be axotomised by traumatic injury to the nervous system. The use of immature, embryo-derived DRG by other groups might be less representative since they have been shown to be less responsive to inhibitory cues in their environment [18, 131].

3.3.2. Axon Growth Promoting Properties of hNP-AC in 2D Cultures

Previous studies had demonstrated that the axon growth promoting properties of experimental animal-derived astroglia are likely to be due to the production of extracellular matrix (including laminin and fibronectin) as well the expression and release of certain growth factors (including bFGF, BDNF and NGF) [113, 329, 463]. It was possible to extend this information by demonstrating that both ECM- and growth factor-mediated mechanisms were also involved in the potent axon-growth promoting effects of the human progenitor-derived astroglia. However, the identification of the specific ECM- and growth factor-related molecules

involved in this process was beyond the scope of the present investigation. The influence of the ECM, particularly of laminin, on axonal growth and regeneration is well established [173, 272]. Therefore PLL/laminin substrate coating was chosen as a positive control for the 2D experiments. Even though this control substrate was able to support extensive neuritic outgrowth, surprisingly greater regeneration was supported by the viable hNP-AC, by hNP-AC-ECM and by hNP-AC-CM. This suggests that hNP-AC represent a promising cell type for consideration in future tissue engineering strategies to promote functional repair in animal models of traumatic CNS and spinal root injury.

3.3.3. Cell-Substrate Interactions of hNP-AC on Orientated Nanofibres

Advances in nanotechnology have led to an interest in cell interactions with substrates in the sub-micron range. Electrospun nanofibres have been used to generate oriented and non-oriented structures that, to some extent, can mimic the properties of the extracellular environment [49, 480]. The ability of nano-structured surfaces or nanofibres to affect the behaviour of non-neural cells [290, 406, 452, 483] as well as neural cells of the PNS has been demonstrated *in vitro* [86, 364]. Cell adhesion, survival and proliferation were well supported but morphology and alignment were altered strikingly by oriented nanofibres, promoting longer axonal growth than seen on the non-oriented fibres [86, 87]. It has therefore become clear that oriented nanofibres may have a significant role in the design of scaffolds intended to promote axon regeneration in the PNS. However, their potential role in bridging CNS lesions remains uncertain. As a first step in assessing this potential, nanofibre-astroglial interactions were studied *in vitro*. Both cell adhesion and migration by hNP-AC were significantly enhanced by nanofibre functionalisation with collagen. However no proliferation on the nanofibres was observed. The lack of an effect of type I collagen on hNP-AC proliferation supports previous *in vitro* investigations, which demonstrated increased proliferation of rat astrocytes only when grown on laminin and fibronectin, but not on type I collagen [296]. Cells grown on the unpatterned PLL substrate spread freely and adopted a pleiomorphic appearance, whereas most of the cells that were seeded onto nanofibres had small cell bodies and long, thin, unipolar- or bipolar morphologies. A clear

relationship between cell spreading and proliferation has been demonstrated by Ingber and colleagues. Cells growing on uniform, unpatterned surfaces showed the highest proliferation rate, whereas cells grown on progressively smaller islands of adhesive substrate showed progressively restricted spreading and lower proliferation rates, and the smallest islands induced apoptosis [77, 384]. Although the present investigation compared cell-substrate interactions on two types of nanofibres, it would have been of interest to include observations of the behaviour of cells seeded onto smooth surfaces coated with either PCL or C/PCL. Such comparisons, enabling the demonstration of the roles played by substrate nanofeatures, were unfortunately not included. Migration of hNP-AC on PCL nanofibres was greater than on the PLL-positive-control substrate. However cells migrated furthest on the C/PCL nanofibers. Cell migration requires the formation of focal-adhesion points between the cell and the extracellular substrate. Focal adhesions are macromolecular complexes that physically link the ECM to the contractile actin cytoskeleton [457]. The most important molecular receptors for ECM binding are integrins [20]. Since integrins bind directly to collagen [254], the improved cell migration of hNP-AC on C/PCL nanofibres might not be a surprise. In addition, an indirect binding between collagen and integrin receptors may be mediated by fibronectin [157]. This may also have occurred in our cell cultures because fibronectin may have been present in the serum-containing medium or may have been secreted by the cells themselves. ECM-integrin interactions are known to activate a variety of intracellular signal cascades. This may result in potential synergistic effects between growth factor and integrin signaling [157]. It might thus be possible to further increase the migratory behaviour of cells on electrospun fibres by (I) incorporation of other ECM molecules, e.g. fibronectin or laminin into the blend for electrospinning; (II) chemical modification of PCL fibres to present specific integrin-activating peptides, such as GRGDS, IKVAV and YIGSR; and (III) combining ECM molecules with soluble factors that may act synergistically with the integrin-activated pathways (e.g., bFGF, TGF-β or PDGF) [47, 97, 135]. Functionalisation of the scaffold, as seen here, by the incorporation of ECM components (i.e., type I collagen) or even by the incorporation of growth factors (or other growth-promoting molecules) has the potential of improving the performance of such scaffolds [214]. The ECM molecule, type I collagen, was chosen for surface functionalisation of the PCL nanofibres because it is a natural polymer that can be mixed and electrospun with PCL and is known to activate axonal and glial inte-

grin receptors capable of supporting cell adhesion and migration [423, 437]. However, it has recently been reported that electrospinning results in the denaturation of up to 99% of the collagen to gelatine, especially when fluoroalcohols are used as a solvent [478]. The extent to which collagen was denatured to gelatine in the present investigation remains uncertain, however, the effect of surface functionalisation of the interactions of hNP-AC were clear.

3.3.4. Cell-substrate Interactions between hNP-AC and Orientated 3D Collagen Scaffolds

Scanning EM demonstrated that the scaffold was composed of large diameter (84±4.5 μm for the shortest distance), highly oriented pores that, when viewed in transverse section had an overall flattened or disk-like appearance. This is somewhat different to honeycomb-like appearance of a small-pore scaffolds that were described earlier [50, 51, 289]. The initial seeding of the scaffolds in the present study was highly efficient with a rapid and even distribution of the hNP-AC throughout the entire structure. This observation is in contrast to the seeding efficiency of the smaller pore sized collagen scaffold reported earlier, where seeding of rat Schwann cells, olfactory ensheathing cells, early postnatal astrocytes or differentiated human neuroblastoma cells (SH-SY5Y) cells showed only limited penetration of the scaffold followed by subsequent migration to deeper regions [51, 289]. The hNP-AC of the present study demonstrated a novel cell-substrate interaction within the scaffold: by 14 days, there was a clear redistribution of the cells such that columns of densely packed hNP-AC could be seen throughout the scaffold. It is possible that this redistribution took place by migration and accumulation of the cells at particular foci, suggesting that cell-cell adhesive interactions between hNP-AC may have been greater than those between the seeded cells and the substrate e.g. [356]. An alternative explanation might be the occurrence of cell death in some regions of the scaffold being counter-balanced by proliferation in others. Counting of the DAPI labelled nuclei did reveal a significant increase of hNP-AC numbers within the scaffold over the 14 days *in vitro* (calculated doubling time of 5.0±0.1 days), but there were no indications of extensive cell death, such as by the presence of nuclear fragmentation. Although others have described type-I collagen to be a poor substrate for astrocyte proliferation in 2D cultures [296], the present data supports the now widely acknowledged notion

that cell behaviour in 2D studies does not necessarily reflect their behaviour in 3D environments [1, 26, 91]. The proliferation of hNP-AC within the scaffold is of major importance because it not only shows the ability of the scaffold to act as a cell carrier but also allows the diffusion of sufficient nutrients to support proliferation.

3.3.5. Axon Growth Promoting Properties of hNP-AC Seeded 3D Scaffolds

Previous studies have demonstrated that non-seeded, micro-structured collagen scaffolds are able to support significant orientated axon regeneration [50, 51, 153, 289]. The present observations revealed that hNP-AC seeded scaffolds support significantly greater DRG axon regrowth than non-seeded scaffolds. Most of the axonal growth through the scaffold was closely associated with bundles of Schwann cells that had migrated out of the DRG explant and which followed the longitudinal orientation of the micro-structured pores. Schwann cells are potent axon growth-promoting cells which present directional cues to regenerating axons [33, 58, 428]. However axonal growth was occasionally not found to be associated with Schwann cells or their processes, but could be seen to be associated with acellular regions of the scaffold or with fibroblasts or hNP-AC. Although DRG axon growth in the acellular regions of orientated collagen scaffolds has been reported by others (e.g [50]), the present investigation extends the understanding of such events by demonstrating that substantial deposits of the ECM molecule, fibronectin, could be found within the porous micro-channels. Fibronectin has already been demonstrated to support axon regeneration and is mainly expressed by fibroblasts, but also by Schwann cells and astroglia [88, 112, 350, 353, 441]. This raises the possibility that axons not only used the type I collagen micro-channel walls as substrates for growth but also local ECM deposits. Others have reported that loading collagen scaffolds with fibronectin leads to axon regeneration by DRG but the authors failed to compare fibronectin containing scaffolds with empty scaffolds [153]. The relatively low seeding density of hNP-AC made it unlikely that contact-mediated mechanisms would account for much of the enhanced DRG axon regeneration. However, it is possible that the release of soluble factors (which would have become trapped and accumulated within the internal micro-architecture of the scaffold) may have influenced the extent of axon regeneration.

Astrocytes have been reported to express a range of growth factors including bFGF, NGF and BDNF [113, 463] and the present investigation has shown that hNP-AC conditioned medium has potent effects on DRG axon growth in simple 2D cultures. It was also feasible that factors produced by hNP-AC may have altered the number of Schwann cells migrating into the scaffold [3, 4], and thus influenced axon growth via an indirect mechanism, however quantification of Schwann cell migration proved that this was not the case.

A surprising observation was the extent to which migrating Schwann cells and fibroblasts intermingled with the seeded hNP-AC. Under normal conditions, Schwann cells and astrocytes form distinct territories with a clear boundary [270], as do fibroblasts and astrocytes [376, 377]. Such boundaries exert considerable influence over the ability of regenerating axons to cross from one territory to the other and their effects have been studied in detail in 2D *in vitro* assays [163, 164, 377]. The present investigation has demonstrated that when these cells encountered each other within an orientated 3D scaffold, substantial intermixing - rather than mutual repulsion was evident. This raises the exciting possibility that the topography of the scaffold may have altered the properties of one or more populations of cells. However, one cannot discount the possibility that the intermixing of the cells was also encouraged by the relatively low densities of the 2 populations of cells within the scaffold. Nonetheless, under other experimental conditions, Schwann cells and astrocytes have also been encouraged to intermingle with each other extensively [56, 61]. Microtransplantation of highly purified populations of Schwann cells, in the form of elongated columns of cells, into the adult rat CNS resulted in the eventual intimate mixing of orientated donor Schwann cell processes with similarly oriented reactive host astrocytic processes within individual basal lamina tubes. The Schwann cells and astrocytes within the resulting chimeric PNS-CNS pathway were subsequently seen to cooperate with each other in supporting directional host axon regeneration [56, 61]. A novel outcome of the present investigation is that the microtopography of the 3D collagen scaffold may have also encouraged a similar type of mixing behaviour between Schwann cells/fibroblasts and hNP-AC.

The ability of biomaterials to influence the behaviour of neural progenitor-derived astrocytes, shifting their shape from a pleiomorphic appearance to a highly oriented one (as seen with nanofibres) and reducing the tendency of CNS and PNS glia to form mutually exclusive territories (as seen with the 3D collagen scaffold), may be of particular interest for CNS-

repair strategies. Lesions to the CNS induce a reactive astroglial response that includes scarring and new basal lamina and chondroitin sulfate proteoglycans deposition. Such reactive astrocytic responses are important for protecting adjacent intact nervous tissue from further damage but also contribute to the axon-growth inhibitory environment at and around the lesion site [129, 376, 396]. However, axon growth-promoting properties of such reactive astrocytes have also been described [265]. Furthermore, the processes of activated/reactive astrocytes can be encouraged to support CNS axon regeneration, effectively chaperoning re-growing axons across a host-graft interface [61, 228]. It is possible that the ability of biomaterials to modify astrocytic morphology/behaviour at graft-host interfaces may be useful in supporting improved graft-host integration; promoting astroglial attachment and aligned migration into the scaffold rather than astroglial scarring which would effectively isolate the graft. Both PCL and collagen reduce astrocytic activation [467]. Thus, implantation of a collagen scaffold or of collagen-PCL nanofibre scaffold might be anticipated to reduce (or at least modify) astrocytic scarring at the graft-host interface and thereby improve oriented cell and tissue integration. However, it is possible that the real extent of scaffold-host tissue interactions may be somewhat different than anticipated in the vastly more complicated setting of *in vivo* implantation.

3.4. Conclusion

The experiments conducted in the present thesis have demonstrated the potent axon growth promoting effects of hNP-AC in simple 2D culture systems. These effects of hNP-AC appear to be due to the production of ECM as well as the production and release of diffusible molecules. The interactions of these cells with nanostructured and microstructured substrates were also investigated *in vitro*. The sPEG-mediated attachment of low density, oriented nanofibres to glass coverslips enables interactions between single cells and single nanofibres to be studied in relatively simple 2D cultures. The potential value of using nanofibres for CNS-based regenerative strategies was addressed by studying astroglia-nanofibre interactions *in vitro*. The morphology and alignment of processes of hNP-AC were strikingly influenced by both types of orientated nanofibres. Furthermore fibre functionalisation greatly enhanced cell adhesion and cell migration. However, hNP-AC revealed no proliferative activity on ei-

ther PCL or C/PCL nanofibres. Both types of nanofibres present strong topographical cues for the oriented growth and migration of hNP-AC. In this context, even small numbers of nanofibres were able to control the orientation of large numbers of cells, suggesting that fewer nanofibres than anticipated may be required to promote directed tissue repair in a 3D scaffold. However, this hypothesis can only be tested by *in vivo* implantation of 3D scaffolds into experimental models of spinal cord injury.

The ability of the topography of a scaffold to influence cell-cell interactions has also been suggested by the present investigations. The fundamental properties of normally mutually repulsive cell types (i.e Schwann cells/fibroblasts and astrocytes) appeared to be over-ridden or modified by the micro-structure of the 3D substrate that they were located in. Although some of the basic principles controlling cell-substrate interactions have already been established in relatively simple 2D systems, the future design of biomaterial-based scaffolds that are intended to promote nervous tissue repair will require a better understanding of such principles in more complex 3D situations.

4. Experimental Spinal Cord Injury

4.1. Introduction

Biomaterial- and tissue engineering-based intervention strategies for the treatment of spinal cord injury (SCI) have become rapidly expanding areas of research. Traumatic spinal cord injury (SCI) causes severe and permanent functional deficits due to the primary mechanical insult followed by secondary tissue degeneration. The loss of function is dramatic and often permanent due to presence of axon-growth inhibitory/repulsive molecules at- and around the lesion site, combined with the presence of a physical barrier presented by the glial scar and the development of fluid-filled cystic cavities [140, 141]. One of the numerous strategies adopted for spinal cord repair has been the grafting of peripheral glia (i.e. Schwann cells [239, 261, 471] and olfactory ensheathing cells [337, 338]), either alone or in combination with a growth promoting scaffold, into the lesion site to promote axon regeneration. However, more recently the potential of stem/progenitor cell-based strategies has become apparent. The potential sources of such donor cells include embryonic- [277], foetal- or adult-derived neural stem cells and neural progenitors (NPC, [321, 322, 367]) and, most recently, induced-pluripotent stem cells (iPS) [436]. Such neural stem/progenitor-based strategies have been reported to promote functional improvement in experimental models of CNS, but the mechanism(s) of action remain poorly defined [52, 114, 121, 156, 306]. However transplantation of neural stem/progenitor-derived oligodendrocytes have been shown to be more efficient for remyelination mediated-repair than grafting non-differentiated or uncommitted cells [62, 481]. Following a similar logic, one may hypothesise that the axon-growth promoting properties of neural stem/progenitor-derived astrocytes will be greater than those of the un-differentiated progenitor cells. Therefore, the present investigation has focussed on the properties of neural stem/progenitor-derived astrocytes for tissue repair. Silver and colleagues showed in the

late 1980s that immature forebrain astrocytes reduced glial scarring and promoted axonal regeneration *in vitro* and *in vivo* [380, 389–391]. Furthermore it was identified that type I astrocytes (rather than type II astrocytes) from the rat are capable of promoting CNS tissue repair in the absence of unwanted side-effects, like allodynia or hyperalgesia [99, 100]. It is highly likely that the orientation of axonal regeneration will play a crucial role in the efficiency of any tissue repair strategy, however, such orientation is only poorly controlled in simple cell transplantation studies. Therefore, a number of orientated scaffolds of varying complexity have been developed to support this behaviour. Simple tubes wrapped around the proximal and distal stumps of transected spinal cord and filled with a gel-like matrix or glial cells were the first attempts for biomaterial-based guidance channels [291, 469, 470]. These guidance channels supported significant axonal in-growth, however the majority of regenerated axons were loacted on the inner surface on the tubes. Further advances in biomaterial engineering have resulted in the development of artificial, 3D, highly orientated and biodegradable matrices [200, 316, 426] which have been transplanted into the injured spinal cord. It has been recognized that such bioengineered matrices can be used to import a range of functional molecules, drugs or cells into areas of pathology.

Since many populations of CNS neurons and their local circuits, both rostral and caudal to the lesion site, remain intact following SCI (e.g. the central pattern generator for stepping movements, [134]), substantial effort has been spent trying to promote functional repair by reconnecting severed nerve fibres to their original targets. These efforts have been encouraged by the fact that only a small percentage (1-10%) of the original nerve fibre projection is needed for the maintenance of useful motor or sensory function [132, 263]. Over recent years, a range of increasingly sophisticated natural and synthetic polymer nerve guides and hydrogels have been developed in an attempt to bridge spinal cord lesions, supporting optimal graft-host integration to allow axon regeneration across both interfaces (i.e. rostral and caudal) of the implant-host transitional zone.

The present investigation follows the hypothesis that implantation of human neural progenitor-derived astrocytes (hNP-AC), alone or in combination with an orientated collagen scaffold will promote functional tissue repair in experimental models of spinal cord injury.

The *in vivo* investigations comprise animals subjected to a spinal cord compression injury by the inflation of a sub-durally positioned balloon. The effects of cell implantation strate-

gies were then assessed. Animal groups of the study were **group I**: lesioned but untreated rats, **group II**: lesioned rats receiving immunosuppression, **group III**: lesioned animals receiving donor human foreskin fibroblasts (hFbl) plus immunosuppression, **group IV**: lesioned animals receiving donor human neural progenitor-derived astrocytes (hNP-AC) plus immunosuppression. As a more sophisticated intervention strategy, a second model of SCI was adopted in which part of the lateral white matter tracts were resected. The effects of a tissue engineering strategy of donor cells plus scaffold were then assessed. Animal groups for these studies were **group I**: lesioned animals receiving naive scaffolds and immunosuppression (control + IS), **group II**: lesioned animals receiving donor hFbl-seeded collagen scaffolds plus immunosuppression, and **group III**: lesioned animals receiving donor hNP-AC-seeded scaffolds with immunosuppression.

4.2. Results

4.2.1. Characterization of hFbl

Human foreskin fibroblasts were chosen to serve as a "neutral" or control cell population for the *in vivo* investigations. They appeared as large flat cells on tissue culture plastic, which grew in an orientated manner and expressed vimentin, CSPG and fibronectin (Figure 4.1A-F). When seeded onto the collagen matrix they also adopted an elongated morphology and followed the orientation of the pores (Figure 4.1G-I). They still expressed large amounts of fibronection, which was deposited throughout the porous microstructure of the scaffold (Figure 4.1H-I).

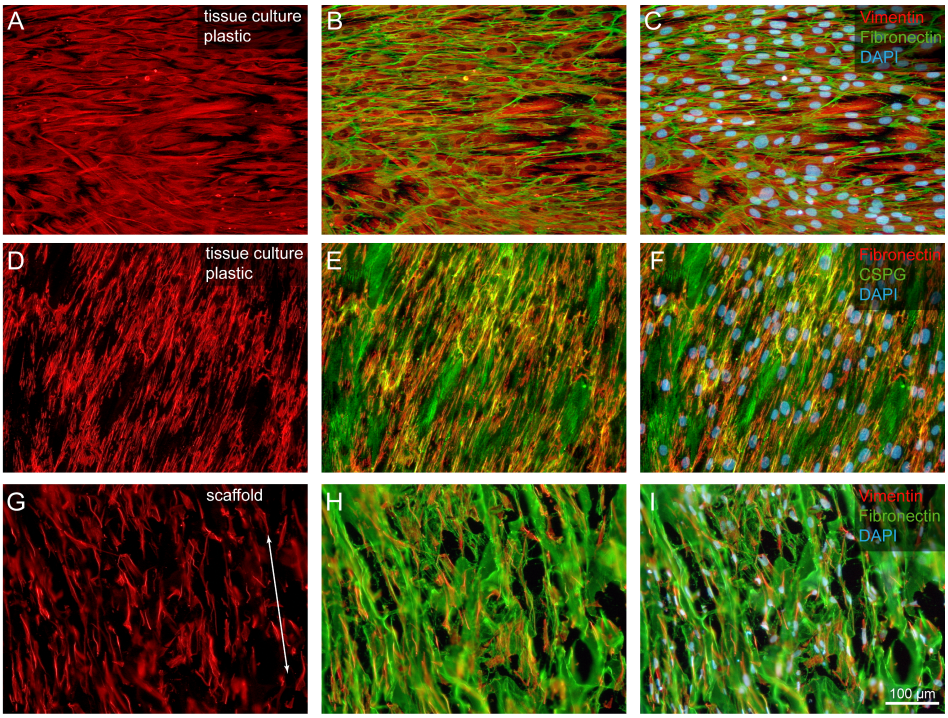

Figure 4.1.: *hFbl express fibronectin and CSPG in tissue culture.* **A-F:** hFbl appear as large flat cells and grow in an orientated manner on normal tissue culture plastic. They express vimentin *(A-C)*, fibronectin *(B, C and D-F)* and CSPG *(E, F)*. **G-I:** When seeded onto the collagen matrix, hFbl also adopt an elongated form which follows the orientation of the pores (double headed arrow). Scale bar in I for A-I.

4.2.2. Balloon Compression Model with Cell Implantation

The results of the behavioural analyses conducted at 5 weeks and 9 weeks were chosen to represent functional outcomes at mid-point and end-point stages of the investigation. For a list of animal numbers per experimental group, see Table 2.4.

Behavioural Analysis

BBB: All animals had a baseline score of 21 (highest possible score), which dropped to an average score of 1 by one week after injury (data not shown). After 5 and 9 weeks groups with cell transplants (hFbl, hNP-AC) showed occasional weight supported stepping, reaching a BBB score of slightly less than 10 at the intermediate time point (5 weeks: 9.9±0.5 and 9,7±0.5 for hFbl and hNP-AC transplants respectively) and above 10 at the end time point (9 weeks: 11.1±0.3 and 10.6±0.5 for hFbl and hNP-AC transplants respectively). This was significantly greater than the score for the control animals (5 weeks: 7±0.7, end-point:

8.6±0.6) for both time points ($p < 0.01$, $p < 0.05$ respectively), but not compared to the control + IS group (5 weeks: 9±0.6, end-point: 9.8±0.5, $p > 0.05$,), which showed some degree of weight support when stationary (Figure 4.2A).

Gridwalk: The overall impression of functional improvement was supported by the gridwalk analysis. Here the animals dropped from the highest possible score of 5 (baseline) to the lowest possible of 0 (data not shown). At the mid- and end-point hFbl (5 weeks: 2.8±0.2, end-point: 3.3±0.2) and control + IS (5 weeks: 2.9±0.2, end-point: 3.2±0.2) groups were significantly better compared to the control group (5 weeks: 1.6±0.3, end-point: 2.3±0.2, $p < 0.01$) At the end-point, the hNP-AC group (5 weeks: 2.2±0.3, end-point: 3.3±0.2) had also reached a significantly better performance than the control ($p < 0.01$; Figure 4.2B).

Hargreaves' heat sensitivity test: All groups showed an increase in the latency of paw withdrawal when exposed to a heat stimulus. This effect increased over time without significant differences between the groups (i.e. hFbl: 5 weeks: 4.2±0.4, end-point: 5.5±0.4; hNP-AC: 5 weeks: 4.9±0.3, end-point: 5.4±0.4; control + IS: 5 weeks: 4.5±0.4, end-point: 5.5±0.4; control: 5 weeks: 4.6±0.3, end-point: 6.2±0.4; Figure 4.2C).

Although there were time-related changes in the extent of functional deficits observed throughout the investigation, the values for all animal groups remained significant below- (i.e. for BBB and gridwalk tests) or above (i.e. for the Hargreaves' heat sensitivity test) their corresponding pre-lesion baseline values ($p < 0.01$; Figure 4.2).

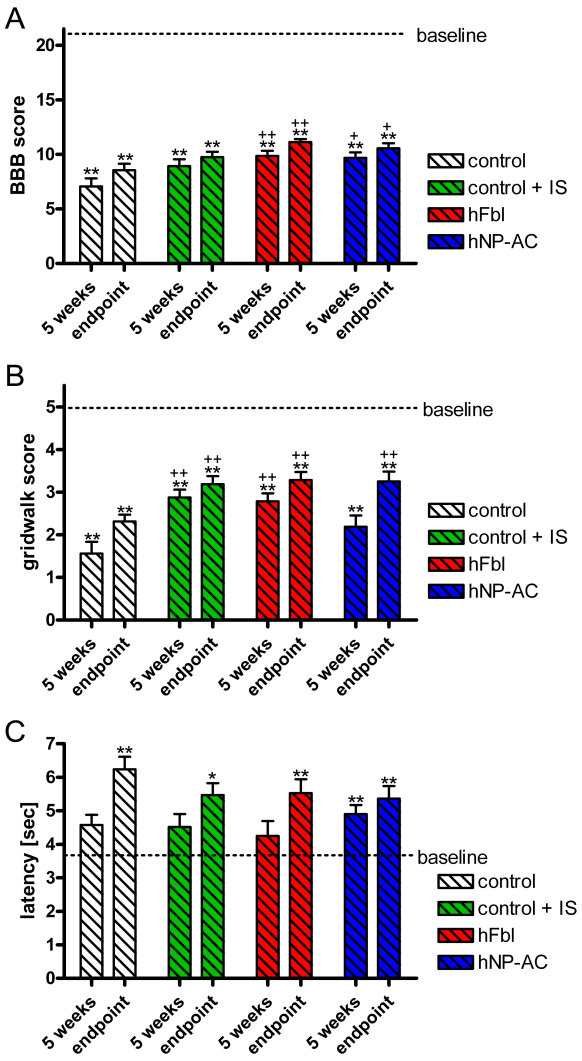

Figure 4.2.: *Animals receiving transplants of cell suspension show better functional recovery than control animals after ballon compression injury.* **A:** *BBB test:* Groups receiving donor cell transplants (i.e. hFbl, hNP-AC) show a statistically greater degree of functional improvement over control animals for both time points ($^{++}$ $p < 0.01$, $^{+}$ $p < 0.05$), but not compared to the control + IS group ($p > 0.05$). **B:** *Gridwalk test:* donor hFbl + IS and control + IS groups performed significantly better compared to the control group ($^{++}$ $p < 0.01$) at 5 weeks post injury. At the end-point, the donor hNP-AC + IS group has also reached a significantly better level of performance than the control group ($^{++}$ $p < 0.01$). **C:** *Hargreaves' heat sensitivity test:* All groups showed an increased latency of paw withdrawal when exposed to heat stimuli (no difference between groups). All groups remained significantly below- (i.e. BBB, gridwalk) or above- (i.e. Hargreaves' heat sensitivity test) the pre-injury baseline values (** $p < 0.01$; control, control + IS and hNP-AC: n=8, hFbl: n=7).

Survival of Transplanted Cells

Transplanted hFbl generally survived well but integrated poorly within the host tissue when transplanted rostral to (Block A, 30%), caudal to (Block C, 70%) and at the lesion site

(Block B, 60%) (Figures 4.3A-I, 4.5A). The donor cells typically formed well defined, elliptical clusters of cells which were strongly fibronectin-positive (Figure 4.3A-D, H, I). Higher magnification demonstrated the close interactions with some host cells, especially at the lesion site, as many human nuclei-negative cells could be found inside of the elliptical clusters (Figure 4.3E-G).

Similarly, transplanted hNP-AC survived and integrated well (Block A: 40%, Block B: 90%, Block C:90%; Figure 4.5A), but in contrast to the donor hFbl, were able to migrate a greater distance in the host tissue, particularly along the longitudinal axis (Figure 4.4A, B, H, I; Figure 4.6A, C). Transverse sections revealed that hNP-AC, despite their longitudinal migration, still showed a tendency to form clusters (Figure 4.4C, D; Figure 4.6B). In general they were able to spread widely throughout the host tissue, in some cases nearly throughout the whole width of the spinal cord section (Figure 4.4A, B; Figure 4.6A) and continued to express GFAP and human nestin (Figure 4.4; Figure 4.6). In the caudal block, donor cells could be found to be relatively evenly distributed throughout the host grey matter, with fewer cells within the white matter. Often they formed larger clusters with closely intermingled processes which surrounded smaller clusters of host cells (Figure 4.4E-G). Individual migrating donor astrocytes, locateds next to the larger clusters of grafted cells, had a more elongated morphology, which followed the axis of the spinal cord (Figure 4.6C, J-L).

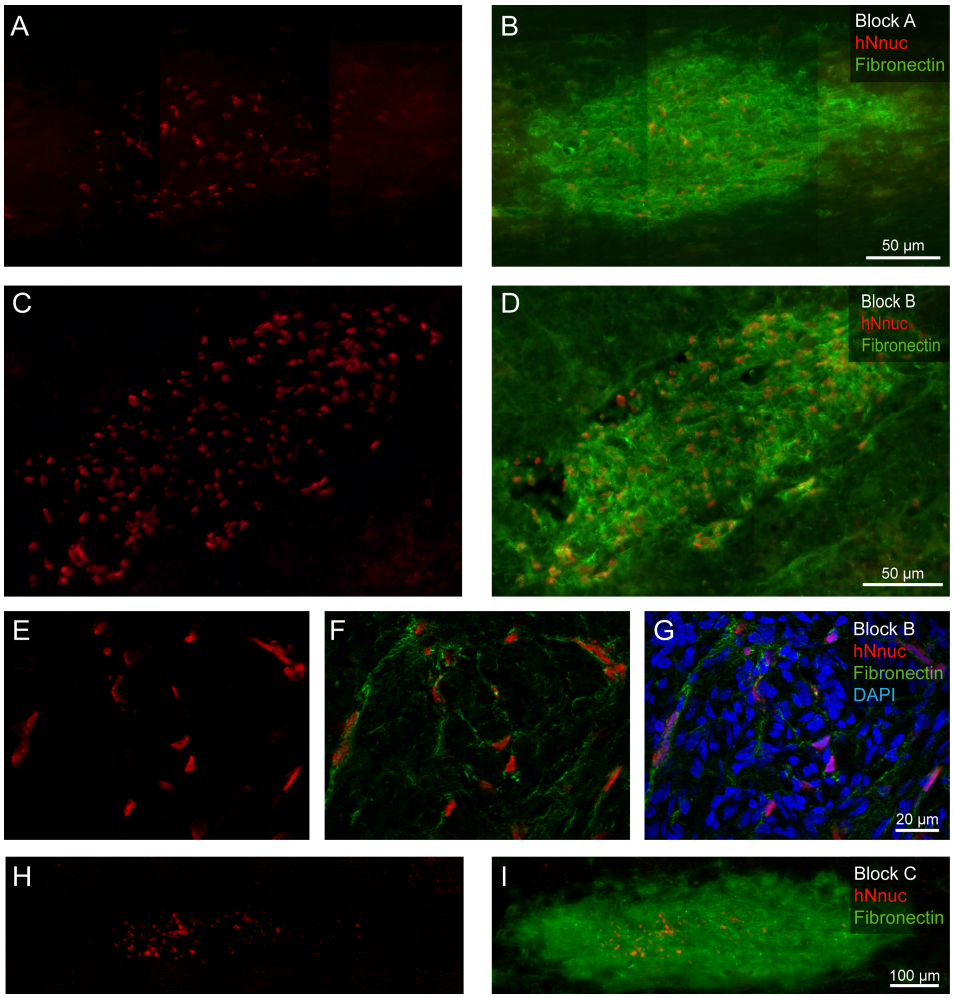

Figure 4.3.: *Donor hFbl survive but intermingle poorly with host cells after transplantation into balloon compression injury of the spinal cord.* **A-D, H, I:** Transplanted cells survive when grafted rostral to- *(A, B)*, within- *(C, D)* and caudal *(H, I)* to the lesion site as shown by the detection of human nuclei-positive staining (hNuc). Donor hFbl form elliptical clusters, which stain strongly for fibronectin *(A-I)*. **E-G:** Higher magnification, together with a nuclear counterstain (DAPI) reveals a high amount of hNuc-negative cells inside of these clusters.

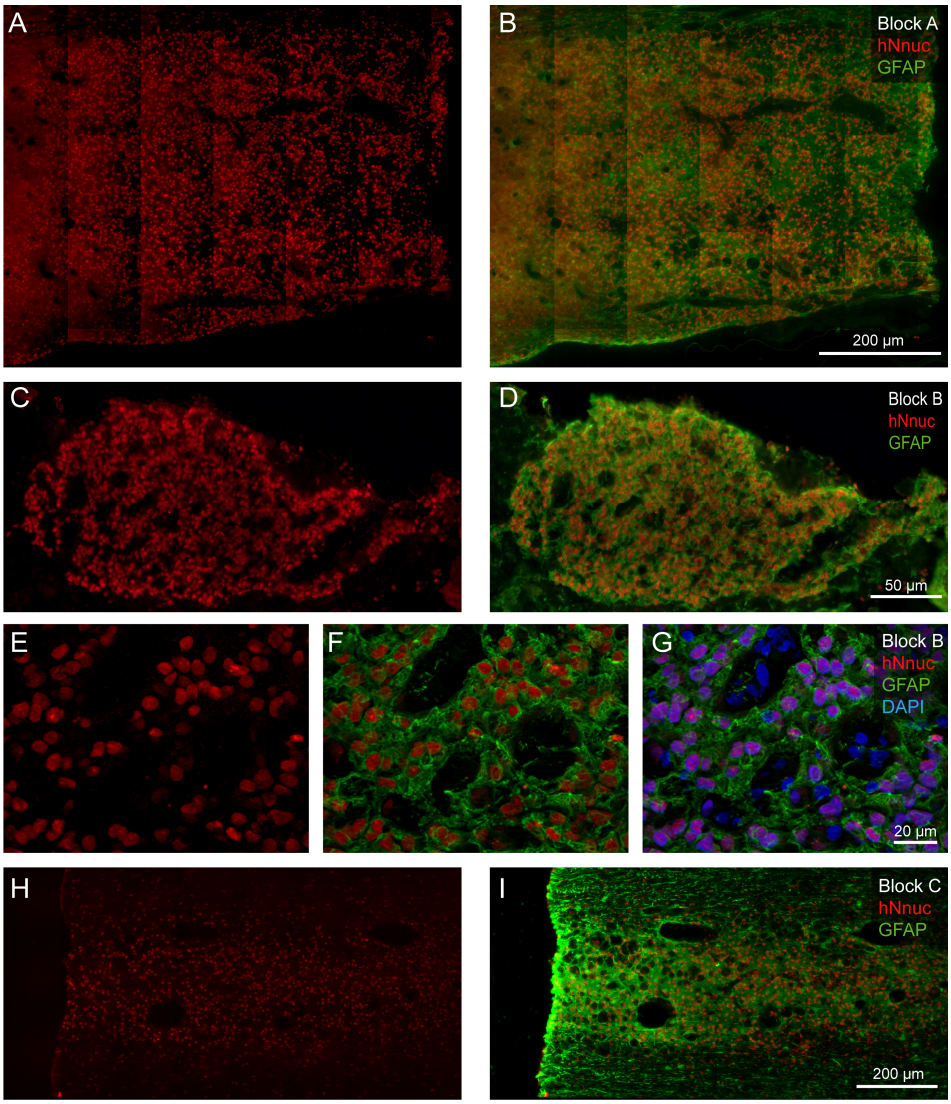

Figure 4.4.: *Donor hNP-AC survive and spread throughout the balloon compression injured spinal cord.* **A, B:** Low magnification image demonstrating that transplanted hNP-AC are capable of spreading throughout the whole width of the spinal cord rostral to the injury site and that they continue to express GFAP after transplantation. **C-G:** Dense cluster of donor hNP-AC at the lesion site. Higher magnification demonstrates that most of the cells are human nuclei- and GFAP-positive *(E-G)*. The GFAP-positive processes inside of the cluster of transplanted cells are non-oriented. **H, I**: Similar to the rostral transplantation site, donor hNP-AC also survive and spread when transplanted caudal to the lesion.

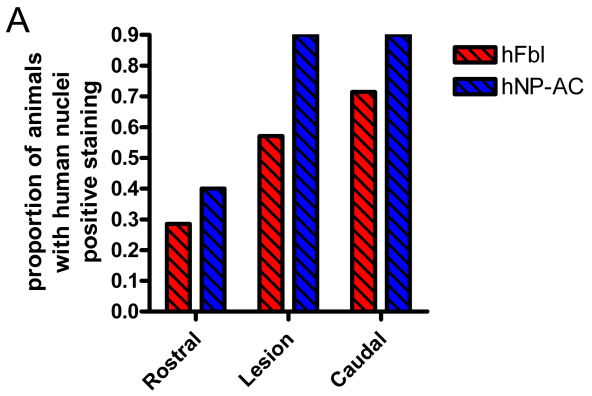

Figure 4.5.: *Proportion of host animals in which surviving donor cells could be identified.* The histogram demonstrates a higher survival rate of donor hNP-AC compared to donor hFbl transplants. Furthermore fewer host animals showed signs of transplanted donor cells at the rostral transplantation site (hNP-AC: n=8, hFbl: n=7).

Regeneration/Sparing of NF200-Positive Axons at the Lesion Site

Quantification of the amount of NF200-positive axons (as indicated by the number of NF-positive pixels) revealed an enhanced ingrowth of neurites into the lesion site of hNP-AC treated animals (23.5±0.7%), which reached statistical significance over the control (20.1±0.7%) and the control + IS (20.1±0.6%, $p < 0.01$), but not over the hFbl (22±0.6%, $p > 0.05$; Figure 4.7E). Donor hFbl supported a significantly greater amount of neurofilament positive axonal ingrowth than the control + IS group ($p < 0.05$). At the lesion epicenter, the distribution of the neurofilament-positive axons was closely associated with laminin-positive structures (Figure 4.7C, D, G, J, H, K) and is most likely to represent regenerating axons. The NF-positive axons in the tissue blocks rostral- and caudal to the epicenter, however, showed a different distribution being more evenly dispersed and showing no co-localisation with laminin-stained structures (e.g. Figure 4.7A, B), probably indicating their intermingling with spared axons. Double immunofluorescence with human nestin demonstrated a close relationship of the regenerating/spared axons with the transplanted hNP-AC rostral, at- and caudal to the lesion site (Figure 4.6D-L). Furthermore, a high density of NF200-positive neurites could be found within the elliptical clusters of laminin-stained cells (Figure 4.7A, B, F, I).

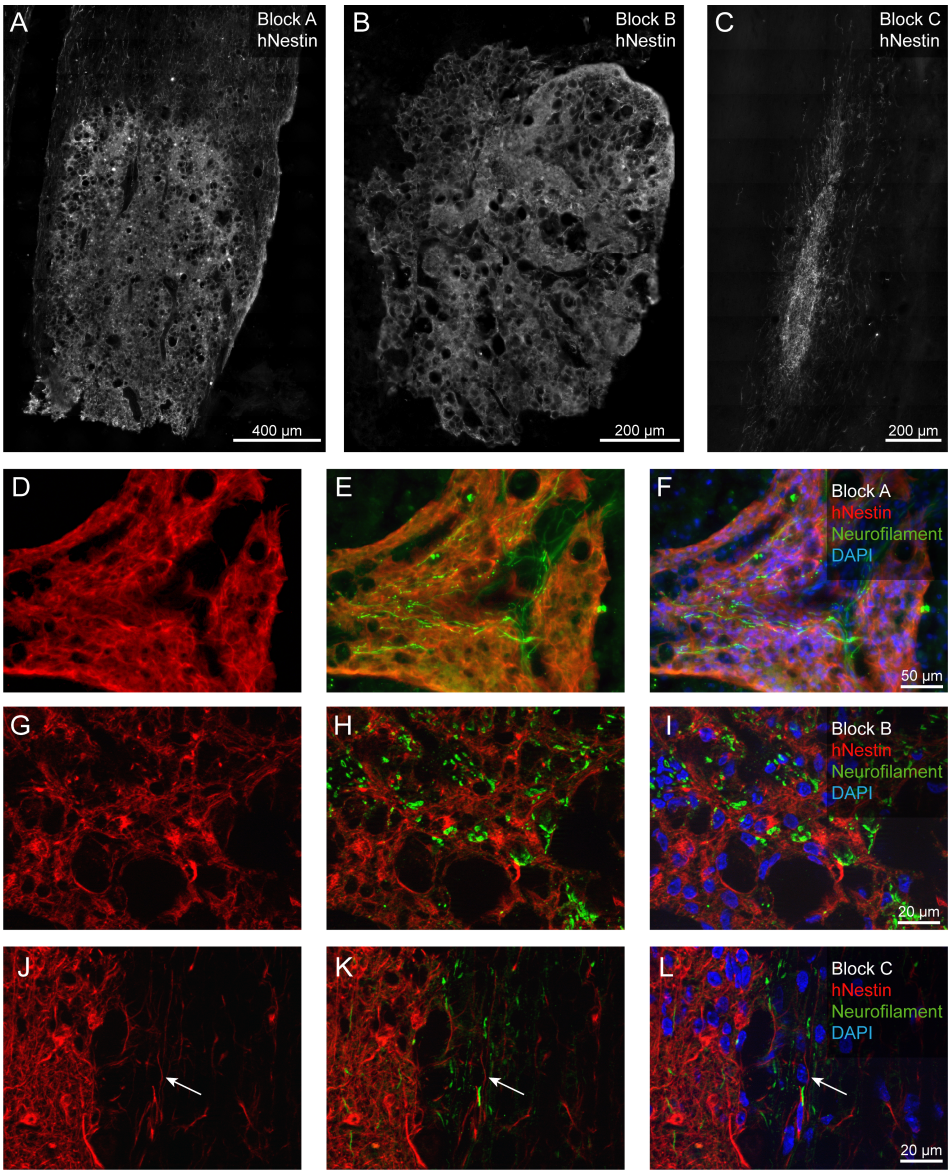

Figure 4.6.: *Regenerating neurites grow along transplanted hNP-AC.* **A-C:** Low magnification image showing the distribution of the hNP-AC at the different transplantation sites (i.e. rostral to- (A), within- (B) and caudal to- (C) the lesion site). The human nestin staining reveals a dense network of donor cells, sometimes elongated, which follows the longitudinal axis of the spinal cord *(C)*. **D-L:** Higher magnification images demonstrating a close spatial relationship between regenerating, neurofilament-positive neurites (green) and the transplanted hNP-AC (human nestin, red) rostral to- *(D-F)*, within- *(G-I)* and caudal to- *(J-L)* to the lesion site. Individual elongated human nestin-positive cells with intermingling processes which followed the longitudinal orientation of the spinal cord (arrows, *J-L*) can be found next to the dense cluster of donor cells.

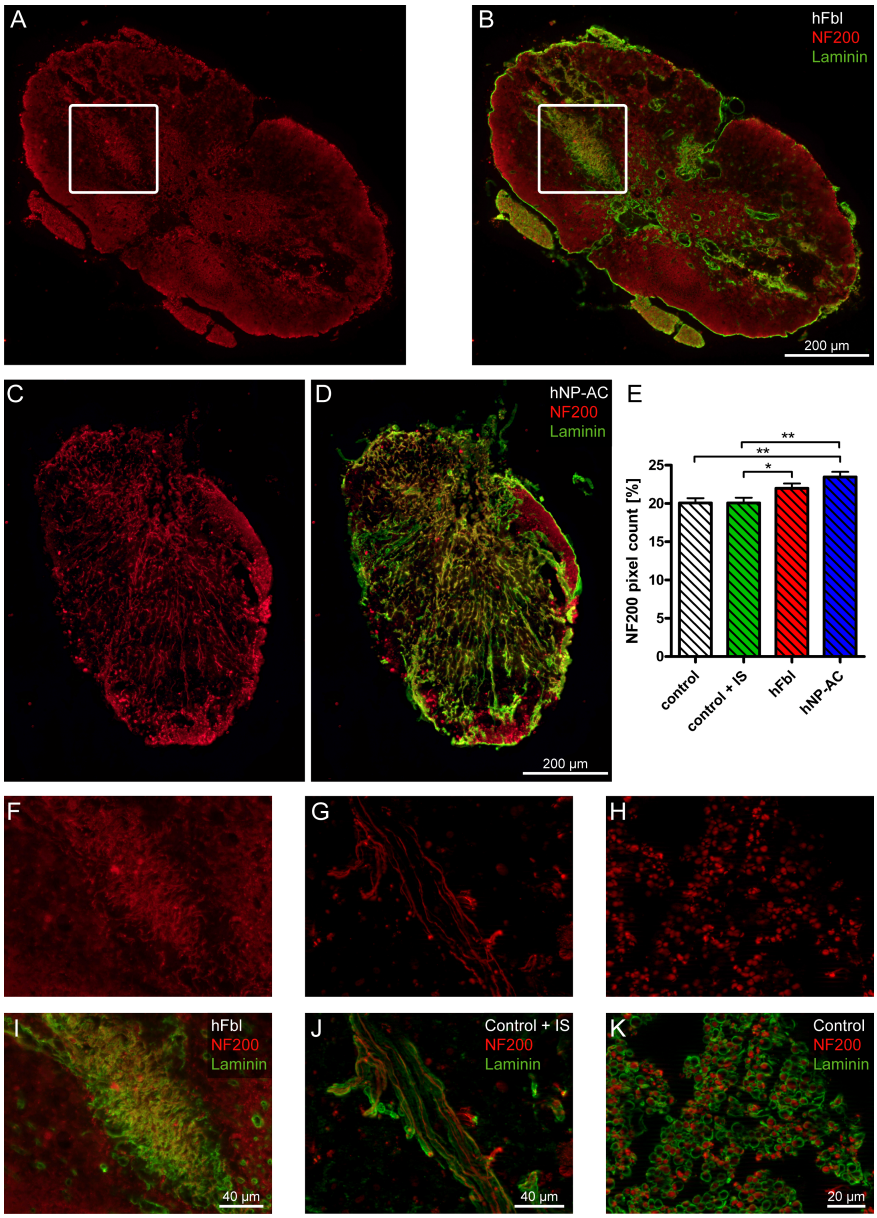

Figure 4.7.: *Donor hNP-AC-grafted animals demonstrate enhanced axonal growth into the lesion site.* **A, B:** Example of a neurofilament- (red) and laminin- (green) staining on a transverse section caudal to the lesion epicentre. The neurofilament immunoreactivity is evenly distributed throughout the whole section, whereas the laminin demonstrates a patchy distribution, apart from one concentrated elliptical region - highlighted (white box shown in greater magnification in *F, I*). **C, D:** Close the lesion epicentre, the neurofilament-positive regenerating axons demonstrate a high degree of colocalisation with the laminin-positive substrate. **F, I:** Higher magnification of the highlighted area in *A, B* showing that the spot of highly concentrated laminin also contains a large amount of neurofilament-positive axons. **G, H, J, K:** The close relationship between laminin-positive and neurofilament-positive structures can be found throughout the sections close to the lesion epicentre. Such relationships can be observed for axons following the orientation of the spinal cord *(H, K)* and also for those growing perpendicular to it *(G, J)*. **E:** Evaluation of the amount of pixel stained for neurofilament immunoreactivity shows that donor hNP-AC promote the greatest in-growth of neurites into the lesion site, which reaches statistical significance over the control and the control + IS groups (** $p < 0.01$), but not over the donor hFbl group ($p > 0.05$). Donor hFbl group demonstrates a significantly greater amount of neurofilament-positive pixels than the control + IS group (* $p < 0.05$, control, control + IS and hNP-AC: n=8, hFbl: n=7).

Schwann Cell Migration into the Lesion Site

Schwann cells (p75-positive host cells) migrated in high numbers into the lesion site (e.g. Figure 4.8A, B). Furthermore an accumulation of p75-positive cells could be found in close relationship with the elliptical cluster of intense fibronectin-immunoreactivity in the hFbl transplanted animals(presumably reflecting clusters of transplanted hFbl) (Figure 4.8C, D). Quantification of the amount of positively stained p75 pixels revealed that the transplantation of hFbl (26.2±0.7%) promoted a signficantly greater Schwann cell migration into the lesion site compared to the other groups ($p < 0.05$ compared to control (24.2±0.5%) and hNP-AC (24±0.5%), $p < 0.01$ compared to control + IS (23.8±0.4%); Figure 4.8G). Transplantation of hNP-AC did not change the amount of p75-positive profiles within the lesion compared to the control and control + IS groups. However, similar to donor hFbl, a close relationship between migrating Schwann cells and donor hNP-AC could be found ($p > 0.05$; Figure 4.8E-F).

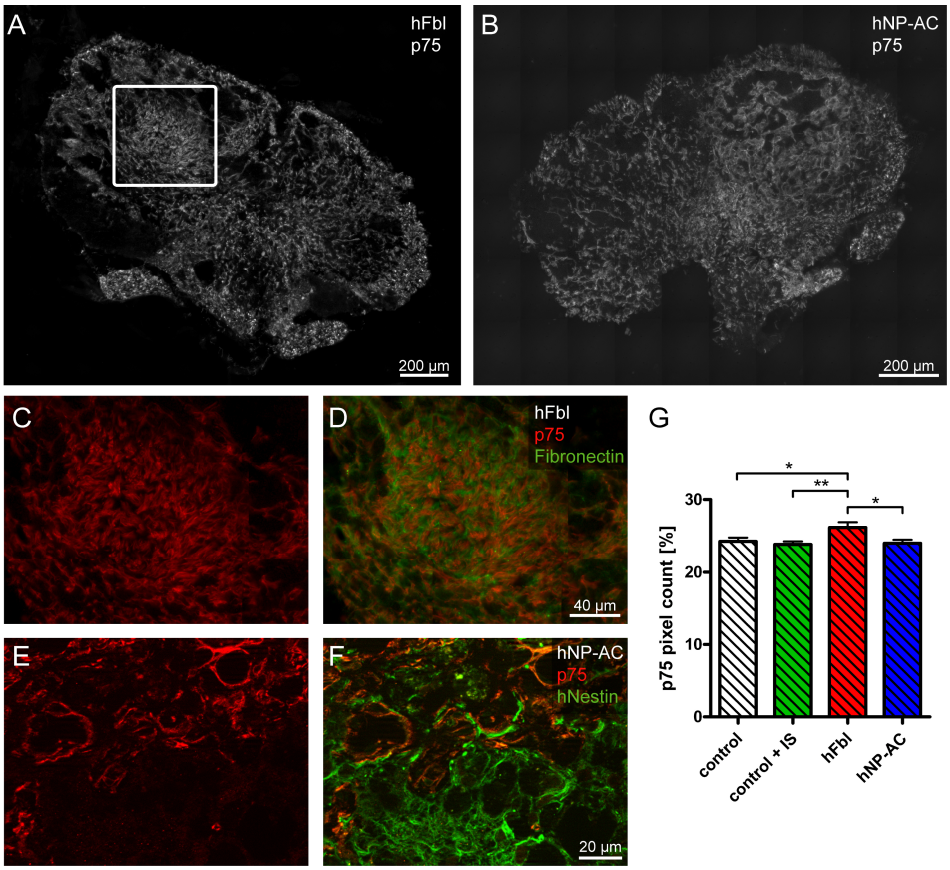

Figure 4.8.: *Schwann cell migration into the lesion site is enhanced by the presence of donor hFbl.* **A, B:** Low magnification images providing an overview of p75-positive Schwann cell migration into the lesion site of animals receiving donor hFbl *(A)* and donor hNP-AC *(B)* cells (control and control + IS groups were similar to the hNP-AC group and are therefore not shown). The highlighted area (white box, *A*) shows an elliptically shaped accumulation of p75-positive cells that is demonstrated at higher magnification in *C, D,* where a close intermingling with fibronectin-immunoreactivity can be seen. **E, F:** Higher magnification demonstrates the close interactions of human nestin- and p75-positive cells. **G:** Estimation of the amount of Schwann cell migration into the lesion site shows that transplantation of donor hFbl promotes a significantly greater degree of Schwann cell migration than seen in any other group (* $p < 0.05$, ** $p < 0.01$). Transplantation of hNP-AC does not change the amount of Schwann cell migration compared to the control and control + IS groups ($p > 0.05$; control, control + IS and hNP-AC: n=8, hFbl: n=7 animals).

GFAP and CSPG Immunoreactivity at the Lesion Site

Reactive host astrocytes (e.g. in the spared white matter) expressed GFAP and CSPG (Figure 4.9A-C). Similary, grafted astrocytes (identified by human nuclei on an adjacent section) also expressed both proteins (Figure 4.9D-F). Nonetheless, CSPG was not exclusivly expressed by astrocytes; GFAP-negative areas at the lesion site also included CSPG expressing cells (presumably host fibroblasts and Schwann cells) (Figure 4.9G-I). Furthermore, the expression of CSPG was especially strong at the elliptical cluster of transplanted

hFbl (Figure 4.9J-L). Evaluation of the intensity of GFAP and CSPG expression demonstrated that transplanted hNP-AC reduced the amount of both proteins compared to the control and the control + IS groups (0.36±0.01, $p < 0.01$ compared to control: 0.48±0.02 and control + IS: 0.46±0.02 groups for GFAP, 0.97±0.01, $p < 0.01$ compared to the control: 1.1±0.02 and $p < 0.05$ compared to control + IS: 1.03±0.02 for CSPG). However, although there was a clear trend for reduced GFAP and CGSP expression in comparison to donor hFbl, the levels never achieved statistical significance ($p > 0.05$, GFAP: 0.41±0.02, CSPG: 1.03±0.02; Figure 4.9M,N). Interestingly, transplantation of hFbl also led to reduced overall GFAP and CSPG levels, despite the high expression of CSPG at the elliptical clusters. However this reduction only reached statistical significance when compared to the control group ($p < 0.01$; Figure 4.9M,N).

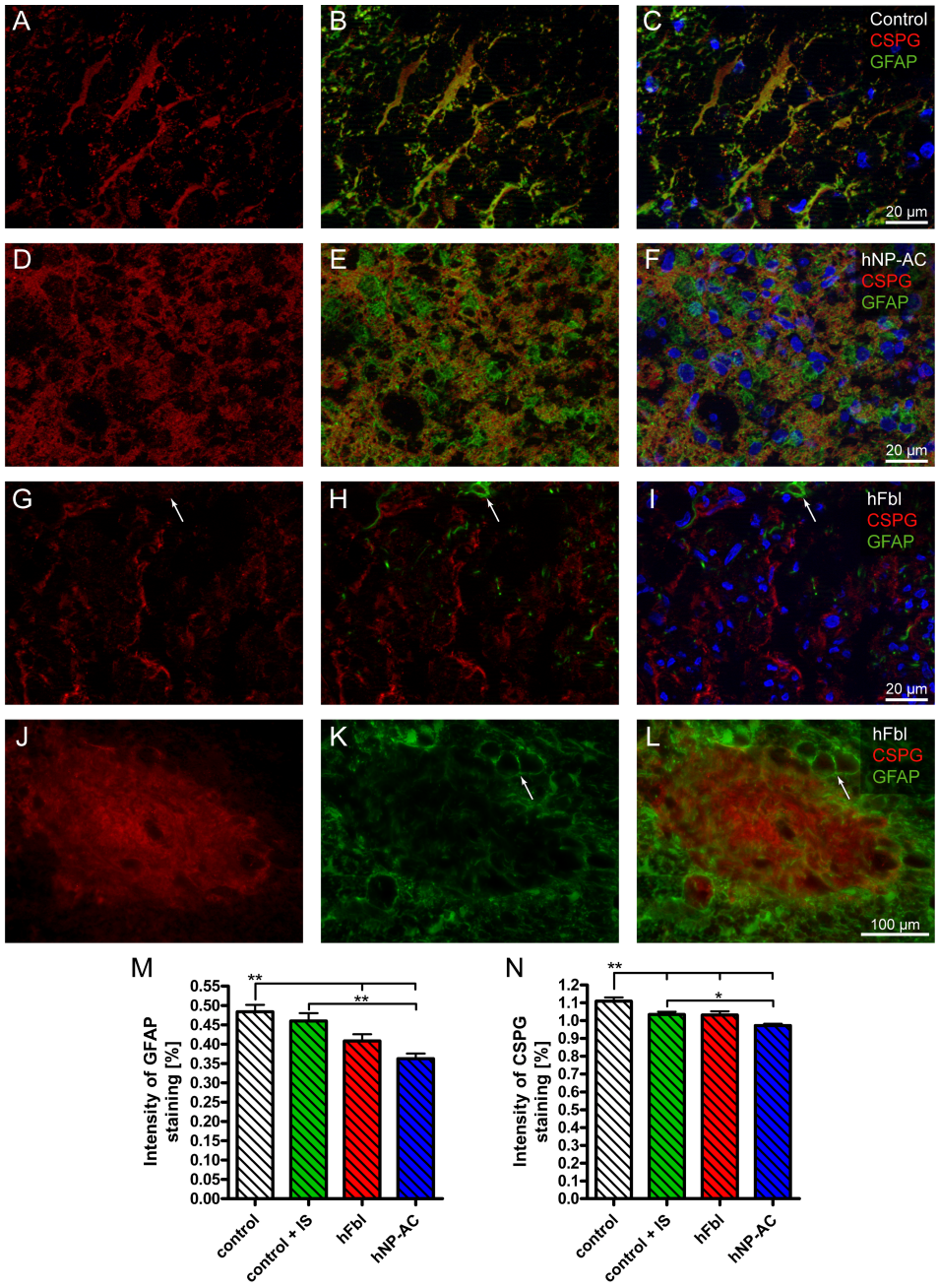

Figure 4.9.: *Donor hNP-AC reduce the amount of intensity of CSPG and GFAP staining at the lesion site.* **A-C:** Reactive host white matter astrocytes (stained for GFAP, green) express CSPG (red). **D-F:** Transplanted hNP-AC (region identified by human nuclei-positive cells in the same area of an adjacent section) also express CSPG. **G-I:** GFAP-negative, CSPG-positive areas demonstrate that GFAP-positive cells are not the only CSPG expressing cells to be found in the samples. Furthermore GFAP-positive cells do not necessarily express large amounts of CSPG (arrows). **J-L:** Transplanted hFbl (region identified by human nuclei-positive cells in the same area of an adjacent section; note the typical elliptical transplant form) also express CSPG. The rounded profiles of astrocytic GFAP (green, arrows in *K* and *L*) demonstrate the isolation and compartmentalisation of the donor fibroblasts by the host tissue. **M, N:** Transplantation of hNP-AC lead to a significant reduction in the intensity of the GFAP *(M)* and CSPG *(N)* staining compared to the control and the control + IS groups (** $p < 0.01$, * $p < 0.05$), but not compared to the donor hFbl group ($p > 0.05$; control, control + IS and hNP-AC: n=8, hFbl: n=7 animals).

Inflammatory Response at the Lesion Site

Iba1-positive macrophages/microglia could be found throughout the lesioned spinal cord (Figure 4.10A,B). At high magnification, the Iba-positive cells could be differentiated by their rounded morphology (Figure 4.10C), sometimes including cell debris (Figure 4.10D), which appeared throughout the section at the lesion epicentre as well as in areas further away, such as white matter tracts undergoing Wallerian degeneration. A ramified morphology was observed, predominantely in the spared grey matter (Figure 4.10E). Evaluation of Iba1-immunoreactivity showed a statistically significant increase for the rounded cells for the control + IS group compared to all groups ($p < 0.01$, control + IS: 0.29±0.01, control: 0.22±0.01, hFbl: 0.23±0.01, hNP-AC: 0.23±0.01) and an increase for the ramified cells compared to the control and the hNP-AC group ($p < 0.01$, control + IS: 0.25±0.01, control: 0.20±0.01, hFbl: 0.23±0.01, hNP-AC: 0.21±0.01; Figure 4.10F). Furthermore the hFbl group demonstrated a higher immunoreactivity for the ramified cells compared to the control ($p < 0.05$; Figure 4.10F).

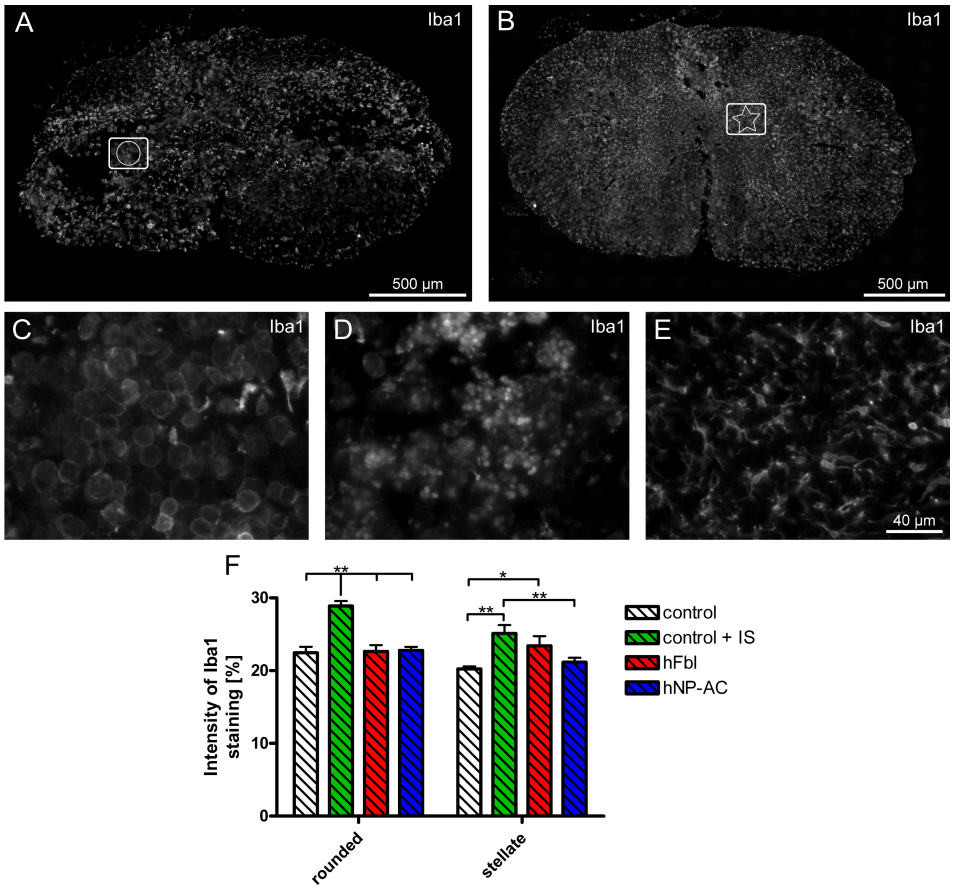

Figure 4.10.: *Iba1 immunoreactivity is increased in the presence of immunosuppression.* **A, B:** Low magnification images of Iba1 close to- *(A)* and caudal to *(B)* the lesion epicenter. Iba1-positive cells can be found throughout the sections. Highlighted areas (white boxes) are shown in higher magnification in **C-E:** The Iba1-positive cells can be broadly divided by their rounded *(C)* or ramified *(E)* morphology. Cells with high amounts of debri *(D)* are included into the rounded group. Cells with rounded morphology are mainly located throughout the sections at the lesion epicentre, but distant from the lesion can be found in the white matter (white box with circle, *A*) whereas cells with the more ramified morphology can be located in the grey matter (white box with asterisk, *B*). **F:** Evaluation of Iba1 immunoreactivity shows a significant increase of the intensity for the control + IS group compared to all groups for the rounded cells (** $p < 0.01$) and an increase compared to the control and the donor hNP-AC group for the ramified cells (** $p < 0.01$). Furthermore, the donor hFbl group demonstrates a higher immunoreactivity for the ramified cells compared to the control (* $p < 0.05$; control, control + IS and hNP-AC: n=8, hFbl: n=7 animals).

Spared Tissue

Only a limited area, if any, of spared tissue could be found at the lesion epicenter of all groups (as indicated by white outlines with shaded areas; Figure 4.11A-E). The amount of spared tissue was enhanced when hFbl were transplanted. This increased tissue sparing reached the level of statistical significance when compared to controls at the epicentre and at -800 μm (epicentre: hFbl: 0.04±0.02, control: 0.0±0.0; -800 μm: hFbl: 0.12±0.05, control: 0.02±0.01; $p < 0.05$) and to the hNP-AC treated animals at 1200 μm epicentre, -400 μm, -800 μm, and -1200 μm (1200 μm: hFbl: 0.1±0.03, hNP-AC: 0.01±0.0; epicentre: hFbl: 0.04±0.02, hNP-AC: 0.0±0.0; -400 μm: hFbl: 0.07±0.03, hNP-AC: 0.0±0.0; -800 μm: hFbl: 0.12±0.05, hNP-AC: 0.0±0.0; -1200 μm: hFbl: 0.12±0.05, hNP-AC: 0.02±0.01; $p < 0.05$). No other statistically significant differences were observed. With increasing distance to the lesion epicentre, rostral and caudal, the amount of spared tissue increased, with reoccurrence of spared grey matter as well (data not shown).

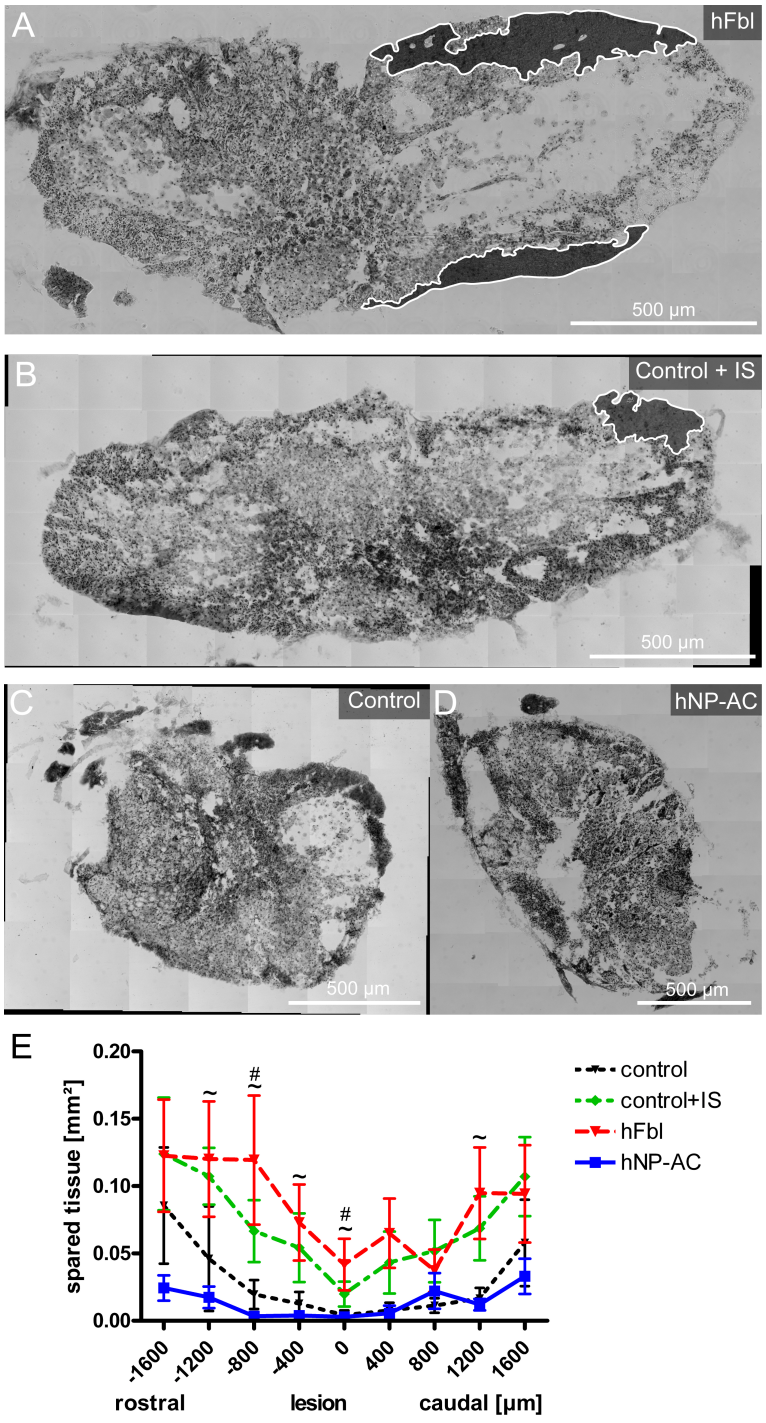

Figure 4.11.: *Transplantation of hFbl excert tissue sparing effects.* **A-D:** Thionin staining of the lesion epicentre for donor hFbl *(A)*, control + IS *(B)*, control *(C)* and donor hNP-AC *(D)* groups. White outlines with shaded areas indicate areas of spared tissue as assessed by inspection of high magnification images *(A, B)*. **E:** Quantification of the amount of spared tissue. Donor hFbl treated animals reveal a significantly greater amount of spared tissue compared to the control group (epicentre, -800 μm; $^{\#}$: $p < 0.05$) and to the hNP-AC group (1200 μm epicentre, -400 μm, -800 μm, -1200 μm; $^{\sim}$: $p < 0.05$; control, control + IS and hNP-AC: n=8, hFbl: n=7 animals).

4.2.3. Tissue Engineering Approach to Promote Repair after Lateral Funiculotomy of the Thoracic Spinal Cord

Behavioural Analysis

Catwalk: All animals (for a list of animal numbers per experimental group, see Table 2.4) were able to support their weight and walk in a coordinated manner 4 weeks after injury, as indicated by the regularity index (i.e. the use of normal step sequence patterns during uninterrupted locomotion) and the stride length, which remained unchanged after injury and scaffold transplantation ($p > 0.05$; Figure 4.12A, B).

Determination of the base of support (BOS) indicated that there was a progressive reduction of the distance between the fore-paws of all experimental groups, which by 8 weeks was significantly different from their pre-injury baseline levels ($p < 0.01$ for all groups). Surprisingly, the fore-paw BOS data for the group receiving hFbl-seeded scaffolds was significantly better (i.e. closer to baseline levels) than that of the group receiving hNP-AC seeded scaffolds ($p < 0.01$). Apart from the above observation, no other differences could be detected between the groups (Figure 4.12C). In contrast to the fore-limb data, the BOS for the hind-limbs all showed an increase in the inter-limb distance in comparison to their pre-surgery baseline levels. Similar to the BOS of the front-paws, the group receiving hFbl-seeded scaffolds was significantly better than the hNP-AC group, and showed no statistically significant difference from the baseline levels. Surprisingly even the control + IS group showed recovery levels that were not statistically different from the baseline (Figure 4.12D).

Print area (complete area covered during the whole stance phase, equivalent to the footprint), max area (largest area in contact with the floor at one particular time point during stance) and the intensity (average intensity of max area) of the affected hind-limb of all groups were significantly reduced by 4 weeks in comparison to the pre-surgery baseline levels ($p < 0.01$; Figure 4.12E-G). Interestingly, the groups receiving cell-seeded scaffolds (i.e. hFbl and hNP-AC) both showed significantly better performances than the empty scaffold + IS control group. All groups subsequently showed a trend for improved function between 4 and 8 weeks to the extent that there were no longer any significant differences between the groups for print area or max area (Figure 4.12E-F). However the values for the recovery of intensity

of paw placement were much better in the group receiving hNP-AC seeded scaffolds, to the extent that by 8 weeks the data for this group was still significantly greater than that of the scaffold plus IS control group and the hFbl-seeded scaffold group ($p < 0.01$ and $p < 0.05$ respectively; Figure 4.12G).

The data for the duty cycle (stance duration divided by the sum of stance and swing duration) and the stance duration showed very similar patterns of recovery. All groups demonstrated a significant reduction in comparison to the pre-surgery baseline values ($p < 0.01$ for all groups). However by 4 weeks post implantation, animal groups receiving hFbl-seeded scaffolds and hNP-AC seeded scaffolds demonstrated a significantly improved duty cycle in comparison to the empty scaffold + IS controls ($p < 0.05$; Figure 4.12H). Improvement in duty cycle values progressed to the extent that, by 8 weeks, all groups remained below pre-implantation baseline values, but the data obtained for groups receiving cell-seeded scaffolds were no longer significantly better than those of the empty scaffold + IS control group. An almost identical pattern of recovery was observed for the stance duration data except that at 4 week post implantation, the group receiving hNP-AC seeded scaffolds had failed to show a significantly greater improvement than that seen in the empty scaffold + IS control group (Figure 4.12I). For swing duration, all animal groups demonstrated a significant increase by 4 weeks in comparison to the baseline levels ($p < 0.01$ for all groups), however, once again, groups receiving the cell-seeded scaffolds performed significantly better than the control + IS group ($p < 0.05$ for both seeded scaffold implantation groups in comparison to the non-seeded control scaffold). Recovery of performance was prominent in all groups between 4 and 8 weeks but none of the groups reached pre-surgery baseline levels. However, by 8 weeks only the hFbl-seeded scaffold group showed a significant improvement in relation to the control scaffold + IS group ($p < 0.05$; Figure 4.12J).

Gridwalk: Similar functional trends were observed in the gridwalk analysis as were observed with the CatWalk. All groups demonstrated a significant increase in the number of footfalls by 4 weeks post surgery ($p < 0\ .01$ for all groups; Figure 4.13A). However, both groups receiving cell-seeded scaffolds showed a significantly better performance than demonstrated by the control group receiving the empty scaffold + IS ($p < 0.05$ for both cell-seeded scaffold groups). Progressive recovery between 4-8 weeks was evident in the control + IS group as well as the group receiving hFbl-seeded scaffolds but not in the hNP-AC seeded

scaffold group. Values for all groups at 8 weeks post surgery were still below the initial baseline values, but no significant differences could be detected between individual groups (Figure 4.13A)

Von Frey filaments: Evaluation of the potential development of allodynia with the von Frey filaments was performed in all 4 paws over the 8 week investigation period. The values obtained for all groups showed substantial variability, to the extent that no statistically significant effects could be demonstrated at any time point ($p > 0.05$; Figure 4.14A-D).

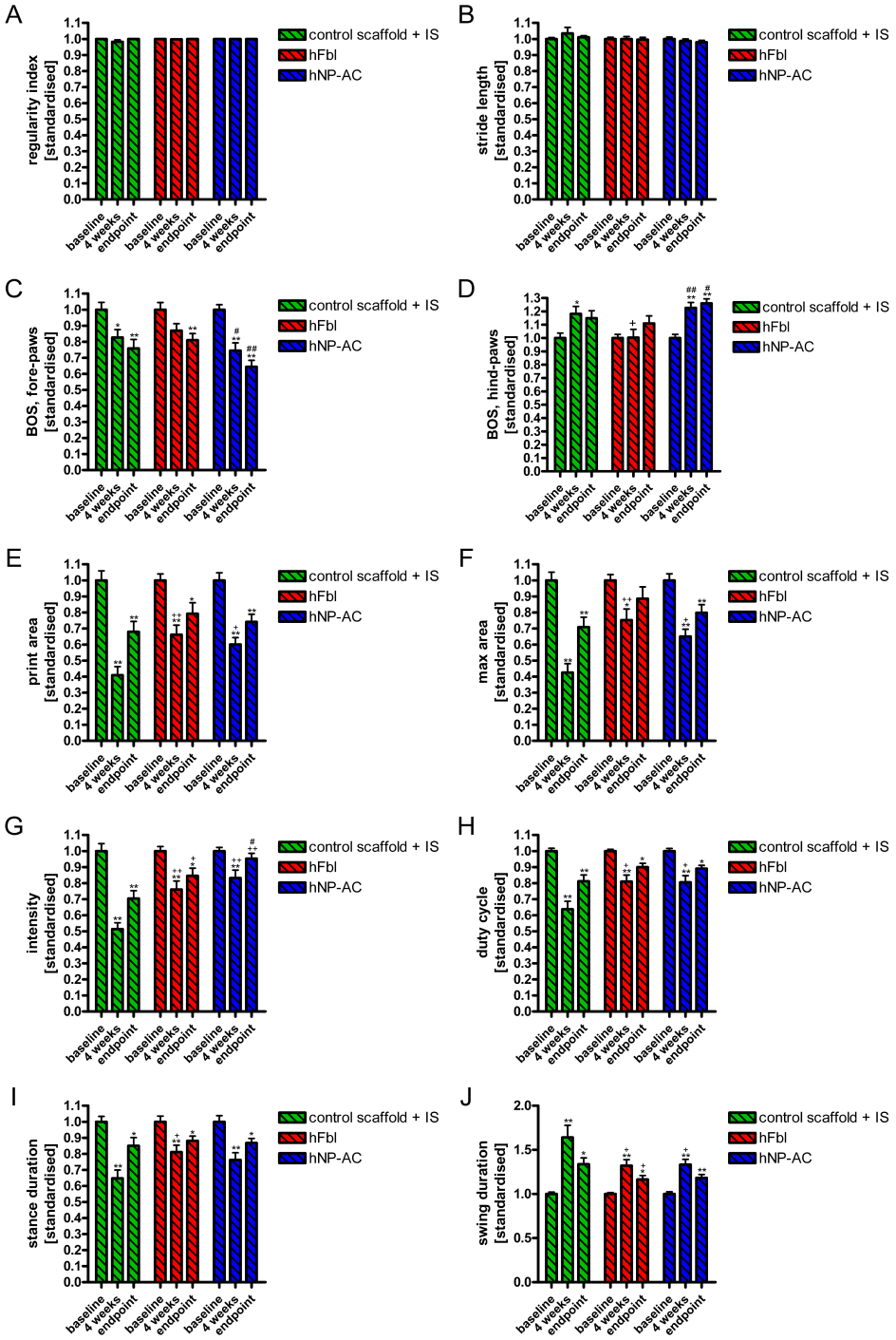

Figure 4.12.: *No recovery of function can be detected after implantation of non-seeded- or cell-seeded scaffolds.* **A, B:** The regularity index and stride length remained unchanged after injury and after scaffold implantation. **C, E, F, G, H, I:** Values for the base of support (BOS) of the fore-paws, print area, max area, intensity (with the exception of the hNP-AC group at the end-point), duty cycle and the stance duration all show reduced values after injury (4 weeks) with a small tendency to recovery back to the (pre-lesion) baseline values. The BOS for the fore-paws reveals a more pronounced narrowing *(C)*. **D, J:** The values for the BOS of the hind-paws and the swing duration increase after injury and show no signs of recovery during the investigation (** $p < 0.01$, * $p < 0.05$ compared to the baseline; $^{++}$ $p < 0.01$, $^{+}$ $p < 0.05$ compared to the control + IS group; ## $p < 0.01$, # $p < 0.05$ compared to the donor hFbl group for all graphs; control + IS: n=9, hFbl: n=10, hNP-AC: n=11 animals).

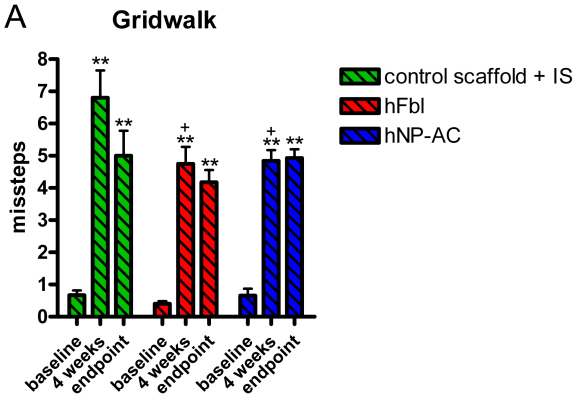

Figure 4.13.: *Cell transplantation increases recovery of fine motor coordination during intermediate time points.* Transplantation of either hFbl or hNP-AC lead to a significant improvement in the number of foot-falls in comparison to the control + IS group by 4 weeks. However, the extent of improvement is no longer significant in comparison to the control + IS group by the end-point. Recovery fails to reach (pre-lesion) baseline values (** $p < 0.01$, compared to the baseline; $^{+}$ $p < 0.05$ compared to the control + IS; control + IS: n=9, hFbl: n=10, hNP-AC: n=11 animals).

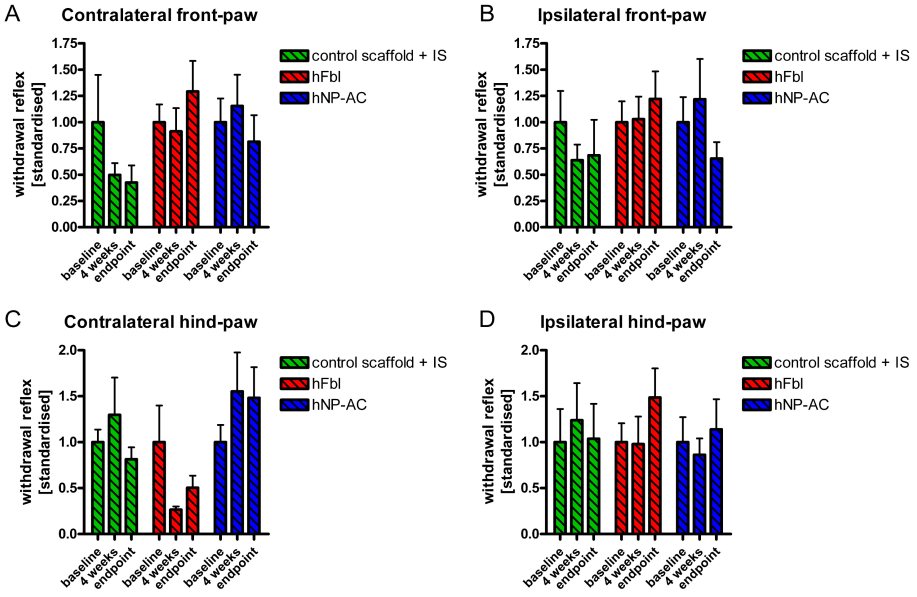

Figure 4.14.: *Evaluation with von Frey filaments shows no signs of allodynia after injury in all groups.* **A-D:** Standardised withdrawal reflex for all four paws. No statistically significant difference can be found at any time point ($p > 0.05$; control + IS: n=9, hFbl: n=10, hNP-AC: n=11 animals).

Survival of Transplanted Cells

In only 10% of the grafted animals could a few human nuclei-positive donor cells be found following implantation of the hFbl-seeded scaffolds. However, the scaffold still demonstrated

an intense staining for the ECM molecule, fibronectin (Figure 4.15A-C, J). Many human nuclei-negative host cells could be found in the immediate vicinity of the donor cells. There was no indication of donor cell migration out of the scaffolds. In contrast, a much better degree of donor cell survival was observed following the implantation of hNP-AC seeded scaffolds (human nuclei-positive donor cells could be found in 55% of the transplanted animals (Figure 4.15D-F, J). Similar to the earlier *in vitro* observations, the donor cells appeared to redistribute themselves and form orientated columns within the scaffolds (Figure 4.15D-F). Nonetheless the amount of surviving cells visible in each section was normally quite low. Furthermore, use of anti-human nestin immunohistochemistry demonstrated that not all donor cells remained within the scaffolds. Individual hNP-AC could be identified within the host white matter, close to the implant, where they had adopted an elongated, (probably) migratory morphology (Figure 4.15G-I).

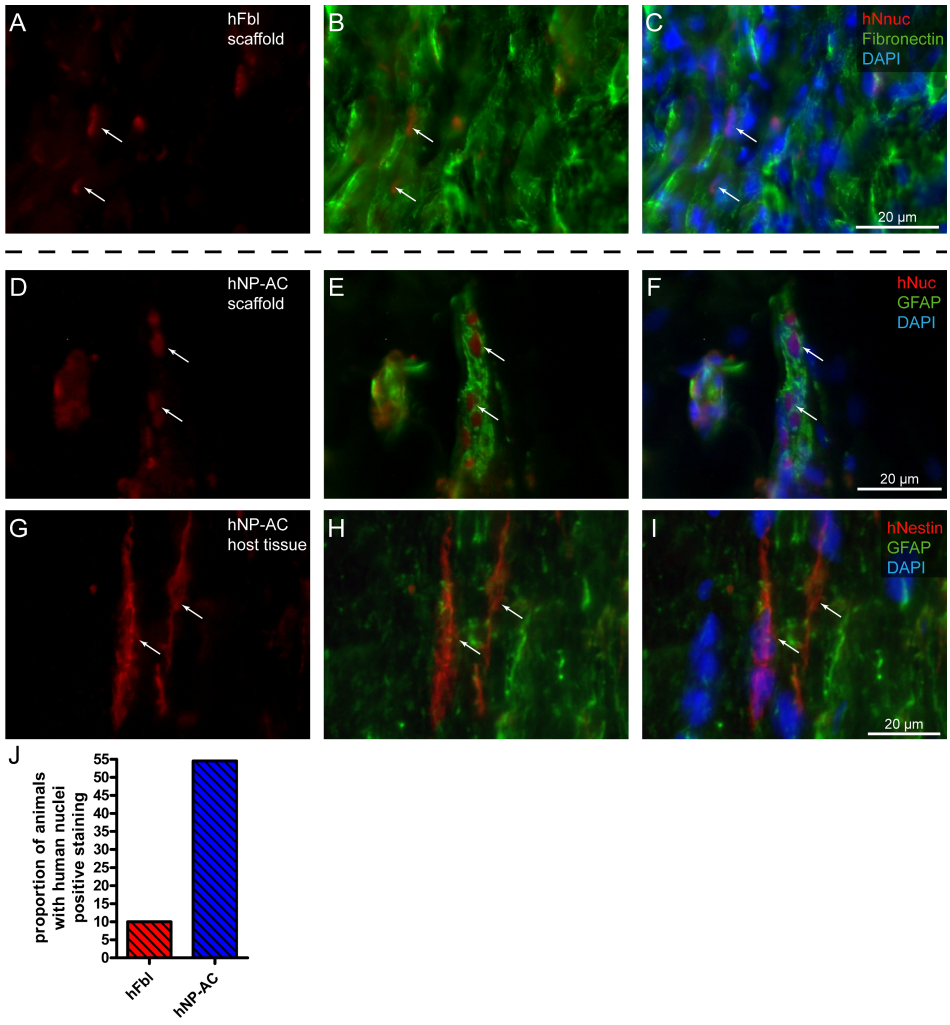

Figure 4.15.: *Implantation of cell-seeded scaffolds into lateral funiculotomies results in only limited donor cell survival.* **A-C:** Only few human nuclei-positive (hNuc) donor cells can be found inside of the hFbl-seeded scaffolds after implantation (arrows). Nonetheless, implanted scaffolds show an intense, evenly distributed, staining for fibronectin. **D-F:** Human nuclei-positive donor hNP-AC cells form columns within the scaffolds (arrows). **G-I:** Furthermore, they may be identified as elongated, migratory cells inside of the adjacent host tissues using antibodies to human nestin (hNestin, arrows). **J:** Only a limited numbers of host animals receiving hFbl-seeded scaffolds show viable human nuclei-positive cells after implantation. In contrast, over 50% of host animals receiving hNP-AC-seeded scaffolds show viable hNuc / hNestin-positive cells (hFbl: n=10, hNP-AC: n=11 animals).

Regeneration of NF200 Positive Axons into the Scaffold

Host axons were able to regenerate into empty and cell-seeded scaffolds. Regenetrating axons clearly followed the orientation of the pores (Figure 4.16A-C). Whereas no clear cell-guided growth could be found in the hFbl and control + IS groups, higher magnification of a hNP-AC-seeded scaffold demonstrated the ability of regenerating axons to grow along GFAP-positive cells within the scaffold, as well as along GFAP-negative areas (Figure 4.16B,

C). Since the survival of transplanted hNP-AC was rather low, most NF-positive axons must have been growing along host GFAP-positive profiles. However, it was clear that donor hNP-AC-seeded scaffolds had promoted a significant increase in the number of regenetrating axons inside of the scaffold, compared to the control empty scaffold + IS group, ($p < 0.05$; Figure 4.16D). The hFbl-seeded scaffold supported axon growth that was intermediate in extent between the values observed for the hNP-AC-seeded and empty scaffolds ($p > 0.05$).

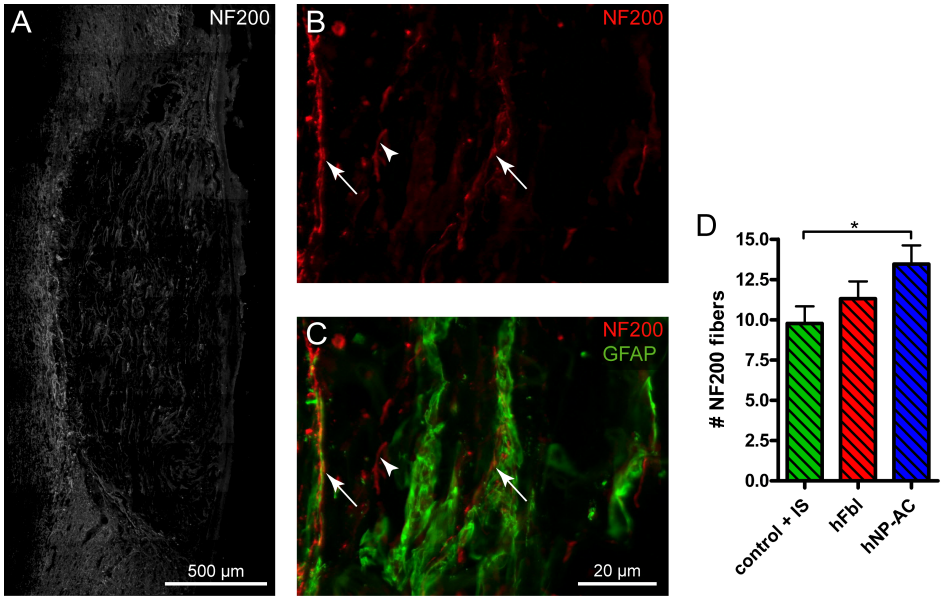

Figure 4.16.: *Implantation of hNP-AC-seeded scaffolds promotes enhanced axon regeneration into the scaffold.* **A:** Example of axon regeneration into the scaffold. The regenerating axons follow the longitudinal orientation of the microchannels within the scaffold in all groups. **B, C:** Higher magnification of an hNP-AC-seeded scaffold demonstrates the ability of axons to grow along GFAP-positive cells (arrows) as well as along GFAP-negative areas (arrowhead). **D:** Quantification of axon regeneration into implanted scaffolds at three different positions (100 μm from the rostral- and caudal- graft-host interface and also at the scaffold midline). hNP-AC seeded scaffolds induce a significantly greater extent of axon regeneration compared to the control group (* $p < 0.05$; control + IS: n=9, hFbl: n=10, hNP-AC: n=11 animals).

GFAP and CSPG Immunoreactivity

Low magnification overview of GFAP stained sections of control + IS (Figure 4.17A), hFbl-seeded (Figure 4.17B) and hNP-AC-seeded (Figure 4.17C) scaffolds highlighted the marked increase of GFAP-positive profiles within the hNP-AC seeded scaffolds, the orientation of which generally followed the longitudinal orientation of the scaffold's pores. Since the GFAP-positive columns could also be found in areas of the scaffold where no human nuclei-positive cells could be demonstrated or even in animals with no identifiable human nuclei at all, it is

likely that such profiles were due to the infiltration of host astrocytic processes. The highly sulphated proteoglycan, CSPG, was clearly associated with the GFAP-positive cells (Figure 4.17G-I), but could also be found in GFAP-negative areas (Figure 4.17D-F). Quantification of the intensity of immunoreactivity revealed that the empty scaffold + IS group demonstrated the greatest degree of astrocytic reactivity (as revealed by increased GFAP expression at the implant host interface). The implantation of either cell-seeded scaffold into the lesioned spinal cord resulted in a significantly reduced intensity of GFAP immunoreactivity in these regions compared to the control + IS group ($p < 0.01$; Figure 4.17J). Quantification of the intensity of CSPG immunoreactivity also revealed that the control + IS group had the highest expression of CSPG. Although both groups that received cell-seeded scaffolds showed reduced mean values in comparison to the control + IS group, only the values for the hFbl-seeded scaffold group reached the level of statistical significance ($p < 0.05$; Figure 4.17K).

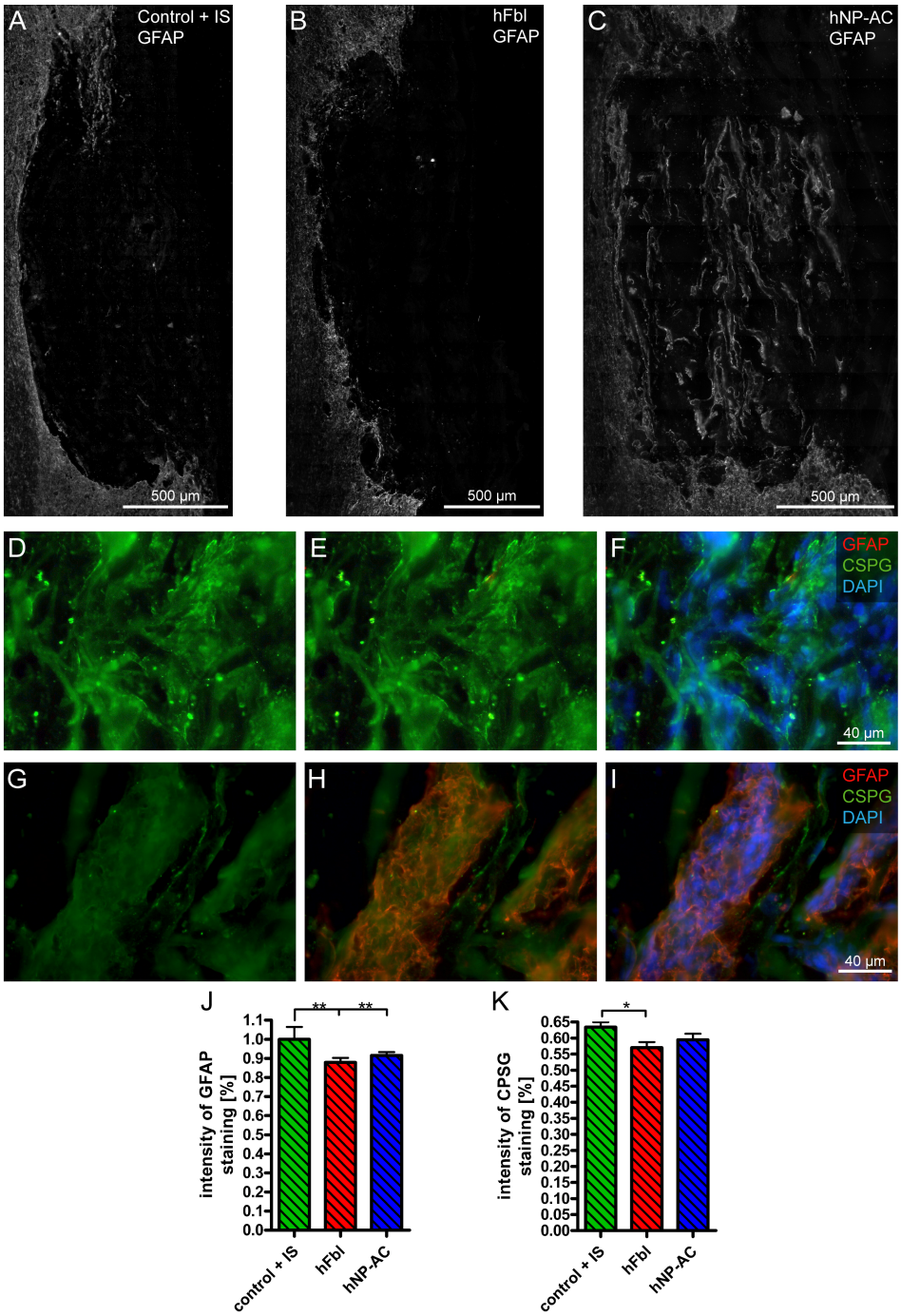

Figure 4.17.: *hNP-AC-seeded scaffolds improve host astrocytic integration.* **A-C:** Low magnification images of GFAP immunohistochemistry in non-seeded- (control + IS, *A*), hFbl-seeded- (*B*) and hNP-AC-seeded- (*C*) scaffolds. The high numbers of GFAP-positive processes within the scaffold and following the orientation of the microchannels, are clearly visible in the hNP-AC-seeded scaffolds (*C*). The extent of GFAP immunoreactivity inside the scaffolds is the same whether implants contain viable donor cells or not (identified by human nuclei staining). **D-F:** CSPG can be found in GFAP-negative areas of hNP-AC-seeded scaffolds (as well as inside of control + IS and hFbl-seeded scaffolds). **G-I:** GFAP-positive columns inside of the scaffold express CSPG. **J:** Cell seeding of the scaffold leads to a reduced intensity of GFAP staining compared to the non-seeded scaffold group (** $p < 0.01$). **K:** The intensity of CSPG staining is reduced for the hFbl-seeded scaffolds compared to the control + IS group (* $p < 0.05$; control + IS: n=9, hFbl: n=10, hNP-AC: n=11 animals).

Inflammatory Response

Immunohistochemistry for ED1 demonstrated cells with a rounded morphology (presumably macrophages) that could be found in the region of the host-scaffold interface (Figure 4.18A, C), with relatively few cells being found deep within the scaffold. The intensity of ED1 immunoreactivity was clearly greatest in the control group receiving the empty scaffold + IS treatment. Implantation of cell-seeded scaffolds reduced the intensity of ED1 immunoreactivity but only the values associated with the hNP-AC seeded scaffolds achieved the level of statistical significance ($p < 0.01$; Figure 4.18E). In stark contrast to the observations made with ED1 staining, Iba1-positive cells could be found throughout the host spinal cord as well as rounded cells at the host-scaffold interface and both rounded- and process bearing morphologies inside of the scaffold (Figure 4.18B). Higher magnification of Iba1-positive cells inside of the scaffold showed that the process bearing cells had adopted an elongated morphology, which followed the orientation of the pores (Figure 4.18D). This is in contrast to the more rounded morphology they show in the host tissue (Figure 4.18G). Both cell-seeded scaffold groups (i.e. hFbl and hNP-AC) demonstrated a reduced intensity of Iba1 staining compared to that seen in the control empty scaffold + IS group ($p < 0.01$; Figure 4.18F).

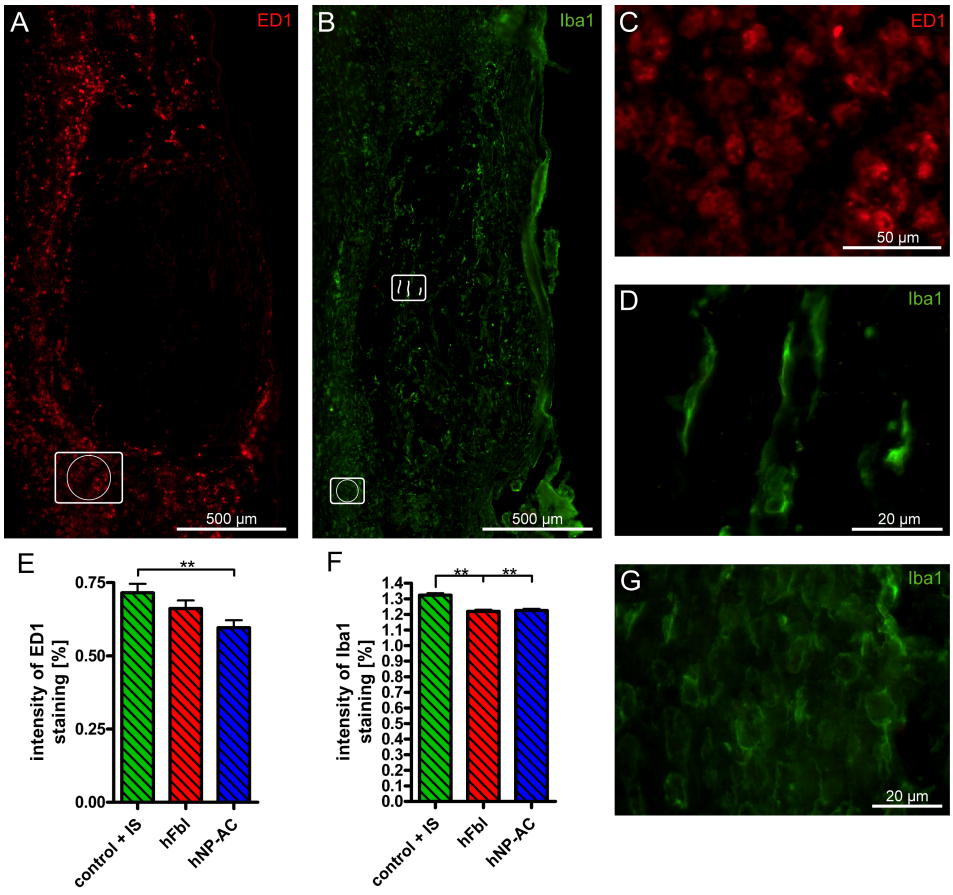

Figure 4.18.: *Implanted hNP-AC-seeded scaffolds modulate the host immune response.* **A:** ED1-positive cells can be found along the host-scaffold interface, but not within the scaffold. **B:** Iba1-positive cells can be found in the host spinal cord, at the interface and within the scaffold. **C:** High magnification of the highlighted area in A (white box with circle). ED1-positive cells demonstrate a rounded morphology. **D:** High magnification of Iba1-positive cells inside of the scaffold (white box with lines in *B*) shows that they adopt an elongated morphology, which follows the orientation of the pores. This is in contrast to the more rounded morphology they show in the host tissues (*G*, highlighted area in *B* (white box with circle)). **E:** Animals transplanted with hNP-AC-seeded scaffolds show a reduced intensity of ED1 compared to the control + IS group (** $p < 0.01$). **F:** Both cell-seeded groups (hFbl and hNP-AC) demonstrate a reduced intensity of Iba1 staining compared to the control + IS group (** $p < 0.01$; control + IS: n=9, hFbl: n=10, hNP-AC: n=11 animals).

4.3. Discussion

Biomaterial- and tissue engineering-based intervention strategies for the treatment of spinal cord injury (SCI) are a fast moving field with a broad range of research. In general, strategies for bridging SCI aim to replace damaged tissue with an axon growth promoting substrate that is able to integrate within the host tissue, supporting neural cell survival, and promoting axon regeneration and functional improvement. In early experimental studies autologous or

allogenic living tissue was used, comprising of foetal spinal cord tissue, peripheral nerve grafts or neuronal tissue [83, 98, 208, 213, 375, 383]. An alternative approach to promote axonal regeneration in SCI has been the transplantation of cell suspensions to bridge the cyst or spinal injury (for reviews see [31, 90, 114, 351, 466]). Most of these studies support some degree of CNS axon regeneration into the grafts, however, there are a number of ethical (e.g. embryonic or foetal tissue/cells) and practical concerns (e.g. the need for immunosuppression in case of allografts and donor site morbidity in case of autologous nerves) for all of these approaches [184, 374]. As the field of regenerative medicine has grown, the focus of many studies has shifted to include the development of artificial growth promoting scaffolds, using natural or synthetic polymers. In this study, the use of hNP-AC either alone (balloon compression injury model), or in combination with an orientated collagen scaffold (lateral funiculotomy, resection injury model) as a tissue engineering-based intervention strategy after spinal cord injury, have been investigated. In both models, we have described the functional outcome (BBB/Gridwalk and Catwalk/Gridwalk respectively), sensitivity (Hargreaves' heat sensitivity test and von Frey filaments respectively), survival of transplanted cells, amount of spared/regenerated axons as well as GFAP, CSPG and Iba1 immunoreactivity. Furthermore, the amount of p75-positive Schwann cell migration into the injury site and the amount of spared tissue were evaluated in the balloon compression injury model as well as ED1 immunoreactivity in the resection injury model.

Human SCI results from a variety of mechanical stresses applied to the spinal cord, but most commonly, acute traumatic SCI consists of both impaction (contusion-type injury) and persistent compression (maceration-type injury). We chose an experimental model of compression injury for our study because it reproduces many of the aspects of severe compression-type injuries seen in the clinical situation [271]. Although the lateral funiculotomy does not represent a common clinical model, it does to some extent reproduce changes caused by spinal cord laceration and allows us to use a more sophisticated intervention strategy; the implantation of the 3D orientated collagen scaffold as a replacement of the resected white matter. Furthermore, an advantage of these models is that animals subjected to experimental SCI show behavioural changes (including recovery) over a number of weeks, thereby allowing assessment of locomotor functions. The lateral funiculotomy model allowed for rapid recovery of postural control and therefore a more sophisticated type of analysis than

the balloon compression injury model (i.e. CatWalk gait analysis system). In any case, it is essential that the lesion model induces a reproducible deficit in at least one area of sensory, motor or autonomic function, otherwise, the model's value for assessing the effectiveness of particular intervention strategies would be compromised [89].

4.3.1. Characterization of hFbl

hFbl were chosen to serve as a "neutral" or control cell population and were characterised by the expression of vimentin, fibronectin and CSPG [72, 332, 333].

4.3.2. Comments on the behavioural analyses of both SCI models

Locomotor recovery after balloon compression injury was monitored using the BBB locomotor rating scale [30]. The CatWalk method is a gait analysis method that allows computer assisted quantification of a large number of locomotor parameters and was used to assess locomotor recovery after lateral funiculotomy [181, 241, 449]. Fine motor coordination was assessed using a horizontal wire grid (also known as the gridwalk) [247]. Furthermore it was important to include the evaluation of the potential development of neuropathic pain. Since grafted cells are intended to support axonal sprouting, synaptogenesis and the formation of new circuitry, it is difficult to exclude the possibility that the donor cells might also promote the formation of aberrant connections, which could cause unwanted side-effects such as enhanced pain perception (hyperalgesia) or the shifting of inocuous sensations to become painful (allodynia). However, the current sensory tests are difficult to interpret because they all depend on a functioning motor response (e.g. paw flexion withdrawal).

Transplantation of hNP-AC after the **balloon compression injury** promoted a better functional recovery (BBB score) compared to the control (lesion only) group, but not when compared to the control + IS group. Although the recovery of the control + IS group showed a trend of being lower than that of the cell implantation groups, it also showed a trend of being better than that of the control (lesion only) group. Interestingly and somewhat surprisingly, the cell control group (hFbl) performed better than the hNP-AC group. This pattern of behavioural responses was also supported by the gridwalk, where both cell implantation groups as well as the control + IS group performed better than the control

group. This demonstrated that all treatment groups revealed a better recovery of fine motor control than was seen in the untreated group. The resulting BBB score of the treated groups is in accordance with previous results for a 15 μl lesion (untreated), where a score of around 10 was achieved after 4 weeks. However, longer time points were not included in that particular study [443]. The slightly lower score in the controls used in the present study may be explained by the lower body weight of the animals and the resulting smaller size of the spinal canal (body weight of ∼270g in the present study compared to ∼315g in the published study [443]). Similar results were obtained with a 12 μl lesion, where the animals (∼315g) reached a BBB score of above 10 after 4 week, but which did not recover further [357]. The compression injury induced in the present study was probably to severe to allow for a better degree of spontaneous recovery and a more detailed analysis of gait. No sign of *thermal* allodynia/hyperalgesia (the Hargreaves test with its long cut off does not discriminate between thermal allodynia and thermal hyperalgesia [472]) could be found using a heat sensitivity test. In the present study, the latency of paw withdrawal tended to increase for all groups over time, with no apparent differences between the groups. However, none of the groups were insensitive (analgesia) to noxious heat stimuli. Similar results have been obtained in a dorsolateral funiculus transection-type injury, where implanted rat BMP4-derived astrocytes (type I astrocytes) induced no signs of thermal allodynia/hyperalgesia, in stark contrast to implanted rat CNTF-derived astrocytes (type II astrocytes) [99]. Unfortunately, a subsequent study comparing using human BMP4- and CNTF-derived astrocytes only concentrated on motor behaviour and failed to include any sensory tests [101].

The Regularity Index initially decreased following **resection injury**, but recovered quickly and completely, as observed by others, demonstrating that the animals were able to cross the runway using a coordinated step pattern [104, 181, 182, 192, 234, 241, 242]. Stride length was not affected by the resection injury, as expected [181, 182]. Hind-limb BOS increased following injury, but this effect was not significant for the hFbl-implanted group. By the endpoint of the experiment hind-limb BOS was also not significantly changed from the baseline values for the control + IS group, and the hNP-AC implanted group showed a BOS value that increased even further over time. This behaviour might be interpreted as a compensation for an unstable gait [181, 182]. Interestingly, a decrease of the BOS of the fore-paws was observed for all groups [181, 182], which may also be interpreted in a similar manner as that for the

changes in hind-limb BOS. The related paw parameters, max- and print contact areas of the affected ipsilateral hind-paw, decreased in all groups, however, with an earlier recovery for the cell-seeded scaffolds. The similar pattern of recovery for both parameters indicates that the toes were not being dragged during gait [181]. The lesion induced decrease in values indicates a reduction of toe spreading and weight loading of the affected hind-paw [182]. This is backed up by the decreased intensity, indicating an unloading of the affected foot as well [182]. It might be suggested that a decreased stepping intensity could be an indication of altered behaviour due to the onset of mechanical allodynia [182, 449]. There were, however, no signs of pain to mechanical stimulation as observed using von Frey filaments. Even the control + IS group, which had the lowest stepping intensity values (being significantly different from both cell implantation groups) showed no sign of allodynia using the von Frey filaments. All groups showed a tendency to recover over time. The stepping intensity value for the hNP-AC implanted group even recovered back to baseline levels, indicating a full return of body weight support by the affected hind-limb. The absence of increased sensitivity to mechanical stimuli is in accordance with the literature, where implanted rat BMP4-derived astrocytes, human fibroblasts and even control animals did not show signs of increased mechanical allodynia in a number of different models of SCI [99, 100, 216, 359]. However, it has been reported that lesioned rats receiving transplanted CNTF-derived astrocytes did show signs of *mechanical* allodynia [99]. However, unfortunately the study assessing human BMP4- and CNTF-derived astrocytes failed to demonstrate any sensory data [101]. Duty cycle and stance duration also decreased after injury, and the swing duration accordingly increased. The changes in all of the above mentioned parameters may be considered as the CatWalk providing a quantitative description of lesion-inducing limping. All of these parameters demonstrated a tendency to recover back to the baseline. Interestingly, others have reported an decrease of swing duration following contusion SCI, whereas dorsal spinal cord transection injuries have been reported to have no effect [181, 182, 192], or to induce increases of this parameter [182, 222]. The gridwalk also showed an early effect of cell-seeded scaffold transplantation, with the control + IS group also demonstrating a pattern of recovery that eventually reached a similar value as that of the hFbl- and hNP-AC-implantation groups.

The results suggest a role of immunosuppression (cyclosporine A and azathioprine) in combination with an anti-inflammatory drug (methlypredisolone) alone on functional recovery,

with a trend to further increased locomotor performance after cell transplantation. Several studies suggest that immunosuppression or anti-inflammatory drugs can act as a promoter of functional recovery after SCI [5, 34, 179, 204], although others have reported no improvement in functional recovery after immunosuppression or anti-inflammatory treatment [100, 178, 205, 283, 335, 336, 415].

Fibroblasts are often used as a cell control group, for comparison with other cell transplants (e.g. NPC) or genetically modified fibroblasts [92, 93, 359, 405]. Interestingly, many groups have found an increased in-growth of axons into spinal cord lesion sites that have been treated with fibroblast grafts [150, 190]. Most studies have reported no improved functional recovery after fibroblasts transplantation [92, 93, 359], but some improvement has been reported by others [405]. Possible mechanisms for the effects of donor fibroblasts on axonal growth and functional recovery are discussed below. Some studies were able to show functional recovery from SCI following the implantation of rat or human glial restricted progenitor BMP4-derived astrocytes (GDA) [99–101], whereas others have reported no- or only temporary functional improvements following the grafting of human GDA or neonatal rat astrocytes [216, 222]. Interestingly the studies assessing human or rat BMP4- and CNTF-derived astrocytes demonstrated a recovery of function using the gridwalk at 4 weeks. This matches with the findings obtained here, where a better recovery was observed for the cell-seeded scaffolds at 4 weeks, but not at the later end-point stage. It is unfortunate that later time points were not investigated in the other studies [99–101]. It is of further interest, that the region of donor cell isolation might also play a role in any transplant mediated effects, apart from the differentiation status (i.e. into type I or type II astrocytes).

Whereas the astrocytes generated in this study, as well as those used by Jin and colleagues, were derived from brain progenitor cells [216], Davies and colleagues employed embryonic (rat) or foetal (human) spinal cord tissue [99–101]. Some differences have been reported between NPC derived from hippocampus or spinal cord [120], and also between NPC derived from hippocampus or subventricular zone [246]. Interestingly, only the Davies group has, so far, been able to demonstrate functional recovery. However only a direct comparison employing the same animal model would clarify whether the different donor cell sources results in different effects on spinal cord regeneration and repair.

Housing animals in an enriched environment has also been reported to increase the extent

of recovery or even to prevent some of the spinal cord contusion-induced parameter changes as measured by CatWalk [182, 251]. Since future experimental treatments for SCI will most likely include the use of different or multiple intervention strategies, it is likely that the use of an enhanced environment could produce added benefits when combined with cell/biomaterial-based strategies. The testing of such a possibility was, however, not within the scope of this investigation.

4.3.3. Survival of transplanted cells

In the balloon compression model, approximately 1x10^6 cells were injected into the spinal cord. Since the 3D scaffolds were trimmed to fit into the resected part of the spinal cord, the estimation of the number of cells transplanted along with the scaffold is rather imprecise, but was in the range of 4-6x10^5. In the literature, the number of cells transplanted after rat SCI has ranged from 1.8x10^5 to 2x10^6 [99–101, 150, 190, 216, 219, 323, 405, 430]. Therefore, the cell number of 1x10^6 is in the middle of the above range and the number of 4-6x10^5 at the lower end.

In earlier transplantation studies a number of nuclear (BrdU, Hoechst) and cytoplasmic dyes (PKH26) have been employed *in vivo* to identify grafted cells (e.g. Schwann cells, NPC, olfactory ensheathing glia [71, 123, 338, 339]). Although the dyes label cells well *in vitro*, once transplanted, the death of the labelled cells may release the dye so that it can be taken up by host cells or label other host structures [12, 193, 198], making identification of the grafted cells very difficult. More recently viral vectors have been employed to deliver genes such as lacZ or GFP to cells *ex vivo* prior to implantation [250]. These early generation delivery systems, however, have suffered from apparent short-term expression due to rapid down-regulation of the inserted gene [46, 191, 352], preventing the long-term tracking of the cell's fate. Here we used a monoclonal antibody against human nuclei [440, 446] to identify donor cells (hNP-AC and hFbl), however axonal association was difficult to identify as the distinct labelling of the cell nucleus made it impossible to detect the entire donor cell morphology. This was somewhat circumvented by the use of the anti-human nestin antibody [286] to identify donor hNP-AC, where regenerating axons could be identified to grow along hNP-AC processes (further discussed below).

The transplantation of suspensions of hNP-AC, either alone or in combination with the 3D collagen scaffold, were found to survive better than suspensions of hFbl. Delayed transplantation appeared to greatly increase the survival of both populations of donor cells, although there are many more factors which might play a role in donor cell survival and which are different in the two models (e.g. type of injury, form of cell transplantation), which make a direct comparison difficult. However, an increased survival after delayed transplantation is in accordance with the literature, where a delayed transplantation (e.g. of Schwann cells and olfactory ensheathing glia) enhanced donor cell survival [195, 324]. At this delayed stage of SCI, the detrimental excitotoxic and inflammatory processes may have declined, but substantial amounts of growth factors, cytokines and neurotrophic factors could be still present that may potentially aid in donor cell survival and differentiation. However for the purpose of promoting rescue of compromised neural cells by neurotrophic activity and stimulating endogenous plasticity, implantation in the early phase after injury may still prove to be most beneficial. The high cell death observed after transplantation of cell-seeded scaffolds might also be due to an inadequate vascularization in the scaffold resulting in decreased oxygen supply, increased carbon dioxide and altered acidity [317]. Although many other studies have demonstrated the survival of transplanted fibroblasts, even a crude analysis of the extent of cell survival (i.e. how many animals still showed signs of the transplanted cells) is often missing [269, 323, 405]. However, similar to the results for the balloon compression injury model, other groups have reported a compact graft morphology with donor fibroblasts staying confined to the transplantation site [150, 359, 405]. The survival of the hNP-AC after acute transplantation (i.e. in association with the 3D collagen scaffolds) was comparable to the survival obtained for BMP4- and CNTF-derived human astrocytes (66% and 50% respectively) [101]. However, survival of donor GDA was better in NOD-scid (athymic) host rats transplanted 9 days after injury, where all animals showed robust survival of transplanted GDA [216]. This is in accordance with the enhanced survival after delayed transplantation in the balloon compression injury model. The reasons for the differences in hNP-AC survival when grafted into the sites rostral- and caudal to the lesion epicentre (balloon compression injury) remain unclear. Previous studies employing olfactory ensheathing glia for SCI repair have rather demonstrated better survival when the cells were transplanted at positions both rostral- and caudal- [144, 338, 339], rather than within [19] the injury site. The lesion and

cavitation after compression extend several segments rostral and caudal from the initial site of injury and it might be that there is a difference in the expression of certain inhibitory substances (e.g. CSPG) at different levels, which could have influenced donor cell survival. However, a comparison of CSPG expression levels in different segments (total length ∼1cm) after contusion injury failed to demonstrate any differences [203].Clearly more animal numbers would be required for this effect (i.e. difference in cell survival related to position of transplant) to be a completely reliable observation.

It is possible that the use of alternative or more potent immunosuppressants (i.e. FK506 (tacrolimus) rather than cyclosporine) could have increased the survival of the donor cells even following transplantation into acute injuries [190]. However immunosuppression can also cause serious side-effects, such as anaemia, infections, chronic kidney damage, increased risk of cardiovascular disease, metabolic syndrome, bone loss, tremors, seizures, and malignancy [257, 347, 399, 445, 477]. Nonetheless, at present, immune suppression seems unavoidable for implanted non-compatible cells or tissues, because it is required to prevent rejection reactions, which themselves may lead not only to the loss of the grafted cells, but also to inflammatory reactions that cause secondary damage [24]. Strategies which harvest autologous cells from the patients themselves (including iPS cells [436]), for *in vitro* expansion and transplantation back into original donor would greatly increase the survival of the transplanted cells, as shown for example for fibroblasts in a primate model of spinal cord injury [439]. Although the sub-acute phase and therefore the time window for transplantation in humans may be longer than in animals, the slower proliferation of human cells and the greater extent of the injury may make it hard to achieve sufficient cell numbers or may even raise additional problems (e.g. insufficient nutrition at the core of the transplant).

Suspensions of hNP-AC that had been transplanted in the absence of a supporting scaffold were able to migrate relatively far through the host spinal cord parenchyma. Even donor hNP-AC that were transplanted with the scaffold were able show some degree of migration into areas close to the host-graft interface. This migratory behaviour of human astrocytes has been demonstrated by others who reported greater migration through spinal cord white matter than through grey matter [101, 216].

4.3.4. Axonal regeneration

In both injury models, donor hNP-AC were able to promote greater axonal growth than the other investigated groups. This is in accordance with the potential such cells have already demonstrated *in vitro* [136]. Although some investigators have reported similar effects of donor rat or human GDA on axonal growth *in vivo* [99–101] others have failed to demonstrate such effects [216]. It is clear that the axons found inside the scaffold can be regarded as having regenerated, but such an interpretation is not so certain in the present balloon compression injury model. However, earlier reports have demonstrated a lack of any spared NF-positive axons at the lesion site early after severe balloon compression injuries [57]. Nonetheless, even when we take the small amount of spared tissue at the lesion epicentre into account (see result section and below), it is highly likely that most of the axons that can be demonstrated at the lesion core must have regenerated. Some of those regenerating axons could be found in close association with transplanted hNP-AC in both injury models, although they showed a greater tendency to grow along laminin-positive structures (i.e. most likely associated with migrating host Schwann cells or newly formed blood vessels) at the lesion site in the balloon compression injury model. Both astrocytes and Schwann cells have already been shown to be capable of directing the orientation of regenerating neurites *in vitro* [38, 103, 373, 428].

Interestingly, large numbers of axons were also detected inside the elliptical clusters of donor hFbl, where a great number of laminin expressing cells could also be found (presumably migrating Schwann cells, [39, 88, 143]). Furthermore, animals receiving fibroblast grafts also showed a tendency for increased axonal regeneration into the lesion site in general, not only into the elliptical clusters. This observation was not totally unexpected since other groups have demonstrated a similar effect of either modified fibroblasts (e.g. for the expression of NGF, Wnt3a, BDNF or NT-3) or native fibroblasts. This may be due to the intrinsic expression of ECM molecules (i.e. fibronectin) or growth factors (e.g. NGF, NT-3, VEGFa and bFGF), or to indirect mechanisms such as the promotion of enhanced Schwann cell migration [150, 219, 298, 405, 430, 438]. Furthermore the importance of a guidance structure to orientate regenerating axons became evident when comparing the patterns of axonal growth in the two different lesion models. Axon growth appeared random

in the balloon compression injury model, while there was clear orientation which followed the longitudinally orientated pores of the collagen scaffold.

It would clearly be of interest for future investigations to use retrograde labelling or more specific axonal markers, such as calcitonin gene-related peptide (CGRP) for sub-populations of sensory DRG axons or 5-hydroxytryptamine (5-HT, serotonin) for serotonergic axons, to allow a more precise analysis of the phenotype of which axonal populations were responding to the presence of particular donor cell types [53, 161, 348].

4.3.5. Schwann cell migration

Whereas a substantial amount of migrating Schwann cells could be found at the lesion site of the balloon compression injury model, very few, if any, Schwann cells were found in the lesion sites of the lateral funiculotomy injury model. The reason for the limited Schwann cell migration in the lateral funiculotomy model could be due to the transection of the nerve roots and the associated severance of the migration route of de-differentiating Schwann cells. The balloon compression injury model, on the other hand, not only compresses the spinal cord but also the local spinal nerve roots. Unlike the resection injury, the damaged nerve roots maintain anatomical continuity with the damaged spinal cord, thus providing a route for significant Schwann cell migration into the lesion site. Schwann cells migration into the compression-, transaction- and contusion type spinal cord injuries has already reported by others. Such studies were also able to demonstrate a close association between regenerating axons and the migrating Schwann cells [57, 60, 61]. However the evaluation and quantification of Schwann cell migration was restricted to the balloon compression model in this investigation because practically none could be detected following the lateral funiculotomy.

In addition to the generally large number of migrating Schwann cells found at the lesion epicentre, a particularly high density of Schwann cells could also be detected at the elliptical clusters of donor hFbl transplantation. The recruitment of large numbers of axon growth-promoting Schwann cells into the lesion site may have contributed to the ability of donor hFbl to promote a degree of functional recovery that was similar to that supported by donor hNP-AC. Schwann cells produce a variety of growth factors (including NGF, BDNF and CNTF), a number of cell adhesion molecules (including integrins, N-cadherin, N-CAM,

L1 and contactin) and extracellular matrix proteins (such as laminin and collagens) which could support axonal growth as well as the survival of damaged neurons close to the lesion site [39, 88, 143]. It is not surprising then, that transplanted Schwann cells have been reported to be able to fill cystic cavities, increase white matter sparing, remyelinate axons of both PNS and CNS origin and to promote axonal regeneration in a variety of SCI models [40, 262, 275, 310, 414, 469]. Furthermore BDNF or GDNF expressing fibroblasts have also been shown to enhance Schwann cell migration after dorsal spinal cord hemisection lesions [41, 42]. However, the above studies failed to demonstrate the extent of Schwann cell migration or functional consequences of such behaviour in their non-treated control group [41, 42].

It is widely acknowledged that the mutually repulsive properties of Schwann cells and astrocytes usually results in boundary formation between populations of these PNS and CNS glia. Such boundaries have been identified as natural barriers to cell migration and axon regeneration [73, 162, 270]. Interestingly, in the present investigation, donor hNP-AC did not hinder the migration of the Schwann cells. This might be due to the immature phenotype of the hNP-AC. However even when some degree of intermingling between host Schwann cells and donor hNP-AC could be observed, it was not as extensive as that seen between the host Schwann cells and the donor hFbl.

4.3.6. GFAP and CSPG expression

GFAP staining was clearly visible in both lesion models, demonstrating the distribution and morphology of host and donor astrocytes. A clear expression of CSPG by host and grafted astrocytes, grafted fibroblasts, and other GFAP-negative host cells (host fibroblasts or Schwann cells) could be demonstrated after balloon compression. After lateral funiculotomy only a weak staining, if any, was visible, which partly colocalised with GFAP-positive cells inside of the scaffold. Only occasionally, could stronger CSPG expression be observed that was associated with GFAP-negative cells (presumably host fibroblasts). Previous studies have demonstrated that CSPGs are generally up-regulated after spinal cord injury, with a peak expression at 1-2 weeks post injury. However after 8 weeks a clear reduction was observed for several members of the CPSG family (e.g neurocan, versican) following transec-

tion injury, which explains the weak staining observed in this study [203, 218]. Spinal cord compression injuries are significantly different and are accompanied by more extensive cell death, inflammation, cavitation and scarring [203]. This might explain the different patterns and extent of CSPG expression in the different types of injury [203]. The present study was able to confirm these findings with the continued expression and clear staining of CSPG after balloon compression injury (compared to the resection injury).

While in the balloon compression model, donor hNP-AC caused a small reduction of both GFAP and CSPG immunoreactivity compared to the control and control + IS, only GFAP was reduced after lateral funiculotomy (compared to the control). Although this seems contradictory, keeping in mind that (host and donor) astrocytes could only be found inside the hNP-AC-seeded scaffolds, it must be emphasised that GFAP-intensity was evaluated, not astrocyte number or area occupied by astrocytic profiles. There was, nonetheless, a trend for reduced CSPG immunoreactivity following hNP-AC transplantation. Interestingly donor hFbl also provoked an overall reduction of GFAP and CSPG levels in both models. This is not so suprising for GFAP as for CSPG, since a high focal expression of CSPG at the hFbl transplantation site (i.e. in the balloon compression injury) could be found. However this local expression seemed not to influence their general beneficial effect. Furthermore despite their low survival after lateral funiculotoy and scaffold implantation, hFbl where able to excert a benfecial effect. Whereas the levels of both proteins were clearly lower after hNP-AC transplantation in the balloon compression model compared to the hFbl, this was reversed in the lateral funiculotomy model. This is most likely due to the presence of reactive host astrocytes and their processes inside the hNP-AC-seeded scaffold. This profound host astroglial response within the scaffolds was apparently absent in the hFbl-seeded scaffolds. This observation may simply reflect that the initial presence of hNP-AC on the scaffolds promoted a better degree of host astroglial integration than seen with the implanted naive or hFbl cell-seeded scaffolds. The fact that substatial GFAP immunoreactivity could be observed, even in scaffolds where no viable donor hNP-AC could be detected, only serves to emphasise the interpreation that such immunoreactivity was derived from host cells. This is in accordance with the literature, where immature rat astrocytes were found to support the integration of millipore filters implanted into the rodent brain [380, 389, 390]. In contrast to the earlier published works which showed infiltration of the surface of the

implanted millipore, the present investigation has clearly demonstrated the novel observation that this effect can be supported throughout the 3D porous microarchitecture of the collagen scaffold. It may well be the case that the phenotype of the host astrocytes may not be as benefical for neurite extension as the donor hNP-AC, but the hNP-AC seeded scaffolds supported significantly greater axonal growth than the non-seeded scaffolds (and a trend for greater axonal growth than the hFbl-seeded scaffolds). Other studies, using different kinds of scaffolds, have demonstrated a close relationship between host GFAP-positive profiles and regenerating axons, even if those host astrocytic profiles showed a limited pentration into the scaffold [158, 226, 328, 467, 471]. This highlights the fact that reactive or activated astrocytes are not only involved in the generation of the glial scar but are also capable of promoting and directing axon regeneration [226, 300, 328, 471]. Interestingly, the few studies which reported astrocyte migration into the implants used scaffolds that were prepared from either collagen or xyloglucan/PDL in their liquid form with gelation after injection [221, 300]. Another factor might be the reduction of the glial scar around the implant, which normally acts as a barrier, not only to regenerating neurites, but also to some populations of migrating cells [24, 381, 397]. Reduced glial scarring and CSPG expression after transplantation of human- or rat-derived immature astrocytes has also been reported by others [216, 388–390]. The reduced glial scarring might therefore have been beneficial for migration of host astrocytes into the scaffold. However there are certainly other mechanism that may be involved (e.g. AQP4, STAT3, integrins [288, 463]) in the enhanced host astrocyte migration since GFAP and CPSG staining at the graft-host interface were also reduced after donor hFbl transplantation (where no significant host astrocyte migration into the scaffold was observed). Nonetheless, it must be reiterated that glial scarring after injury is beneficial to overall tissue integrity during the acute phase (1-2 weeks) after spinal cord injury [127, 305, 342]. The formation of an astroglial barrier is responsible for the protection of adjacent, non-injured spinal cord tissues, but such protection comes at the price of reducing spontaneous axon regeneration. The mechanisms that control the phenotype of reactive astrocytes to be either scarring/axon growth inhibitory or axon growth promoting remain unclear at present. However, future research into such behaviour may substantially help the development of tissue engineering strategies aimed at promoting spinal cord repair.

It is also possible that the presence of donor hNP-AC may have assisted in tissue repair,

supporting the remyleination of demylinated, spared axons. Endogenous oligodendrocyte precursor cells have been reported to be unable to remyelinate axons in the absence of astrocytes [417].

4.3.7. Inflammatory response

The balloon compression injury model greatly affected both grey and white matter microglia. Microglial responses to traumatic injuries are, to some extent, more severe in white matter than in grey matter [105, 365] and it has been shown that in damaged white matter, microglia became enlarged, often with retracted processes while in damaged grey matter they remained ramified [279]. Therefore the analysis of Iba1 immunoreactivity following compression injury was divided between cells of a rounded morphology and those of a ramified morphology. In contrast, the evaluation of inflammatory response after lateral funiculotomy was restricted only to white matter microglia (with the inclusion of supplementary ED1 immunohistochemistry). Iba1 identifies the ionized calcium binding adapter molecule 1 [207], which is expressed by microglia and monocytes [215]. After CNS injury Iba1 is upregulated in activated microglia close to and at the primary injury site [209, 210, 442]. ED1 (CD68) recognizes a single chain glycoprotein that is predominantly expressed on the lysosomal compartment of activated monocytes and macrophages, and is absent in the normal CNS [106, 238, 334]. Following acute traumatic injuries, ED1 antigen is expressed rapidly on microglia that are engaged in phagocytosis of tissue debris (i.e. on reactive microglia) [106, 403]. However, ED1 expression is restricted to the most severe areas of insult [210].

Since an increased expression of Iba1 has been reported in the spinal cord after injury [442, 447], we analysed the intensity (mean grey value) of Iba1 staining after injury and implantation of the scaffold.

After **balloon compression injury** and accompanying immunsuppression, Iba1 expression increased in both types of microglia. However the number of microglia and the intensity of staining are not completely independent paramters, since an increase in the number of microglia could also lead to an increase in the intensity of an image. In this context, others have reported that the neuroprotective effect of FK506 on motor neuron survival after sciatic nerve transection was accompanied by increased microglia numbers (compared to an

untreated control). However, reactive microglia, as indicated by MHC-II expression, were reduced after FK506 treatment [361]. Similarly, in the context of activation, earlier studies have also demonstrated that methylpredisolone and cyclosporine reduced the number of activated microglia after CNS injury [309, 424]. It might be hypothesised that the triple immunosuppresion used in the present study had a similar effect (i.e. increasing microglial numbers in response to injury but modifying their staus of activation). However, since MHC-II expression has also been reported to be present in non-reactive ramified microglia and may not be a consistent surface marker for reactive microglia [403], it was not included in the present investigation.

Interestingly the effect of the immunosuppression was apparently counteracted by the cell transplantation, especially for the rounded white matter microglia. In this context, it is well established that both astrocytes and fibroblasts have modulatory effects on monocyte/microglia [63, 244, 392]. However, it is at present difficult to understand why donor hFbl exerted a different effect on grey and white matter microglia.

After **lateral funiculotomy and scaffold implantation**, Iba1 and ED1 distribution were quite distinct. The Iba1-positive cells could be found around and and within the scaffold, while ED1-positive cells remained around the scaffold. Although the origin of microglia is under debate, it is widely acknowledged that circulating (ED1 positive) monocytes, which have a higher migratory capacity then microglia [403], do enter the pathological CNS where they can differentiate into cells that are phenotypically and morphologically indistinguishable from resident microglia [189]. The Iba1 positive cells detected inside the scaffold may therefore be derived from monocytes which had migrated into the scaffold and differentiated into non-reactive (i.e. ED1 negative) microglia. Previous studies have reported that Iba1-positive, ED1-negative, activated microglia, were involved in neuronal regeneration within the axotomized motor nucleus [168, 209].

However the expression profiles of surface and cytoplasmic antigens often overlap, making it difficult to assign a definitive phenotype or function to a given cell type [189], therefore it is difficult to pin down the exact type of inflammatory cell that is inside of the scaffold or even around.

Similar to the results obtained with the balloon compression injury, the intensity of Iba1 was reduced after implantation of the cell-seeded scaffolds as compared to the control animal

which received naive scaffolds plus immunosuppression. Interestingly, ED1 intensity was only reduced following the implantation of hNP-AC-seeded scaffolds, although a trend for a reduced intensity was also observed with hFbl-seeded scaffolds. This might not only indicate reduced macrophage activation, but also reduced reactive microglia. However it remains unclear if this effect was overall beneficial or detrimental, since the inflammatory response is known as having both an early neurodegenerative component and a later neuroprotective component [74, 248]. Since the present investigation was only able to demonstrate the morphology and phenotype of the microglia/macrophages at 8 weeks after injury, future studies will be required to assess whether the effects of implanting cell-seeded scaffolds are mediated through modification of early (i.e. detrimental) inflammatory events or the later (i.e. beneficial) inflammatory events.

4.3.8. Spared tissue

After balloon compression injury and hFbl transplantation, enhanced Schwann cell migration and a reduction of lesion size at its epicenter could be detected. The effects of fibroblast implantation on tissue sparing are relatively unknown, although a trend for increased tissue sparing was also observed when these cells were used as a control cell population in a model of contusion-type SCI [359]. The ability of Schwann cells to increase tissue sparing is fairly well documented and, since we have already demonstrated that donor hFbl supported enhanced Schwann cell migration into the lesion site, it is tempting to speculate that the tissue sparing may have been due to indirect mechanisms mediated through Schwann cells [40, 262, 275, 310, 414, 469]. However, other as yet unidentified mechanisms (e.g. growth factor expression, see above) cannot be discounted. Nonetheless, since the sparing of as little as 1-10% of spinal cord axons can have significant benefits on functional outcome [43, 45, 115], the beneficial effects of donor hFbl (via direct or indirect mechanisms) may have been mediated by such an outcome.

Despite otherwise promising results, donor hNP-AC failed to demonstrate any recognisable tissue sparing effect: the amount of spared tissue was even smaller than that induced by the donor hFbl. However, it is possible that the relatively good survival of the donor hNP-AC and their intimate integration into host tissues may have resulted in observer misinterpretation

of the extent of tissue sparing. It is conceivable that mixed donor/host regions may have been interpreted as cell-rich areas of lesion site rather than cell-rich areas of spared tissue.

The control + IS group showed a general trend for a reduced lesion size. However, most of the previous published results of the effect of cyclosporine on lesion size showed no statistical effect as well [190, 204, 335]. Only rarely could a beneficial effect of immunosuppression be observed [249]. Methylpredisolone demonstrated reduced lesion volumes and functional benefits in some studies [85, 179, 307], however other studies failed to reproduce these effects [167, 179, 336]. The effect of azathioprine is less well studied, but some promising results have been demonstrated [5].

4.4. Conclusion

Balloon compression model: Both hNP-AC and hFbl cell transplants resulted in a greater degree of functional recovery than the untreated control. However, no significant differences were observed between the extent of recovery supported by cell transplantation groups and the control + IS group. The beneficial effects observed with the different strategies might result from a number of different mechanism: (I) immunosuppresion greatly affected the intensity of Iba1 and therefore may have altered the inflammatory response leading to some degree of tissue sparing, (II) donor hFbl promoted a greater degree of Schwann cells migration into the lesion site, leading to enhanced axon regeneration as well as tissue sparing, (III) donor hNP-AC promoted the least amount of glial scarring at the graft-host interface (as indicated by the intensity of GFAP- and CSPG-immunoreactivity) as well as the greatest extent of axon regeneration.

Tissue engineering strategy: Donor hNP-AC promoted also the greatest degree of axon regeneration and host astrocytic migration and integration into the implanted scaffold. Despite these promising results, hNP-AC failed to support a greater degree of functional recovery when compared to the other animal groups. The mechanism behind the enhanced behavioural recovery seen following implantation of hFbl-seeded scaffolds is likely to be different from that suggested for the balloon compression injury model since Schwann cell migration was not observed in these experiments. However animals receiving hFbl-seeded scaffolds showed reduced GFAP and CSPG intensity at the graft-host interface and a moder-

ate effect on neurite growth into the scaffold. Both cell-scaffold transplantation groups also demonstrated reduced intensity of ED1 and Iba1 immunoreactivity, however the relevance of this observation remains obscure. It is feasible that the relatively poor survival of the transplanted cells in this experimental model might have contributed to the lack of clear and unequivocal effects. Future experiments that maintain the survival of large numbers of donor cells will, thus, be important for the clearer understanding of the therapeutic value hNP-AC in regenerative medicine, in particular for spinal cord injury.

5. General Discussion

The notion that stem/progenitor cells represent an inexhaustible source of neurons and glia for cell replacement therapies (in particular for the treatment of SCI) is no longer a scientific hope, but a realistic goal. Recent discussions and concerns relate to the relative merits of therapeutic potential when comparing cells from different sources (e.g. embryonic-, foetal-, adult- or iPS-stem/progenitor cells) as well as which particular phenotype (e.g. undifferentiated, lineage restricted or fully differentiated) of cell will provide the best regenerative benefit. Biomaterials are also a new and rapidly expanding discipline in the field of regenerative medicine, and have showed great potential for promoting tissue repair in combination with stem/progenitor cells and their derivatives [402]. However, promoting functional recovery after spinal cord injury is at present still a challenge and there is still a long way before we can move to the clinic. However, some clinical trials assessing the potential of human neural progenitor cells are currently being conducted [435].

Here we adopted and developed further the relatively simple concept that immature rat astrocytes were capable of promoting axon regeneration and improved scaffold integration [236, 380, 389–391] and the main hypothesis that was proposed in the present thesis was:

"That human immature neural progenitor-derived astrocytes are capable of promoting axon regeneration and scaffold integration, similar to properties demonstrated for immature rat astrocytes."

To address this hypothesis, the following four goals were formulated and the achievements presented in this thesis will be discussed shortly.

5.1. To generate highly enriched populations of immature astrocytes from human neural progenitor cells (hNP-AC)

After the characterisation of the undifferentiated cells, the ability to differentiate hNPC into highly enriched populations of immature type I astrocytes was demonstrated. Following the reports that immature rat astrocytes promoted axon regeneration [236, 380, 389–391], rat neural progenitor cell-derived type I astrocytes were shown, in stark contrast to type II astrocytes, to be able to promote recovery as well as limiting allodynia after SCI [99]. As an alternative of obtaining NPC from aborted foetuses, recent advances in stem cell technology have indicated that it may be possible to generate NPC from somatic cells, taken from the patients themselves. This could be done either using therapeutic cloning techniques, or by the generation of inducible pluripotent stem (iPS) cells by "reprogramming" somatic cells [284, 297, 312, 413]. Since the donor cells would be derived from the patients themselves, the ethical and immunological issues often raised in regard to the use of embryonic- or foetal-derived NPC would be avoided. However, a significant drawback of such an approach may be that such cells would only be generated for therapeutic use after the patient had been involved in an accident. Thus, it would be unlikely that such cells could be used to treat the acute phase of an injury. Moreover, quality control of these cells is likely to be difficult and expensive, since each individual patient will require a separate batch of iPS cells to be produced.

5.2. To determine cell-substrate interactions between hNP-AC and orientated bioengineered substrates

(I) When associated with the orientated PCL and C/PCL nanofibres, hNP-AC adopted an elongated morphology, following the orientation of the fibres. Functionalisation of the nanofibres with collagen did not affect the proliferation or process length of hNP-AC, whereas

adhesion and migration were enhanced. The sPEG-mediated attachment of low density, oriented nanofibers to glass cover-slips enabled the interactions between single cells and single nanofibers to be studied in relatively simple "2D" cultures [159]. Improving the functional properties of such scaffolds to support greater axonal regeneration, host- and donor-cell survival (tissue sparing), proliferation and migration by the incorporation of ECM components (i.e. type I collagen), or their functional peptide sequences (e.g. DGEA [362]) is an area of increasing interest in regenerative medicine [159]. Furthermore, the development of such approaches requires the technology to move from relatively simple 2D into a 3D orientated scaffolds, ready for further *in vitro* and *in vivo* testing.

(II) hNP-AC seeded onto orientated 3D collagen scaffolds continued to proliferate and formed columns of orientated cells which followed the orientation of the micro-channels. Furthermore, in addition to the observed cell-substrate interactions, novel cell-cell interactions were also documented: the intermingling of seeded hNP-AC with migrating fibroblasts and Schwann cells within the collagen scaffolds represented a surprising finding. Astrocytes and Schwann cells/fibroblast normally demonstrate mutually repulsive properties and distinct boundaries are formed where the two cell types meet. Such boundaries exert considerable influence over the ability of regenerating axons to cross from one territory to the other and their effects have been studied in detail in 2D *in vitro* assays [163, 164, 377]. The present investigation has demonstrated that when these cells encountered each other within an orientated 3D scaffold, substantial intermixing- rather than mutual repulsion was evident. This raises the possibility that the topography of the scaffold may have altered the properties of one or more populations of cells. However the observed effect could also be due to the immature nature of the astrocytes, although a possible role of both factors is most likely. Although some of the basic principles controlling cell-substrate and cell-cell interactions have already been established in relatively simple 2D systems, the future design of biomaterial-based scaffolds that are intended to promote nervous tissue repair depend a better understanding of such principles in more complex 3D environments, which resemble the *in vivo* situation more closely [1, 136].

5.3. To identify the axon growth-promoting properties of the hNP-AC in 2D and 3D systems using adult neuronal populations

(I) hNP-AC demonstrated their ability to promote neurite regeneration in a simple 2D assay using dissociated adult DRG neurons. Surprisingly, axon growth was even greater than that observed over the PLL/laminin positive control substrate. This effect was due to contact-mediated mechanisms and the release of diffusible substances into the medium. It has already been demonstrated that immature rat astrocytes are able to promote neurite regeneration of embryonic neuronal populations [391], however the extension of this axon growth promoting behaviour to human cells and its demonstration with adult neuronal populations had, until now, never been reported. The identification of the specific ECM- and growth factor-related molecules involved in this behaviour was not included in the present investigation, but a precise analysis of the mechanisms behind the growth promoting properties of the hNP-AC could help in the development of improved cell- and biomaterial-based intervention strategies for nerve regeneration.

(II) Seeding of the 3D collagen scaffold with hNP-AC promoted a greater ingrowth of regenerating neurites from hemisected adult DRG compared to the non-seeded, control scaffolds. The present investigation showed that the topography of the scaffold helped guide axonal growth. This is widely regarded as a crucial step in nerve repair. Furthermore, the translation of the growth promoting properties of the hNP-AC from 2D- to a 3D environment has been demonstrated. This phase of the investigation should not be regarded as the simple validation of the results obtained in 2D, since many aspects of cell form and function (i.e. morphology, ECM & integrin expression) are known to be different in 3D culture systems [1, 91].

5.4. To determine the axon growth promoting properties/ graft-host interactions of hNP-AC when implanted into experimental models of SCI, either alone- or in combination with a 3D collagen scaffold

In the **first SCI model** investigated, hNP-AC cell suspensions were transplanted one week after compression injury of the spinal cord. In the **second SCI model**, hNP-AC-seeded 3D collagen scaffolds were implanted into an acute spinal cord resection injury. Although donor hNP-AC cell suspensions promoted greater functional recovery than was seen in non-transplanted controls in the first SCI model, no functional improvement could be observed following implantation of the hNP-AC-seeded scaffolds in the second SCI model. Some other studies were able to show functional recovery following the implantation of rat or human glial restricted progenitor BMP4-derived astrocytes (GDA) after 4 weeks [99–101], whereas others reported no- or only temporary functional improvements following the grafting of human or neonatal rat GDA [216, 222]. Unfortunately, the other investigations did not include a "neutral" cell control group, such as the hFbl used in the present investigation. Different time scales and injury models further complicate a direct comparison between results obtained from different publications. Therefore, it remains unclear if transplantation of progenitor-derived type I astrocytes has beneficial effects or no effects on functional recovery after spinal cord injury. It might be that different combinations of cell populations and biomaterials could be more suitable for a specific type of injury or best used at different time points after injury (e.g. for acute, delayed or even chronic injuries), but such eventualities still require verification by further studies. The world-wide adoption of standardised techniques would facilitate such studies and more readily allow the comparison of data that was obtained by different groups.

No sign of graft-induced allodynia/hyperalgesia could be found in either model of SCI. Similar results have been obtained with rat BMP4-derived astrocytes (type I astrocytes), in stark contrast to implanted rat CNTF-derived astrocytes (type II astrocytes) [99]. Unfortunately, a subsequent study comparing human BMP4- and CNTF-derived astrocytes only

concentrated on motor behaviour and failed to include any sensory tests [101]. The present investigation was only able to conclude that human type I astrocytes do not promote allodynia, similar to the rat type I astrocytes; however human type II astrocytes were not included in the present investigation. The differences of donor type I and type II astrocytes on functional and sensitivity outcomes [99] demonstrates the importance of including tests for possible unwanted side-effects, an issue that has, to date, largely been over-looked.

Morphological investigations demonstrated that hNP-AC survived and integrated well into the balloon compression injured spinal cords. In contrast, only limited donor cell survival was observed after implantation of cell-seeded scaffolds. This effect may have been due to the delayed transplantation of the cell suspension, since the detrimental excitotoxic and inflammatory processes at the lesion epicentre may have declined at that stage, but substantial amounts of growth factors, cytokines and neurotrophic factors could still be present that may have assisted donor cell survival. However the two models are so different in severity and type of lesion as well as in the means of importing donor cells into the spinal cord that direct comparison is not possible. The survival of the hNP-AC after acute transplantation (i.e. in the second model) was comparable to the survival obtained for acutely transplanted BMP4- and CNTF-derived human astrocytes (66% and 50% respectively) [101]. However, survival of donor BMP4-derived astrocytes was better in NOD-scid (athymic) host rats transplanted 9 days after injury, where all animals showed robust survival of transplanted GDA [216]. The poor survival of donor cells after implantation might have prevented a better functional outcome. However, some early beneficial effects, despite low cell survival, were demonstrated, also by others [101]. The duration of cell survival is uncertain and it might be that donor cells were able have beneficial effects, which declined when donor cell death occurred.

Most spinal cord injured patients have an almost normal life expectancy and the functional benefits observed in animal models are, at most, restricted to a few months. Thus, a robust survival of transplanted cells might be crucial for long lasting beneficial effects. Furthermore the size of injuries suffered by patients is much greater compared to the rat counterpart and nutritional deficits and an insufficient blood supply might increase the difficulties of cell/biomaterial-based intervention strategies in humans. Nonetheless, if the beneficial effects of donor cell transplantation are via improved host cell survival/neuroprotection (rather then neurite regeneration) it may be anticipated that any improved functional consequences will

be seen at relatively early survival times.

Reduced host glial scarring was observed in both models and despite limited donor cell survival, donor hNP-AC-seeded scaffolds promoted a greater degree of graft-host tissue integration than seen in controls. Similar results were obtained with immature rat astrocytes, which were found to support the integration of millipore filters implanted into the rodent brain [380, 389, 390]. In contrast to the earlier published works which only showed infiltration of the surface of the implanted millipore, the present investigation has clearly demonstrated the novel observation that this effect can be supported throughout the 3D microarchitecture of the porous collagen scaffold. Another factor might be the reduction of the glial scarring around the implant, which normally acts as a barrier, not only to regenerating neurites, but also to some populations of migrating cells [24, 381, 397]. Reduced glial scarring and CSPG expression after transplantation of human- or rat-derived immature astrocytes has also been reported by others [216, 388–390]. The reduced glial scarring might therefore have been beneficial for migration of host astrocytes into the scaffold. Within the scaffold, similar to the *in vitro* studies, the few surviving hNP-AC formed columns of orientated cells. Some hNP-AC even migrated out of the scaffold and into the surrounding host tissue, where they adopted an elongated, migratory, morphology which was similar to the migratory capacity of the cells observed in the balloon compression model.

Donor hNP-AC were able to enhance axonal regeneration in both models of SCI. Some of those regenerating neurites were found in close contact with donor cells. A clear effect of donor cell-mediated axonal guidance could be observed when the two different models were compared: non-oriented neurite regeneration was observed in the first SCI model but orientated growth that followed the direction of the donor cells within the micro-channels was observed in the second SCI model. The enhanced neurite regeneration indicates that the promising results obtained *in vitro* were translated to the *in vivo* situation. This is in accordance with the literature, where human- and rat immature astrocytes were able to promote neurite regeneration in different CNS injury models [101, 236, 380, 389, 390]. Further investigations will be required to clarify the reasons for the apparent inability of the donor hNP-AC to promote any significant functional improvement. However, despite the fact that there is an impressive (and growing) list of treatments focusing on neurite regeneration, there are at least three important caveats that need to be borne in mind for such studies:

(I) the contribution of axonal regeneration to any demonstrated functional recovery may be inferred but largely remains unproven, (II) the proportion of fibres that regenerate is small, (III) the distances covered by regrowing axons is usually modest, especially when considering the size of comparable human lesions [52].

Interestingly, donor hNP-AC did not reduce the number of migrating Schwann cells (SC) into the lesion site, whereas donor hFbl actually supported greater SC migration. This suggests that the close interaction of hNP-AC with either migrating fibroblasts or Schwann cells within the 3D collagen scaffold may have been due to the intrinsic properties of the hNP-AC rather than to the topography of the scaffold. However, this point remains to be elucidated. Unfortunately no SC migration was observed in the second SCI model. This is likely to be due to the manner in which the spinal cord resection injuries were made: the cutting and removal of part of the lateral funiculus may have also severed a number of spinal nerve roots. The loss of physical continuity between the roots and lesioned spinal cord may thus have prevented the migration of any reactive, de-differentiated cells. Irrespective of the mechanism(s) by which the hNP-AC-seeded scaffolds supported better cell intermingling, the present data suggests that the use of such intervention strategies may also be appropriate for the bridging of injured dorsal and ventral roots to the spinal cord (i.e. avulsion-type injuries), where boundaries between astrocytes and Schwann cells/fibroblasts naturally occur [73, 147, 148, 162, 270].

Microglial activation, which was increased by immunosuppression (IS), was counter-balanced by the presence of donor hNP-AC and hFbl after balloon compression. In the absence of a control group of animals which were lesioned but lacked IS, it remains unclear if the IS also led to an increased microglial activation in the lateral funiculotomy/scaffold implantation model as well. Nonetheless, a reduced microglial activation of the cell-seeded scaffolds compared to the control scaffold + IS was observed, supporting the effects observed in the compression injury model. However, it remains unclear from the present data whether this effect had an overall beneficial or detrimental influence on scaffold-host integration and axon regeneration. This uncertainty is compounded by the fact that the inflammatory response is known as having both an early neurodegenerative component and a later neuroprotective component [74, 248]. Further experiments will be required to address this specific question.

Despite otherwise promising results, hNP-AC failed to demonstrate a detectable tissue

sparing effect in the compression injury model, and tissue sparing was not the focus of the lateral funiculotomy model. However, it is possible that the relatively good survival of the donor hNP-AC in the compression model and their intimate integration into the host tissues may have resulted in observer misinterpretation of the extent of tissue sparing. It is conceivable that mixed donor/host regions may have been interpreted as cell-rich areas of lesion site rather than cell-rich areas of spared tissue.

Nonetheless although the achievement of complete functional recovery by long distance axon regeneration following SCI is a worthwhile aspiration, a more realistic goal would be the induction of short distance axon regeneration resulting in the effective lowering of the level of the spinal deficit. Even seemingly small improvements in function can have a disproportionately large impact on the quality of life of SCI patients. For example, a treatment-induced return in the ability to grip with the hands or to regain some degree of manual dexterity could lead to the patient being able to regain a greater degree of independence of patients suffering from cervical spinal cord injuries.

5.5. Conclusion

The *in vitro* results demonstrated a more detailed characterisation of the hNP and their differentiated progeny: the hNP-AC. The basic axon growth promoting properties of the differentiated cells have been demonstrated in tissue culture as well as the cell-substrate interactions with bioengineered materials in 2D (orientated nanofibres) and 3D (collagen scaffold) studies. The ability of the hNP-AC-seeded scaffolds to support improved graft-host integration and host axonal growth, and hNP-AC supensions to improve host axonal growth *in vivo* have also been demonstrated in experimental models of spinal cord injury. It is now clear that ***hNP-AC do indeed have similar properties to their rat counterpart***. However, donor cells failed to exert any substantial functional improvement in the *in vivo* models of spinal cord injury. Further investigations will be required to clarify the reasons for the apparent inability of the donor hNP-AC to promote any significant functional improvement.

Bibliography

[1] A. Abbott. Cell culture: biology's new dimension. *Nature*, 424(6951):870–872, Aug 2003. doi: 10.1038/424870a. URL http://dx.doi.org/10.1038/424870a.

[2] K. H. Adcock, D. J. Brown, M. C. Shearer, D. Shewan, M. Schachner, G. M. Smith, H. M. Geller, and J. W. Fawcett. Axon behaviour at schwann cell - astrocyte boundaries: manipulation of axon signalling pathways and the neural adhesion molecule l1 can enable axons to cross. *Eur J Neurosci*, 20(6):1425–1435, Sep 2004. doi: 10.1111/j.1460-9568.2004.03573.x. URL http://dx.doi.org/10.1111/j.1460-9568.2004.03573.x.

[3] F. T. Afshari, J. C. Kwok, and J. W. Fawcett. Astrocyte-produced ephrins inhibit schwann cell migration via vav2 signaling. *J Neurosci*, 30(12):4246–4255, Mar 2010. doi: 10.1523/JNEUROSCI.3351-09.2010. URL http://dx.doi.org/10.1523/JNEUROSCI.3351-09.2010.

[4] F. T. Afshari, J. C. Kwok, L. White, and J. W. Fawcett. Schwann cell migration is integrin-dependent and inhibited by astrocyte-produced aggrecan. *Glia*, 58(7):857–869, May 2010. doi: 10.1002/glia.20970. URL http://dx.doi.org/10.1002/glia.20970.

[5] S. Akgun, A. Tekeli, O. Kurtkaya, A. Civelek, S. C. Isbir, K. Ak, S. Arsan, and A. Sav. Neuroprotective effects of fk-506, l-carnitine and azathioprine on spinal cord ischemia-reperfusion injury. *Eur J Cardiothorac Surg*, 25(1):105–110, Jan 2004.

[6] J. Altman and G. D. Das. Post-natal origin of microneurones in the rat brain. *Nature*, 207(5000): 953–956, Aug 1965.

[7] A. Alvarez-Buylla and C. Lois. Neuronal stem cells in the brain of adult vertebrates. *Stem Cells*, 13(3):263–272, May 1995. doi: 10.1002/stem.5530130307. URL http://dx.doi.org/10.1002/stem.5530130307.

[8] A. P. Amar and M. L. Levy. Pathogenesis and pharmacological strategies for mitigating secondary damage in acute spinal cord injury. *Neurosurgery*, 44(5):1027–39; discussion 1039–40, May 1999.

[9] A. J. Anderson. Mechanisms and pathways of inflammatory responses in cns trauma: spinal cord injury. *J Spinal Cord Med*, 25(2):70–9; discussion 80, 2002.

[10] D. K. Anderson, D. R. Howland, and P. J. Reier. Fetal neural grafts and repair of the injured spinal cord. *Brain Pathol*, 5(4):451–457, Oct 1995.

[11] D. P. Ankeny, D. M. McTigue, and L. B. Jakeman. Bone marrow transplants provide tissue protection and directional guidance for axons after contusive spinal cord injury in rats. *Exp Neurol*, 190(1):17–31, Nov 2004. doi: 10.1016/j.expneurol.2004.05.045. URL `http://dx.doi.org/10.1016/j.expneurol.2004.05.045`.

[12] A. D. Ansselin, T. Fink, and D. F. Davey. Peripheral nerve regeneration through nerve guides seeded with adult schwann cells. *Neuropathol Appl Neurobiol*, 23(5):387–398, Oct 1997.

[13] S. J. Archibald, J. Shefner, C. Krarup, and R. D. Madison. Monkey median nerve repaired by nerve graft or collagen nerve guide tube. *J Neurosci*, 15(5 Pt 2):4109–4123, May 1995.

[14] O. Arosarena. Tissue engineering. *Curr Opin Otolaryngol Head Neck Surg*, 13(4):233–241, Aug 2005.

[15] J. K. Atwal, J. Pinkston-Gosse, J. Syken, S. Stawicki, Y. Wu, C. Shatz, and M. Tessier-Lavigne. Pirb is a functional receptor for myelin inhibitors of axonal regeneration. *Science*, 322(5903):967–970, Nov 2008. doi: 10.1126/science.1161151. URL `http://dx.doi.org/10.1126/science.1161151`.

[16] S. A. Azizi, D. Stokes, B. J. Augelli, C. DiGirolamo, and D. J. Prockop. Engraftment and migration of human bone marrow stromal cells implanted in the brains of albino rats–similarities to astrocyte grafts. *Proc Natl Acad Sci U S A*, 95(7):3908–3913, Mar 1998.

[17] J. D. Balentine. Pathology of experimental spinal cord trauma. i. the necrotic lesion as a function of vascular injury. *Lab Invest*, 39(3):236–253, Sep 1978.

[18] C. E. Bandtlow and J. Löschinger. Developmental changes in neuronal responsiveness to the cns myelin-associated neurite growth inhibitor ni-35/250. *Eur J Neurosci*, 9(12):2743–2752, Dec 1997.

[19] D. J. Barakat, S. M. Gaglani, S. R. Neravetla, A. R. Sanchez, C. M. Andrade, Y. Pressman, R. Puzis, M. S. Garg, M. B. Bunge, and D. D. Pearse. Survival, integration, and axon growth support of glia transplanted into the chronically contused spinal cord. *Cell Transplant*, 14(4):225–240, 2005.

[20] M. Barczyk, S. Carracedo, and D. Gullberg. Integrins. *Cell Tissue Res*, 339(1):269–280, Jan 2010. doi: 10.1007/s00441-009-0834-6. URL `http://dx.doi.org/10.1007/s00441-009-0834-6`.

[21] F. M. Bareyre. Neuronal repair and replacement in spinal cord injury. *J Neurol Sci*, 265(1-2):63–72, Feb 2008. doi: 10.1016/j.jns.2007.05.004. URL `http://dx.doi.org/10.1016/j.jns.2007.05.004`.

[22] F. M. Bareyre, B. Haudenschild, and M. E. Schwab. Long-lasting sprouting and gene expression changes induced by the monoclonal antibody in-1 in the adult spinal cord. *J Neurosci*, 22(16):7097–7110, Aug 2002. doi: 20026733. URL `http://dx.doi.org/20026733`.

[23] F. M. Bareyre, M. Kerschensteiner, O. Raineteau, T. C. Mettenleiter, O. Weinmann, and M. E. Schwab. The injured spinal cord spontaneously forms a new intraspinal circuit in adult rats. *Nat Neurosci*, 7(3):269–277, Mar 2004. doi: 10.1038/nn1195. URL `http://dx.doi.org/10.1038/nn1195`.

[24] F. Barnabé-Heider and J. Frisén. Stem cells for spinal cord repair. *Cell Stem Cell*, 3(1):16–24, Jul 2008. doi: 10.1016/j.stem.2008.06.011. URL `http://dx.doi.org/10.1016/j.stem.2008.06.011`.

[25] R. Barouch and M. Schwartz. Autoreactive t cells induce neurotrophin production by immune and neural cells in injured rat optic nerve: implications for protective autoimmunity. *FASEB J*, 16(10): 1304–1306, Aug 2002. doi: 10.1096/fj.01-0467fje. URL `http://dx.doi.org/10.1096/fj.01-0467fje`.

[26] J. E. Barralet, L. Wang, M. Lawson, J. T. Triffitt, P. R. Cooper, and R. M. Shelton. Comparison of bone marrow cell growth on 2d and 3d alginate hydrogels. *J Mater Sci Mater Med*, 16(6):515–519, Jun 2005. doi: 10.1007/s10856-005-0526-z. URL `http://dx.doi.org/10.1007/s10856-005-0526-z`.

[27] C. P. Barrett, L. Guth, E. J. Donati, and J. G. Krikorian. Astroglial reaction in the gray matter lumbar segments after midthoracic transection of the adult rat spinal cord. *Exp Neurol*, 73(2):365–377, Aug 1981.

[28] C. P. Barrett, E. J. Donati, and L. Guth. Differences between adult and neonatal rats in their astroglial response to spinal injury. *Exp Neurol*, 84(2):374–385, May 1984.

[29] U. Bartsch, C. E. Bandtlow, L. Schnell, S. Bartsch, A. A. Spillmann, B. P. Rubin, R. Hillenbrand, D. Montag, M. E. Schwab, and M. Schachner. Lack of evidence that myelin-associated glycoprotein is a major inhibitor of axonal regeneration in the cns. *Neuron*, 15(6):1375–1381, Dec 1995.

[30] D. M. Basso, M. S. Beattie, and J. C. Bresnahan. A sensitive and reliable locomotor rating scale for open field testing in rats. *J Neurotrauma*, 12(1):1–21, Feb 1995.

[31] L. Bauchet, N. Lonjon, F.-E. Perrin, C. Gilbert, A. Privat, and C. Fattal. Strategies for spinal cord repair after injury: a review of the literature and information. *Ann Phys Rehabil Med*, 52(4):330–351, May 2009.

[32] S. Bavetta, P. J. Hamlyn, G. Burnstock, A. R. Lieberman, and P. N. Anderson. The effects of fk506 on dorsal column axons following spinal cord injury in adult rats: neuroprotection and local regeneration. *Exp Neurol*, 158(2):382–393, Aug 1999. doi: 10.1006/exnr.1999.7119. URL `http://dx.doi.org/10.1006/exnr.1999.7119`.

[33] M. S. Beattie, J. C. Bresnahan, J. Komon, C. A. Tovar, M. V. Meter, D. K. Anderson, A. I. Faden, C. Y. Hsu, L. J. Noble, S. Salzman, and W. Young. Endogenous repair after spinal cord contusion injuries in the rat. *Exp Neurol*, 148(2):453–463, Dec 1997. doi: 10.1006/exnr.1997.6695. URL `http://dx.doi.org/10.1006/exnr.1997.6695`.

[34] D. L. Behrmann, J. C. Bresnahan, and M. S. Beattie. Modeling of acute spinal cord injury in the rat: neuroprotection and enhanced recovery with methylprednisolone, u-74006f and ym-14673. *Exp Neurol*, 126(1):61–75, Mar 1994. doi: 10.1006/exnr.1994.1042. URL `http://dx.doi.org/10.1006/exnr.1994.1042`.

[35] C. Berthold, J. Fraher, R. King, and M. Rydmark. *Microscopic Anatomy of the Peripheral Nervous System. In Perpheral Neuropathy.* Elsevier Saunders, Pennsylvania., 2005.

[36] J. R. Bethea. Spinal cord injury-induced inflammation: a dual-edged sword. *Prog Brain Res*, 128:33–42, 2000. doi: 10.1016/S0079-6123(00)28005-9. URL `http://dx.doi.org/10.1016/S0079-6123(00)28005-9`.

[37] J. R. Bethea, H. Nagashima, M. C. Acosta, C. Briceno, F. Gomez, A. E. Marcillo, K. Loor, J. Green, and W. D. Dietrich. Systemically administered interleukin-10 reduces tumor necrosis factor-alpha production and significantly improves functional recovery following traumatic spinal cord injury in rats. *J Neurotrauma*, 16(10):851–863, Oct 1999.

[38] R. Biran, M. D. Noble, and P. A. Tresco. Directed nerve outgrowth is enhanced by engineered glial substrates. *Exp Neurol*, 184(1):141–152, Nov 2003.

[39] J. L. Bixby, J. Lilien, and L. F. Reichardt. Identification of the major proteins that promote neuronal process outgrowth on schwann cells in vitro. *J Cell Biol*, 107(1):353–361, Jul 1988.

[40] W. F. Blakemore, R. A. Eames, K. J. Smith, and W. I. McDonald. Remyelination in the spinal cord of the cat following intraspinal injections of lysolecithin. *J Neurol Sci*, 33(1-2):31–43, Aug 1977.

[41] A. Blesch and M. H. Tuszynski. Cellular gdnf delivery promotes growth of motor and dorsal column sensory axons after partial and complete spinal cord transections and induces remyelination. *J Comp Neurol*, 467(3):403–417, Dec 2003. doi: 10.1002/cne.10934. URL `http://dx.doi.org/10.1002/cne.10934`.

[42] A. Blesch and M. H. Tuszynski. Transient growth factor delivery sustains regenerated axons after spinal cord injury. *J Neurosci*, 27(39):10535–10545, Sep 2007. doi: 10.1523/JNEUROSCI.1903-07.2007. URL `http://dx.doi.org/10.1523/JNEUROSCI.1903-07.2007`.

[43] A. R. Blight. Cellular morphology of chronic spinal cord injury in the cat: analysis of myelinated axons by line-sampling. *Neuroscience*, 10(2):521–543, Oct 1983.

[44] A. R. Blight. Effects of silica on the outcome from experimental spinal cord injury: implication of macrophages in secondary tissue damage. *Neuroscience*, 60(1):263–273, May 1994.

[45] A. R. Blight and V. Decrescito. Morphometric analysis of experimental spinal cord injury in the cat: the relation of injury intensity to survival of myelinated axons. *Neuroscience*, 19(1):321–341, Sep 1986.

[46] B. Blits, P. A. Dijkhuizen, T. P. Carlstedt, H. Poldervaart, S. Schiemanck, G. J. Boer, and J. Verhaagen. Adenoviral vector-mediated expression of a foreign gene in peripheral nerve tissue bridges implanted in the injured peripheral and central nervous system. *Exp Neurol*, 160(1):256–267, Nov 1999. doi: 10.1006/exnr.1999.7204. URL http://dx.doi.org/10.1006/exnr.1999.7204.

[47] J. Bockelmann, K. Klinkhammer, A. von Holst, N. Seiler, A. Faissner, G. A. Brook, D. Klee, and J. Mey. Functionalization of electrospun poly(epsilon-caprolactone) fibers with the extracellular matrix-derived peptide grgds improves guidance of schwann cell migration and axonal growth. *Tissue Eng Part A*, 17(3-4):475–486, Feb 2011. doi: 10.1089/ten.TEA.2010.0369. URL http://dx.doi.org/10.1089/ten.TEA.2010.0369.

[48] Y. Bomstein, J. B. Marder, K. Vitner, I. Smirnov, G. Lisaey, O. Butovsky, V. Fulga, and E. Yoles. Features of skin-coincubated macrophages that promote recovery from spinal cord injury. *J Neuroimmunol*, 142(1-2):10–16, Sep 2003.

[49] U. Boudriot, R. Dersch, A. Greiner, and J. H. Wendorff. Electrospinning approaches toward scaffold engineering–a brief overview. *Artif Organs*, 30(10):785–792, Oct 2006. doi: 10.1111/j.1525-1594.2006.00301.x. URL http://dx.doi.org/10.1111/j.1525-1594.2006.00301.x.

[50] A. Bozkurt, G. A. Brook, S. Moellers, F. Lassner, B. Sellhaus, J. Weis, M. Woeltje, J. Tank, C. Beckmann, P. Fuchs, L. O. Damink, F. Schügner, I. Heschel, and N. Pallua. In vitro assessment of axonal growth using dorsal root ganglia explants in a novel three-dimensional collagen matrix. *Tissue Eng*, 13(12):2971–2979, Dec 2007. doi: 10.1089/ten.2007.0116. URL http://dx.doi.org/10.1089/ten.2007.0116.

[51] A. Bozkurt, R. Deumens, C. Beckmann, L. O. Damink, F. Schügner, I. Heschel, B. Sellhaus, J. Weis, W. Jahnen-Dechent, G. A. Brook, and N. Pallua. In vitro cell alignment obtained with a schwann cell enriched microstructured nerve guide with longitudinal guidance channels. *Biomaterials*, 30(2):169–179, Jan 2009. doi: 10.1016/j.biomaterials.2008.09.017. URL http://dx.doi.org/10.1016/j.biomaterials.2008.09.017.

[52] E. J. Bradbury and S. B. McMahon. Spinal cord repair strategies: why do they work? *Nat Rev Neurosci*, 7(8):644–653, Aug 2006. doi: 10.1038/nrn1964. URL http://dx.doi.org/10.1038/nrn1964.

[53] J. M. Braz and A. I. Basbaum. Genetically expressed transneuronal tracer reveals direct and indirect serotonergic descending control circuits. *J Comp Neurol*, 507(6):1990–2003, Apr 2008. doi: 10.1002/cne.21665. URL http://dx.doi.org/10.1002/cne.21665.

[54] B. S. Bregman, E. Kunkel-Bagden, L. Schnell, H. N. Dai, D. Gao, and M. E. Schwab. Recovery from spinal cord injury mediated by antibodies to neurite growth inhibitors. *Nature*, 378(6556):498–501, Nov 1995. doi: 10.1038/378498a0. URL http://dx.doi.org/10.1038/378498a0.

[55] K. L. Brewer, J. R. Bethea, and R. P. Yezierski. Neuroprotective effects of interleukin-10 following excitotoxic spinal cord injury. *Exp Neurol*, 159(2):484–493, Oct 1999. doi: 10.1006/exnr.1999.7173. URL `http://dx.doi.org/10.1006/exnr.1999.7173`.

[56] G. A. Brook, J. M. Lawrence, B. Shah, and G. Raisman. Extrusion transplantation of schwann cells into the adult rat thalamus induces directional host axon growth. *Exp Neurol*, 126(1):31–43, Mar 1994. doi: 10.1006/exnr.1994.1040. URL `http://dx.doi.org/10.1006/exnr.1994.1040`.

[57] G. A. Brook, D. Plate, R. Franzen, D. Martin, G. Moonen, J. Schoenen, A. B. Schmitt, J. Noth, and W. Nacimiento. Spontaneous longitudinally orientated axonal regeneration is associated with the schwann cell framework within the lesion site following spinal cord compression injury of the rat. *J Neurosci Res*, 53(1):51–65, Jul 1998.

[58] G. A. Brook, C. Spitzer, W. Nacimiento, P. L. Woodhams, and J. Noth. A novel early component of the cell body response in axotomized clarke's nucleus neurons revealed by monoclonal antibody py. *Exp Neurol*, 149(1):64–72, Jan 1998. doi: 10.1006/exnr.1997.6714. URL `http://dx.doi.org/10.1006/exnr.1997.6714`.

[59] G. A. Brook, A. Pérez-Bouza, J. Noth, and W. Nacimiento. Astrocytes re-express nestin in deafferented target territories of the adult rat hippocampus. *Neuroreport*, 10(5):1007–1011, Apr 1999.

[60] G. A. Brook, D. A. Houweling, R. G. Gieling, T. Hermanns, E. A. Joosten, D. P. Bär, W. H. Gispen, A. B. Schmitt, P. Leprince, J. Noth, and W. Nacimiento. Attempted endogenous tissue repair following experimental spinal cord injury in the rat: involvement of cell adhesion molecules l1 and ncam? *Eur J Neurosci*, 12(9):3224–3238, Sep 2000.

[61] G. A. Brook, J. M. Lawrence, and G. Raisman. Columns of schwann cells extruded into the cns induce in-growth of astrocytes to form organized new glial pathways. *Glia*, 33(2):118–130, Feb 2001.

[62] O. Brüstle, K. N. Jones, R. D. Learish, K. Karram, K. Choudhary, O. D. Wiestler, I. D. Duncan, and R. D. McKay. Embryonic stem cell-derived glial precursors: a source of myelinating transplants. *Science*, 285(5428):754–756, Jul 1999.

[63] C. D. Buckley, D. Pilling, J. M. Lord, A. N. Akbar, D. Scheel-Toellner, and M. Salmon. Fibroblasts regulate the switch from acute resolving to chronic persistent inflammation. *Trends Immunol*, 22(4): 199–204, Apr 2001.

[64] M. B. Bunge. Transplantation of purified populations of schwann cells into lesioned adult rat spinal cord. *J Neurol*, 242(1 Suppl 1):S36–S39, Dec 1994.

[65] R. P. Bunge, W. R. Puckett, J. L. Becerra, A. Marcillo, and R. M. Quencer. Observations on the pathology of human spinal cord injury. a review and classification of 22 new cases with details from a case of chronic cord compression with extensive focal demyelination. *Adv Neurol*, 59:75–89, 1993.

[66] R. P. Bunge, W. R. Puckett, and E. D. Hiester. Observations on the pathology of several types of human spinal cord injury, with emphasis on the astrocyte response to penetrating injuries. *Adv Neurol*, 72:305–315, 1997.

[67] T. G. Bush, N. Puvanachandra, C. H. Horner, A. Polito, T. Ostenfeld, C. N. Svendsen, L. Mucke, M. H. Johnson, and M. V. Sofroniew. Leukocyte infiltration, neuronal degeneration, and neurite outgrowth after ablation of scar-forming, reactive astrocytes in adult transgenic mice. *Neuron*, 23(2):297–308, Jun 1999.

[68] A. Buss and M. E. Schwab. Sequential loss of myelin proteins during wallerian degeneration in the rat spinal cord. *Glia*, 42(4):424–432, Jun 2003. doi: 10.1002/glia.10220. URL `http://dx.doi.org/10.1002/glia.10220`.

[69] S. R. Y. Cajal. *Degeneration and Regeneration of the Nervous System, Vol. 1*, volume 1. New York: Oxford University Press, American Branch, 1928.

[70] S. R. Y. Cajal. *Degeneration and Regeneration of the Nervous System, Vol. 2*, volume 2. New York: Oxford University Press, American Branch, 1928.

[71] Q. L. Cao, Y. P. Zhang, R. M. Howard, W. M. Walters, P. Tsoulfas, and S. R. Whittemore. Pluripotent stem cells engrafted into the normal or lesioned adult rat spinal cord are restricted to a glial lineage. *Exp Neurol*, 167(1):48–58, Jan 2001. doi: 10.1006/exnr.2000.7536. URL `http://dx.doi.org/10.1006/exnr.2000.7536`.

[72] I. Carlstedt, L. Cöster, and A. Malmström. Isolation and characterization of dermatan sulphate and heparan sulphate proteoglycans from fibroblast culture. *Biochem J*, 197(1):217–225, Jul 1981.

[73] T. Carlstedt. Nerve fibre regeneration across the peripheral-central transitional zone. *J Anat*, 190 (Pt 1):51–56, Jan 1997.

[74] C. C. M. Chan. Inflammation: beneficial or detrimental after spinal cord injury? *Recent Pat CNS Drug Discov*, 3(3):189–199, Nov 2008.

[75] S. R. Chaplan, F. W. Bach, J. W. Pogrel, J. M. Chung, and T. L. Yaksh. Quantitative assessment of tactile allodynia in the rat paw. *J Neurosci Methods*, 53(1):55–63, Jul 1994.

[76] C. H. Chau, D. K. Y. Shum, H. Li, J. Pei, Y. Y. Lui, L. Wirthlin, Y. S. Chan, and X.-M. Xu. Chondroitinase abc enhances axonal regrowth through schwann cell-seeded guidance channels after spinal cord injury. *FASEB J*, 18(1):194–196, Jan 2004. doi: 10.1096/fj.03-0196fje. URL `http://dx.doi.org/10.1096/fj.03-0196fje`.

[77] C. S. Chen, M. Mrksich, S. Huang, G. M. Whitesides, and D. E. Ingber. Geometric control of cell life and death. *Science*, 276(5317):1425–1428, May 1997.

[78] C. S. Chen, M. Mrksich, S. Huang, G. M. Whitesides, and D. E. Ingber. Micropatterned surfaces for control of cell shape, position, and function. *Biotechnol Prog*, 14(3):356–363, 1998. doi: 10.1021/bp980031m. URL http://dx.doi.org/10.1021/bp980031m.

[79] M. S. Chen, A. B. Huber, M. E. van der Haar, M. Frank, L. Schnell, A. A. Spillmann, F. Christ, and M. E. Schwab. Nogo-a is a myelin-associated neurite outgrowth inhibitor and an antigen for monoclonal antibody in-1. *Nature*, 403(6768):434–439, Jan 2000. doi: 10.1038/35000219. URL http://dx.doi.org/10.1038/35000219.

[80] Y. Chen, N. E. Vartiainen, W. Ying, P. H. Chan, J. Koistinaho, and R. A. Swanson. Astrocytes protect neurons from nitric oxide toxicity by a glutathione-dependent mechanism. *J Neurochem*, 77 (6):1601–1610, Jun 2001.

[81] S. R. Clarke, A. K. Shetty, J. L. Bradley, and D. A. Turner. Reactive astrocytes express the embryonic intermediate neurofilament nestin. *Neuroreport*, 5(15):1885–1888, Oct 1994.

[82] C. D. Clemente. Regeneration in the vertebrate central nervous system. *Int Rev Neurobiol*, 6:257–301, 1964.

[83] G. Clowry, K. Sieradzan, and G. Vrbová. Grafts of embryonic tissue into spinal cord: a possible strategy for treating neuromuscular disorders. *Neuromuscul Disord*, 1(2):87–92, 1991.

[84] W. Colin and R. B. Donoff. Nerve regeneration through collagen tubes. *J Dent Res*, 63(7):987–993, Jul 1984.

[85] S. Constantini and W. Young. The effects of methylprednisolone and the ganglioside gm1 on acute spinal cord injury in rats. *J Neurosurg*, 80(1):97–111, Jan 1994. doi: 10.3171/jns.1994.80.1.0097. URL http://dx.doi.org/10.3171/jns.1994.80.1.0097.

[86] J. M. Corey, D. Y. Lin, K. B. Mycek, Q. Chen, S. Samuel, E. L. Feldman, and D. C. Martin. Aligned electrospun nanofibers specify the direction of dorsal root ganglia neurite growth. *J Biomed Mater Res A*, 83(3):636–645, Dec 2007. doi: 10.1002/jbm.a.31285. URL http://dx.doi.org/10.1002/jbm.a.31285.

[87] J. M. Corey, C. C. Gertz, B.-S. Wang, L. K. Birrell, S. L. Johnson, D. C. Martin, and E. L. Feldman. The design of electrospun plla nanofiber scaffolds compatible with serum-free growth of primary motor and sensory neurons. *Acta Biomater*, 4(4):863–875, Jul 2008. doi: 10.1016/j.actbio.2008.02.020. URL http://dx.doi.org/10.1016/j.actbio.2008.02.020.

[88] C. J. Cornbrooks, D. J. Carey, J. A. McDonald, R. Timpl, and R. P. Bunge. In vivo and in vitro observations on laminin production by schwann cells. *Proc Natl Acad Sci U S A*, 80(12):3850–3854, Jun 1983.

[89] G. Courtine, M. B. Bunge, J. W. Fawcett, R. G. Grossman, J. H. Kaas, R. Lemon, I. Maier, J. Martin, R. J. Nudo, A. Ramon-Cueto, E. M. Rouiller, L. Schnell, T. Wannier, M. E. Schwab, and V. R. Edgerton. Can experiments in nonhuman primates expedite the translation of treatments for spinal cord injury in humans? *Nat Med*, 13(5):561–566, May 2007. doi: 10.1038/nm1595. URL `http://dx.doi.org/10.1038/nm1595`.

[90] M. Coutts and H. S. Keirstead. Stem cells for the treatment of spinal cord injury. *Exp Neurol*, 209(2):368–377, Feb 2008. doi: 10.1016/j.expneurol.2007.09.002. URL `http://dx.doi.org/10.1016/j.expneurol.2007.09.002`.

[91] E. Cukierman, R. Pankov, D. R. Stevens, and K. M. Yamada. Taking cell-matrix adhesions to the third dimension. *Science*, 294(5547):1708–1712, Nov 2001. doi: 10.1126/science.1064829. URL `http://dx.doi.org/10.1126/science.1064829`.

[92] B. J. Cummings, N. Uchida, S. J. Tamaki, D. L. Salazar, M. Hooshmand, R. Summers, F. H. Gage, and A. J. Anderson. Human neural stem cells differentiate and promote locomotor recovery in spinal cord-injured mice. *Proc Natl Acad Sci U S A*, 102(39):14069–14074, Sep 2005. doi: 10.1073/pnas.0507063102. URL `http://dx.doi.org/10.1073/pnas.0507063102`.

[93] B. J. Cummings, N. Uchida, S. J. Tamaki, and A. J. Anderson. Human neural stem cell differentiation following transplantation into spinal cord injured mice: association with recovery of locomotor function. *Neurol Res*, 28(5):474–481, Jul 2006. doi: 10.1179/016164106X115116. URL `http://dx.doi.org/10.1179/016164106X115116`.

[94] R. Curtis, D. Green, R. M. Lindsay, and G. P. Wilkin. Up-regulation of gap-43 and growth of axons in rat spinal cord after compression injury. *J Neurocytol*, 22(1):51–64, Jan 1993.

[95] D. Dahl, A. Bignami, K. Weber, and M. Osborn. Filament proteins in rat optic nerves undergoing wallerian degeneration: localization of vimentin, the fibroblastic 100-a filament protein, in normal and reactive astrocytes. *Exp Neurol*, 73(2):496–506, Aug 1981.

[96] D. Dahl, D. C. Rueger, A. Bignami, K. Weber, and M. Osborn. Vimentin, the 57 000 molecular weight protein of fibroblast filaments, is the major cytoskeletal component in immature glia. *Eur J Cell Biol*, 24(2):191–196, Jun 1981.

[97] P. D. Dalton and J. Mey. Neural interactions with materials. *Front Biosci*, 14:769–795, 2009.

[98] S. David and A. J. Aguayo. Axonal elongation into peripheral nervous system "bridges" after central nervous system injury in adult rats. *Science*, 214(4523):931–933, Nov 1981.

[99] J. Davies, C. Pröschel, N. Zhang, M. Noble, M. Mayer-Pröschel, and S. Davies. Transplanted astrocytes derived from bmp- or cntf-treated glial-restricted precursors have opposite effects on recovery and allodynia after spinal cord injury. *J Biol*, 7(7):24, Sep 2008. doi: 10.1186/jbiol85. URL `http://dx.doi.org/10.1186/jbiol85`.

[100] J. E. Davies, C. Huang, C. Proschel, M. Noble, M. Mayer-Proschel, and S. J. Davies. Astrocytes derived from glial-restricted precursors promote spinal cord repair. *J Biol*, 5(3):7, 2006. doi: 10.1186/jbiol35. URL `http://dx.doi.org/10.1186/jbiol35`.

[101] S. J. A. Davies, C.-H. Shih, M. Noble, M. Mayer-Proschel, J. E. Davies, and C. Proschel. Transplantation of specific human astrocytes promotes functional recovery after spinal cord injury. *PLoS One*, 6(3):e173, Mar 2011. doi: doi:10.1371/journal.pone.0017328.

[102] P. Delree, P. Leprince, J. Schoenen, and G. Moonen. Purification and culture of adult rat dorsal root ganglia neurons. *J Neurosci Res*, 23(2):198–206, Jun 1989. doi: 10.1002/jnr.490230210. URL `http://dx.doi.org/10.1002/jnr.490230210`.

[103] R. Deumens, G. C. Koopmans, C. G. J. D. Bakker, V. Maquet, S. Blacher, W. M. M. Honig, R. Jérôme, J.-P. Pirard, H. W. M. Steinbusch, and E. A. J. Joosten. Alignment of glial cells stimulates directional neurite growth of cns neurons in vitro. *Neuroscience*, 125(3):591–604, 2004. doi: 10.1016/j.neuroscience.2004.02.010. URL `http://dx.doi.org/10.1016/j.neuroscience.2004.02.010`.

[104] R. Deumens, G. C. Koopmans, W. M. M. Honig, F. P. T. Hamers, V. Maquet, R. Jérôme, H. W. M. Steinbusch, and E. A. J. Joosten. Olfactory ensheathing cells, olfactory nerve fibroblasts and biomatrices to promote long-distance axon regrowth and functional recovery in the dorsally hemisected adult rat spinal cord. *Exp Neurol*, 200(1):89–103, Jul 2006. doi: 10.1016/j.expneurol.2006.01.030. URL `http://dx.doi.org/10.1016/j.expneurol.2006.01.030`.

[105] P. Dibaj, F. Nadrigny, H. Steffens, A. Scheller, J. Hirrlinger, E. D. Schomburg, C. Neusch, and F. Kirchhoff. No mediates microglial response to acute spinal cord injury under atp control in vivo. *Glia*, 58(9):1133–1144, Jul 2010. doi: 10.1002/glia.20993. URL `http://dx.doi.org/10.1002/glia.20993`.

[106] C. D. Dijkstra, E. A. Döpp, P. Joling, and G. Kraal. The heterogeneity of mononuclear phagocytes in lymphoid organs: distinct macrophage subpopulations in the rat recognized by monoclonal antibodies ed1, ed2 and ed3. *Immunology*, 54(3):589–599, Mar 1985.

[107] L. E. Dike, C. S. Chen, M. Mrksich, J. Tien, G. M. Whitesides, and D. E. Ingber. Geometric control of switching between growth, apoptosis, and differentiation during angiogenesis using micropatterned substrates. *In Vitro Cell Dev Biol Anim*, 35(8):441–448, Sep 1999. doi: 10.1007/s11626-999-0050-4. URL `http://dx.doi.org/10.1007/s11626-999-0050-4`.

[108] W. J. Dixon. Efficient analysis of experimental observations. *Annu Rev Pharmacol Toxicol*, 20:441–462, 1980. doi: 10.1146/annurev.pa.20.040180.002301. URL http://dx.doi.org/10.1146/annurev.pa.20.040180.002301.

[109] M. Domeniconi, Z. Cao, T. Spencer, R. Sivasankaran, K. Wang, E. Nikulina, N. Kimura, H. Cai, K. Deng, Y. Gao, Z. He, and M. Filbin. Myelin-associated glycoprotein interacts with the nogo66 receptor to inhibit neurite outgrowth. *Neuron*, 35(2):283–290, Jul 2002.

[110] K. Drögemüller, U. Helmuth, A. Brunn, M. Sakowicz-Burkiewicz, D. H. Gutmann, W. Mueller, M. Deckert, and D. Schlüter. Astrocyte gp130 expression is critical for the control of toxoplasma encephalitis. *J Immunol*, 181(4):2683–2693, Aug 2008.

[111] I. Dusart and M. E. Schwab. Secondary cell death and the inflammatory reaction after dorsal hemisection of the rat spinal cord. *Eur J Neurosci*, 6(5):712–724, May 1994.

[112] P. A. Eccleston, R. Mirsky, and K. R. Jessen. Spontaneous immortalisation of schwann cells in culture: short-term cultured schwann cells secrete growth inhibitory activity. *Development*, 112(1):33–42, May 1991.

[113] M. Eddleston and L. Mucke. Molecular profile of reactive astrocytes–implications for their role in neurologic disease.eddleston1993a. *Neuroscience*, 54(1):15–36, May 1993.

[114] E. Eftekharpour, S. Karimi-Abdolrezaee, and M. G. Fehlings. Current status of experimental cell replacement approaches to spinal cord injury. *Neurosurg Focus*, 24(3-4):E19, 2008. doi: 10.3171/FOC/2008/24/3-4/E18. URL http://dx.doi.org/10.3171/FOC/2008/24/3-4/E18.

[115] E. Eidelberg, D. Straehley, R. Erspamer, and C. J. Watkins. Relationship between residual hindlimb-assisted locomotion and surviving axons after incomplete spinal cord injuries. *Exp Neurol*, 56(2): 312–322, Aug 1977.

[116] S. Elkabes, E. M. DiCicco-Bloom, and I. B. Black. Brain microglia/macrophages express neurotrophins that selectively regulate microglial proliferation and function. *J Neurosci*, 16(8):2508–2521, Apr 1996.

[117] E. Emery, P. Aldana, M. B. Bunge, W. Puckett, A. Srinivasan, R. W. Keane, J. Bethea, and A. D. Levi. Apoptosis after traumatic human spinal cord injury. *J Neurosurg*, 89(6):911–920, Dec 1998. doi: 10.3171/jns.1998.89.6.0911. URL http://dx.doi.org/10.3171/jns.1998.89.6.0911.

[118] C. J. Emmett, W. Jaques-Berg, and P. J. Seeley. Microtransplantation of neural cells into adult rat brain. *Neuroscience*, 38(1):213–222, 1990.

[119] L. F. Eng. Glial fibrillary acidic protein (gfap): the major protein of glial intermediate filaments in differentiated astrocytes. *J Neuroimmunol*, 8(4-6):203–214, Jun 1985.

[120] M. Enomoto, K. Shinomiya, and S. Okabe. Migration and differentiation of neural progenitor cells from two different regions of embryonic central nervous system after transplantation into the intact spinal cord. *Eur J Neurosci*, 17(6):1223–1232, Mar 2003.

[121] G. U. Enzmann, R. L. Benton, J. F. Talbott, Q. Cao, and S. R. Whittemore. Functional considerations of stem cell transplantation therapy for spinal cord repair. *J Neurotrauma*, 23(3-4):479–495, 2006. doi: 10.1089/neu.2006.23.479. URL `http://dx.doi.org/10.1089/neu.2006.23.479`.

[122] P. S. Eriksson, E. Perfilieva, T. Björk-Eriksson, A. M. Alborn, C. Nordborg, D. A. Peterson, and F. H. Gage. Neurogenesis in the adult human hippocampus. *Nat Med*, 4(11):1313–1317, Nov 1998. doi: 10.1038/3305. URL `http://dx.doi.org/10.1038/3305`.

[123] A. B.-V. Evercooren, A. Gansmüller, E. Clerin, and M. Gumpel. Hoechst 33342 a suitable fluorescent marker for schwann cells after transplantation in the mouse spinal cord. *Neurosci Lett*, 131(2):241–244, Oct 1991.

[124] J. R. Fallon. Neurite guidance by non-neuronal cells in culture: preferential outgrowth of peripheral neurites on glial as compared to nonglial cell surfaces. *J Neurosci*, 5(12):3169–3177, Dec 1985.

[125] J. R. Fallon. Preferential outgrowth of central nervous system neurites on astrocytes and schwann cells as compared with nonglial cells in vitro. *J Cell Biol*, 100(1):198–207, Jan 1985.

[126] J. Faulkner and H. S. Keirstead. Human embryonic stem cell-derived oligodendrocyte progenitors for the treatment of spinal cord injury. *Transpl Immunol*, 15(2):131–142, Dec 2005. doi: 10.1016/j.trim.2005.09.007. URL `http://dx.doi.org/10.1016/j.trim.2005.09.007`.

[127] J. R. Faulkner, J. E. Herrmann, M. J. Woo, K. E. Tansey, N. B. Doan, and M. V. Sofroniew. Reactive astrocytes protect tissue and preserve function after spinal cord injury. *J Neurosci*, 24(9):2143–2155, Mar 2004. doi: 10.1523/JNEUROSCI.3547-03.2004. URL `http://dx.doi.org/10.1523/JNEUROSCI.3547-03.2004`.

[128] J. W. Fawcett. Intrinsic neuronal determinants of regeneration. *Trends Neurosci*, 15(1):5–8, Jan 1992.

[129] J. W. Fawcett. Overcoming inhibition in the damaged spinal cord. *J Neurotrauma*, 23(3-4):371–383, 2006. doi: 10.1089/neu.2006.23.371. URL `http://dx.doi.org/10.1089/neu.2006.23.371`.

[130] J. W. Fawcett and R. A. Asher. The glial scar and central nervous system repair. *Brain Res Bull*, 49 (6):377–391, Aug 1999.

[131] J. W. Fawcett, E. Housden, L. Smith-Thomas, and R. L. Meyer. The growth of axons in three-dimensional astrocyte cultures. *Dev Biol*, 135(2):449–458, Oct 1989.

[132] M. G. Fehlings and C. H. Tator. The relationships among the severity of spinal cord injury, residual neurological function, axon counts, and counts of retrogradely labeled neurons after experimental spinal cord injury. *Exp Neurol*, 132(2):220–228, Apr 1995.

[133] R. E. Feldmann and R. Mattern. The human brain and its neural stem cells postmortem: from dead brains to live therapy. *Int J Legal Med*, 120(4):201–211, Jul 2006. doi: 10.1007/s00414-005-0037-y. URL `http://dx.doi.org/10.1007/s00414-005-0037-y`.

[134] D. Feraboli-Lohnherr, D. Orsal, A. Yakovleff, M. G. y Ribotta, and A. Privat. Recovery of locomotor activity in the adult chronic spinal rat after sublesional transplantation of embryonic nervous cells: specific role of serotonergic neurons. *Exp Brain Res*, 113(3):443–454, Mar 1997.

[135] C. ffrench Constant and H. Colognato. Integrins: versatile integrators of extracellular signals. *Trends Cell Biol*, 14(12):678–686, Dec 2004. doi: 10.1016/j.tcb.2004.10.005. URL `http://dx.doi.org/10.1016/j.tcb.2004.10.005`.

[136] T. Führmann, L. M. Hillen, K. Montzka, M. Wöltje, and G. A. Brook. Cell-cell interactions of human neural progenitor-derived astrocytes within a microstructured 3d-scaffold. *Biomaterials*, 31(30):7705–7715, Oct 2010. doi: 10.1016/j.biomaterials.2010.06.060. URL `http://dx.doi.org/10.1016/j.biomaterials.2010.06.060`.

[137] T. Führmann, K. Montzka, L. M. Hillen, D. Hodde, A. Dreier, A. Bozkurt, M. Wöltje, and G. A. Brook. Axon growth-promoting properties of human bone marrow mesenchymal stromal cells. *Neurosci Lett*, 474(1):37–41, Apr 2010. doi: 10.1016/j.neulet.2010.03.002. URL `http://dx.doi.org/10.1016/j.neulet.2010.03.002`.

[138] D. F. Fiorentino, A. Zlotnik, T. R. Mosmann, M. Howard, and A. O'Garra. Il-10 inhibits cytokine production by activated macrophages. *J Immunol*, 147(11):3815–3822, Dec 1991.

[139] D. F. Fiorentino, A. Zlotnik, P. Vieira, T. R. Mosmann, M. Howard, K. W. Moore, and A. O'Garra. Il-10 acts on the antigen-presenting cell to inhibit cytokine production by th1 cells. *J Immunol*, 146 (10):3444–3451, May 1991.

[140] M. T. Fitch and J. Silver. Cns injury, glial scars, and inflammation: Inhibitory extracellular matrices and regeneration failure. *Exp Neurol*, 209(2):294–301, Feb 2008. doi: 10.1016/j.expneurol.2007.05.014. URL `http://dx.doi.org/10.1016/j.expneurol.2007.05.014`.

[141] M. T. Fitch, C. Doller, C. K. Combs, G. E. Landreth, and J. Silver. Cellular and molecular mechanisms of glial scarring and progressive cavitation: in vivo and in vitro analysis of inflammation-induced secondary injury after cns trauma. *J Neurosci*, 19(19):8182–8198, Oct 1999.

[142] J. C. Fleming, M. D. Norenberg, D. A. Ramsay, G. A. Dekaban, A. E. Marcillo, A. D. Saenz, M. Pasquale-Styles, W. D. Dietrich, and L. C. Weaver. The cellular inflammatory response in human spinal cords after injury. *Brain*, 129(Pt 12):3249–3269, Dec 2006. doi: 10.1093/brain/awl296. URL `http://dx.doi.org/10.1093/brain/awl296`.

[143] J. Fortun, C. E. Hill, and M. B. Bunge. Combinatorial strategies with schwann cell transplantation to improve repair of the injured spinal cord. *Neurosci Lett*, 456(3):124–132, Jun 2009. doi: 10.1016/j.neulet.2008.08.092. URL `http://dx.doi.org/10.1016/j.neulet.2008.08.092`.

[144] K. Fouad, L. Schnell, M. B. Bunge, M. E. Schwab, T. Liebscher, and D. D. Pearse. Combining schwann cell bridges and olfactory-ensheathing glia grafts with chondroitinase promotes locomotor recovery after complete transection of the spinal cord. *J Neurosci*, 25(5):1169–1178, Feb 2005. doi: 10.1523/JNEUROSCI.3562-04.2005. URL `http://dx.doi.org/10.1523/JNEUROSCI.3562-04.2005`.

[145] A. E. Fournier and S. M. Strittmatter. Repulsive factors and axon regeneration in the cns. *Curr Opin Neurobiol*, 11(1):89–94, Feb 2001.

[146] A. E. Fournier, T. GrandPre, and S. M. Strittmatter. Identification of a receptor mediating nogo-66 inhibition of axonal regeneration. *Nature*, 409(6818):341–346, Jan 2001. doi: 10.1038/35053072. URL `http://dx.doi.org/10.1038/35053072`.

[147] J. P. Fraher. Axon-glial relationships in early cns-pns transitional zone development: an ultrastructural study. *J Neurocytol*, 26(1):41–52, Jan 1997.

[148] J. P. Fraher. The transitional zone and cns regeneration. *J Anat*, 196 (Pt 1):137–158, Jan 2000.

[149] R. J. Franklin and W. F. Blakemore. The peripheral nervous system–central nervous system regeneration dichotomy: a role for glial cell transplantation. *J Cell Sci*, 95 (Pt 2):185–190, Feb 1990.

[150] R. Franzen, D. Martin, A. Daloze, G. Moonen, and J. Schoenen. Grafts of meningeal fibroblasts in adult rat spinal cord lesion promote axonal regrowth. *Neuroreport*, 10(7):1551–1556, May 1999.

[151] E. Freire, F. C. A. Gomes, T. Jotha-Mattos, V. M. Neto, F. C. S. Filho, and T. Coelho-Sampaio. Sialic acid residues on astrocytes regulate neuritogenesis by controlling the assembly of laminin matrices. *J Cell Sci*, 117(Pt 18):4067–4076, Aug 2004. doi: 10.1242/jcs.01276. URL `http://dx.doi.org/10.1242/jcs.01276`.

[152] J. Frisén, C. B. Johansson, C. Török, M. Risling, and U. Lendahl. Rapid, widespread, and longlasting induction of nestin contributes to the generation of glial scar tissue after cns injury. *J Cell Biol*, 131 (2):453–464, Oct 1995.

[153] K. Fukushima, M. Enomoto, S. Tomizawa, M. Takahashi, Y. Wakabayashi, S. Itoh, Y. Kuboki, and K. Shinomiya. The axonal regeneration across a honeycomb collagen sponge applied to the transected spinal cord. *J Med Dent Sci*, 55(1):71–79, Mar 2008.

[154] F. H. Gage. Mammalian neural stem cells. *Science*, 287(5457):1433–1438, Feb 2000.

[155] F. H. Gage, P. W. Coates, T. D. Palmer, H. G. Kuhn, L. J. Fisher, J. O. Suhonen, D. A. Peterson, S. T. Suhr, and J. Ray. Survival and differentiation of adult neuronal progenitor cells transplanted to the adult brain. *Proc Natl Acad Sci U S A*, 92(25):11879–11883, Dec 1995.

[156] D. Garbossa, M. Fontanella, C. Fronda, C. Benevello, G. Muraca, A. Ducati, and A. Vercelli. New strategies for repairing the injured spinal cord: the role of stem cells. *Neurol Res*, 28(5):500–504, Jul 2006. doi: 10.1179/016164106X115152. URL `http://dx.doi.org/10.1179/016164106X115152`.

[157] B. Geiger, A. Bershadsky, R. Pankov, and K. M. Yamada. Transmembrane crosstalk between the extracellular matrix–cytoskeleton crosstalk. *Nat Rev Mol Cell Biol*, 2(11):793–805, Nov 2001. doi: 10.1038/35099066. URL `http://dx.doi.org/10.1038/35099066`.

[158] F. Gelain, S. Panseri, S. Antonini, C. Cunha, M. Donega, J. Lowery, F. Taraballi, G. Cerri, M. Montagna, F. Baldissera, and A. Vescovi. Transplantation of nanostructured composite scaffolds results in the regeneration of chronically injured spinal cords. *ACS Nano*, 5(1):227–236, Jan 2011. doi: 10.1021/nn102461w. URL `http://dx.doi.org/10.1021/nn102461w`.

[159] J. Gerardo-Nava, T. Führmann, K. Klinkhammer, N. Seiler, J. Mey, D. Klee, M. Möller, P. D. Dalton, and G. A. Brook. Human neural cell interactions with orientated electrospun nanofibers in vitro. *Nanomed*, 4(1):11–30, Jan 2009. doi: 10.2217/17435889.4.1.11. URL `http://dx.doi.org/10.2217/17435889.4.1.11`.

[160] R. S. Ghirnikar, Y. L. Lee, and L. F. Eng. Chemokine antagonist infusion attenuates cellular infiltration following spinal cord contusion injury in rat. *J Neurosci Res*, 59(1):63–73, Jan 2000.

[161] A. Ghosh, F. Haiss, E. Sydekum, R. Schneider, M. Gullo, M. T. Wyss, T. Mueggler, C. Baltes, M. Rudin, B. Weber, and M. E. Schwab. Rewiring of hindlimb corticospinal neurons after spinal cord injury. *Nat Neurosci*, 13(1):97–104, Jan 2010. doi: 10.1038/nn.2448. URL `http://dx.doi.org/10.1038/nn.2448`.

[162] J. Golding, D. Shewan, and J. Cohen. Maturation of the mammalian dorsal root entry zone–from entry to no entry. *Trends Neurosci*, 20(7):303–308, Jul 1997.

[163] J. P. Golding, D. Shewan, M. Berry, and J. Cohen. An in vitro model of the rat dorsal root entry zone reveals developmental changes in the extent of sensory axon growth into the

spinal cord. *Mol Cell Neurosci*, 7(3):191–203, Mar 1996. doi: 10.1006/mcne.1996.0015. URL http://dx.doi.org/10.1006/mcne.1996.0015.

[164] J. P. Golding, C. Bird, S. McMahon, and J. Cohen. Behaviour of drg sensory neurites at the intact and injured adult rat dorsal root entry zone: postnatal neurites become paralysed, whilst injury improves the growth of embryonic neurites. *Glia*, 26(4):309–323, Jun 1999.

[165] S. Goldman. Stem and progenitor cell-based therapy of the human central nervous system. *Nat Biotechnol*, 23(7):862–871, Jul 2005. doi: 10.1038/nbt1119. URL http://dx.doi.org/10.1038/nbt1119.

[166] R. R. Gonzenbach and M. E. Schwab. Disinhibition of neurite growth to repair the injured adult cns: focusing on nogo. *Cell Mol Life Sci*, 65(1):161–176, Jan 2008. doi: 10.1007/s00018-007-7170-3. URL http://dx.doi.org/10.1007/s00018-007-7170-3.

[167] A. Gorio, L. Madaschi, B. D. Stefano, S. Carelli, A. M. D. Giulio, S. D. Biasi, T. Coleman, A. Cerami, and M. Brines. Methylprednisolone neutralizes the beneficial effects of erythropoietin in experimental spinal cord injury. *Proc Natl Acad Sci U S A*, 102(45):16379–16384, Nov 2005. doi: 10.1073/pnas.0508479102. URL http://dx.doi.org/10.1073/pnas.0508479102.

[168] M. B. Graeber, F. López-Redondo, E. Ikoma, M. Ishikawa, Y. Imai, K. Nakajima, G. W. Kreutzberg, and S. Kohsaka. The microglia/macrophage response in the neonatal rat facial nucleus following axotomy. *Brain Res*, 813(2):241–253, Dec 1998.

[169] D. Grafahrend, K.-H. Heffels, M. V. Beer, P. Gasteier, M. Möller, G. Boehm, P. D. Dalton, and J. Groll. Degradable polyester scaffolds with controlled surface chemistry combining minimal protein adsorption with specific bioactivation. *Nat Mater*, 10(1):67–73, Jan 2011. doi: 10.1038/nmat2904. URL http://dx.doi.org/10.1038/nmat2904.

[170] T. GrandPré, F. Nakamura, T. Vartanian, and S. M. Strittmatter. Identification of the nogo inhibitor of axon regeneration as a reticulon protein. *Nature*, 403(6768):439–444, Jan 2000. doi: 10.1038/35000226. URL http://dx.doi.org/10.1038/35000226.

[171] R. Grill, K. Murai, A. Blesch, F. H. Gage, and M. H. Tuszynski. Cellular delivery of neurotrophin-3 promotes corticospinal axonal growth and partial functional recovery after spinal cord injury. *J Neurosci*, 17(14):5560–5572, Jul 1997.

[172] R. J. Grill, A. Blesch, and M. H. Tuszynski. Robust growth of chronically injured spinal cord axons induced by grafts of genetically modified ngf-secreting cells. *Exp Neurol*, 148(2):444–452, Dec 1997. doi: 10.1006/exnr.1997.6704. URL http://dx.doi.org/10.1006/exnr.1997.6704.

[173] B. Grimpe and J. Silver. The extracellular matrix in axon regeneration. *Prog Brain Res*, 137:333–349, 2002.

[174] P. Gris, A. Tighe, D. Levin, R. Sharma, and A. Brown. Transcriptional regulation of scar gene expression in primary astrocytes. *Glia*, 55(11):1145–1155, Aug 2007. doi: 10.1002/glia.20537. URL http://dx.doi.org/10.1002/glia.20537.

[175] J. Groll, J. Fiedler, E. Engelhard, T. Ameringer, S. Tugulu, H.-A. Klok, R. E. Brenner, and M. Moeller. A novel star peg-derived surface coating for specific cell adhesion. *J Biomed Mater Res A*, 74(4):607–617, Sep 2005. doi: 10.1002/jbm.a.30335. URL http://dx.doi.org/10.1002/jbm.a.30335.

[176] L. Guth. Regeneration in the mammalian peripheral nervous system. *Physiol Rev*, 36(4):441–478, Oct 1956.

[177] L. Guth, C. P. Barrett, E. J. Donati, F. D. Anderson, M. V. Smith, and M. Lifson. Essentiality of a specific cellular terrain for growth of axons into a spinal cord lesion. *Exp Neurol*, 88(1):1–12, Apr 1985.

[178] S. S. Haghighi, S. K. Agrawal, D. Surdell, R. Plambeck, S. Agrawal, G. C. Johnson, and A. Walker. Effects of methylprednisolone and mk-801 on functional recovery after experimental chronic spinal cord injury. *Spinal Cord*, 38(12):733–740, Dec 2000.

[179] N. P. Hailer. Immunosuppression after traumatic or ischemic cns damage: it is neuroprotective and illuminates the role of microglial cells. *Prog Neurobiol*, 84(3):211–233, Mar 2008. doi: 10.1016/j.pneurobio.2007.12.001. URL http://dx.doi.org/10.1016/j.pneurobio.2007.12.001.

[180] S. M. Hall. Regeneration in the peripheral nervous system. *Neuropathol Appl Neurobiol*, 15(6):513–529, 1989.

[181] F. P. Hamers, A. J. Lankhorst, T. J. van Laar, W. B. Veldhuis, and W. H. Gispen. Automated quantitative gait analysis during overground locomotion in the rat: its application to spinal cord contusion and transection injuries. *J Neurotrauma*, 18(2):187–201, Feb 2001. doi: 10.1089/08977150150502613. URL http://dx.doi.org/10.1089/08977150150502613.

[182] F. P. T. Hamers, G. C. Koopmans, and E. A. J. Joosten. Catwalk-assisted gait analysis in the assessment of spinal cord injury. *J Neurotrauma*, 23(3-4):537–548, 2006. doi: 10.1089/neu.2006.23.537. URL http://dx.doi.org/10.1089/neu.2006.23.537.

[183] K. Hargreaves, R. Dubner, F. Brown, C. Flores, and J. Joris. A new and sensitive method for measuring thermal nociception in cutaneous hyperalgesia. *Pain*, 32(1):77–88, Jan 1988.

[184] T. P. Harrower and R. A. Barker. Is there a future for neural transplantation? *BioDrugs*, 18(3): 141–153, 2004.

[185] M. E. Hatten, R. K. Liem, M. L. Shelanski, and C. A. Mason. Astroglia in cns injury. *Glia*, 4(2): 233–243, 1991. doi: 10.1002/glia.440040215. URL http://dx.doi.org/10.1002/glia.440040215.

[186] E. Hauben, O. Butovsky, U. Nevo, E. Yoles, G. Moalem, E. Agranov, F. Mor, R. Leibowitz-Amit, E. Pevsner, S. Akselrod, M. Neeman, I. R. Cohen, and M. Schwartz. Passive or active immunization with myelin basic protein promotes recovery from spinal cord contusion. *J Neurosci*, 20(17):6421–6430, Sep 2000.

[187] E. Hauben, E. Agranov, A. Gothilf, U. Nevo, A. Cohen, I. Smirnov, L. Steinman, and M. Schwartz. Posttraumatic therapeutic vaccination with modified myelin self-antigen prevents complete paralysis while avoiding autoimmune disease. *J Clin Invest*, 108(4):591–599, Aug 2001. doi: 10.1172/JCI12837. URL `http://dx.doi.org/10.1172/JCI12837`.

[188] E. Hauben, A. Ibarra, T. Mizrahi, R. Barouch, E. Agranov, and M. Schwartz. Vaccination with a nogo-a-derived peptide after incomplete spinal-cord injury promotes recovery via a t-cell-mediated neuroprotective response: comparison with other myelin antigens. *Proc Natl Acad Sci U S A*, 98(26):15173–15178, Dec 2001. doi: 10.1073/pnas.011585298. URL `http://dx.doi.org/10.1073/pnas.011585298`.

[189] A. L. Hawthorne and P. G. Popovich. Emerging concepts in myeloid cell biology after spinal cord injury. *Neurotherapeutics*, Mar 2011. doi: 10.1007/s13311-011-0032-6. URL `http://dx.doi.org/10.1007/s13311-011-0032-6`.

[190] Y. Hayashi, J. S. Shumsky, T. Connors, T. Otsuka, I. Fischer, A. Tessler, and M. Murray. Immunosuppression with either cyclosporine a or fk506 supports survival of transplanted fibroblasts and promotes growth of host axons into the transplant after spinal cord injury. *J Neurotrauma*, 22(11):1267–1281, Nov 2005. doi: 10.1089/neu.2005.22.1267. URL `http://dx.doi.org/10.1089/neu.2005.22.1267`.

[191] W. T. Hendriks, M. J. Ruitenberg, B. Blits, G. J. Boer, and J. Verhaagen. Viral vector-mediated gene transfer of neurotrophins to promote regeneration of the injured spinal cord. *Prog Brain Res*, 146:451–476, 2004. doi: 10.1016/S0079-6123(03)46029-9. URL `http://dx.doi.org/10.1016/S0079-6123(03)46029-9`.

[192] W. T. J. Hendriks, R. Eggers, M. J. Ruitenberg, B. Blits, F. P. T. Hamers, J. Verhaagen, and G. J. Boer. Profound differences in spontaneous long-term functional recovery after defined spinal tract lesions in the rat. *J Neurotrauma*, 23(1):18–35, Jan 2006. doi: 10.1089/neu.2006.23.18. URL `http://dx.doi.org/10.1089/neu.2006.23.18`.

[193] S. Hermanns, G. Wunderlich, C. Rosenbaum, C. O. Hanemann, H. W. Müller, and C. C. Stichel. Lack of immune responses to immediate or delayed implanted allogeneic and xenogeneic schwann cell suspensions. *Glia*, 21(3):299–314, Nov 1997.

[194] J. E. Herrmann, T. Imura, B. Song, J. Qi, Y. Ao, T. K. Nguyen, R. A. Korsak, K. Takeda, S. Akira, and M. V. Sofroniew. Stat3 is a critical regulator of astrogliosis and scar formation after spinal

cord injury. *J Neurosci*, 28(28):7231–7243, Jul 2008. doi: 10.1523/JNEUROSCI.1709-08.2008. URL http://dx.doi.org/10.1523/JNEUROSCI.1709-08.2008.

[195] C. E. Hill, L. D. F. Moon, P. M. Wood, and M. B. Bunge. Labeled schwann cell transplantation: cell loss, host schwann cell replacement, and strategies to enhance survival. *Glia*, 53(3):338–343, Feb 2006. doi: 10.1002/glia.20287. URL http://dx.doi.org/10.1002/glia.20287.

[196] C. P. Hofstetter, E. J. Schwarz, D. Hess, J. Widenfalk, A. E. Manira, D. J. Prockop, and L. Olson. Marrow stromal cells form guiding strands in the injured spinal cord and promote recovery. *Proc Natl Acad Sci U S A*, 99(4):2199–2204, Feb 2002. doi: 10.1073/pnas.042678299. URL http://dx.doi.org/10.1073/pnas.042678299.

[197] C. P. Hofstetter, N. A. V. Holmström, J. A. Lilja, P. Schweinhardt, J. Hao, C. Spenger, Z. Wiesenfeld-Hallin, S. N. Kurpad, J. Frisén, and L. Olson. Allodynia limits the usefulness of intraspinal neural stem cell grafts; directed differentiation improves outcome. *Nat Neurosci*, 8(3):346–353, Mar 2005. doi: 10.1038/nn1405. URL http://dx.doi.org/10.1038/nn1405.

[198] P. K. Horan and S. E. Slezak. Stable cell membrane labelling. *Nature*, 340(6229):167–168, Jul 1989. doi: 10.1038/340167a0. URL http://dx.doi.org/10.1038/340167a0.

[199] P. J. Horner and F. H. Gage. Regenerating the damaged central nervous system. *Nature*, 407(6807): 963–970, Oct 2000. doi: 10.1038/35039559. URL http://dx.doi.org/10.1038/35039559.

[200] Y.-C. Huang, Y.-Y. Huang, C.-C. Huang, and H.-C. Liu. Manufacture of porous polymer nerve conduits through a lyophilizing and wire-heating process. *J Biomed Mater Res B Appl Biomater*, 74 (1):659–664, Jul 2005. doi: 10.1002/jbm.b.30267. URL http://dx.doi.org/10.1002/jbm.b.30267.

[201] C. E. Hulsebosch. Recent advances in pathophysiology and treatment of spinal cord injury. *Adv Physiol Educ*, 26(1-4):238–255, Dec 2002.

[202] D. L. Hynds and D. M. Snow. Fibronectin and laminin elicit differential behaviors from sh-sy5y growth cones contacting inhibitory chondroitin sulfate proteoglycans. *J Neurosci Res*, 66(4):630–642, Nov 2001.

[203] J. F. Iaci, A. M. Vecchione, M. P. Zimber, and A. O. Caggiano. Chondroitin sulfate proteoglycans in spinal cord contusion injury and the effects of chondroitinase treatment. *J Neurotrauma*, 24(11):1743–1759, Nov 2007. doi: 10.1089/neu.2007.0366. URL http://dx.doi.org/10.1089/neu.2007.0366.

[204] A. Ibarra, D. Correa, K. Willms, M. T. Merchant, G. Guizar-Sahagún, I. Grijalva, and I. Madrazo. Effects of cyclosporin-a on immune response, tissue protection and motor function of rats subjected to spinal cord injury. *Brain Res*, 979(1-2):165–178, Jul 2003.

[205] A. Ibarra, E. Hernández, J. Lomeli, D. Pineda, M. Buenrostro, S. Martiñón, E. Garcia, N. Flores, G. Guizar-Sahagun, D. Correa, and I. Madrazo. Cyclosporin-a enhances non-functional axonal growing after complete spinal cord transection. *Brain Res*, 1149:200–209, May 2007. doi: 10.1016/j.brainres.2007.02.056. URL `http://dx.doi.org/10.1016/j.brainres.2007.02.056`.

[206] T. Ikegami, M. Nakamura, J. Yamane, H. Katoh, S. Okada, A. Iwanami, K. Watanabe, K. Ishii, F. Kato, H. Fujita, T. Takahashi, H. J. Okano, Y. Toyama, and H. Okano. Chondroitinase abc combined with neural stem/progenitor cell transplantation enhances graft cell migration and outgrowth of growth-associated protein-43-positive fibers after rat spinal cord injury. *Eur J Neurosci*, 22(12):3036–3046, Dec 2005. doi: 10.1111/j.1460-9568.2005.04492.x. URL `http://dx.doi.org/10.1111/j.1460-9568.2005.04492.x`.

[207] Y. Imai, I. Ibata, D. Ito, K. Ohsawa, and S. Kohsaka. A novel gene iba1 in the major histocompatibility complex class iii region encoding an ef hand protein expressed in a monocytic lineage. *Biochem Biophys Res Commun*, 224(3):855–862, Jul 1996. doi: 10.1006/bbrc.1996.1112. URL `http://dx.doi.org/10.1006/bbrc.1996.1112`.

[208] H. K. Inoue, S. Kobayashi, and K. Ohbayashi. Regeneration of hemisectioned spinal cords with and without supporting materials. *Neurol Med Chir (Tokyo)*, 37(8):600–605, Aug 1997.

[209] D. Ito, Y. Imai, K. Ohsawa, K. Nakajima, Y. Fukuuchi, and S. Kohsaka. Microglia-specific localisation of a novel calcium binding protein, iba1. *Brain Res Mol Brain Res*, 57(1):1–9, Jun 1998.

[210] D. Ito, K. Tanaka, S. Suzuki, T. Dembo, and Y. Fukuuchi. Enhanced expression of iba1, ionized calcium-binding adapter molecule 1, after transient focal cerebral ischemia in rat brain. *Stroke*, 32(5): 1208–1215, May 2001.

[211] S. Itoh, K. Takakuda, S. Kawabata, Y. Aso, K. Kasai, H. Itoh, and K. Shinomiya. Evaluation of cross-linking procedures of collagen tubes used in peripheral nerve repair. *Biomaterials*, 23(23):4475–4481, Dec 2002.

[212] A. Iwanami, S. Kaneko, M. Nakamura, Y. Kanemura, H. Mori, S. Kobayashi, M. Yamasaki, S. Momoshima, H. Ishii, K. Ando, Y. Tanioka, N. Tamaoki, T. Nomura, Y. Toyama, and H. Okano. Transplantation of human neural stem cells for spinal cord injury in primates. *J Neurosci Res*, 80(2):182–190, Apr 2005. doi: 10.1002/jnr.20436. URL `http://dx.doi.org/10.1002/jnr.20436`.

[213] C. B. Jaeger, J. P. Toombs, and R. B. Borgens. Grafting in acute spinal cord injury: morphological and immunological aspects of transplanted adult rat enteric ganglia. *Neuroscience*, 52(2):333–346, Jan 1993.

[214] A. Jain, Y.-T. Kim, R. J. McKeon, and R. V. Bellamkonda. In situ gelling hydrogels for conformal repair of spinal cord defects, and local delivery of bdnf after spinal cord injury. *Biomaterials*, 27(3):497–504, Jan 2006. doi: 10.1016/j.biomaterials.2005.07.008. URL `http://dx.doi.org/10.1016/j.biomaterials.2005.07.008`.

[215] K.-A. Ji, M.-S. Yang, H.-K. Jeong, K.-J. Min, S.-H. Kang, I. Jou, and E.-H. Joe. Resident microglia die and infiltrated neutrophils and monocytes become major inflammatory cells in lipopolysaccharide-injected brain. *Glia*, 55(15):1577–1588, Nov 2007. doi: 10.1002/glia.20571. URL `http://dx.doi.org/10.1002/glia.20571`.

[216] Y. Jin, B. Neuhuber, A. Singh, J. Bouyer, A. Lepore, J. Bonner, T. Himes, J. Campanelli, and I. Fischer. Transplantation of human glial restricted progenitors and derived astrocytes into a contusion model of spinal cord injury. *J Neurotrauma*, Jan 2011. doi: 10.1089/neu.2010.1626. URL `http://dx.doi.org/10.1089/neu.2010.1626`.

[217] L. L. Jones, M. Oudega, M. B. Bunge, and M. H. Tuszynski. Neurotrophic factors, cellular bridges and gene therapy for spinal cord injury. *J Physiol*, 533(Pt 1):83–89, May 2001.

[218] L. L. Jones, R. U. Margolis, and M. H. Tuszynski. The chondroitin sulfate proteoglycans neurocan, brevican, phosphacan, and versican are differentially regulated following spinal cord injury. *Exp Neurol*, 182(2):399–411, Aug 2003.

[219] L. L. Jones, D. Sajed, and M. H. Tuszynski. Axonal regeneration through regions of chondroitin sulfate proteoglycan deposition after spinal cord injury: a balance of permissiveness and inhibition. *J Neurosci*, 23(28):9276–9288, Oct 2003.

[220] T. B. Jones, R. P. Hart, and P. G. Popovich. Molecular control of physiological and pathological t-cell recruitment after mouse spinal cord injury. *J Neurosci*, 25(28):6576–6583, Jul 2005. doi: 10.1523/JNEUROSCI.0305-05.2005. URL `http://dx.doi.org/10.1523/JNEUROSCI.0305-05.2005`.

[221] E. A. Joosten, P. R. Bär, and W. H. Gispen. Collagen implants and cortico-spinal axonal growth after mid-thoracic spinal cord lesion in the adult rat. *J Neurosci Res*, 41(4):481–490, Jul 1995. doi: 10.1002/jnr.490410407. URL `http://dx.doi.org/10.1002/jnr.490410407`.

[222] E. A. J. Joosten, W. B. Veldhuis, and F. P. T. Hamers. Collagen containing neonatal astrocytes stimulates regrowth of injured fibers and promotes modest locomotor recovery after spinal cord injury. *J Neurosci Res*, 77(1):127–142, Jul 2004. doi: 10.1002/jnr.20088. URL `http://dx.doi.org/10.1002/jnr.20088`.

[223] M. S. Kaplan and J. W. Hinds. Neurogenesis in the adult rat: electron microscopic analysis of light radioautographs. *Science*, 197(4308):1092–1094, Sep 1977.

[224] S. Karimi-Abdolrezaee, E. Eftekharpour, J. Wang, C. M. Morshead, and M. G. Fehlings. Delayed transplantation of adult neural precursor cells promotes remyelination and functional neurological recovery after spinal cord injury. *J Neurosci*, 26(13):3377–3389, Mar 2006. doi: 10.1523/JNEUROSCI.4184-05.2006. URL `http://dx.doi.org/10.1523/JNEUROSCI.4184-05.2006`.

[225] S. Karimi-Abdolrezaee, E. Eftekharpour, J. Wang, D. Schut, and M. G. Fehlings. Synergistic effects of transplanted adult neural stem/progenitor cells, chondroitinase, and growth factors promote functional repair and plasticity of the chronically injured spinal cord. *J Neurosci*, 30(5):1657–1676, Feb 2010. doi: 10.1523/JNEUROSCI.3111-09.2010. URL `http://dx.doi.org/10.1523/JNEUROSCI.3111-09.2010`.

[226] K. Kataoka, Y. Suzuki, M. Kitada, T. Hashimoto, H. Chou, H. Bai, M. Ohta, S. Wu, K. Suzuki, and C. Ide. Alginate enhances elongation of early regenerating axons in spinal cord of young rats. *Tissue Eng*, 10(3-4):493–504, 2004. doi: 10.1089/107632704323061852. URL `http://dx.doi.org/10.1089/107632704323061852`.

[227] R. Katoh-Semba, M. Matsuda, K. Kato, and A. Oohira. Chondroitin sulphate proteoglycans in the rat brain: candidates for axon barriers of sensory neurons and the possible modification by laminin of their actions. *Eur J Neurosci*, 7(4):613–621, Apr 1995.

[228] M. D. Kawaja and F. H. Gage. Reactive astrocytes are substrates for the growth of adult cns axons in the presence of elevated levels of nerve growth factor. *Neuron*, 7(6):1019–1030, Dec 1991.

[229] Y. Ke, L. Chi, R. Xu, C. Luo, D. Gozal, and R. Liu. Early response of endogenous adult neural progenitor cells to acute spinal cord injury in mice. *Stem Cells*, 24(4):1011–1019, Apr 2006. doi: 10.1634/stemcells.2005-0249. URL `http://dx.doi.org/10.1634/stemcells.2005-0249`.

[230] H. S. Keirstead, G. Nistor, G. Bernal, M. Totoiu, F. Cloutier, K. Sharp, and O. Steward. Human embryonic stem cell-derived oligodendrocyte progenitor cell transplants remyelinate and restore locomotion after spinal cord injury. *J Neurosci*, 25(19):4694–4705, May 2005. doi: 10.1523/JNEUROSCI.0311-05.2005. URL `http://dx.doi.org/10.1523/JNEUROSCI.0311-05.2005`.

[231] B. G. Kim, Y. M. Kang, J. H. Phi, Y.-H. Kim, D. H. Hwang, J. Y. Choi, S. Ryu, A.-E. Elastal, S. H. Paek, K.-C. Wang, S.-H. Lee, S. U. Kim, and B.-W. Yoon. Implantation of polymer scaffolds seeded with neural stem cells in a canine spinal cord injury model. *Cytotherapy*, 12(6):841–845, Oct 2010. doi: 10.3109/14653249.2010.501784. URL `http://dx.doi.org/10.3109/14653249.2010.501784`.

[232] H. M. Kim, D. H. Hwang, J. E. Lee, S. U. Kim, and B. G. Kim. Ex vivo vegf delivery by neural stem cells enhances proliferation of glial progenitors, angiogenesis, and tissue sparing after spinal cord injury. *PLoS One*, 4(3):e4987, 2009. doi: 10.1371/journal.pone.0004987. URL `http://dx.doi.org/10.1371/journal.pone.0004987`.

[233] J. Kipnis, E. Yoles, H. Schori, E. Hauben, I. Shaked, and M. Schwartz. Neuronal survival after cns insult is determined by a genetically encoded autoimmune response. *J Neurosci*, 21(13):4564–4571, Jul 2001.

[234] N. Klapka, S. Hermanns, G. Straten, C. Masanneck, S. Duis, F. P. T. Hamers, D. Müller, W. Zuschratter, and H. W. Müller. Suppression of fibrous scarring in spinal cord injury of rat promotes long-distance regeneration of corticospinal tract axons, rescue of primary motoneurons in somatosensory cortex and significant functional recovery. *Eur J Neurosci*, 22(12):3047–3058, Dec 2005. doi: 10.1111/j.1460-9568.2005.04495.x. URL `http://dx.doi.org/10.1111/j.1460-9568.2005.04495.x`.

[235] I. Klimanskaya, Y. Chung, S. Becker, S.-J. Lu, and R. Lanza. Human embryonic stem cell lines derived from single blastomeres. *Nature*, 444(7118):481–485, Nov 2006. doi: 10.1038/nature05142. URL `http://dx.doi.org/10.1038/nature05142`.

[236] M. Kliot, G. M. Smith, J. D. Siegal, and J. Silver. Astrocyte-polymer implants promote regeneration of dorsal root fibers into the adult mammalian spinal cord. *Exp Neurol*, 109(1):57–69, Jul 1990.

[237] I. Klusman and M. E. Schwab. Effects of pro-inflammatory cytokines in experimental spinal cord injury. *Brain Res*, 762(1-2):173–184, Jul 1997.

[238] W. Knapp, B. Dörken, P. Rieber, R. E. Schmidt, H. Stein, and A. E. von dem Borne. Cd antigens 1989. *Blood*, 74(4):1448–1450, Sep 1989.

[239] I. Kohama, K. L. Lankford, J. Preiningerova, F. A. White, T. L. Vollmer, and J. D. Kocsis. Transplantation of cryopreserved adult human schwann cells enhances axonal conduction in demyelinated spinal cord. *J Neurosci*, 21(3):944–950, Feb 2001.

[240] M. Koistinaho, S. Lin, X. Wu, M. Esterman, D. Koger, J. Hanson, R. Higgs, F. Liu, S. Malkani, K. R. Bales, and S. M. Paul. Apolipoprotein e promotes astrocyte colocalization and degradation of deposited amyloid-beta peptides. *Nat Med*, 10(7):719–726, Jul 2004. doi: 10.1038/nm1058. URL `http://dx.doi.org/10.1038/nm1058`.

[241] G. C. Koopmans, R. Deumens, W. M. M. Honig, F. P. T. Hamers, H. W. M. Steinbusch, and E. A. J. Joosten. The assessment of locomotor function in spinal cord injured rats: the importance of objective analysis of coordination. *J Neurotrauma*, 22(2):214–225, Feb 2005. doi: 10.1089/neu.2005.22.214. URL `http://dx.doi.org/10.1089/neu.2005.22.214`.

[242] G. C. Koopmans, R. Deumens, A. Buss, L. Geoghegan, A. M. Myint, W. H. H. Honig, N. Kern, E. A. Joosten, J. Noth, and G. A. Brook. Acute rolipram/thalidomide treatment improves tissue sparing and locomotion after experimental spinal cord injury. *Exp Neurol*, 216(2):490–498, Apr 2009.

[243] G. C. Kopen, D. J. Prockop, and D. G. Phinney. Marrow stromal cells migrate throughout forebrain and cerebellum, and they differentiate into astrocytes after injection into neonatal mouse brains. *Proc Natl Acad Sci U S A*, 96(19):10711–10716, Sep 1999.

[244] A. M. Kostianovsky, L. M. Maier, R. C. Anderson, J. N. Bruce, and D. E. Anderson. Astrocytic regulation of human monocytic/microglial activation. *J Immunol*, 181(8):5425–5432, Oct 2008.

[245] V. Kroehne, I. Heschel, F. Schügner, D. Lasrich, J. W. Bartsch, and H. Jockusch. Use of a novel collagen matrix with oriented pore structure for muscle cell differentiation in cell culture and in grafts. *J Cell Mol Med*, 12(5A):1640–1648, 2008. doi: 10.1111/j.1582-4934.2008.00238.x. URL `http://dx.doi.org/10.1111/j.1582-4934.2008.00238.x`.

[246] V. G. Kukekov, E. D. Laywell, O. Suslov, K. Davies, B. Scheffler, L. B. Thomas, T. F. O'Brien, M. Kusakabe, and D. A. Steindler. Multipotent stem/progenitor cells with similar properties arise from two neurogenic regions of adult human brain. *Exp Neurol*, 156(2):333–344, Apr 1999. doi: 10.1006/exnr.1999.7028. URL `http://dx.doi.org/10.1006/exnr.1999.7028`.

[247] E. Kunkel-Bagden, H. N. Dai, and B. S. Bregman. Methods to assess the development and recovery of locomotor function after spinal cord injury in rats.kunkel-bagden1993. *Exp Neurol*, 119(2):153–164, Feb 1993. doi: 10.1006/exnr.1993.1017. URL `http://dx.doi.org/10.1006/exnr.1993.1017`.

[248] B. K. Kwon, W. Tetzlaff, J. N. Grauer, J. Beiner, and A. R. Vaccaro. Pathophysiology and pharmacologic treatment of acute spinal cord injury. *Spine J*, 4(4):451–464, 2004. doi: 10.1016/j.spinee.2003.07.007. URL `http://dx.doi.org/10.1016/j.spinee.2003.07.007`.

[249] H.-Z. Lü, Y.-X. Wang, J.-S. Zhou, F.-C. Wang, and J.-G. Hu. Cyclosporin a increases recovery after spinal cord injury but does not improve myelination by oligodendrocyte progenitor cell transplantation. *BMC Neurosci*, 11:127, 2010. doi: 10.1186/1471-2202-11-127. URL `http://dx.doi.org/10.1186/1471-2202-11-127`.

[250] L. A. Langford and G. C. Owens. Resolution of the pathway taken by implanted schwann cells to a spinal cord lesion by prior infection with a retrovirus encoding beta-galactosidase. *Acta Neuropathol*, 80(5):514–520, 1990.

[251] A. J. Lankhorst, M. P. ter Laak, T. J. van Laar, N. L. van Meeteren, J. C. de Groot, L. H. Schrama, F. P. Hamers, and W. H. Gispen. Effects of enriched housing on functional recovery after spinal cord contusive injury in the adult rat. *J Neurotrauma*, 18(2):203–215, Feb 2001. doi: 10.1089/08977150150502622. URL `http://dx.doi.org/10.1089/08977150150502622`.

[252] E. D. Laywell, V. G. Kukekov, and D. A. Steindler. Multipotent neurospheres can be derived from forebrain subependymal zone and spinal cord of adult mice after protracted post-

mortem intervals. *Exp Neurol*, 156(2):430–433, Apr 1999. doi: 10.1006/exnr.1999.7029. URL http://dx.doi.org/10.1006/exnr.1999.7029.

[253] J. C. Lee, M. Mayer-Proschel, and M. S. Rao. Gliogenesis in the central nervous system. *Glia*, 30(2): 105–121, Apr 2000.

[254] B. Leitinger and E. Hohenester. Mammalian collagen receptors. *Matrix Biol*, 26(3):146–155, Apr 2007. doi: 10.1016/j.matbio.2006.10.007. URL http://dx.doi.org/10.1016/j.matbio.2006.10.007.

[255] K. B. Lemström, A. K. Räisänen-Sokolowski, P. J. Häyry, and P. K. Koskinen. Triple drug immunosuppression significantly reduces aortic allograft arteriosclerosis in the rat. *Arterioscler Thromb Vasc Biol*, 16(4):553–564, Apr 1996.

[256] U. Lendahl, L. B. Zimmerman, and R. D. McKay. Cns stem cells express a new class of intermediate filament protein. *Cell*, 60(4):585–595, Feb 1990.

[257] J. Levitsky. Operational tolerance: past lessons and future prospects. *Liver Transpl*, 17(3):222–232, Mar 2011. doi: 10.1002/lt.22265. URL http://dx.doi.org/10.1002/lt.22265.

[258] L. Li, A. Lundkvist, D. Andersson, U. Wilhelmsson, N. Nagai, A. C. Pardo, C. Nodin, A. Ståhlberg, K. Aprico, K. Larsson, T. Yabe, L. Moons, A. Fotheringham, I. Davies, P. Carmeliet, J. P. Schwartz, M. Pekna, M. Kubista, F. Blomstrand, N. Maragakis, M. Nilsson, and M. Pekny. Protective role of reactive astrocytes in brain ischemia. *J Cereb Blood Flow Metab*, 28(3):468–481, Mar 2008. doi: 10.1038/sj.jcbfm.9600546. URL http://dx.doi.org/10.1038/sj.jcbfm.9600546.

[259] M. Li, A. Shibata, C. Li, P. E. Braun, L. McKerracher, J. Roder, S. B. Kater, and S. David. Myelin-associated glycoprotein inhibits neurite/axon growth and causes growth cone collapse. *J Neurosci Res*, 46(4):404–414, Nov 1996. doi: gt;3.0.CO;2-K. URL http://dx.doi.org/gt;3.0.CO;2-K.

[260] S. Li and S. M. Strittmatter. Delayed systemic nogo-66 receptor antagonist promotes recovery from spinal cord injury. *J Neurosci*, 23(10):4219–4227, May 2003.

[261] Y. Li and G. Raisman. Schwann cells induce sprouting in motor and sensory axons in the adult rat spinal cord. *J Neurosci*, 14(7):4050–4063, Jul 1994.

[262] Y. Li and G. Raisman. Integration of transplanted cultured schwann cells into the long myelinated fiber tracts of the adult spinal cord. *Exp Neurol*, 145(2 Pt 1):397–411, Jun 1997. doi: 10.1006/exnr.1997.6502. URL http://dx.doi.org/10.1006/exnr.1997.6502.

[263] Y. Li, P. M. Field, and G. Raisman. Regeneration of adult rat corticospinal axons induced by transplanted olfactory ensheathing cells. *J Neurosci*, 18(24):10514–10524, Dec 1998.

[264] P. Liang, L. hong Jin, T. Liang, E. zhong Liu, and S. guang Zhao. Human neural stem cells promote corticospinal axons regeneration and synapse reformation in injured spinal cord of rats. *Chin Med J (Engl)*, 119(16):1331–1338, Aug 2006.

[265] C. M. Liberto, P. J. Albrecht, L. M. Herx, V. W. Yong, and S. W. Levison. Pro-regenerative properties of cytokine-activated astrocytes. *J Neurochem*, 89(5):1092–1100, Jun 2004. doi: 10.1111/j.1471-4159.2004.02420.x. URL `http://dx.doi.org/10.1111/j.1471-4159.2004.02420.x`.

[266] M. Lietz, L. Dreesmann, M. Hoss, S. Oberhoffner, and B. Schlosshauer. Neuro tissue engineering of glial nerve guides and the impact of different cell types. *Biomaterials*, 27(8):1425–1436, Mar 2006. doi: 10.1016/j.biomaterials.2005.08.007. URL `http://dx.doi.org/10.1016/j.biomaterials.2005.08.007`.

[267] J. Lin and W. Cai. Effect of vimentin on reactive gliosis: in vitro and in vivo analysis. *J Neurotrauma*, 21(11):1671–1682, Nov 2004. doi: 10.1089/neu.2004.21.1671. URL `http://dx.doi.org/10.1089/neu.2004.21.1671`.

[268] J. H.-C. Lin, N. Lou, N. Kang, T. Takano, F. Hu, X. Han, Q. Xu, D. Lovatt, A. Torres, K. Willecke, J. Yang, J. Kang, and M. Nedergaard. A central role of connexin 43 in hypoxic preconditioning. *J Neurosci*, 28(3):681–695, Jan 2008. doi: 10.1523/JNEUROSCI.3827-07.2008. URL `http://dx.doi.org/10.1523/JNEUROSCI.3827-07.2008`.

[269] Y. Liu, D. Kim, B. T. Himes, S. Y. Chow, T. Schallert, M. Murray, A. Tessler, and I. Fischer. Transplants of fibroblasts genetically modified to express bdnf promote regeneration of adult rat rubrospinal axons and recovery of forelimb function. *J Neurosci*, 19(11):4370–4387, Jun 1999.

[270] F. J. Liuzzi and R. J. Lasek. Astrocytes block axonal regeneration in mammals by activating the physiological stop pathway. *Science*, 237(4815):642–645, Aug 1987.

[271] N. Lonjon, P. Kouyoumdjian, M. Prieto, L. Bauchet, H. Haton, M. Gaviria, A. Privat, and F. E. Perrin. Early functional outcomes and histological analysis after spinal cord compression injury in rats. *J Neurosurg Spine*, 12(1):106–113, Jan 2010. doi: 10.3171/2009.7.SPINE0989. URL `http://dx.doi.org/10.3171/2009.7.SPINE0989`.

[272] L. Luckenbill-Edds. Laminin and the mechanism of neuronal outgrowth. *Brain Res Brain Res Rev*, 23 (1-2):1–27, Feb 1997.

[273] M. B. Luskin. Restricted proliferation and migration of postnatally generated neurons derived from the forebrain subventricular zone. *Neuron*, 11(1):173–189, Jul 1993.

[274] D. K. Ma, M. A. Bonaguidi, G.-L. Ming, and H. Song. Adult neural stem cells in the mammalian central nervous system. *Cell Res*, 19(6):672–682, Jun 2009. doi: 10.1038/cr.2009.56. URL `http://dx.doi.org/10.1038/cr.2009.56`.

[275] D. Martin, P. Robe, R. Franzen, P. Delrée, J. Schoenen, A. Stevenaert, and G. Moonen. Effects of schwann cell transplantation in a contusion model of rat spinal cord injury. *J Neurosci Res*, 45(5): 588–597, Sep 1996. doi: gt;3.0.CO;2-8. URL `http://dx.doi.org/gt;3.0.CO;2-8`.

[276] R. Martini. Expression and functional roles of neural cell surface molecules and extracellular matrix components during development and regeneration of peripheral nerves. *J Neurocytol*, 23(1):1–28, Jan 1994.

[277] J. W. McDonald, X. Z. Liu, Y. Qu, S. Liu, S. K. Mickey, D. Turetsky, D. I. Gottlieb, and D. W. Choi. Transplanted embryonic stem cells survive, differentiate and promote recovery in injured rat spinal cord. *Nat Med*, 5(12):1410–1412, Dec 1999. doi: 10.1038/70986. URL `http://dx.doi.org/10.1038/70986`.

[278] R. McKay. Stem cells in the central nervous system. *Science*, 276(5309):66–71, Apr 1997.

[279] S. M. McKay, D. J. Brooks, P. Hu, and E. M. McLachlan. Distinct types of microglial activation in white and grey matter of rat lumbosacral cord after mid-thoracic spinal transection. *J Neuropathol Exp Neurol*, 66(8):698–710, Aug 2007.

[280] R. J. McKeon, R. C. Schreiber, J. S. Rudge, and J. Silver. Reduction of neurite outgrowth in a model of glial scarring following cns injury is correlated with the expression of inhibitory molecules on reactive astrocytes. *J Neurosci*, 11(11):3398–3411, Nov 1991.

[281] R. J. McKeon, M. J. Jurynec, and C. R. Buck. The chondroitin sulfate proteoglycans neurocan and phosphacan are expressed by reactive astrocytes in the chronic cns glial scar. *J Neurosci*, 19(24): 10778–10788, Dec 1999.

[282] L. McKerracher, S. David, D. L. Jackson, V. Kottis, R. J. Dunn, and P. E. Braun. Identification of myelin-associated glycoprotein as a major myelin-derived inhibitor of neurite growth. *Neuron*, 13(4): 805–811, Oct 1994.

[283] S. S. McMahon, S. Albermann, G. E. Rooney, C. Moran, J. Hynes, Y. Garcia, P. Dockery, T. O'Brien, A. J. Windebank, and F. P. Barry. Effect of cyclosporin a on functional recovery in the spinal cord following contusion injury. *J Anat*, 215(3):267–279, Sep 2009. doi: 10.1111/j.1469-7580.2009.01107.x. URL `http://dx.doi.org/10.1111/j.1469-7580.2009.01107.x`.

[284] A. Meissner, M. Wernig, and R. Jaenisch. Direct reprogramming of genetically unmodified fibroblasts into pluripotent stem cells. *Nat Biotechnol*, 25(10):1177–1181, Oct 2007. doi: 10.1038/nbt1335. URL `http://dx.doi.org/10.1038/nbt1335`.

[285] P. Menei, C. Montero-Menei, S. R. Whittemore, R. P. Bunge, and M. B. Bunge. Schwann cells genetically modified to secrete human bdnf promote enhanced axonal regrowth across transected adult rat spinal cord. *Eur J Neurosci*, 10(2):607–621, Feb 1998.

[286] C. A. Messam, J. Hou, and E. O. Major. Coexpression of nestin in neural and glial cells in the developing human cns defined by a human-specific anti-nestin antibody. *Exp Neurol*, 161(2):585–596, Feb 2000. doi: 10.1006/exnr.1999.7319. URL `http://dx.doi.org/10.1006/exnr.1999.7319`.

[287] R. Milner and I. L. Campbell. Cytokines regulate microglial adhesion to laminin and astrocyte extracellular matrix via protein kinase c-dependent activation of the alpha6beta1 integrin. *J Neurosci*, 22 (5):1562–1572, Mar 2002.

[288] R. Milner, X. Huang, J. Wu, S. Nishimura, R. Pytela, D. Sheppard, and C. ffrench Constant. Distinct roles for astrocyte alphavbeta5 and alphavbeta8 integrins in adhesion and migration. *J Cell Sci*, 112 (Pt 23):4271–4279, Dec 1999.

[289] S. Möllers, I. Heschel, L. H. H. O. Damink, F. Schügner, R. Deumens, B. Müller, A. Bozkurt, J. G. Nava, J. Noth, and G. A. Brook. Cytocompatibility of a novel, longitudinally microstructured collagen scaffold intended for nerve tissue repair. *Tissue Eng Part A*, 15(3):461–472, Mar 2009. doi: 10.1089/ten.tea.2007.0107. URL `http://dx.doi.org/10.1089/ten.tea.2007.0107`.

[290] X. M. Mo, C. Y. Xu, M. Kotaki, and S. Ramakrishna. Electrospun p(lla-cl) nanofiber: a biomimetic extracellular matrix for smooth muscle cell and endothelial cell proliferation. *Biomaterials*, 25(10): 1883–1890, May 2004.

[291] C. T. Montgomery, E. A. Tenaglia, and J. A. Robson. Axonal growth into tubes implanted within lesions in the spinal cords of adult rats. *Exp Neurol*, 137(2):277–290, Feb 1996. doi: 10.1006/exnr.1996.0026. URL `http://dx.doi.org/10.1006/exnr.1996.0026`.

[292] D. A. Morgenstern, R. A. Asher, and J. W. Fawcett. Chondroitin sulphate proteoglycans in the cns injury response. *Prog Brain Res*, 137:313–332, 2002.

[293] G. Mukhopadhyay, P. Doherty, F. S. Walsh, P. R. Crocker, and M. T. Filbin. A novel role for myelin-associated glycoprotein as an inhibitor of axonal regeneration. *Neuron*, 13(3):757–767, Sep 1994.

[294] M. Murray and I. Fischer. Transplantation and gene therapy: combined approaches for repair of spinal cord injury. *Neuroscientist*, 7(1):28–41, Feb 2001.

[295] D. J. Myer, G. G. Gurkoff, S. M. Lee, D. A. Hovda, and M. V. Sofroniew. Essential protective roles of reactive astrocytes in traumatic brain injury. *Brain*, 129(Pt 10):2761–2772, Oct 2006. doi: 10.1093/brain/awl165. URL `http://dx.doi.org/10.1093/brain/awl165`.

[296] N. Nagano, M. Aoyagi, and K. Hirakawa. Extracellular matrix modulates the proliferation of rat astrocytes in serum-free culture. *Glia*, 8(2):71–76, Jun 1993. doi: 10.1002/glia.440080202. URL `http://dx.doi.org/10.1002/glia.440080202`.

[297] M. Nakagawa, M. Koyanagi, K. Tanabe, K. Takahashi, T. Ichisaka, T. Aoi, K. Okita, Y. Mochiduki, N. Takizawa, and S. Yamanaka. Generation of induced pluripotent stem cells without myc from mouse and human fibroblasts. *Nat Biotechnol*, 26(1):101–106, Jan 2008. doi: 10.1038/nbt1374. URL `http://dx.doi.org/10.1038/nbt1374`.

[298] C. Nicaise, D. Mitrecic, and R. Pochet. Brain and spinal cord affected by amyotrophic lateral sclerosis induce differential growth factors expression in rat mesenchymal and neural stem cells. *Neuropathol Appl Neurobiol*, 37(2):179–188, Feb 2011. doi: 10.1111/j.1365-2990.2010.01124.x. URL `http://dx.doi.org/10.1111/j.1365-2990.2010.01124.x`.

[299] B. Niederöst, T. Oertle, J. Fritsche, R. A. McKinney, and C. E. Bandtlow. Nogo-a and myelin-associated glycoprotein mediate neurite growth inhibition by antagonistic regulation of rhoa and rac1. *J Neurosci*, 22(23):10368–10376, Dec 2002.

[300] D. R. Nisbet, A. E. Rodda, M. K. Horne, J. S. Forsythe, and D. I. Finkelstein. Implantation of functionalized thermally gelling xyloglucan hydrogel within the brain: associated neurite infiltration and inflammatory response. *Tissue Eng Part A*, 16(9):2833–2842, Sep 2010. doi: 10.1089/ten.TEA.2009.0677. URL `http://dx.doi.org/10.1089/ten.TEA.2009.0677`.

[301] G. I. Nistor, M. O. Totoiu, N. Haque, M. K. Carpenter, and H. S. Keirstead. Human embryonic stem cells differentiate into oligodendrocytes in high purity and myelinate after spinal cord transplantation. *Glia*, 49(3):385–396, Feb 2005. doi: 10.1002/glia.20127. URL `http://dx.doi.org/10.1002/glia.20127`.

[302] M. Noble, J. Fok-Seang, and J. Cohen. Glia are a unique substrate for the in vitro growth of central nervous system neurons. *J Neurosci*, 4(7):1892–1903, Jul 1984.

[303] H. Nornes, A. Björklund, and U. Stenevi. Reinnervation of the denervated adult spinal cord of rats by intraspinal transplants of embryonic brain stem neurons. *Cell Tissue Res*, 230(1):15–35, 1983.

[304] Y. Ogawa, K. Sawamoto, T. Miyata, S. Miyao, M. Watanabe, M. Nakamura, B. S. Bregman, M. Koike, Y. Uchiyama, Y. Toyama, and H. Okano. Transplantation of in vitro-expanded fetal neural progenitor cells results in neurogenesis and functional recovery after spinal cord contusion injury in adult rats. *J Neurosci Res*, 69(6):925–933, Sep 2002. doi: 10.1002/jnr.10341. URL `http://dx.doi.org/10.1002/jnr.10341`.

[305] S. Okada, M. Nakamura, H. Katoh, T. Miyao, T. Shimazaki, K. Ishii, J. Yamane, A. Yoshimura, Y. Iwamoto, Y. Toyama, and H. Okano. Conditional ablation of stat3 or socs3 discloses a dual role for reactive astrocytes after spinal cord injury. *Nat Med*, 12(7):829–834, Jul 2006. doi: 10.1038/nm1425. URL `http://dx.doi.org/10.1038/nm1425`.

[306] H. Okano, S. Kaneko, S. Okada, A. Iwanami, M. Nakamura, and Y. Toyama. Regeneration-based therapies for spinal cord injuries. *Neurochem Int*, 51(2-4):68–73, 2007. doi: 10.1016/j.neuint.2007.04.013. URL http://dx.doi.org/10.1016/j.neuint.2007.04.013.

[307] D. O. Okonkwo, T. B. Reece, J. J. Laurent, A. S. Hawkins, P. I. Ellman, J. Linden, I. L. Kron, C. G. Tribble, J. R. Stone, and J. A. Kern. A comparison of adenosine a2a agonism and methylprednisolone in attenuating neuronal damage and improving functional outcome after experimental traumatic spinal cord injury in rabbits. *J Neurosurg Spine*, 4(1):64–70, Jan 2006. doi: 10.3171/spi.2006.4.1.64. URL http://dx.doi.org/10.3171/spi.2006.4.1.64.

[308] G. Orive, E. Anitua, J. L. Pedraz, and D. F. Emerich. Biomaterials for promoting brain protection, repair and regeneration. *Nat Rev Neurosci*, 10(9):682–692, Sep 2009. doi: 10.1038/nrn2685. URL http://dx.doi.org/10.1038/nrn2685.

[309] M. Oudega, C. G. Vargas, A. B. Weber, N. Kleitman, and M. B. Bunge. Long-term effects of methylprednisolone following transection of adult rat spinal cord. *Eur J Neurosci*, 11(7):2453–2464, Jul 1999.

[310] C. L. Paíno, C. Fernandez-Valle, M. L. Bates, and M. B. Bunge. Regrowth of axons in lesioned adult rat spinal cord: promotion by implants of cultured schwann cells. *J Neurocytol*, 23(7):433–452, Jul 1994.

[311] H. C. Park, Y. S. Shim, Y. Ha, S. H. Yoon, S. R. Park, B. H. Choi, and H. S. Park. Treatment of complete spinal cord injury patients by autologous bone marrow cell transplantation and administration of granulocyte-macrophage colony stimulating factor. *Tissue Eng*, 11(5-6):913–922, 2005. doi: 10.1089/ten.2005.11.913. URL http://dx.doi.org/10.1089/ten.2005.11.913.

[312] I.-H. Park, P. H. Lerou, R. Zhao, H. Huo, and G. Q. Daley. Generation of human-induced pluripotent stem cells. *Nat Protoc*, 3(7):1180–1186, 2008. doi: 10.1038/nprot.2008.92. URL http://dx.doi.org/10.1038/nprot.2008.92.

[313] K. K. Park, K. Liu, Y. Hu, P. D. Smith, C. Wang, B. Cai, B. Xu, L. Connolly, I. Kramvis, M. Sahin, and Z. He. Promoting axon regeneration in the adult cns by modulation of the pten/mtor pathway. *Science*, 322(5903):963–966, Nov 2008. doi: 10.1126/science.1161566. URL http://dx.doi.org/10.1126/science.1161566.

[314] A. M. Parr, I. Kulbatski, and C. H. Tator. Transplantation of adult rat spinal cord stem/progenitor cells for spinal cord injury. *J Neurotrauma*, 24(5):835–845, May 2007. doi: 10.1089/neu.2006.3771. URL http://dx.doi.org/10.1089/neu.2006.3771.

[315] R. J. Pasterkamp, R. J. Giger, M. J. Ruitenberg, A. J. Holtmaat, J. D. Wit, F. D. Winter, and J. Verhaagen. Expression of the gene encoding the chemorepellent semaphorin iii is induced in the fibroblast component of neural scar tissue formed following injuries of adult but not neonatal cns. *Mol Cell Neurosci*, 13(2):143–166, Feb 1999. doi: 10.1006/mcne.1999.0738. URL `http://dx.doi.org/10.1006/mcne.1999.0738`.

[316] C. M. Patist, M. B. Mulder, S. E. Gautier, V. Maquet, R. Jérôme, and M. Oudega. Freeze-dried poly(d,l-lactic acid) macroporous guidance scaffolds impregnated with brain-derived neurotrophic factor in the transected adult rat thoracic spinal cord. *Biomaterials*, 25(9):1569–1582, Apr 2004.

[317] D. D. Pearse, A. R. Sanchez, F. C. Pereira, C. M. Andrade, R. Puzis, Y. Pressman, K. Golden, B. M. Kitay, B. Blits, P. M. Wood, and M. B. Bunge. Transplantation of schwann cells and/or olfactory ensheathing glia into the contused spinal cord: Survival, migration, axon association, and functional recovery. *Glia*, 55(9):976–1000, Jul 2007. doi: 10.1002/glia.20490. URL `http://dx.doi.org/10.1002/glia.20490`.

[318] E. B. Pedersen, J. Zimmer, and B. Finsen. Triple immunosuppression protects murine intracerebral, hippocampal xenografts in adult rat hosts: effects on cellular infiltration, major histocompatibility complex antigen induction and blood-brain barrier leakage. *Neuroscience*, 78(3):685–701, Jun 1997.

[319] D. B. Pettigrew and K. A. Crutcher. White matter of the cns supports or inhibits neurite outgrowth in vitro depending on geometry. *J Neurosci*, 19(19):8358–8366, Oct 1999.

[320] D. B. Pettigrew, K. P. Shockley, and K. A. Crutcher. Disruption of spinal cord white matter and sciatic nerve geometry inhibits axonal growth in vitro in the absence of glial scarring. *BMC Neurosci*, 2:8, 2001.

[321] K. Pfeifer, M. Vroemen, A. Blesch, and N. Weidner. Adult neural progenitor cells provide a permissive guiding substrate for corticospinal axon growth following spinal cord injury. *Eur J Neurosci*, 20(7):1695–1704, Oct 2004. doi: 10.1111/j.1460-9568.2004.03657.x. URL `http://dx.doi.org/10.1111/j.1460-9568.2004.03657.x`.

[322] K. Pfeifer, M. Vroemen, M. Caioni, L. Aigner, U. Bogdahn, and N. Weidner. Autologous adult rodent neural progenitor cell transplantation represents a feasible strategy to promote structural repair in the chronically injured spinal cord. *Regen Med*, 1(2):255–266, Mar 2006. doi: 10.2217/17460751.1.2.255. URL `http://dx.doi.org/10.2217/17460751.1.2.255`.

[323] M. A. Pizzi and M. J. Crowe. Transplantation of fibroblasts that overexpress matrix metalloproteinase-3 into the site of spinal cord injury in rats. *J Neurotrauma*, 23(12):1750–1765, Dec 2006. doi: 10.1089/neu.2006.23.1750. URL `http://dx.doi.org/10.1089/neu.2006.23.1750`.

[324] G. W. Plant, C. L. Christensen, M. Oudega, and M. B. Bunge. Delayed transplantation of olfactory ensheathing glia promotes sparing/regeneration of supraspinal axons in the contused adult rat spinal cord. *J Neurotrauma*, 20(1):1–16, Jan 2003. doi: 10.1089/08977150360517146. URL `http://dx.doi.org/10.1089/08977150360517146`.

[325] P. G. Popovich, Z. Guan, P. Wei, I. Huitinga, N. van Rooijen, and B. T. Stokes. Depletion of hematogenous macrophages promotes partial hindlimb recovery and neuroanatomical repair after experimental spinal cord injury. *Exp Neurol*, 158(2):351–365, Aug 1999. doi: 10.1006/exnr.1999.7118. URL `http://dx.doi.org/10.1006/exnr.1999.7118`.

[326] P. G. Popovich, Z. Guan, V. McGaughy, L. Fisher, W. F. Hickey, and D. M. Basso. The neuropathological and behavioral consequences of intraspinal microglial/macrophage activation. *J Neuropathol Exp Neurol*, 61(7):623–633, Jul 2002.

[327] W. Potter, R. E. Kalil, and W. J. Kao. Biomimetic material systems for neural progenitor cell-based therapy. *Front Biosci*, 13:806–821, 2008.

[328] P. Prang, R. Müller, A. Eljaouhari, K. Heckmann, W. Kunz, T. Weber, C. Faber, M. Vroemen, U. Bogdahn, and N. Weidner. The promotion of oriented axonal regrowth in the injured spinal cord by alginate-based anisotropic capillary hydrogels. *Biomaterials*, 27(19):3560–3569, Jul 2006. doi: 10.1016/j.biomaterials.2006.01.053. URL `http://dx.doi.org/10.1016/j.biomaterials.2006.01.053`.

[329] J. Price and R. O. Hynes. Astrocytes in culture synthesize and secrete a variant form of fibronectin. *J Neurosci*, 5(8):2205–2211, Aug 1985.

[330] R. Prinjha, S. E. Moore, M. Vinson, S. Blake, R. Morrow, G. Christie, D. Michalovich, D. L. Simmons, and F. S. Walsh. Inhibitor of neurite outgrowth in humans. *Nature*, 403(6768):383–384, Jan 2000. doi: 10.1038/35000287. URL `http://dx.doi.org/10.1038/35000287`.

[331] D. J. Prockop. Marrow stromal cells as stem cells for nonhematopoietic tissues. *Science*, 276(5309): 71–74, Apr 1997.

[332] A. B. J. Prowse, L. R. McQuade, K. J. Bryant, D. D. V. Dyk, B. E. Tuch, and P. P. Gray. A proteome analysis of conditioned media from human neonatal fibroblasts used in the maintenance of human embryonic stem cells. *Proteomics*, 5(4):978–989, Mar 2005. doi: 10.1002/pmic.200401087. URL `http://dx.doi.org/10.1002/pmic.200401087`.

[333] A. B. J. Prowse, L. R. McQuade, K. J. Bryant, H. Marcal, and P. P. Gray. Identification of potential pluripotency determinants for human embryonic stem cells following proteomic analysis of human and mouse fibroblast conditioned media. *J Proteome Res*, 6(9):3796–3807, Sep 2007. doi: 10.1021/pr0702262. URL `http://dx.doi.org/10.1021/pr0702262`.

[334] K. A. Pulford, A. Sipos, J. L. Cordell, W. P. Stross, and D. Y. Mason. Distribution of the cd68 macrophage/myeloid associated antigen. *Int Immunol*, 2(10):973–980, 1990.

[335] A. G. Rabchevsky, I. Fugaccia, P. G. Sullivan, and S. W. Scheff. Cyclosporin a treatment following spinal cord injury to the rat: behavioral effects and stereological assessment of tissue sparing. *J Neurotrauma*, 18(5):513–522, May 2001. doi: 10.1089/089771501300227314. URL `http://dx.doi.org/10.1089/089771501300227314`.

[336] A. G. Rabchevsky, I. Fugaccia, P. G. Sullivan, D. A. Blades, and S. W. Scheff. Efficacy of methylprednisolone therapy for the injured rat spinal cord. *J Neurosci Res*, 68(1):7–18, Apr 2002.

[337] A. Ramón-Cueto and M. Nieto-Sampedro. Regeneration into the spinal cord of transected dorsal root axons is promoted by ensheathing glia transplants. *Exp Neurol*, 127(2):232–244, Jun 1994. doi: 10.1006/exnr.1994.1099. URL `http://dx.doi.org/10.1006/exnr.1994.1099`.

[338] A. Ramón-Cueto, G. W. Plant, J. Avila, and M. B. Bunge. Long-distance axonal regeneration in the transected adult rat spinal cord is promoted by olfactory ensheathing glia transplants. *J Neurosci*, 18 (10):3803–3815, May 1998.

[339] A. Ramón-Cueto, M. I. Cordero, F. F. Santos-Benito, and J. Avila. Functional recovery of paraplegic rats and motor axon regeneration in their spinal cords by olfactory ensheathing glia. *Neuron*, 25(2): 425–435, Feb 2000.

[340] K. V. R. Rao, K. S. Panickar, A. R. Jayakumar, and M. D. Norenberg. Astrocytes protect neurons from ammonia toxicity. *Neurochem Res*, 30(10):1311–1318, Oct 2005. doi: 10.1007/s11064-005-8803-2. URL `http://dx.doi.org/10.1007/s11064-005-8803-2`.

[341] O. Rapalino, O. Lazarov-Spiegler, E. Agranov, G. J. Velan, E. Yoles, M. Fraidakis, A. Solomon, R. Gepstein, A. Katz, M. Belkin, M. Hadani, and M. Schwartz. Implantation of stimulated homologous macrophages results in partial recovery of paraplegic rats. *Nat Med*, 4(7):814–821, Jul 1998.

[342] F. Renault-Mihara, S. Okada, S. Shibata, M. Nakamura, Y. Toyama, and H. Okano. Spinal cord injury: emerging beneficial role of reactive astrocytes' migration. *Int J Biochem Cell Biol*, 40(9):1649–1653, 2008. doi: 10.1016/j.biocel.2008.03.009. URL `http://dx.doi.org/10.1016/j.biocel.2008.03.009`.

[343] B. A. Reynolds and R. L. Rietze. Neural stem cells and neurospheres–re-evaluating the relationship. *Nat Methods*, 2(5):333–336, May 2005. doi: 10.1038/nmeth758. URL `http://dx.doi.org/10.1038/nmeth758`.

[344] B. A. Reynolds and S. Weiss. Generation of neurons and astrocytes from isolated cells of the adult mammalian central nervous system. *Science*, 255(5052):1707–1710, Mar 1992.

[345] J. L. Ridet, S. K. Malhotra, A. Privat, and F. H. Gage. Reactive astrocytes: cellular and molecular cues to biological function. *Trends Neurosci*, 20(12):570–577, Dec 1997.

[346] L. B. Rocha, G. Goissis, and M. A. Rossi. Biocompatibility of anionic collagen matrix as scaffold for bone healing. *Biomaterials*, 23(2):449–456, Jan 2002.

[347] J. Rosenberger, A. M. Geckova, J. P. Dijk, R. Roland, W. J. Heuvel, and J. W. G. F. Factors modifying stress from adverse effects of immunosuppressive medication in kidney transplant recipients. *Clin Transplant*, 19(1):70–76, Feb 2005. doi: 10.1111/j.1399-0012.2004.00300.x. URL `http://dx.doi.org/10.1111/j.1399-0012.2004.00300.x`.

[348] M. G. Rosenfeld, J. J. Mermod, S. G. Amara, L. W. Swanson, P. E. Sawchenko, J. Rivier, W. W. Vale, and R. M. Evans. Production of a novel neuropeptide encoded by the calcitonin gene via tissue-specific rna processing. *Nature*, 304(5922):129–135, 1983.

[349] J. D. Rothstein, M. Dykes-Hoberg, C. A. Pardo, L. A. Bristol, L. Jin, R. W. Kuncl, Y. Kanai, M. A. Hediger, Y. Wang, J. P. Schielke, and D. F. Welty. Knockout of glutamate transporters reveals a major role for astroglial transport in excitotoxicity and clearance of glutamate. *Neuron*, 16(3):675–686, Mar 1996.

[350] D. G. Roufa, M. I. Johnson, and M. B. Bunge. Influence of ganglion age, nonneuronal cells and substratum on neurite outgrowth in culture. *Dev Biol*, 99(1):225–239, Sep 1983.

[351] J. W. Rowland, G. W. J. Hawryluk, B. Kwon, and M. G. Fehlings. Current status of acute spinal cord injury pathophysiology and emerging therapies: promise on the horizon. *Neurosurg Focus*, 25(5):E2, 2008. doi: 10.3171/FOC.2008.25.11.E2. URL `http://dx.doi.org/10.3171/FOC.2008.25.11.E2`.

[352] M. J. Ruitenberg, G. W. Plant, C. L. Christensen, B. Blits, S. P. Niclou, A. R. Harvey, G. J. Boer, and J. Verhaagen. Viral vector-mediated gene expression in olfactory ensheathing glia implants in the lesioned rat spinal cord. *Gene Ther*, 9(2):135–146, Jan 2002. doi: 10.1038/sj.gt.3301626. URL `http://dx.doi.org/10.1038/sj.gt.3301626`.

[353] E. Ruoslahti and A. Vaheri. Novel human serum protein from fibroblast plasma membrane. *Nature*, 248(5451):789–791, Apr 1974.

[354] Z. Ruszczak. Effect of collagen matrices on dermal wound healing. *Adv Drug Deliv Rev*, 55(12): 1595–1611, Nov 2003.

[355] Z. Ruszczak and W. Friess. Collagen as a carrier for on-site delivery of antibacterial drugs. *Adv Drug Deliv Rev*, 55(12):1679–1698, Nov 2003.

[356] P. L. Ryan, R. A. Foty, J. Kohn, and M. S. Steinberg. Tissue spreading on implantable substrates is a competitive outcome of cell-cell vs. cell-substratum adhesivity. *Proc Natl Acad Sci U S A*, 98(8):4323–4327, Apr 2001. doi: 10.1073/pnas.071615398. URL `http://dx.doi.org/10.1073/pnas.071615398`.

[357] K. Saganová, J. Orendácová, I. Sulla, P. Filipcík, D. Cízková, and I. Vanický. Effects of long-term fk506 administration on functional and histopathological outcome after spinal cord injury in adult rat. *Cell Mol Neurobiol*, 29(6-7):1045–1051, Sep 2009. doi: 10.1007/s10571-009-9395-1. URL `http://dx.doi.org/10.1007/s10571-009-9395-1`.

[358] S. Sakakibara, T. Imai, K. Hamaguchi, M. Okabe, J. Aruga, K. Nakajima, D. Yasutomi, T. Nagata, Y. Kurihara, S. Uesugi, T. Miyata, M. Ogawa, K. Mikoshiba, and H. Okano. Mouse-musashi-1, a neural rna-binding protein highly enriched in the mammalian cns stem cell. *Dev Biol*, 176(2):230–242, Jun 1996.

[359] D. L. Salazar, N. Uchida, F. P. T. Hamers, B. J. Cummings, and A. J. Anderson. Human neural stem cells differentiate and promote locomotor recovery in an early chronic spinal cord injury nod-scid mouse model. *PLoS One*, 5(8):e12272, 2010. doi: 10.1371/journal.pone.0012272. URL `http://dx.doi.org/10.1371/journal.pone.0012272`.

[360] S. Saunders. *Peripheral nerve trunks. In Nerves and Nerve Injuries.* Churchill Livingstone, Edinburgh London and New York., 1978.

[361] K. Saxena, N. Patro, and I. Patro. Fk506 protects neurons following peripheral nerve injury via immunosuppression. *Cell Mol Neurobiol*, 27(8):1049–1057, Dec 2007. doi: 10.1007/s10571-007-9221-6. URL `http://dx.doi.org/10.1007/s10571-007-9221-6`.

[362] J. C. Schense and J. A. Hubbell. Cross-linking exogenous bifunctional peptides into fibrin gels with factor xiiia. *Bioconjug Chem*, 10(1):75–81, 1999. doi: 10.1021/bc9800769. URL `http://dx.doi.org/10.1021/bc9800769`.

[363] C. E. Schmidt and J. B. Leach. Neural tissue engineering: strategies for repair and regeneration. *Annu Rev Biomed Eng*, 5:293–347, 2003. doi: 10.1146/annurev.bioeng.5.011303.120731. URL `http://dx.doi.org/10.1146/annurev.bioeng.5.011303.120731`.

[364] E. Schnell, K. Klinkhammer, S. Balzer, G. Brook, D. Klee, P. Dalton, and J. Mey. Guidance of glial cell migration and axonal growth on electrospun nanofibers of poly-epsilon-caprolactone and a collagen/poly-epsilon-caprolactone blend. *Biomaterials*, 28(19):3012–3025, Jul 2007. doi: 10.1016/j.biomaterials.2007.03.009. URL `http://dx.doi.org/10.1016/j.biomaterials.2007.03.009`.

[365] L. Schnell, S. Fearn, H. Klassen, M. E. Schwab, and V. H. Perry. Acute inflammatory responses to mechanical lesions in the cns: differences between brain and spinal cord. *Eur J Neurosci*, 11(10): 3648–3658, Oct 1999.

[366] J. Schoenen, P. Delree, P. Leprince, and G. Moonen. Neurotransmitter phenotype plasticity in cultured dissociated adult rat dorsal root ganglia: an immunocytochemical study. *J Neurosci Res*, 22(4):473–487, Apr 1989. doi: 10.1002/jnr.490220414. URL `http://dx.doi.org/10.1002/jnr.490220414`.

[367] S. S. Schultz. Adult stem cell application in spinal cord injury. *Curr Drug Targets*, 6(1):63–73, Feb 2005.

[368] J. M. Schwab, K. Brechtel, C.-A. Mueller, V. Failli, H.-P. Kaps, S. K. Tuli, and H. J. Schluesener. Experimental strategies to promote spinal cord regeneration–an integrative perspective. *Prog Neurobiol*, 78(2):91–116, Feb 2006. doi: 10.1016/j.pneurobio.2005.12.004. URL `http://dx.doi.org/10.1016/j.pneurobio.2005.12.004`.

[369] M. E. Schwab and D. Bartholdi. Degeneration and regeneration of axons in the lesioned spinal cord. *Physiol Rev*, 76(2):319–370, Apr 1996.

[370] M. Schwartz. Protective autoimmunity as a t-cell response to central nervous system trauma: prospects for therapeutic vaccines. *Prog Neurobiol*, 65(5):489–496, Dec 2001.

[371] P. H. Schwartz, P. J. Bryant, T. J. Fuja, H. Su, D. K. O'Dowd, and H. Klassen. Isolation and characterization of neural progenitor cells from post-mortem human cortex. *J Neurosci Res*, 74(6): 838–851, Dec 2003. doi: 10.1002/jnr.10854. URL `http://dx.doi.org/10.1002/jnr.10854`.

[372] R. M. Seaberg and D. van der Kooy. Stem and progenitor cells: the premature desertion of rigorous definitions. *Trends Neurosci*, 26(3):125–131, Mar 2003.

[373] A. M. Seggio, A. Narayanaswamy, B. Roysam, and D. M. Thompson. Self-aligned schwann cell monolayers demonstrate an inherent ability to direct neurite outgrowth. *J Neural Eng*, 7(4):046001, Aug 2010. doi: 10.1088/1741-2560/7/4/046001. URL `http://dx.doi.org/10.1088/1741-2560/7/4/046001`.

[374] A. Seiger. Collection and use of fetal central nervous system tissue. *Fetal Ther*, 4 Suppl 1:104–107, 1989.

[375] E. Senoo, N. Tamaki, E. Fujimoto, and C. Ide. Effects of prelesioned peripheral nerve graft on nerve regeneration in the rat spinal cord. *Neurosurgery*, 42(6):1347–1356, Jun 1998.

[376] M. C. Shearer and J. W. Fawcett. The astrocyte/meningeal cell interface–a barrier to successful nerve regeneration? *Cell Tissue Res*, 305(2):267–273, Aug 2001.

[377] M. C. Shearer, S. P. Niclou, D. Brown, R. A. Asher, A. J. G. D. Holtmaat, J. M. Levine, J. Verhaagen, and J. W. Fawcett. The astrocyte/meningeal cell interface is a barrier to neurite outgrowth which can be overcome by manipulation of inhibitory molecules or axonal signalling pathways. *Mol Cell Neurosci*, 24(4):913–925, Dec 2003.

[378] A. Y. Shih, D. A. Johnson, G. Wong, A. D. Kraft, L. Jiang, H. Erb, J. A. Johnson, and T. H. Murphy. Coordinate regulation of glutathione biosynthesis and release by nrf2-expressing glia potently protects neurons from oxidative stress. *J Neurosci*, 23(8):3394–3406, Apr 2003.

[379] L. S. Shihabuddin, P. J. Horner, J. Ray, and F. H. Gage. Adult spinal cord stem cells generate neurons after transplantation in the adult dentate gyrus. *J Neurosci*, 20(23):8727–8735, Dec 2000.

[380] J. Silver. Transplantation strategies using embryonic astroglial cells to promote cns axon regeneration in neonatal and adult mammals. *Clin Res*, 36(3):196–199, Apr 1988.

[381] J. Silver and J. H. Miller. Regeneration beyond the glial scar. *Nat Rev Neurosci*, 5(2):146–156, Feb 2004. doi: 10.1038/nrn1326. URL `http://dx.doi.org/10.1038/nrn1326`.

[382] J. Silver and M. Y. Ogawa. Postnatally induced formation of the corpus callosum in acallosal mice on glia-coated cellulose bridges. *Science*, 220(4601):1067–1069, Jun 1983.

[383] T. J. Sims, M. B. Durgun, and S. A. Gilmore. Transplantation of sciatic nerve segments into normal and glia-depleted spinal cords. *Exp Brain Res*, 125(4):495–501, Apr 1999.

[384] R. Singhvi, A. Kumar, G. P. Lopez, G. N. Stephanopoulos, D. I. Wang, G. M. Whitesides, and D. E. Ingber. Engineering cell shape and function. *Science*, 264(5159):696–698, Apr 1994.

[385] R. Singhvi, G. Stephanopoulos, and D. I. Wang. Effects of substratum morphology on cell physiology. *Biotechnol Bioeng*, 43(8):764–771, Apr 1994. doi: 10.1002/bit.260430811. URL `http://dx.doi.org/10.1002/bit.260430811`.

[386] R. M. Smeal and P. A. Tresco. The influence of substrate curvature on neurite outgrowth is cell type dependent. *Exp Neurol*, 213(2):281–292, Oct 2008. doi: 10.1016/j.expneurol.2008.05.026. URL `http://dx.doi.org/10.1016/j.expneurol.2008.05.026`.

[387] R. M. Smeal, R. Rabbitt, R. Biran, and P. A. Tresco. Substrate curvature influences the direction of nerve outgrowth. *Ann Biomed Eng*, 33(3):376–382, Mar 2005.

[388] G. M. Smith and R. H. Miller. Immature type-1 astrocytes suppress glial scar formation, are motile and interact with blood vessels. *Brain Res*, 543(1):111–122, Mar 1991.

[389] G. M. Smith and J. Silver. Transplantation of immature and mature astrocytes and their effect on scar formation in the lesioned central nervous system. *Prog Brain Res*, 78:353–361, 1988.

[390] G. M. Smith, R. H. Miller, and J. Silver. Changing role of forebrain astrocytes during development, regenerative failure, and induced regeneration upon transplantation. *J Comp Neurol*, 251(1):23–43, Sep 1986. doi: 10.1002/cne.902510103. URL `http://dx.doi.org/10.1002/cne.902510103`.

[391] G. M. Smith, U. Rutishauser, J. Silver, and R. H. Miller. Maturation of astrocytes in vitro alters the extent and molecular basis of neurite outgrowth. *Dev Biol*, 138(2):377–390, Apr 1990.

[392] R. S. Smith, T. J. Smith, T. M. Blieden, and R. P. Phipps. Fibroblasts as sentinel cells. synthesis of chemokines and regulation of inflammation. *Am J Pathol*, 151(2):317–322, Aug 1997.

[393] D. M. Snow, V. Lemmon, D. A. Carrino, A. I. Caplan, and J. Silver. Sulfated proteoglycans in astroglial barriers inhibit neurite outgrowth in vitro. *Exp Neurol*, 109(1):111–130, Jul 1990.

[394] D. M. Snow, E. M. Brown, and P. C. Letourneau. Growth cone behavior in the presence of soluble chondroitin sulfate proteoglycan (cspg), compared to behavior on cspg bound to laminin or fibronectin. *Int J Dev Neurosci*, 14(3):331–349, Jun 1996.

[395] E. Y. Snyder, C. Yoon, J. D. Flax, and J. D. Macklis. Multipotent neural precursors can differentiate toward replacement of neurons undergoing targeted apoptotic degeneration in adult mouse neocortex. *Proc Natl Acad Sci U S A*, 94(21):11663–11668, Oct 1997.

[396] M. V. Sofroniew. Reactive astrocytes in neural repair and protection. *Neuroscientist*, 11(5):400–407, Oct 2005. doi: 10.1177/1073858405278321. URL `http://dx.doi.org/10.1177/1073858405278321`.

[397] M. V. Sofroniew and H. V. Vinters. Astrocytes: biology and pathology. *Acta Neuropathol*, 119(1):7–35, Jan 2010. doi: 10.1007/s00401-009-0619-8. URL `http://dx.doi.org/10.1007/s00401-009-0619-8`.

[398] U. S. Sohur, J. G. Emsley, B. D. Mitchell, and J. D. Macklis. Adult neurogenesis and cellular brain repair with neural progenitors, precursors and stem cells. *Philos Trans R Soc Lond B Biol Sci*, 361(1473):1477–1497, Sep 2006. doi: 10.1098/rstb.2006.1887. URL `http://dx.doi.org/10.1098/rstb.2006.1887`.

[399] T. R. Srinivas and H.-U. Meier-Kriesche. Minimizing immunosuppression, an alternative approach to reducing side effects: objectives and interim result. *Clin J Am Soc Nephrol*, 3 Suppl 2:S101–S116, Mar 2008. doi: 10.2215/CJN.03510807. URL `http://dx.doi.org/10.2215/CJN.03510807`.

[400] D. P. Stirling, K. Khodarahmi, J. Liu, L. T. McPhail, C. B. McBride, J. D. Steeves, M. S. Ramer, and W. Tetzlaff. Minocycline treatment reduces delayed oligodendrocyte death, attenuates axonal dieback, and improves functional outcome after spinal cord injury. *J Neurosci*, 24(9):2182–2190, Mar 2004. doi: 10.1523/JNEUROSCI.5275-03.2004. URL `http://dx.doi.org/10.1523/JNEUROSCI.5275-03.2004`.

[401] G. Stoll, S. Jander, and R. R. Myers. Degeneration and regeneration of the peripheral nervous system: from augustus waller's observations to neuroinflammation. *J Peripher Nerv Syst*, 7(1):13–27, Mar 2002.

[402] K. S. Straley, C. W. P. Foo, and S. C. Heilshorn. Biomaterial design strategies for the treatment of spinal cord injuries. *J Neurotrauma*, 27(1):1–19, Jan 2010. doi: 10.1089/neu.2009.0948. URL `http://dx.doi.org/10.1089/neu.2009.0948`.

[403] W. J. Streit and Q.-S. Xue. Life and death of microglia. *J Neuroimmune Pharmacol*, 4(4):371–379, Dec 2009. doi: 10.1007/s11481-009-9163-5. URL `http://dx.doi.org/10.1007/s11481-009-9163-5`.

[404] W. J. Streit, S. L. Semple-Rowland, S. D. Hurley, R. C. Miller, P. G. Popovich, and B. T. Stokes. Cytokine mrna profiles in contused spinal cord and axotomized facial nucleus suggest a beneficial role for inflammation and gliosis. *Exp Neurol*, 152(1):74–87, Jul 1998. doi: 10.1006/exnr.1998.6835. URL `http://dx.doi.org/10.1006/exnr.1998.6835`.

[405] H. I. Suh, J. Min, K. H. Choi, S. W. Kim, K. S. Kim, and S. R. Jeon. Axonal regeneration effects of wnt3a-secreting fibroblast transplantation in spinal cord-injured rats. *Acta Neurochir (Wien)*, Jan 2011. doi: 10.1007/s00701-011-0945-1. URL `http://dx.doi.org/10.1007/s00701-011-0945-1`.

[406] T. Sun, S. Mai, D. Norton, J. W. Haycock, A. J. Ryan, and S. MacNeil. Self-organization of skin cells in three-dimensional electrospun polystyrene scaffolds. *Tissue Eng*, 11(7-8):1023–1033, 2005. doi: 10.1089/ten.2005.11.1023. URL `http://dx.doi.org/10.1089/ten.2005.11.1023`.

[407] M. Suzuki and G. Raisman. The glial framework of central white matter tracts: segmented rows of contiguous interfascicular oligodendrocytes and solitary astrocytes give rise to a continuous meshwork of transverse and longitudinal processes in the adult rat fimbria. *Glia*, 6(3):222–235, 1992. doi: 10.1002/glia.440060310. URL `http://dx.doi.org/10.1002/glia.440060310`.

[408] M. Suzuki and G. Raisman. Multifocal pattern of postnatal development of the macroglial framework of the rat fimbria. *Glia*, 12(4):294–308, Dec 1994. doi: 10.1002/glia.440120406. URL `http://dx.doi.org/10.1002/glia.440120406`.

[409] C. N. Svendsen, M. A. Caldwell, and T. Ostenfeld. Human neural stem cells: isolation, expansion and transplantation. *Brain Pathol*, 9(3):499–513, Jul 1999.

[410] R. A. Swanson, W. Ying, and T. M. Kauppinen. Astrocyte influences on ischemic neuronal death. *Curr Mol Med*, 4(2):193–205, Mar 2004.

[411] E. Syková and P. Jendelová. Magnetic resonance tracking of implanted adult and embryonic stem cells in injured brain and spinal cord. *Ann N Y Acad Sci*, 1049:146–160, May 2005. doi: 10.1196/annals.1334.014. URL `http://dx.doi.org/10.1196/annals.1334.014`.

[412] E. Syková, A. Homola, R. Mazanec, H. Lachmann, S. L. Konrádová, P. Kobylka, R. Pádr, J. Neuwirth, V. Komrska, V. Vávra, J. Stulík, and M. Bojar. Autologous bone marrow transplantation in patients with subacute and chronic spinal cord injury. *Cell Transplant*, 15(8-9):675–687, 2006.

[413] K. Takahashi, K. Okita, M. Nakagawa, and S. Yamanaka. Induction of pluripotent stem cells from fibroblast cultures. *Nat Protoc*, 2(12):3081–3089, 2007. doi: 10.1038/nprot.2007.418. URL `http://dx.doi.org/10.1038/nprot.2007.418`.

[414] T. Takami, M. Oudega, M. L. Bates, P. M. Wood, N. Kleitman, and M. B. Bunge. Schwann cell but not olfactory ensheathing glia transplants improve hindlimb locomotor performance in the moderately contused adult rat thoracic spinal cord. *J Neurosci*, 22(15):6670–6681, Aug 2002. doi: 20026636. URL `http://dx.doi.org/20026636`.

[415] T. Takami, M. Oudega, J. R. Bethea, P. M. Wood, N. Kleitman, and M. B. Bunge. Methylprednisolone and interleukin-10 reduce gray matter damage in the contused fischer rat thoracic spinal cord but do not improve functional outcome. *J Neurotrauma*, 19(5):653–666, May 2002. doi: 10.1089/089771502753754118. URL `http://dx.doi.org/10.1089/089771502753754118`.

[416] R. Talac, J. A. Friedman, M. J. Moore, L. Lu, E. Jabbari, A. J. Windebank, B. L. Currier, and M. J. Yaszemski. Animal models of spinal cord injury for evaluation of tissue engineering treatment strategies. *Biomaterials*, 25(9):1505–1510, Apr 2004.

[417] J. F. Talbott, D. N. Loy, Y. Liu, M. S. Qiu, M. B. Bunge, M. S. Rao, and S. R. Whittemore. Endogenous nkx2.2+/olig2+ oligodendrocyte precursor cells fail to remyelinate the demyelinated adult rat spinal cord in the absence of astrocytes. *Exp Neurol*, 192(1):11–24, Mar 2005. doi: 10.1016/j.expneurol.2004.05.038. URL `http://dx.doi.org/10.1016/j.expneurol.2004.05.038`.

[418] X. Tang, J. E. Davies, and S. J. A. Davies. Changes in distribution, cell associations, and protein expression levels of ng2, neurocan, phosphacan, brevican, versican v2, and tenascin-c during acute to chronic maturation of spinal cord scar tissue. *J Neurosci Res*, 71(3):427–444, Feb 2003. doi: 10.1002/jnr.10523. URL `http://dx.doi.org/10.1002/jnr.10523`.

[419] Y. Taoka and K. Okajima. Role of leukocytes in spinal cord injury in rats. *J Neurotrauma*, 17(3): 219–229, Mar 2000.

[420] Y. Taoka, K. Okajima, M. Uchiba, K. Murakami, N. Harada, M. Johno, and M. Naruo. Activated protein c reduces the severity of compression-induced spinal cord injury in rats by inhibiting activation of leukocytes. *J Neurosci*, 18(4):1393–1398, Feb 1998.

[421] Y. I. Tarasenko, J. Gao, L. Nie, K. M. Johnson, J. J. Grady, C. E. Hulsebosch, D. J. McAdoo, and P. Wu. Human fetal neural stem cells grafted into contusion-injured rat spinal

cords improve behavior. *J Neurosci Res*, 85(1):47–57, Jan 2007. doi: 10.1002/jnr.21098. URL http://dx.doi.org/10.1002/jnr.21098.

[422] C. C. Tate, M. C. Tate, and M. C. LaPlaca. Fibronectin and laminin increase in the mouse brain after controlled cortical impact injury. *J Neurotrauma*, 24(1):226–230, Jan 2007. doi: 10.1089/neu.2006.0043. URL http://dx.doi.org/10.1089/neu.2006.0043.

[423] N. J. Tawil, M. Houde, R. Blacher, F. Esch, L. F. Reichardt, D. C. Turner, and S. Carbonetto. Alpha 1 beta 1 integrin heterodimer functions as a dual laminin/collagen receptor in neural cells. *Biochemistry*, 29(27):6540–6544, Jul 1990.

[424] A. Teichner, E. Morselli, F. R. Buttarelli, B. Caronti, F. E. Pontieri, G. Venturini, and G. Palladini. Treatment with cyclosporine a promotes axonal regeneration in rats submitted to transverse section of the spinal cord. *J Hirnforsch*, 34(3):343–349, 1993.

[425] S. Temple. The development of neural stem cells. *Nature*, 414(6859):112–117, Nov 2001. doi: 10.1038/35102174. URL http://dx.doi.org/10.1038/35102174.

[426] Y. D. Teng, E. B. Lavik, X. Qu, K. I. Park, J. Ourednik, D. Zurakowski, R. Langer, and E. Y. Snyder. Functional recovery following traumatic spinal cord injury mediated by a unique polymer scaffold seeded with neural stem cells. *Proc Natl Acad Sci U S A*, 99(5):3024–3029, Mar 2002. doi: 10.1073/pnas.052678899. URL http://dx.doi.org/10.1073/pnas.052678899.

[427] M. Thallmair, G. A. Metz, W. J. Z'Graggen, O. Raineteau, G. L. Kartje, and M. E. Schwab. Neurite growth inhibitors restrict plasticity and functional recovery following corticospinal tract lesions. *Nat Neurosci*, 1(2):124–131, Jun 1998. doi: 10.1038/373. URL http://dx.doi.org/10.1038/373.

[428] D. M. Thompson and H. M. Buettner. Neurite outgrowth is directed by schwann cell alignment in the absence of other guidance cues. *Ann Biomed Eng*, 34(1):161–168, Jan 2006. doi: 10.1007/s10439-005-9013-4. URL http://dx.doi.org/10.1007/s10439-005-9013-4.

[429] J. A. Thomson, J. Itskovitz-Eldor, S. S. Shapiro, M. A. Waknitz, J. J. Swiergiel, V. S. Marshall, and J. M. Jones. Embryonic stem cell lines derived from human blastocysts. *Science*, 282(5391):1145–1147, Nov 1998.

[430] C. A. Tobias, J. S. Shumsky, M. Shibata, M. H. Tuszynski, I. Fischer, A. Tessler, and M. Murray. Delayed grafting of bdnf and nt-3 producing fibroblasts into the injured spinal cord stimulates sprouting, partially rescues axotomized red nucleus neurons from loss and atrophy, and provides limited regeneration. *Exp Neurol*, 184(1):97–113, Nov 2003.

[431] V. J. Tom, C. M. Doller, A. T. Malouf, and J. Silver. Astrocyte-associated fibronectin is critical for axonal regeneration in adult white matter. *J Neurosci*, 24(42):9282–9290, Oct 2004. doi: 10.1523/JNEUROSCI.2120-04.2004. URL http://dx.doi.org/10.1523/JNEUROSCI.2120-04.2004.

[432] V. J. Tom, H. R. Sandrow-Feinberg, K. Miller, L. Santi, T. Connors, M. A. Lemay, and J. D. Houlé. Combining peripheral nerve grafts and chondroitinase promotes functional axonal regeneration in the chronically injured spinal cord. *J Neurosci*, 29(47):14881–14890, Nov 2009. doi: 10.1523/JNEUROSCI.3641-09.2009. URL `http://dx.doi.org/10.1523/JNEUROSCI.3641-09.2009`.

[433] K. J. Tomaselli, L. F. Reichardt, and J. L. Bixby. Distinct molecular interactions mediate neuronal process outgrowth on non-neuronal cell surfaces and extracellular matrices. *J Cell Biol*, 103(6 Pt 2): 2659–2672, Dec 1986.

[434] K. J. Tomaselli, K. M. Neugebauer, J. L. Bixby, J. Lilien, and L. F. Reichardt. N-cadherin and integrins: two receptor systems that mediate neuronal process outgrowth on astrocyte surfaces. *Neuron*, 1(1): 33–43, Mar 1988.

[435] A. Trounson, R. G. Thakar, G. Lomax, and D. Gibbons. Clinical trials for stem cell therapies. *BMC Med*, 9:52, 2011. doi: 10.1186/1741-7015-9-52. URL `http://dx.doi.org/10.1186/1741-7015-9-52`.

[436] O. Tsuji, K. Miura, Y. Okada, K. Fujiyoshi, M. Mukaino, N. Nagoshi, K. Kitamura, G. Kumagai, M. Nishino, S. Tomisato, H. Higashi, T. Nagai, H. Katoh, K. Kohda, Y. Matsuzaki, M. Yuzaki, E. Ikeda, Y. Toyama, M. Nakamura, S. Yamanaka, and H. Okano. Therapeutic potential of appropriately evaluated safe-induced pluripotent stem cells for spinal cord injury. *Proc Natl Acad Sci U S A*, 107(28):12704–12709, Jul 2010. doi: 10.1073/pnas.0910106107. URL `http://dx.doi.org/10.1073/pnas.0910106107`.

[437] D. C. Turner, L. A. Flier, and S. Carbonetto. Identification of a cell-surface protein involved in pc12 cell-substratum adhesion and neurite outgrowth on laminin and collagen. *J Neurosci*, 9(9):3287–3296, Sep 1989.

[438] M. H. Tuszynski, D. A. Peterson, J. Ray, A. Baird, Y. Nakahara, and F. H. Gage. Fibroblasts genetically modified to produce nerve growth factor induce robust neuritic ingrowth after grafting to the spinal cord. *Exp Neurol*, 126(1):1–14, Mar 1994.

[439] M. H. Tuszynski, R. Grill, L. L. Jones, H. M. McKay, and A. Blesch. Spontaneous and augmented growth of axons in the primate spinal cord: effects of local injury and nerve growth factor-secreting cell grafts. *J Comp Neurol*, 449(1):88–101, Jul 2002. doi: 10.1002/cne.10266. URL `http://dx.doi.org/10.1002/cne.10266`.

[440] N. Uchida, D. W. Buck, D. He, M. J. Reitsma, M. Masek, T. V. Phan, A. S. Tsukamoto, F. H. Gage, and I. L. Weissman. Direct isolation of human central nervous system stem cells. *Proc Natl Acad Sci U S A*, 97(26):14720–14725, Dec 2000. doi: 10.1073/pnas.97.26.14720. URL `http://dx.doi.org/10.1073/pnas.97.26.14720`.

[441] A. Vaheri, E. Ruoslahti, B. Westermark, and J. Ponten. A common cell-type specific surface antigen in cultured human glial cells and fibroblasts: loss in malignant cells. *J Exp Med*, 143(1):64–72, Jan 1976.

[442] S. van Neerven, E. A. J. Joosten, G. A. Brook, C. A. Lambert, J. Mey, J. Weis, M. A. Marcus, H. W. Steinbusch, M. van Kleef, J. Patijn, and R. Deumens. Repetitive intrathecal vegf(165) treatment has limited therapeutic effects after spinal cord injury in the rat. *J Neurotrauma*, 27(10):1781–1791, Oct 2010. doi: 10.1089/neu.2010.1484. URL `http://dx.doi.org/10.1089/neu.2010.1484`.

[443] I. Vanický, L. Urdzíková, K. Saganová, D. Cízková, and J. Gálik. A simple and reproducible model of spinal cord injury induced by epidural balloon inflation in the rat. *J Neurotrauma*, 18(12):1399–1407, Dec 2001. doi: 10.1089/08977150152725687. URL `http://dx.doi.org/10.1089/08977150152725687`.

[444] M. R. Vargas, D. A. Johnson, D. W. Sirkis, A. Messing, and J. A. Johnson. Nrf2 activation in astrocytes protects against neurodegeneration in mouse models of familial amyotrophic lateral sclerosis. *J Neurosci*, 28(50):13574–13581, Dec 2008. doi: 10.1523/JNEUROSCI.4099-08.2008. URL `http://dx.doi.org/10.1523/JNEUROSCI.4099-08.2008`.

[445] J. P. Vella and M. H. Sayegh. Maintenance pharmacological immunosuppressive strategies in renal transplantation. *Postgrad Med J*, 73(861):386–390, Jul 1997.

[446] A. L. Vescovi, E. A. Parati, A. Gritti, P. Poulin, M. Ferrario, E. Wanke, P. Frölichsthal-Schoeller, L. Cova, M. Arcellana-Panlilio, A. Colombo, and R. Galli. Isolation and cloning of multipotential stem cells from the embryonic human cns and establishment of transplantable human neural stem cell lines by epigenetic stimulation. *Exp Neurol*, 156(1):71–83, Mar 1999. doi: 10.1006/exnr.1998.6998. URL `http://dx.doi.org/10.1006/exnr.1998.6998`.

[447] G. Villa, S. Ceruti, M. Zanardelli, G. Magni, L. Jasmin, P. T. Ohara, and M. P. Abbracchio. Temporomandibular joint inflammation activates glial and immune cells in both the trigeminal ganglia and in the spinal trigeminal nucleus. *Mol Pain*, 6:89, 2010. doi: 10.1186/1744-8069-6-89. URL `http://dx.doi.org/10.1186/1744-8069-6-89`.

[448] R. R. Voskuhl, R. S. Peterson, B. Song, Y. Ao, L. B. J. Morales, S. Tiwari-Woodruff, and M. V. Sofroniew. Reactive astrocytes form scar-like perivascular barriers to leukocytes during adaptive immune inflammation of the cns. *J Neurosci*, 29(37):11511–11522, Sep 2009. doi: 10.1523/JNEUROSCI.1514-09.2009. URL `http://dx.doi.org/10.1523/JNEUROSCI.1514-09.2009`.

[449] D. H. Vrinten and F. F. T. Hamers. 'catwalk' automated quantitative gait analysis as a novel method to assess mechanical allodynia in the rat; a comparison with von frey testing. *Pain*, 102(1-2):203–209, Mar 2003.

[450] M. Vroemen, L. Aigner, J. Winkler, and N. Weidner. Adult neural progenitor cell grafts survive after acute spinal cord injury and integrate along axonal pathways. *Eur J Neurosci*, 18(4):743–751, Aug 2003.

[451] F.-P. Wachs, S. Couillard-Despres, M. Engelhardt, D. Wilhelm, S. Ploetz, M. Vroemen, J. Kaesbauer, G. Uyanik, J. Klucken, C. Karl, J. Tebbing, C. Svendsen, N. Weidner, H.-G. Kuhn, J. Winkler, and L. Aigner. High efficacy of clonal growth and expansion of adult neural stem cells. *Lab Invest*, 83(7): 949–962, Jul 2003.

[452] J. F. Walsh, M. E. Manwaring, and P. A. Tresco. Directional neurite outgrowth is enhanced by engineered meningeal cell-coated substrates. *Tissue Eng*, 11(7-8):1085–1094, 2005. doi: 10.1089/ten.2005.11.1085. URL `http://dx.doi.org/10.1089/ten.2005.11.1085`.

[453] A. W. Wamil, B. D. Wamil, and C. G. Hellerqvist. Cm101-mediated recovery of walking ability in adult mice paralyzed by spinal cord injury. *Proc Natl Acad Sci U S A*, 95(22):13188–13193, Oct 1998.

[454] J. J. Wang, M. I. Chuah, D. T. Yew, P. C. Leung, and D. S. Tsang. Effects of astrocyte implantation into the hemisected adult rat spinal cord. *Neuroscience*, 65(4):973–981, Apr 1995.

[455] K. C. Wang, J. A. Kim, R. Sivasankaran, R. Segal, and Z. He. P75 interacts with the nogo receptor as a co-receptor for nogo, mag and omgp. *Nature*, 420(6911):74–78, Nov 2002. doi: 10.1038/nature01176. URL `http://dx.doi.org/10.1038/nature01176`.

[456] K. C. Wang, V. Koprivica, J. A. Kim, R. Sivasankaran, Y. Guo, R. L. Neve, and Z. He. Oligodendrocyte-myelin glycoprotein is a nogo receptor ligand that inhibits neurite outgrowth. *Nature*, 417(6892):941–944, Jun 2002. doi: 10.1038/nature00867. URL `http://dx.doi.org/10.1038/nature00867`.

[457] N. Wang, J. P. Butler, and D. E. Ingber. Mechanotransduction across the cell surface and through the cytoskeleton. *Science*, 260(5111):1124–1127, May 1993.

[458] Z. H. Wang, G. F. Walter, and L. Gerhard. The expression of nerve growth factor receptor on schwann cells and the effect of these cells on the regeneration of axons in traumatically injured human spinal cord. *Acta Neuropathol*, 91(2):180–184, 1996.

[459] I. B. Wanner, A. Deik, M. Torres, A. Rosendahl, J. T. Neary, V. P. Lemmon, and J. L. Bixby. A new in vitro model of the glial scar inhibits axon growth. *Glia*, 56(15):1691–1709, Nov 2008. doi: 10.1002/glia.20721. URL `http://dx.doi.org/10.1002/glia.20721`.

[460] K. Watanabe, M. Nakamura, A. Iwanami, Y. Fujita, Y. Kanemura, Y. Toyama, and H. Okano. Comparison between fetal spinal-cord- and forebrain-derived neural stem/progenitor cells as a source of

transplantation for spinal cord injury. *Dev Neurosci*, 26(2-4):275–287, 2004. doi: 10.1159/000082144. URL http://dx.doi.org/10.1159/000082144.

[461] M. W. Weible and T. Chan-Ling. Phenotypic characterization of neural stem cells from human fetal spinal cord: Synergistic effect of lif and bmp4 to generate astrocytes. *Glia*, 55(11):1156–1168, Aug 2007. doi: 10.1002/glia.20539. URL http://dx.doi.org/10.1002/glia.20539.

[462] X. Wen and P. A. Tresco. Effect of filament diameter and extracellular matrix molecule precoating on neurite outgrowth and schwann cell behavior on multifilament entubulation bridging device in vitro. *J Biomed Mater Res A*, 76(3):626–637, Mar 2006. doi: 10.1002/jbm.a.30520. URL http://dx.doi.org/10.1002/jbm.a.30520.

[463] R. E. White and L. B. Jakeman. Don't fence me in: harnessing the beneficial roles of astrocytes for spinal cord repair. *Restor Neurol Neurosci*, 26(2-3):197–214, 2008.

[464] M. J. Wilby, E. M. Muir, J. Fok-Seang, B. J. Gour, O. W. Blaschuk, and J. W. Fawcett. N-cadherin inhibits schwann cell migration on astrocytes. *Mol Cell Neurosci*, 14(1):66–84, Jul 1999. doi: 10.1006/mcne.1999.0766. URL http://dx.doi.org/10.1006/mcne.1999.0766.

[465] U. Wilhelmsson, L. Li, M. Pekna, C.-H. Berthold, S. Blom, C. Eliasson, O. Renner, E. Bushong, M. Ellisman, T. E. Morgan, and M. Pekny. Absence of glial fibrillary acidic protein and vimentin prevents hypertrophy of astrocytic processes and improves post-traumatic regeneration. *J Neurosci*, 24(21):5016–5021, May 2004. doi: 10.1523/JNEUROSCI.0820-04.2004. URL http://dx.doi.org/10.1523/JNEUROSCI.0820-04.2004.

[466] S. M. Willerth and S. E. Sakiyama-Elbert. Cell therapy for spinal cord regeneration. *Adv Drug Deliv Rev*, 60(2):263–276, Jan 2008. doi: 10.1016/j.addr.2007.08.028. URL http://dx.doi.org/10.1016/j.addr.2007.08.028.

[467] D. Y. Wong, S. J. Hollister, P. H. Krebsbach, and C. Nosrat. Poly(epsilon-caprolactone) and poly (l-lactic-co-glycolic acid) degradable polymer sponges attenuate astrocyte response and lesion growth in acute traumatic brain injury. *Tissue Eng*, 13(10):2515–2523, Oct 2007. doi: 10.1089/ten.2006.0440. URL http://dx.doi.org/10.1089/ten.2006.0440.

[468] S. Wu, Y. Suzuki, T. Noda, H. Bai, M. Kitada, K. Kataoka, Y. Nishimura, and C. Ide. Immunohistochemical and electron microscopic study of invasion and differentiation in spinal cord lesion of neural stem cells grafted through cerebrospinal fluid in rat. *J Neurosci Res*, 69(6):940–945, Sep 2002. doi: 10.1002/jnr.10346. URL http://dx.doi.org/10.1002/jnr.10346.

[469] X. M. Xu, V. Guénard, N. Kleitman, and M. B. Bunge. Axonal regeneration into schwann cell-seeded guidance channels grafted into transected adult rat spinal cord. *J Comp Neurol*, 351(1):145–160, Jan 1995. doi: 10.1002/cne.903510113. URL http://dx.doi.org/10.1002/cne.903510113.

[470] X. M. Xu, A. Chen, V. Guénard, N. Kleitman, and M. B. Bunge. Bridging schwann cell transplants promote axonal regeneration from both the rostral and caudal stumps of transected adult rat spinal cord. *J Neurocytol*, 26(1):1–16, Jan 1997.

[471] X. M. Xu, S. X. Zhang, H. Li, P. Aebischer, and M. B. Bunge. Regrowth of axons into the distal spinal cord through a schwann-cell-seeded mini-channel implanted into hemisected adult rat spinal cord. *Eur J Neurosci*, 11(5):1723–1740, May 1999.

[472] I. Yalcin, A. Charlet, M.-J. Freund-Mercier, M. Barrot, and P. Poisbeau. Differentiating thermal allodynia and hyperalgesia using dynamic hot and cold plate in rodents. *J Pain*, 10(7):767–773, Jul 2009. doi: 10.1016/j.jpain.2009.01.325. URL `http://dx.doi.org/10.1016/j.jpain.2009.01.325`.

[473] G. Yiu and Z. He. Glial inhibition of cns axon regeneration. *Nat Rev Neurosci*, 7(8):617–627, Aug 2006. doi: 10.1038/nrn1956. URL `http://dx.doi.org/10.1038/nrn1956`.

[474] E. Yoles, E. Hauben, O. Palgi, E. Agranov, A. Gothilf, A. Cohen, V. Kuchroo, I. R. Cohen, H. Weiner, and M. Schwartz. Protective autoimmunity is a physiological response to cns trauma. *J Neurosci*, 21 (11):3740–3748, Jun 2001.

[475] Z. Zador, S. Stiver, V. Wang, and G. T. Manley. Role of aquaporin-4 in cerebral edema and stroke. *Handb Exp Pharmacol*, 190(190):159–170, 2009.

[476] M. V. Zappone, R. Galli, R. Catena, N. Meani, S. D. Biasi, E. Mattei, C. Tiveron, A. L. Vescovi, R. Lovell-Badge, S. Ottolenghi, and S. K. Nicolis. Sox2 regulatory sequences direct expression of a (beta)-geo transgene to telencephalic neural stem cells and precursors of the mouse embryo, revealing regionalization of gene expression in cns stem cells. *Development*, 127(11):2367–2382, Jun 2000.

[477] M. M. Zdanowicz. The pharmacology of immunosuppression. *Am J Pharm Educ*, 73(8):144, Dec 2009.

[478] D. I. Zeugolis, S. T. Khew, E. S. Y. Yew, A. K. Ekaputra, Y. W. Tong, L.-Y. L. Yung, D. W. Hutmacher, C. Sheppard, and M. Raghunath. Electro-spinning of pure collagen nano-fibres - just an expensive way to make gelatin? *Biomaterials*, 29(15):2293–2305, May 2008. doi: 10.1016/j.biomaterials.2008.02.009. URL `http://dx.doi.org/10.1016/j.biomaterials.2008.02.009`.

[479] W. J. Z'Graggen, G. A. Metz, G. L. Kartje, M. Thallmair, and M. E. Schwab. Functional recovery and enhanced corticofugal plasticity after unilateral pyramidal tract lesion and blockade of myelin-associated neurite growth inhibitors in adult rats. *J Neurosci*, 18(12):4744–4757, Jun 1998.

[480] N. Zhang, H. Yan, and X. Wen. Tissue-engineering approaches for axonal guidance. *Brain Res Brain Res Rev*, 49(1):48–64, Jul 2005. doi: 10.1016/j.brainresrev.2004.11.002. URL `http://dx.doi.org/10.1016/j.brainresrev.2004.11.002`.

[481] S. C. Zhang, B. Ge, and I. D. Duncan. Adult brain retains the potential to generate oligodendroglial progenitors with extensive myelination capacity. *Proc Natl Acad Sci U S A*, 96(7):4089–4094, Mar 1999.

[482] Z. Zhang, C. J. Krebs, and L. Guth. Experimental analysis of progressive necrosis after spinal cord trauma in the rat: etiological role of the inflammatory response. *Exp Neurol*, 143(1):141–152, Jan 1997. doi: 10.1006/exnr.1996.6355. URL `http://dx.doi.org/10.1006/exnr.1996.6355`.

[483] S. Zhong, W. E. Teo, X. Zhu, R. W. Beuerman, S. Ramakrishna, and L. Y. L. Yung. An aligned nanofibrous collagen scaffold by electrospinning and its effects on in vitro fibroblast culture. *J Biomed Mater Res A*, 79(3):456–463, Dec 2006. doi: 10.1002/jbm.a.30870. URL `http://dx.doi.org/10.1002/jbm.a.30870`.

[484] N. P. Ziats, K. M. Miller, and J. M. Anderson. In vitro and in vivo interactions of cells with biomaterials. *Biomaterials*, 9(1):5–13, Jan 1988.

[485] B. Zörner and M. E. Schwab. Anti-nogo on the go: from animal models to a clinical trial. *Ann N Y Acad Sci*, 1198 Suppl 1:E22–E34, Jun 2010. doi: 10.1111/j.1749-6632.2010.05566.x. URL `http://dx.doi.org/10.1111/j.1749-6632.2010.05566.x`.

A. Publications

T. Führmann, L. M. Hillen, K. Montzka, M. Wöltje, G. A. Brook. Novel Cell-Cell Interactions of Human Neural Progenitor-Derived Astrocytes within a Microstructured 3D-Scaffold. *Biomaterials 2010,* ***31****:7705-7715*

T. Führmann, K. Montzka, L.M. Hillen, D. Hodde, A. Dreier, A. Bozkurt, M. Wöltje, G.A. Brook. Axon growth-promoting properties of human bone marrow mesenchymal stromal cells. *Neuroscience Letters 2010,* ***474****:37-41*

J. Gerardo-Nava*, **T. Führmann***, K. Klinkhammer, N. Seiler, J. Mey, D. Klee, M. Möller, P.D. Dalton, G.A. Brook. Human Neural and Glial Interactions with Electrospun Nanofibres in vitro. *Nanomedicine 2009, Jan;****4****(1):11-30*
*These authors contributed equally to this work and are first authors

K. Montzka, **T. Führmann**, J. Müller-Ehmsen, M. Wöltje and G. A. Brook. Growth factor and cytokine expression of human mesenchymal stromal cells is not altered in an in vitro model of tissue damage. *Cytotherapy 2010,* ***Nov;12(7)****:870-80.*

K. Montzka, **T. Führmann**, M. Wöltje, G.A. Brook. Expansion of human bone marrow-derived mesenchymal stromal cells: serum-reduced medium is better than conventional medium *Cytotherapy 2010,* ***Sep;12(5)****:587-92*

A. Bozkurt*, R. Deumens*, J Scheffel, D.M. O'Dey, J. Weis, E.A. Joosten, **T. Führmann**, G.A. Brook, N. Pallua. CatWalk gait analysis in assessment of functional recovery after sciatic nerve injury. *Journal of Neuroscience Methods 2008,* ***173****:91-98*
*These authors contributed equally to this work and are first authors

K. Montzka*, N. Lassonczyk*, B. Tschöke, S. Neuss, **T. Führmann**, R. Franzen, R. Smeets, G.A. Brook, M. Wöltje. Neural differentiation potential of human bone marrow derived mesenchymal stromal cells: misleading marker gene expression. *BMC Neuroscience 2009,* ***10****:16.*
*These authors contributed equally to this work and are first authors

Book article

T. Führmann, J. Gerardo-Nava, G. A. Brook *(2010) Tissue Engineering: Central Nervous System.* **Chapter 12. pp 221-244.** In Tissue Engineering. From Lab to Clinic. Eds Pallua N, Suschek C. Springer Verlag, London, Heidelberg, Dordrecht, New York. DOI: 10.1007/978-3-642-02824-3.

B. Acknowledgments

As with almost every PhD student I had help from various sources and I would like to take the time to thank some of them here at the end of the manuscript. It cannot be a complete list and for anyone who happens to read this thesis and feels like he should have been acknowledged: I would like to thank you first for your greatly appreciated help.

Gary, I thank you for your scientific guidance during my PhD, your constant support, provided in form of discussions and practical help, especially while performing the different operations in Aachen or Liege. The many hours of your time spent correcting the spelling of various manuscripts, abstracts or this thesis has been greatly appreciated. I would also like to thank you for providing me with the opportunity to visit so many different places in Europe and for the great times we had during those lab visits or meetings and I hope we will share some more in the future.

Katrin ich danke dir dafür, dass ich den langen Weg zum Doktor nicht alleine machen musste. Für deine moralische Unterstüzung und deiner Hilfe im Labor, sei es bei molekularbiologischen Fragen, Auswertung von Rattenvideos, Kryoschnitten oder sonstigem Allerlei. Ohne dich wäre der Weg sicherlich beschwerlicher gewesen. Deine Bereitschaft die Freude über Publikationen oder Preise zu teilen hat mir auch immer wieder Spass gemacht, ebenfalls wären die Meetings ohne dich nur halb so lustig gewesen. Ich wünsche dir für deine Zukunft in der Urologie und auch Abseits der Wissenschaft alles Gute.

Lisa, ich danke dir für deine immer positive Art, deine Begeisterung für nahezu alle Bereiche der Medizin war immer wieder beeindruckend, genauso wie deine Motivation deine eigene Doktorarbeit zu bewältigen. Ich hoffe du wirst deine neuen Mitarbeiter in Maastricht ebenfalls mit deiner Begeisterung anstecken.

Doro, ich danke dir für deine immer hilfsbereite Art, ganz besonders für deine große Hilfe bei der Zellkultur, die vielen unterhaltsamen Stunden im Labor und Büro, aber auch für deine moralische Unterstützung. Ich wünsche dir alles Gute bei deinem Weg zum Doktor, ich hoffe ich kann dir dabei ebenfalls behilflich sein.

José, I would like to thank you for your support and help during my thesis, which includes, but is not restricted to, the preparation of the nanofibers. It was a pleasure working with you and I would like to wish you all the best for your thesis and offer my help to you as well.

Ron, I thank you for all your help, especially for teaching us how to perform and analyse the different behavioural tests. Your one year "abroad" in Aachen and your willingness to share your experience and knowledge was greatly appreciated.

Prof. Wagner, Ich danke Ihnen, dass Sie mir die Möglichkeit gegeben haben, in Ihrem Institut zu promovieren und Ihren Anregungen für meine Arbeit während des Kanditatenseminars.

I would like to thank **all members of the EU rescue project** for the interesting discussions during the EU-meetings, **Florence E. Perrin** for supporting us with the fibroblasts and especially **Rachelle Franzen and Renauld Quertainmont**, you provided us with the necessary knowledge and tools to perform the balloon compression injury at your institute. Furthermore, Renaud you were always willing to take care of the animals, a necessary task that was greatly appreciated. Without your help the *in vivo* chapter would have been reduced by half.

Zuletzt möchte ich meiner **Familie** danken, meinen Geschwistern und ihren Familien: Tina, Pauline, "Nr.2" und Thorsten; Fabian, Marie und Anja; sowie meinen Eltern, Claudia und Wolfgang. Ihr alle habt immer wieder Interesse an meiner Arbeit gezeigt, dafür und für so vieles mehr bin ich euch sehr dankbar.